Credits

Table of Contents

Review Article

Short Communication

First Record of the Ladder Gudgeon *Bostrychus scalaris* Larson, 2008 (Gobiiformes: Eleotridae: Butinae) from Mangrove Estuary of South Sumatra, Indonesia

Rusdianto Rusdianto[1]*, Gema Wahyudewantoro[1], Kunto Wibowo[1]

1)Museum Zoologicum Bogoriense, Research Center for Biosystematics and Evolution, National Research and Innovation Agency (BRIN), Jl. Raya Bogor KM 46, Cibinong, Bogor, West Java 16911, Indonesia
* Corresponding author, email: rusdi.jati77@gmail.com

ABSTRACT

A single specimen of *Bostrychus scalaris* was collected from the mangrove estuary of Banyuasin Regency, South Sumatra, Indonesia. The species was originally described as a new species based on a single specimen collected from the disturbed mangrove site in Sementa River, Selangor State, Malaysia. Subsequently, the species was known to have been distributed in Singapore based on a watercolour painting by a French naturalist also in Mekong River in Soc Trang Province, Vietnam. The present specimen of *B. scalaris* represents the first record of the species from Indonesian water and southernmost record of the species.

The genus *Bostrychus* characterised in having 7 dorsal spines; 9 dorsal soft rays; 1 anal spine; 8 anal soft rays; and 27 vertebrae (Larson 2008; Kottelat 2013) consists of eight valid species, viz., *Bostrychus sinensis* Lacepède, 1801, *Bostrychus africanus* (Steindachner, 1879), *Bostrychus zonatus* Weber, 1907, *Bostrychus aruensis* Weber, 1911, *Bostrychus expatria* (Herre, 1927), *Bostrychus strigogenys* Nichols, 1937, *Bostrychus microphthalmus* Hoese & Kottelat, 2005, and *Bostrychus scalaris* Larson, 2008 (Parenti 2021). The distribution of this genus covers Asia, Africa, Indo-West Pacific, and Oceania where three species have been recorded in Indonesian waters, namely *B. aruensis* (Aru Islands), *B. strigogenys* (Papua Province), and *B. microphthalmus* (South Sulawesi) (Miller & Wongrat 1990; Parenti 2021). Most of the genus *Bostrychus* are recorded inhabiting freshwater, brackish, and marine habitats. Most of this genus also inhabit estuaries and are mangrove ecosystem types.

The ladder gudgeon *B. scalaris* was previously reported with a limited geographical distribution in Malaysia (Larson 2008; Kottelat 2013; Huang et al. 2014; Parenti 2021), Singapore (Loneux 2006; Larson et al. 2016), and Vietnam (Tran et al. 2021; Taki et al. 2021). This species was originally described as a new species by Larson (2008) based on a single specimen collected from the Sementa River near Klang, Selangor State, Malaysia. Apart from being reported in Malaysia, this species' distribution in Singapore is suspected based on notes in a watercolour painting (number 607; genus unknown) by the French naturalist F. L. de

Castelnau. Other records also mention that *B. scalaris* is also found in mangrove habitats around Mekong River tributaries in Cu Lao Dung District, Soc Trang Province, Vietnam. The single specimen collection in this report represents the first record of this species in Indonesia, distributed in irrigated oil palm plantations in Banyuasin Regency, South Sumatra Province.

Counts and measurements of the body and its parts of a single specimen of *B. scalaris* follow Larson (2008). Measurements and meristic calculations were performed using Mitutoyo ABS digital caliper 500-151-30 0-150mm and a stereo microscope. Standard, total, and head lengths were abbreviated as SL, TL, and HL, respectively. Head length was measured from the base of the operculum to the tip of the mouth. Data of body proportion measurement is shown in both real scale and percentage of standard length, while head proportion data is shown in both real scale and percentage of head length. The character descriptions are based on a single specimen in Indonesia which was cataloged and deposited at the Museum Zoologicum Bogoriense (MZB) under the Directorate of Scientific Collections Management, Nasional Research and Innovation Agency, Indonesia.

Taxonomy
Gigaclass Actinopterygii
Superclass Actinopteri
Class Teleostei
Order Gobiiformes
Family Eleotridae Bonaparte, 1835
Subfamily Butinae Bleeker, 1874
Genus *Bostrychus* Lacepède, 1801
Bostrychus scalaris Larson, 2008
(Standard English name: Ladder gudgeon)
Figures 1–2

Material examined. MZB.26591, single specimen, 103.6 mm SL, brackish water flow in small plantation ditches, Sungsang IV Village, Banyuasin II District, Banyuasin Regency, South Sumatra Province, Sumatra Island, Indonesia, 2°21'00.5"S 104°51'49.4"E, throwing nets, Rusdianto, 31 May 2020.

Description. Head broad, compressed, flat, with a slightly protruding area in the centre of the nape extending parallel to the body axis towards the back, broadest area located in the area vertically aligned with preopercular margin. Total length (TL) 126.5 mm; head length (HL) 30.68 mm (29.61% of SL); head width at preopercular margin 23.99 mm (78.19% of HL). Mouth terminal, large and slightly oblique, forming an angle of about 30° with the body axis. The length of the upper and lower jaws are 18.45 mm (60.14% of HL) and 19.58 mm (63.82% of HL), respectively; posterior end of jaw just below eye. Upper lip free; lower lip joins with chin anteriorly; inner area of lip with fine fimbriae. Teeth in the upper and lower jaws are small, flat, arranged in a cone shape with slightly blunt tips. Teeth arranged in six to seven rows anteriorly and four to five rows posteriorly. Conical vomer teeth, six to eight-rows. Large tongue with rounded tip. Snout length 10.31 mm (33.60% of HL); broad, curved, and blunt in appearance when viewed dorsally, and curved and slightly pointed in ventral view. Eyes small, laterally arranged with a diameter of 2.93 mm (16.07% of HL). Interorbital broad, fleshy, with a width of 8.92 mm (8.61% of HL). Anterior naris small, with a long tube at the edge of upper lip; posterior naris oval, with short tube. Gill opening wide, ex-

tending forward to below the posterior preopercle. Preopercular pores five, with a single median anterior interorbital pore, posterior interorbital pores paired, anterior nasal pores small, located close to the edge of the upper lip. Six pores eye (oculoscular canal damaged). Sensory papillae in a transverse pattern, mandibular papillae *i* in several short transverse rows and mostly arranged in eight or nine irregular groups, a pair of papillae *i* groups on the chin.

Body slender, slightly rounded in anterior region, compressed posteriorly; body depth 19.04 mm (18.37% of SL); body width 15.70 mm (15.15% of HL); predorsal length 13.4 mm (12.93% of HL), preanal length 60.73 mm (58.61% of HL); preventral length 23.70 mm (22.87% of HL); dorsal fin base length 10.8 mm (I) (10.42% of SL), 19.70 (II) (19.01% of SL); first dorsal fin length 11.92 mm (11.50% of SL), second dorsal fin length 25.09 mm (24.21% of SL), ventral fin length 19.53 mm (18.85% of SL); anal fin base length 13.06 mm (12.60% of SL); anal fin length 17.68 mm (17.06% of SL); prepectoral fin length 19.90 mm (19.2% of HL); caudal peduncle height 11.56 mm (11.16% of SL); distance between base of dorsal fin (II) and caudal peduncle 20.30 mm (19.59% of SL). The body and head covered by small cycloid scales. Scales on the head embedded in the fleshy skin (difficult to see without dissection). Opercles covered with small cycloid scales. Preopercle covered with small cycloid scales covering most of the cheeks, especially in the area near the rows of papillae. Prepelvic region with small embedded cycloid scales extending forward. Base of pectoral fins covered with small cycloid scales. Predorsal scales small, cycloid-shaped, extending forward the operculum with embedded cycloid scales. First dorsal fin low and pointed (tips of third and fourth spines curved); the tip of the depressed fin reaching base of second dorsal fin; about 17 small scales between first and second dorsal fins. Height of second dorsal and anal fins are slightly greater than the first dorsal fin. The posterior fin is slightly longer than the anterior fin but not overly so. The posterior radius is much shorter than the base of the caudal fin. Pectoral fins broadly rounded, rays unbranched. Caudal fins oblong and rounded posteriorly; pelvic fins slender and pointed, extending less than half the distance to anus.

The characters of the single specimen of *Bostrychus scalaris* collected from South Sumatra, Indonesia, follow the characters of the holotype specimen first described by Larson (2008). This species is distinguished from all other species of the genus *Bostrychus* by the following combination of characters: 9 total dorsal soft rays; 8 total anal soft rays; 16 total pectoral rays; and 135 left-sided linea lateralis scales. Head is broad and flat, the body slender and compact; pectoral fin with distinct dark brown markings; throughout lateral surface of body with ca. 24–25 dark vertical bars; and a convoluted pattern along the body (Larson 2008; this study). Larson (2008) stated that the number of linea lateralis on the left side of the body is 135. Still, in this latest study, the number of linea lateralis scales could not be counted because the scales on the left side of the body had been damaged due to the removal of tissue for DNA analysis. The detailed comparisons between *B. scalaris* to each other species of the genus are given in Larson (2008).

The Indonesian specimen of *B. scalaris* is larger than the holotype from Malaysia (103.6 mm vs. 93 mm SL). This size is followed by slightly larger or shorter in several morphometric proportions, e.g., head length (29.61% in the former vs. 25.7% of SL in the latter), head width (78.19% vs. 75.7% of SL), eye diameter (16.07% vs. 15.9% of HL), maxillary length (60.14% vs. 56.5% of HL), pectoral fin length (19.20% vs. 16.9% of SL), snout length (33.60% vs 32.2% of HL), and body depth (18.37% vs

15.5% of SL), caudal peduncle depth (11.16% vs 12.3% of SL). Several morphometrics (lengths of mandible, predorsal, preanal, second dorsal fin, and ventral fin) that previously not reported in its original description were examined in this study (see Description). Indonesian specimen could not be compared with the Vietnam specimen because the Vietnam specimen was not mentioned in detail regarding its morphometric measurements or meristic counts.

Preserved coloration. Based on a single specimen preserved in 70% alcohol, a dark brown dorsal head covers the entire surface of the scalp perfectly from the snout to the nape. Towards the ventral side, the dark brown fades and is incompletely distributed, resulting in an irregular pattern of spots around the eyes, cheeks, and operculum; the dark brown continues to fade ventrally, leaving small spots on the ventral 1/3 of the head. Dark brown centre upper lip then fades towards the lower side lip to leave small spots. The ventral head is perfectly white, and the chin is purplish (Figure 2a). Deep purple iris, outer edge of iris mottled purple-black, white pupil.

The dark brown dorsal body extends from the nape to the base of the tail. Ventrally, the dark brown is undistributed and does not completely cover the body, resulting in a pattern of light brown short vertical bars on the lateral body. The light brown short vertical bars number about 24 to 25, forming a ladder-like pattern, extending from the operculum to the base of the tail; some verticals are straight, crooked, and some are wavy. Some ends of the light brown short vertical bars are fused to each other in the centre of the bar, some ends are fused together in the ventral region, and some are separated from each other. At the ends of the vertical bars towards the abdomen and ventral region, the light brown colour fades, leaving small light brown spots along the sides of the body.

Figure 1. Preserved *Bostrychus scalaris* specimen, MZB.26591, 103.6 mm SL, collected from Banyuasin Regency, South Sumatra Province, Indonesia.

The base of pectoral fin light brown; near base of the fin, a short brown bar running parallel from the first to the last pectoral ray, producing 2 transverse, curved bands. Tip fin wide, blackish-brown band. The first dorsal fin mostly folded down, pale white base and with brownish tip. Second dorsal fin base white, purple-black patches alternating vertically with white; blackish dorsal fin tip. The first dorsal fin to the last dorsal soft ray purple-black produces a pattern of 4 horizontally aligned purple-black bands. Anal fin pale yellowish-white; two pale purple, thin, horizontally transverse bands; tip purplish with a narrow, pale white band just on the outer edge. Base of the upper lateral caudal fin, 2 mm diameter black spot, surrounded by a circular light brown; five dark brown bands, vertically curved and irregular. Tip of the outermost area black.
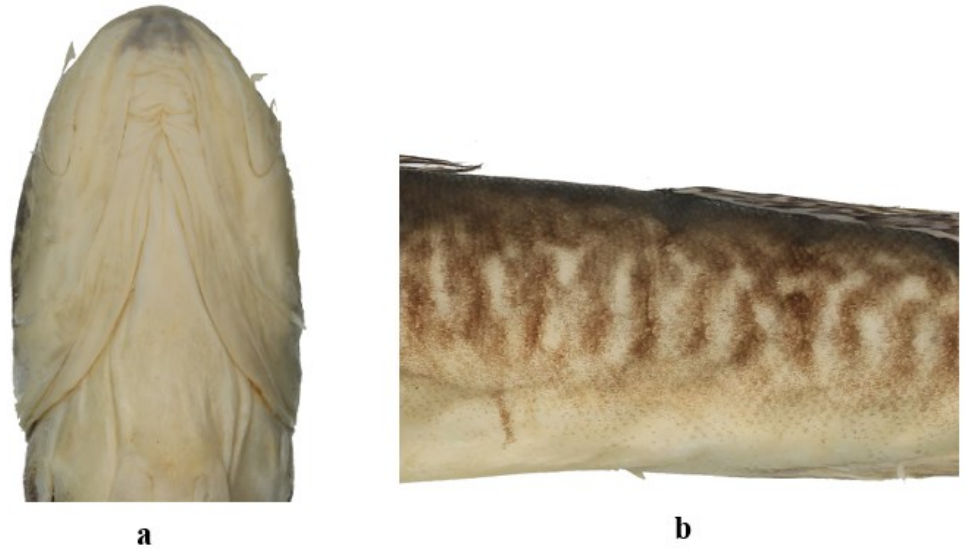
Figure 2. Enlargement of the body part of *B. scalaris* showing: **a)** pattern of folds on the ventral part of the head, **b)** a ladder-like pattern in the body, as one of the distinguishing characters.

The Indonesian specimen was not documented when it was fresh or alive, however, the colour of preserved specimen apparently did not differ much from the colour when it was still alive. All dark markings in the fin rays, dark spot in the dorsal base of caudal fin, and ladder-like pattern of dark bars a long side of the body in the live individual are still retained in the preserved specimen (see Larson 2008: Figure 1-2). At that time, Indonesian specimen was immediately tissue harvested for DNA analysis and then preserved.

Habitat. A single specimen collected from a small ditch that irrigated the oil palm plantation area (Figure 3). Measuring width of the ditch about 1.5 m and less than 1 m in depth. The riparian vegetation is dominated by shrub vegetation with muddy bottom. The water source in this ditch flows from a mixture of fresh water at the estuary of the Musi River and salt water in the South China Sea which is directly adjacent to the Bangka Islands with a salinity level of 18.5 ppt (Hernawati et al. 2023).

Figure 3. Brackish waters in Banyuasin Regency, South Sumatra, which are the habitat of *Bostrychus scalaris*. Photograph: Rena Tri Hernawati (2020).

The single specimen from Indonesia was collected from brackish waters close to the mouth of the Musi River which borders the salty waters of the South China Sea. These waters flow inland through small ditches into plantations. These conditions are similar to the collection sites in Malaysia and Vietnam which are also brackish waters, but the salinity levels of the collection sites in Malaysia are slightly higher (20 ppt vs. 18.5 ppt in this study), while the collection sites in Vietnam have a lower salinity range than the collection sites in Indonesia and Malaysia (14 ppt - 16.8 ppt) (Larson 2008; Tran et al. 2021). This sampling area is dominated by *Derris* sp. and *Nypa* sp. (Dalimunthe et al. 2022; Hernawati et al. 2023), other species from the Fabacea family dominate in mangrove areas in Sungsang Subdistrict and around Payung Island, South Sumatra (Figure 3), while site collection in Malaysia and Vietnam are dominated by mangrove vegetation (Larson 2008; Tran et al. 2021). Site locations in Indonesia are slightly turbid, with slow currents and substrates of soil or mud. This data also emphasises the most suitable ecological niche conditions for *B. scalaris*, namely in brackish water habitats around estuary ecosystems with mangrove vegetation.

Distribution. *Bostrychus scalaris* was previously in Sementa River, near Klang, Selangor State, on the west coast of peninsular Malaysia (Larson 2008; Kottelat 2013; Huang et al. 2014; Parenti 2021); in Singapore based on scientific watercolour paintings illustrated by French naturalist F. L. de Castelnau in 1858–1862 (Loneux 2006; Larson et al. 2016); and in the mangrove habitat at the mouth of the Mekong River in Cu Lao Dung Province, Vietnam (Tran et al. 2021; Taki et al. 2021) (Figure 4). The present specimen from South Sumatra represent the first record of *B. scalaris* in Indonesian water and the southernmost record of this species.
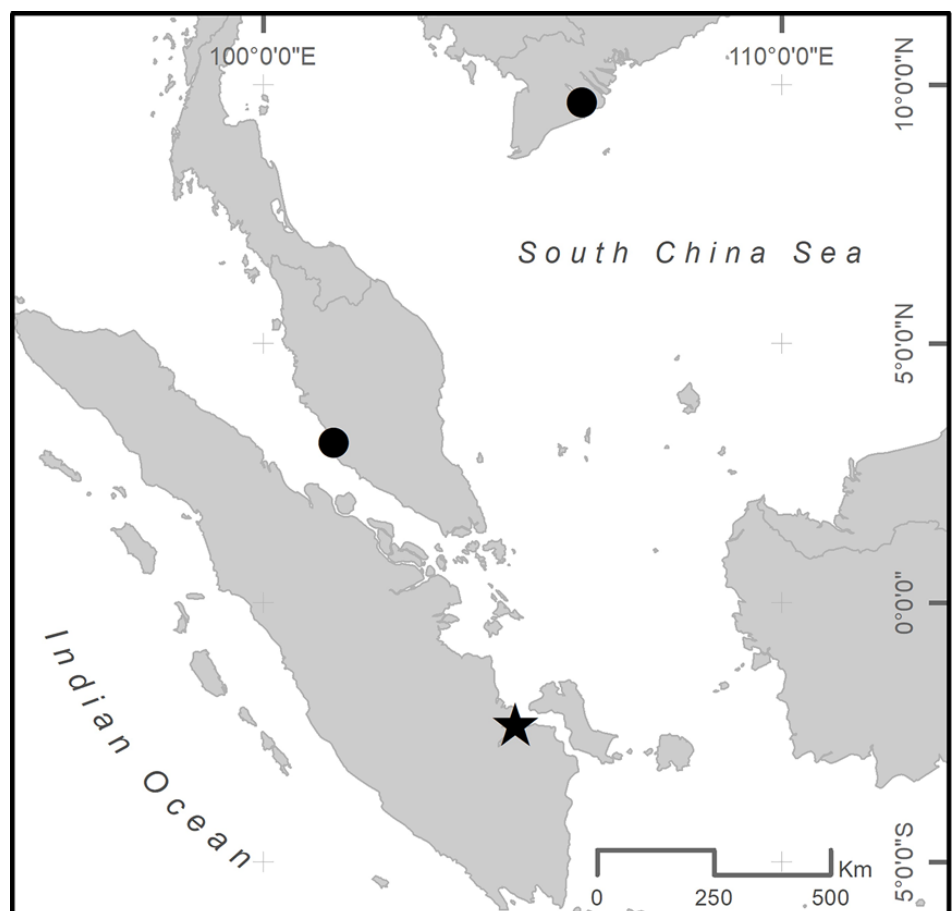
Figure 4. *Bostrychus scalaris* distribution records based on previous studies (circles) and new records based on recent studies (star).

This species almost found in a relatively small number of individuals at each site, especially scientific reports from Malaysia and Indonesia which indicate a solitary species in its distribution. Another assumption leads to a low reproductive rate which causes its distribution to be less abundant, especially in its juvenile phase. Therefore, further research is essential to prove these assumptions. It is also important to develop an on-site conservation strategy to prevent potential damage to natural habitats, considering that the reported distribution of this species in Indonesia is only in brackish waters in plantations which are very vulnerable to degradation and damage due to land use change. This is also to prevent habitat destruction as happened in Malaysia, where it was reported that the holotype's natural habitat had been reclaimed (Larson 2008)

The present record of *Bostrychus scalaris* in Indonesian waters confirms the geographic distribution of this species in the Indo-West Pacific, especially in the South China Sea. In addition, this record of *B. scalaris* in South Sumatra also completes the distribution records of four species of *Bostrychus* in the Indonesian water after i.e., of *B. aruensis* in the Aru Islands, *B. strigogenys* in Papua, *B. microphthalmos*, and most recently, *B. scalaris* in South Sumatra (Nichols 1937; Allen 1991; Hoese & Kottelat 2005).

Bostrychus scalaris does not yet have a protection status from either the IUCN Red List or CITES. The small number of individuals and its limited natural distribution means that data and information on the species is still lacking. Further assessment is really important to determine its protection status immediately and to evaluate its population trends in nature, followed by the preparation of further management strategies. In terms of potential utilisation, the unique body colour of with a brownish staircase pattern along its body give an attractive value of this species as an ornamental aquarium fish.

A partial mitochondrial DNA sequence of the Cytochrome C Oxidase Subunit I (COI) gene of approximately 686 bp was obtained from this sample. Currently, the reference sequence of *B. scalaris* is not available in several GenBanks such as NCBI or BOLD SYSTEM. Uploading the COI sequence of *B. scalaris* from the results of this study in GenBank will be the first time so that it can be used as a reference for future research. The nucleotide BLAST results showed that the sequence of *B. scalaris* was different from the sequences of *B. sinensis* and *B. zonatus*, but it was more similar to *Oxyeleotris marmorata*. This is due to the limited reference sequences of *B. scalaris*, both its partial mtDNA and full genome mtDNA. Details of BLAST similarity values with *O. marmorata* results are maximum score 662, total score 662, query coverage 93%, E value 0, and percent identity 85.78%. Further research using molecular approaches is important, including to determine the phylogenetic position of *B. scalaris* with other species of the genus *Bostrychus*.

AUTHORS CONTRIBUTION

R. designed the study, collected the specimens, and wrote the original draft. G.W. collected and analysed the morphometric and meristic data, KW documented the specimens, reviewed, and edited the manuscript. All authors have read and approved the final version of the manuscript.

(Directorate of Scientific Collection Management-BRIN), who has assisted in providing catalog number for specimen. This research was funded by LIPI (Currently the National Research and Innovation Agency).

CONFLICT OF INTEREST

The authors declare they have no conflict of interest relating to the study.

REFERENCES

Allen, G.R., 1991. *Field guide to the freshwater fishes of New Guinea*, Madang, Papua New Guinea: Christensen Research Institute.

Dalimunthe, S.H. et al., 2022. Species Diversity and Conservation Status of Mangroves in Payung Island, South Sumatra, Indonesia. *Bul. Plasma Nutfah*, 28(1), pp.13–24. doi: 10.21082/blpn.v28n1.2022.p13 -24.

Hernawati, R.T. et al., 2023. Update on fish community in the mangrove ecosystems of Banyuasin Regency, South Sumatra, Indonesia, with the addition of the first record of the genus *Bostrychus. IOP Conference Series: Earth and Environmental Science*, 1191, 012005. doi: 10.1088/1755-1315/1191/1/012005.

Hoese, D.F. & Kottelat, M., 2005. *Bostrychus microphthalmus*, a new microphthalmic cavefish from Sulawesi (Teleostei: Gobiidae). *Ichthyological Exploration of Freshwaters*, 16(2), pp.183-191.

Huang, S.P. et al., 2013. An annotated checklist of gobioid fishes from the mangrove estuary of Matang, Malay Peninsula, with comments on a new *Pseudogobius* (Teleostei: Gobiidae) species. *Journal of Marine Science and Technology*, 21, pp.106-116. doi: 10.6119/JMST-013-1219-8.

Kottelat, M., 2013. The Fishes of The Inland Waters of Southeast Asia: A Catalogue and Core Bibliography of The Fishes Known to Occur in Freshwaters, Mangroves and Estuaries. *Raffles Bulletin of Zoology*, 27, pp.1-663.

Larson, H.K., 2008. A new species of the gudgeon Bostrychus (Teleostei: Gobioidei Eleotridae), from peninsular Malaysia. *The Beagle: Records of the Museums and Art Galleries of the Northern Territory*, 24, pp.147–150. doi: 10.3316/informit.102769078693983.

Larson, H.K. et al., 2016. An updated checklist of the gobioid fishes of Singapore. *Raffles Bulletin of Zoology*, 34, pp.744–757.

Loneux. M., 2006. The Castelnau's fish collection and watercolour notebooks. *Proceedings of the 3rd GBIF Science Symposium - Tropical Biodiversity: Science, Data, Conservation*, pp.91-94.

Miller, P.J & Wongrat, P., 1991. Eleotridae. In *Checklist of the Fishes of the Eastern tropical Atlantic*, 2, pp.952-957.

Nichols, J.T., 1937. Results of the Archbold expeditions. No. 15. A new fish of the genus *Bostrychus* from New Guinea. *American Museum Novitates*, 922, pp.1-2.

Parenti, P., 2021. A checklist of the gobioid fishes of the world (Percomorpha: Gobiiformes). *Iranian Journal of Ichthyology*, 8, pp.1-480. doi: 10.22034/iji.v8i0.556.

Taki, Y. et al., 2021. *Fishes of the Indochinese Mekong*, Tokyo, Japan: Nagao Natural Environment Foundation, pp.1-546.

Tran, D.D. et al., 2021. Fish species composition variability in cu Lao dung, Soc Trang, Vietnam. *Aquaculture, Aquarium, Conservation & Legislation*, 14(4), pp.1865-1876.

Short Communications

The First Record of an Hourglass Toad (*Leptophryne borbonica*) in The Core Zone of Bromo Tengger Semeru National Park and Its Ecological Aspects

Berry Fakhry Hanifa[1]*****, **Muhamad Aslam Fadhilah**[1], **Sandra Rafika Devi**[2], **Muhammad Asmuni Hasyim**[1], **Luhur Septiadi**[3]

1) Biology Study Program. Faculty of Science and Technology, Universitas Islam Negeri Maulana Malik Ibrahim Malang, Malang, East Java 65144, Indonesia
2) Faculty of Biology, Universitas Gadjah Mada, D.I. Yogyakarta 55281, Indonesia
3) Wildlife Conservation Society – Indonesia Program, Bogor, West Java 16128, Indonesia
* Corresponding author, email: berryfhanifa@uin-malang.ac.id

ABSTRACT

Leptophryne borbonica is an amphibian species known for its sensitivity to environmental changes. Within the expansive Bromo Tengger Semeru National Park (TNBTS), new occurrences of *L. borbonica* have been discovered for the second time in another region of TNBTS (core area in Ireng-Ireng Block, Lumajang). This research provides the newest finding of *L. borbonica* and insights into the habitat assessment and potential food preferences of *L. borbonica* within TNBTS. The methodology involved the examination of morphology and meristics in *L. borbonica*. Habitat assessment and potential food indicated stable values. However, continued vigilance is essential due to vulnerability to volcanic threats.

The Bromo Tengger Semeru Mountains area is a natural preserve that maintains its biodiversity, yet it needs comprehensive data on its animal population, especially amphibians. This circumstance presents a significant opportunity to explore and comprehend the diversity within the TNBTS and its surrounding areas (BBTNBTS 2010). TNBTS holds many mysteries and lacks of data, particularly in the case of reptiles and amphibians (Septiadi et al. 2023a). A species of amphibian was recently discovered as a new distribution record while our team explored the core zone (Blok Ireng-Ireng), namely *Leptophryne borbonica* (Astriyantika et al. 2014).

The *Leptophryne* genus has three species: *L. cruentata*, *L. javanica*, and *L. borbonica*. *L cruentata* is only distributed in West Java and Central Java (Mumpuni 2001). Hence, it is in the Critically Endangered conservation status (IUCN SSC Amphibian Specialist Group 2019). The bleeding toad is now included in the IUCN Red List as Critically Endangered (Kusrini et al. 2019). At the same time, *L. javanica* was discovered in 2018 and is strictly distributed in West Java and Central Java.

The discovery of new *Leptophryne* populations continued in 2019 when our team found two *L. borbonica* populations in East Java, to be precise in the Coban Cinde and Coban Siuk natural tourism areas, Malang

district (Erfanda et al. 2019). This discovery was the latest finding on the distribution of the easternmost *L. borbonica* species on Java Island at that time. Furthermore, we later found a new population in the core area of TNBTS, East Java, which we are still studying. We also found significant differences in morphometrics and webbing formulas in the three East Java populations. From this information, it can be concluded temporarily that the potential presence of *L. borbonica* is still very high, especially on Java Island, and several findings indicate significant morphological differences. Coupled with *L. borbonica* found on the islands of Sumatra and Kalimantan, whose identity remains unclear (Chan & Grismer 2019; Hamidy et al. 2019). Thus, this species must be studied more deeply.

L. borbonica (Tschudi, 1838), or the hourglass toad, is a relatively small toad with an hourglass pattern on its dorsal part (Ardiansyah et al. 2014). In research on the distribution of hourglass toads in the East Java region of the Tengger Mountains, the results showed that information related to isolated *L. borbonica* populations is very vulnerable to ecological disturbances, future ecotourism development, infectious diseases, population loss, and local extinction (Erfanda et al. 2019). Therefore, it is fascinating to conduct further research regarding vegetation assessment and potential food preferences in different populations within the same type of mountain.

Research on amphibian diversity has predominantly focused on unveiling cryptic species. At the same time, investigations into other facets of biodiversity, such as habitat assessment and potential food, have progressed slowly and received limited attention (Iskandar 2020). However, it is essential to note that amphibians worldwide encounter a series of direct threats to their long-term survival (Stuart et al. 2008). They are considered more endangered and experiencing more rapid population declines than birds and mammals, necessitating urgent global conservation efforts. Many amphibians in Java inhabit specific micro-habitats, lack reported life histories, are highly sensitive to environmental changes, and are susceptible to local extinction (Cahyadi & Arifin 2019).

Consequently, long-term monitoring is essential to ensure the sustainability of their populations (Storfer 2003). Given the need for more information, conducting a population ecology study focusing on habitat assessment and potential food preferences of *L borbonica* in TNBTS is imperative. Thus, we aim to record the new distribution of *L. borbonica* in the core zone of TNBTS and to provide the habitat assessment and potential food preference.

This research was conducted from February to March 2022 by collecting specimens of *L. borbonica* downstream of the Ireng-Ireng River, located within SPTN Region III of Bromo Tengger Semeru National Park, Senduro District, Lumajang, East Java Province (BBTNBTS 2010) at coordinates 8°06'08"S and 113°04'39"E, has an elevation of 1,200 m.a.s.l (Figure 1).

L. borbonica sampling using a virtual encounter survey. A total of 45 individuals, consisting of 36 males and nine females, were collected, recorded, and stored for preservation with alcohol 70% (Matsui 1984). Specimens were selected from one adult male and one adult female (SVL: >20 mm). Morphometric data were measured using digital calipers, following the methods described by Hamidy et al. (2018) and Watters et al. (2016). Measurement results were digitally recorded using the Procreate software.

Data collection related to habitat assessment involved observing vegetation from the Ireng-Ireng River to the bridge (200-300 meters) through purposive sampling survey activities. Exploratory data collec-

tion techniques were employed, including direct exploration and documentation methods. The researcher aimed to gather comprehensive information about the plant species at each observation location (Arini & Kinho 2012; Andries et al. 2022).
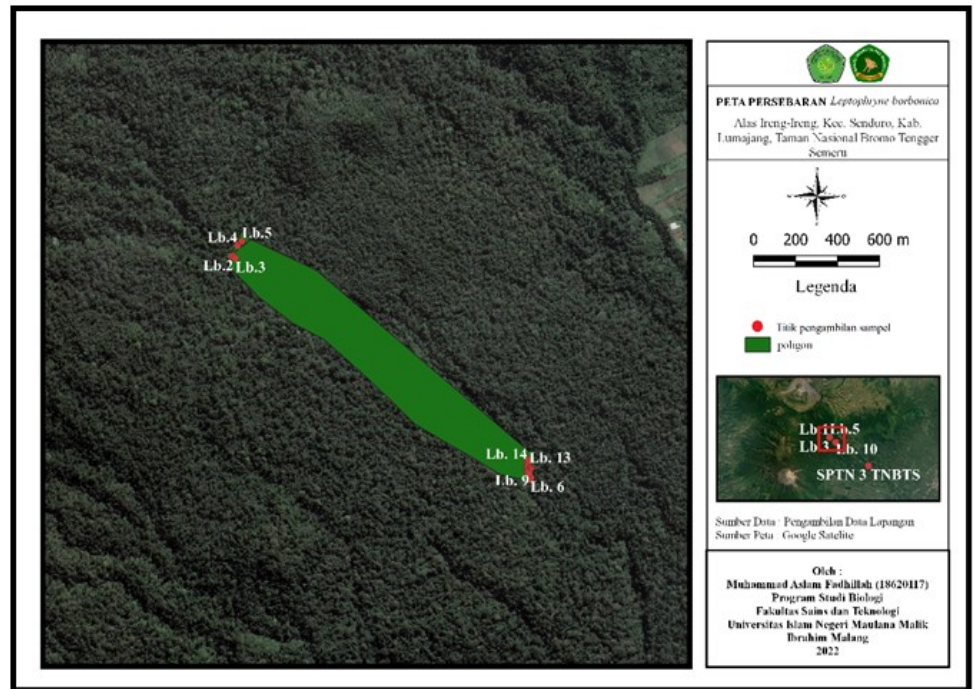
Figure 1. Location of the Ireng-Ireng Block (projected by QGIS Desktop 3.36.3).
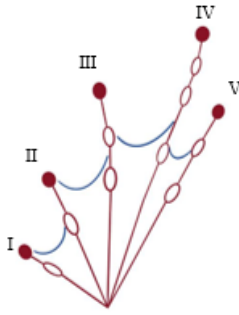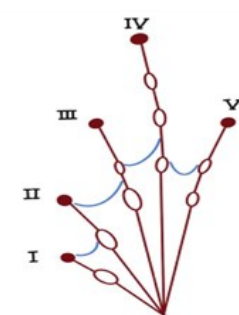
Data collection regarding potential food was accomplished using insect traps (Pitfall Traps) and hand sorting. Pitfall traps were used to capture ground-surface insects (Southwood & Henderson 2009). Fifteen plots, spaced 10 meters apart and divided into three sets with three repetitions, were used to install Pitfall traps. Subsequently, the collected samples underwent initial hand sorting.

Morphologically, *L. borbonica*) in the Ireng-Ireng, TNBTS exhibits several distinctive characteristics. These include a slender body structure with a Snout-Vent Length (SVL) ranging from 20 to 26 mm in males and 30 to 40 mm in females. The dorsal aspect features a black triangular mark with a rough skin texture and black spots on a light brown body, as depicted in Table 1 (A) and (B). The tympanum is not visible, and the snout protrudes upwards. The orbital region displays a horizontal pupil, while the supra labial region showcases black and white striped motifs and faint parathyroid glands, as shown in Table 1(C). The skin from the cloaca to the supra-orbital region appears rough and wrinkled. The ventral portion is predominantly white, with black markings on the sublabial region (Table 1(D)). The dorsal surface of the femur displays brown colouring with black spots, transitioning to red from the femur to the ventral tibia. The digits of the hand terminate in rounded, lumpy tubercles, as depicted in Table 1 (E), while the metatarsals of the legs appear red. The swimming membrane spans 5 mm on each digit and features black tubercles. Some fresh specimens showed greenish coloration in the dorsum area (Table 1 (F)).

Meristically, *L. borbonica* in the Ireng-Ireng Block of TNBTS exhibits distinct leg webbing patterns (Table 1), which vary between male and female specimens. For male samples from the Ireng-Ireng River population, the membrane formula/webbing formula yielded the following results: (I 0-1 II 0-2½ III 2-2½ IV 3½-1 V) when considering the outer to

inner digits. On the other hand, female samples from the Ireng-Ireng River population exhibited the following webbing formula: (I 0-1 II 0-2½ III 2-2½ IV 3½-1 V).

Table 1. The morphology of the *L. borbonica* in the Ireng-Ireng, TNBTS.

Webbing formula	Documentation	Sex
		Male (I 0-1 II 0-2½ III 2-2½ IV 3½-1 V).
		Female (I 0-1 II 0-2½ III 2-2½ IV 3½-1 V).

Sample documentation of *Leptophyne borbonica*	
	A & B. Dorsum C. Lateral view of the head D ventral views E. left hindlimb F. left forelimb

Based on the information provided above, most morphological characteristics align with the description of *L. borbonica*, as documented by Inger and Stuebing (2005), Erfanda et al. (2019), and Hamidy et al. (2018), hourglass toads are typically tiny, with males having a snout-vent length (SVL) of approximately 23.5 mm and an average SVL of 26.10 mm for the species. They exhibit a slender body habitus characterised by long forelegs and short hind legs, with no discernible bone crest. The snout protrudes slightly above the mouth in profile, and the tip digits are rounded rather than expanded. Parathyroid glands are indistinct, and a distinctive black hourglass mark is on the dorsum. Tympanum and a median singular vocal sac with a vocal slit are evident in males. The skin exhibits a wrinkled texture, covering all body regions, including the forefoot and hindfoot dorsal surface, while the supratympanic fold is notably

absent. In terms of coloration, they feature a mottled brown back adorned with black spots on the head, back, and limbs. The groin and ventral surfaces of the fore and hind legs display a reddish hue, with reddish webbing on the back and belly. The abdomen typically exhibits a brownish hue with black and white markings. The chest and throat are blackish, and the limbs bear a distinct black line on the back and a black line on the upper lip. A netted black pattern marks their golden iris. Notably, there is no black triangle marking behind the eye, in contrast to the observations made by Iskandar (1998), who reported black triangles on several specimens from different regions. When compared with Alhadi et al. (2021), differences were found in the snout, which was short and tapered, and the tympanum was oval.

Based on the results of environmental factor measurements during the research (Table 2), the air temperature at the research location ranged from 21.8-24.5°C, humidity levels at 93-94%. Amphibians exhibit a wide temperature tolerance range. They can inhabit temperatures ranging from 0-40°C (Stebbins & Cohen 2021). Meanwhile, species from the same genus, namely *L javanica*, are typically found in environments with temperatures ranging from 15-19.3°C and water temperatures of 16°-18.7°C. Biologically, water temperature affects metabolism, growth, behaviour, interspecific competition, susceptibility to disease, and organism mortality (Coutant 1999). Physically, it can impact the concentration of dissolved gases (Beschta et al. 1987). *L. borbonica*, is not considered an actual aquatic toad and spends most of its life near water bodies, slow-flowing rivers (Iskandar 1998).

Table 2. Habitat Parameters of research locations in the Ireng-Ireng, TNBTS.

Repetition	Physical Parameters	
	Temperature	Humidity
Upstream	21.8°C	93 %
Downstream	24.5°C	94 %

A positive correlation exists between the abundance of *L. borbonica* and temperature, albeit weak. Amphibians exhibit specific temperature tolerances and tend to occupy habitats within ranges that support their survival (Freda & Dunson 1986). Anurans, in particular, require higher humidity levels compared to reptiles and other terrestrial animals (Ludwig 1945). Amphibians possess permeable skin that must remain moist, making some anuran species highly dependent on aquatic habitats for survival (Becker et al. 2007; Silva et al. 2014; Hidayah et al. 2018; Devi et al. 2019). It also plays a vital role in anuran communication, thereby contributing to the success of their reproductive processes (Duellman & Trueb 1994; Oseen & Wassersug 2002; Wong et al. 2004).

Besides directly affecting *L. borbonica*, physical factors also influence the vegetation near its habitats. This research also documented the types of vegetation thriving in areas where *L. borbonica* was encountered. It is significant, given that vegetation is crucial in providing shelter for *L. borbonica*, protecting them from predators and UV radiation, and serving as a food source. The protection offered by forest canopy cover also has repercussions for aquatic microhabitats (Paul & Gwynn-Jones 2003). The vegetation identified in this study was riparian vegetation, which typically grows alongside water bodies. Riparian was established that the riverside zone is a refuge for biodiversity and productivity, making it pivotal in land resource and wildlife management. In addition, riverine forest canopies play a crucial role in conserving amphibian diversity, partic-

ularly for species specialised in forest habitats (Lemckert 1999; Skelly et al. 2002; Popescu et al. 2012; Provete et al. 2014; Lipinski et al. 2016). Hence, forest vegetation structure is considered a key indicator of biodiversity (Guo et al. 2017), and the present research established a relevant noteworthy correlation.

Vegetation found in the *L. borbonica* encounter area in the Ireng-Ireng, TNBTS (Figure 2), some of the identified vegetation species included: a) *Ageratum conyzoides* b) *Ageratina riparia* c) *Begonia formosana* d) *Dryopteris filix-mas* e) *Homalomena* sp. f) *Impatiens hawkeri* g) *Mallotus barbatus* h) *Mitragyna speciosa* i) *Pilea melastomoides* j) *Plantago major* k) *Schismatoglottis asperata* i) *Selaginella mayeri*. Some *L. borbonica* are often found attached to low-lying leaves near rivers. In contrast, others are located on the soil surface or rocks near watercourses, and some even inhabit the watercourses themselves (Iskandar 1998). *L. borbonica* primarily selects rocks and leaves as substrates for its activities. Many anuran species commonly use substrate as camouflage to deceive predators, preferring those with similar colours to their bodies.

Figure 2. Vegetation found in the *L. borbonica* encounter area in the Ireng-Ireng, TNBTS: a) *Ageratum conyzoides* b) *Ageratina riparia* c) *Begonia formosana* d) *Dryopteris filix-mas* e) *Homalomena* sp. f) *Impatiens hawkeri* g) *Mallotus barbatus* h) *Mitragyna speciosa* i) *Pilea melastomoides* j) *Plantago major* k) *Schismatoglottis asperata* i) *Selaginella mayeri*.

L. borbonica is not an actual semi-aquatic toad. However, most of these toads are known to spend their entire lives around water areas (Figure 3). This toad is often found around clear, fast-flowing rivers, and indicates soil fertility (Iskandar 1998; Kusrini 2013). It often attached to short herbaceous leaves around rivers; others are found on the surface of soil or rocks around water flows.

The availability of food sources is one factor that determines a species' survival in nature. *Leptophryne*, an insectivorous animal, feeds primarily on small arthropods from the Order Hymenoptera, such as Formicidae and Pheidole (Kusrini et al. 2007). Observation data on *L. borbonica*'s food availability in the TNBTS indicated criteria similar to those

obtained using pitfall and hand-sorting methods. In the pitfall method, 491 arthropods were collected (Table 3), resulting in a diversity index of 1.447, a species evenness index of 0.1932 (in the low category), and a medium species richness index of 3.389. Meanwhile, the hand-sorting method yielded 88 types of arthropods, with a diversity index of 2.039, a medium evenness index of 0.5485, and a medium richness index of 2.904.

Figure 3. Habitat type of *Leptophryne borbonica* in Ireng-Ireng, TNBTS: a) semi-aquatic habitat b) aquatic habitat (Photographed by Muhamad Aslam Fadhillah).

Amphibian diversity is related to environmental conditions because amphibians are very sensitive to environmental changes (Tanjung et al. 2023). Amphibians also play an important role in the food chain, both as predators and prey (Hocking & Babbit 2014; Kanagavel et al. 2017; Carlsson & Tyden 2018; Priambodo et al. 2019). Amphibian responses to the environment are also different for each species. Habitat heterogeneity can influence amphibian richness (Luja et al. 2017). However, habitat heterogeneity can be disturbed due to habitat degradation, natural disasters and anthropogenic activities (Badillo-Saldaña et al. 2016; Berriozabal-Islas et al. 2018). Therefore, monitoring the population must remain a priority (Gillespie et al. 2015)

The greater the diversity, richness, and evenness of ground surface insect species in a given land area, the more stable the forest ecosystem. Dominant orders in the pitfall trap method included Entomobryomorpha (228 individuals), Amphipoda (180 individuals), Orthoptera (27 individuals), and Hymenoptera (27 individuals). In the hand-sorting method, dominant orders included Amphipoda (40 individuals) and Hymenoptera (17 individuals). However, amphibians selectively choose their food based on the available options within their habitat niche. Hence, they can differentiate between different types of prey (Freed 1982). Food preference in amphibians is often linked to their morphology, physiological characteristics, and behaviour (Solé & Rödder 2010). Food availability, particularly from the orders Hymenoptera and Orthoptera, is crucial for maintaining the presence of *L. borbonica* in this niche. Research *on L. cruentata* suggests that their diet predominantly comprises Hymenoptera (ants) at 60.38% and Orthoptera at 6.60% (Freed 1982). It is worth noting that most members of the Hymenoptera order are active explorers, both aerial and terrestrial (Silva et al. 2014; Jaapar et al. 2018).

Among the three *Leptophryne* species in Indonesia (*L. borbonica, cruentata, L. javanica*), *L. borbonica* is considered the species of least concern by the IUCN because of its wide distribution (Cahyadi & Arifin 2019; IUCN SSC Amphibian Specialist Group 2019). In fact, as a small amphibian inhabiting the Java region, land use changes and deforestation very quickly. This species is also threatened by anthropological and volcanic activity (Erfanda et al. 2019; Septiadi et al. 2023b). The threat of infection

by the fungus *Batrachochytrium dendrobatidis* (Bd) can also be a threat to this type because, in West Java, cases of this fungus have been found to have infected several amphibians (Kusrini et al. 2008).

Table 3. Arthropod as potential food preference for *L. borbonica* in TNBTS.

Index	Metode	
	Pitfall	Hand Sorted
Total	491	88
Shannon Wiener	1.447	2.039
Evenness	0.1932	0.5485
Margalef	3.389	2.904

Pitfall Method		
Ordo	**Family**	**Total**
Araneae	Gnaposidae	3
	Pholcidae	1
Entomobryomorpha	Entomobryidae	228
Amphipoda	Talitridae	180
Coleoptera	Curculionidae	2
	Staphylinidae	3
	Nitidulidae	1
Orthoptera	Gryllidae	27
Blattodea	Corydiidae	1
Poduromorpha	Hypogastruridae	2
Hemiptera	Miridae	10
	Cicadellidae	3
Mesostigmata	Arasitidae	3
Hymenoptera	Formicidae	27
Total		**491**

Hand Sorted Method		
Araneae	Gnaposidae	7
Orthoptera	Acrididae	4
Entomobyorpha	Entomobryidae	3
Amphipoda	Talitridae	40
Coleoptera	Staphylinidae	5
	Scarabaeidae	4
Chilopoda	Scolopendridae	2
Mesostigmata	Arasitidae	3
Hemiptera	Coreidae	3
Hymenoptera	Formicidae	17
Total		**88**

AUTHORS CONTRIBUTION
B.F.H., M.A.H., and L.S. contributed concepts, ideas, research funds, and research equipment, MAF collected data, data preservation, and analysis, and SRD collected data, and wrote the original draft.

CONFLICT OF INTEREST
All authors declare no conflict of interests.

REFERENCES

Alhadi, F. et al., 2021. *Amfibi Pulau Jawa: Panduan Bergambar dan Identifikasi*, Perkumpulan Amfibi Reptil Sumatera.

Andries, A.E., Koneri, R. & Maabuat, P.V., 2022. Inventarisasi Tumbuhan Paku di Ruang Terbuka Hijau Kampus Universitas Sam Ratulangi Manado, Sulawesi Utara. *Jurnal Bios Logos.*, 12(2),pp.140-148. doi: 10.35799/jbl.v12i2.42343.

Ardiansyah, D. et al., 2014. Kelimpahan Kodok Jam Pasir *Leptophryne borbonica* di Sepanjang Aliran Sungai Cisuren, Bodogol, Taman Nasional Gunung Gede Pangrango. *Bioma*, 10(2), pp.11-18. doi: 10.21009/bioma10(2).2.

Arini, D.I.D. & Kinho, J., 2012. Keragaman Jenis Tumbuhan Paku di Cagar Alam Gunung Ambang Sulawesi Utara. *Info BPK Manado*, 2(1), pp.17- 40.

Astriyantika, M., Aried, H. & Sunarminto, T., 2014. Studi Konservasi Sumberdaya Alam Hayati Pada Masyarakat Tengger Di Resort Ranu Pani, Taman Nasional Bromo Tengger Semeru. *Media Konservasi*, 19(1), pp.1–11. doi: 10.29243/medkon.19.1.%p

Badillo-Saldaña, L.M., Ramírez-Bautista, A. & Wilson, L.D., 2016. Effects of establishment of grazing areas on diversity of amphibian communities in tropical evergreen forests and mountain cloud forests of the Sierra Madre Oriental. *Rev Mex Biodivers*, 87(1), pp.133-139. doi: 10.1016/j.rmb.2015.09.019.

BBTNBTS., 2010. *Laporan Inventarisasi Flora Fauna Di Taman Nasional Bromo Tengger Semeru*, Balai Besar Taman Nasional Bromo Tengger Semeru.

Becker, C.G. et al., 2007. Habitat split and the global decline of amphibians. *Science*, 318(5857), pp.1775–1777. doi: 10.1126/science.1149374

Berriozabal-Islas, C. et al., 2018. Modification of landscape as promoter of change in structure and taxonomic diversity of reptile's communities: An example in tropical landscape in the central region of Mexico. *Nat Conserv.* 28, pp.33-49. doi: 10.3897/natureconservation.28.26186

Beschta, R.L. et al., 1987. Stream temperature and aquatic habitat: fisheries and forestry interactions. *Streamside Management: Forestry and Fishery Interactions*, College of Forest Resources, University of Washington.

Cahyadi, G. & Arifin, U., 2019. Potential and challenges on amphibians and reptiles research in West Java. *Jurnal Biodjati*, 4(2), pp.149-162. doi: 10.15575/biodjati.v4i2.4820.

Carlsson, G. & Tydén, E., 2018. Development and evaluation of gene expression biomarkers for chemical pollution in common frog (*Rana temporaria*) tadpoles. *Environ Sci Pollut Res Intl*, 25(33), pp.33131-33139. doi: 10.1007/s11356-018-3260-z.

Chan, K.O. & Grismer, L.L., 2019. To split or not to split? Multilocus phylogeny and molecular species delimitation of southeast Asian toads (family: Bufonidae). *BMC Evolutionary Biology*, 19(1), 95. doi: 10.1186/s12862-019-1422-3.

Coutant, C.C., 1999. *Perspectives on temperature in the Pacific Northwest's fresh waters*, Oak Ridge National Lab.

Devi, S.R. et al., 2019. Struktur Komunitas Ordo Anura di Lokasi Wisata Bedengan Desa Selorejo Kecamatan Dau Kabupaten Malang. *Jurnal Riset Biologi dan Aplikasinya*, 1(2), pp.71-79. doi: 10.26740/jrba.v1n2.p71-79.

Duellman, W.E. & Trueb, L., 1994. *Biology of amphibians*, Johns Hopkins University Press

Erfanda, M.P. et al., 2019. Distribution Record of *Leptophryne borbonica* (Tschudi, 1838) (Anura: Bufonidae) from Malang, East Java: Description, Microhabitat, and Possible Threats. *Journal of Tropical Biodiversity and Biotechnology*, 4(2), pp.82-89. doi: 10.22146/jtbb.45355.

Freda, J. & Dunson, W.A., 1986. Effects of low pH and other chemical variables on the local distribution of amphibians. *Copeia*, 1968(2), pp.454–466. doi: 10.2307/1445003

Freed, A.N., 1982. A treefrog's menu: selection for an evening's meal. *Oecologia*, 53, pp.20–26. doi:10.1007/BF00377131.

Gillespie, G.R. et al., 2015. Responses of tropical forest herpetofauna to moderate anthropogenic disturbance and effects of natural habitat variation in Sulawesi, Indonesia. *Biol Conserv*, 192, pp.161-173. doi: 10.1016/j.biocon.2015.08.034.

Guo, X. et al., 2017. Regional mapping of vegetation structure for biodiversity monitoring using airborne lidar data. *Ecol Inform*, 38, pp.50–61.doi: 10.1016/j.ecoinf.2017.01.005.

Hamidy, A. et al., 2018. Detection of Cryptic taxa in the genus *Leptophryne* (Fitzinger, 1843) (Amphibia; Bufonidae) and the description of a new species from Java, Indonesia. *Zootaxa*, 4450(4), pp.427-44. doi: 10.11646/zootaxa.4450.4.2

Hidayah, A. et al., 2018. Keanekaragaman Herpetofauna di Kawasan Wisata Alam Coban Putri Desa Tlekung Kecamatan Junrejo Kota Batu Jawa Timur. *Prosiding Seminar Nasional Hayati*, 6, pp.79-91. doi: 10.29407/hayati.v6i1.660

Hocking, D.J. & Babbit, K.J., 2014. Amphibian contributions to ecosystem services. *Herpetol Conserv Biol*, 9(1), e86854. doi: 10.1371/journal.pone.0086854.

Inger, R.F. & Stuebing, R.B., 2005. *Field Guide of Borneo Frog*, Natural History Publications.

Iskandar, D.T., 1998, *The Amphibians of Java and Bali*, Research and Development Centre for Biology-LIPI.

Iskandar, D.T., 2020. Tropical biodiversity with special emphasis on characteristic species. *AIP Conference Proceedings*, 2231, 020004. doi: 10.1063/5.0007501

IUCN SSC Amphibian Specialist Group, 2019, '*Leptophryne cruentata*' in *The IUCN Red List of Threatened Species 2019: e.T138045255A3020276,* viewed 1 July 2024 from https://dx.doi.org/10.2305/IUCN.UK.2019-1.RLTS.T138045255A3020276.en

Jaapar, M.F. et al., 2018. Foraging behavior of stingless bee *Heterotrigona itama* (Cockerell, 1918) (Hymenoptera: Apidae: Meliponini). *AIP Conference Proceedings,* 1940, 020037. doi: 10.1063/1.5027952.

Kanagavel, A. et al., 2017. Do frogs really eat cardamom? Understanding the myth of crop damage by amphibians in the Western Ghats, India. *Ambio,* 46, pp.695-705. doi: 10.1007/s13280-017-0908-8.

Kusrini, M.D. et al., 2007. Preliminary study on the distribution and biology of the bleeding toad, *Leptophryne cruentata* Tschudi, 1838. In *Frogs of Gede Pangrango: A Follow up Project for the Conservation of Frogs in West Java Indonesia. Book 1: Main Report.* Technical report submitted to the BP Conservation Programme.

Kusrini, M.D. et al., 2008. Chytridiomycosis in frogs of Mount Gede Pangrango, Indonesia. *Diseases of Aquatic organisms,* 82(3), pp.187–194. doi: 10.3354/dao01981.

Kusrini, M.D., 2013. *Panduan Bergambar Identifikasi Amfibi Jawa barat,* Fakultas Kehutanan IPB dan Direktorat Konservasi Keanekaragaman Hayati.

Kusrini, M.D., Denok, R. & Fitri, A., 2019. *Usulan Perlindungan Kodok Merah,* Konservasi Sumberdaya Hutan & Ekosiwata IPB.

Lemckert, F., 1999. Impacts of selective logging on frogs in a forested area of northern New South Wales. *Biol. Conserv,* 89, pp.321–328. doi: 10.1016/S0006- 3207(98)00117-7.

Lipinski, V.M., Santos, T.G. & Schuch, A.P., 2016. An UV-sensitive anuran species as an indicator of environmental quality of the Southern Atlantic rainforest. *Journal of Photochem Photobiol,* 165, pp.174–181. doi: 10.1016/j.jphotobiol.2016. 10.025.

Ludwig, D., 1945. The effects of atmospheric humidity on animal life. *Physiological Zoology,* 18(2), pp.103–135. doi: 10.1086/physzool.18.2.30151858.

Luja, V.H. et al., 2017. Herpetofauna inside and outside from a natural protected area: The case of Reserva Estatal de la Biósfera Sierra San Juan, Nayarit, Mexico. *Nat Conserv,* 21, pp.15-38. doi: 10.3897/natureconservation.21.12875.

Matsui, M., 1984. Morphometric variation analyses and revision of the Japanese toads (Genus Bufo, Bufonidae), *Contributions from the Biological Laboratory, Kyoto University.*

Mumpuni, M., 2001. Keanekaragaman Herpetofauna di Taman Nasional Gunung Halimun, Jawa Barat. *Berita Biologi,* 5(6), pp.711-720. doi: 10.14203/beritabiologi.v5i6.1078.

Oseen, K.L. & Wassersug, R.J., 2002. Environmental factors influencing calling in sympatric anurans. *Oecologia,* 133(4), pp.616–625. doi: 10.1007/s00442-002-1067-5

Paul, N.D. & Gwynn-Jones, D., 2003. Ecological roles of solar UV radiation: towards an integrated approach. *Trends in Ecology & Evolution,* 18(1), pp.48-55. doi: 10.1016/S0169-5347(02)00014-9

Popescu, V.D., 2012. The role of forest harvesting and subsequent vegetative regrowth in determining patterns of amphibian habitat use. *For. Ecol. Manag.,* 270, pp.163–174. doi: 10.1016/j.foreco.2012. 01.027.

Priambodo, B. et al., 2019. Characteristics of water sources in Malang, based on the diversity, community structure, and the role of herpetofauna as bioindicators. *EurAsian Journal of BiScien*, 13(2), pp.2279 -2283.

Provete, D.B. et al., 2014. Broad-scale spatial patterns of canopy cover and pond morphology affect the structure of a Neotropical amphibian metacommunity. *Hydrobiologia*, 734, pp.69–79. doi: 10.1007/ s10750-014-1870-0.

Septiadi, L. et al., 2023a. Found but forgotten: on the records, misidentification, and potential rediscovery of the rare bromo Tengger Semeru mountain endemic snake (Serpentes: Colubridae*: Tetralepis fruhstorferi*). *Russian Journal of Herpetology*, 30(4), pp.249-254. doi: 10.30906/1026-2296-2023-30-4-249-254

Septiadi, L. et al. 2023b. Preliminary observations on population structure, mating behaviour, and the fig-feeding tadpoles of the Hourglass Toad, *Leptophryne borbonica* (Tschudi, 1838), from Malang, East Java Province, Indonesia. *Herpetology Notes*, 16, pp.813-821.

Silva, A.G. et al., 2014. Foraging distance of Melipona subnitida Ducke (Hymenoptera: Apidae). *Sociobiology*, 61(4), pp.494–501. doi: 10.13102/sociobiology. v61i4.494-501.

Skelly, D.K., Freidenberg, L.K. & Kiesecker, J.M., 2002. Forest canopy and the performance of larval amphibians. *Ecology*, 83, pp.983–992. doi: 10.1890/0012- 9658(2002)083[0983:FCATPO]2.0.CO;2.

Solé, M. & Rödder, D., 2010. Dietary assessments of adult amphibians. In *Amphibian ecology and conservation: a handbook of techniques*. Oxford: Oxford University Press, pp.167-184. doi: 10.1093/ oso/9780199541188.003.0010

Southwood, T.R.E. & Henderson, P.A., 2009. *Ecological methods*, John Wiley & Sons.

Stebbins, R.C. & Cohen, N.W., 2021. *A natural history of amphibians*, Princeton: Princeton University Press.

Storfer, A., 2003. Amphibian declines: future directions. *Diversity and distributions*, 9(2), pp.151-163. doi: 10.1046/j.1472-4642.2003.00014.x

Stuart, S.N et al., 2008. *Threatened amphibians of the world*, Lynx Edicions.

Tanjung, R.D. et al., 2023. Amphibian Community Structure In Isau-Isau Wildlife Reserve, South Sumatra, Indonesia. *Biodiversitas Journal of Biological Diversity*, 24(12), pp.6836-6843. doi: 10.13057/biodiv/ d241244

Watters, J.L. et al., 2016. Review of morphometric measurements used in anuran species descriptions and recommendations for a standardized approach. *Zootaxa*, 4072(4), pp.477–495. doi: 10.11646/ zootaxa.4072.4.6

Wong, B. et al., 2004. Do temperature and social environment interact to affect call rate in frogs (*Crinia signifera*)? *Austral Ecology*, 29(2), pp.209–214. doi: 10.1111/j.1442-9993.2004.tb00312.

Short Communications

Praxelis (Asteraceae: Eupatorieae), A Newly Naturalised Genus for Kalimantan and Sumatra, Indonesia

Muhammad Rifqi Hariri[1,2]*, Arifin Surya Dwipa Irsyam[3], Ria Windi Lestari[4], Peniwidiyanti[5], Lutfi Rahmaningtiyas[6], Rizmoon Nurul Zulkarnaen[7,8], Aulia Hasan Widjaya[8], Saripudin[8], Dian Latifah[8], Ponco Yuliyanto[9], Noviana Budianti[3], Yoyo Suhaya[3], Dian Rosleine[3], Endah Sulistyawati[3]

1) Research Center for Biosystematics and Evolution, National Research and Innovation Agency (BRIN), Jl. Raya Jakarta-Bogor Km. 46, Cibinong, West Java, 16911, Indonesia.
2) Botani Tropika Indonesia Foundation (BOTANIKA), Jl. Seruni No. 25, Loji, Bogor, West Java, 16117, Indonesia.
3) School of Life Sciences and Technology (SITH), Institut Teknologi Bandung (ITB), Jl. Ganesha No. 10, Bandung, West Java, 40132, Indonesia.
4) Study Program of Biology, Faculty of Mathematics and Life Sciences, Universitas Palangka Raya, Jl. Yos Sudarso, Palangka Raya, 27111, Indonesia.
5) Research Center for Ecology and Ethnobiology, National Research and Innovation Agency (BRIN), Jl. Raya Jakarta-Bogor Km. 46, Cibinong, West Java, 16911, Indonesia.
6) Directorate of Scientific Collection Management, National Research and Innovation Agency (BRIN), Jl. Raya Jakarta-Bogor Km. 46, Cibinong, West Java, 16911, Indonesia.
7) Environmental and Life Science Department, Faculty of Science, University Brunei Darussalam, BE1410, Brunei Darussalam
8) Research Center for Applied Botany, National Research and Innovation Agency (BRIN), Jl. Raya Jakarta-Bogor Km. 46, Cibinong, West Java, 16911, Indonesia.
9) Research Center for Food Technology and Processing, National Research and Innovation Agency (BRIN), Jln. Yogya-Wonosari Km. 3, Yogyakarta, 55861, Indonesia.
* Corresponding author, email: muhammadrifqihariri@gmail.com

ABSTRACT

The southern American genus *Praxelis* Cass. has 18 species. In Singapore and Indonesia, notably Java, *P. clematidea* R.M.King & H.Rob. has naturalised. The first record in Indonesia was in Bogor in 2018, although it is unverified elsewhere. *Praxelis clematidea* was found in Bangka, Belitung, Jambi, Lampung, and Palangka Raya during our exploratory field research in 2020–2023. The naturalised populations proliferate in roadsides, ditches, open spaces, and disturbed areas. It thrives in a small swampy peat environment in Palangka Raya. *Praxelis clematidea* has been found outside Java, suggesting it could become an invasive alien species in Kalimantan and Sumatra.

Asteraceae is one of the largest groups of Angiosperm families, with 1701 genera distributed worldwide except in Antarctica (Funk et al. 2007). As many as 150 genera are found in Malesia, and 70 are naturalised genera (van Steenis 1987; Holmes et al. 2023). The Asteraceae family still has to be revised for the Flora Malesiana. Furthermore, many newly recorded alien species of Asteraceae were reported in Malesia within the past eight years, such as Singapore (Chen et al. 2018) and Java (Irsyam & Hariri 2016; Tjitrosoedirjo & Wahyuni 2018; Irsyam & Irwanto 2019; Irsyam et al. 2020a; Irsyam et al. 2020b; Al Anshori et al. 2022). These findings imply that further taxonomic research on newly discovered

Asteraceae is required to update and improve the knowledge of the Asteraceae of Malesia.

Praxelis Cass is a group of Eupatorieae that is primarily found in South America and comprises 20 species (King & Robinson 1987). Taxonomically, *Praxelis* was previously placed under the *Eupatorium* sect. *Praxelis* (Cass.) Benth. ex Baker, but King and Robinson (1970) reinstated it at the generic level. The genus *Praxelis* is recognised by its caducous involucral bracts, conical receptacle, lack of paleae, the inner surface of corolla lobes with dense papillose hairs, baluster form anther collars, obcompressed achene, asymmetrical carpopodia, and pappus composed of many capillary bristles (King & Robinson 1970; King & Robinson 1987; Hind & Robinson 2007; Grossi et al. 2020).

According to previous studies, only one species of *Praxelis* occurred in Malesia, namely *P. clematidea* (Hieron. ex Kuntze) R.M.King & H.Rob. The species have been naturalised in Singapore and Java (Chen et al. 2018; Tjitrosoedirdjo & Wahyuni 2018). During our field studies from 2020 to 2023, the spontaneous populations of *P. clematidea* were collected in Kalimantan (Central Kalimantan) and Sumatra (Bangka Belitung Islands, Jambi, Lampung, and South Sumatra). The species is considered new to Kalimantan and Sumatra. Hence, this study aimed to report the presence of *Praxelis* in Kalimantan and Sumatra as part of a database update for the Asteraceae of Malesia, particularly Indonesia. Moreover, discovering new alien species and assessing their naturalisation status are essential for their proper management.

This work is based on five field botanical surveys in Kalimantan (Central Kalimantan) and Sumatra (Bangka Belitung Islands, Jambi, Lampung, and South Sumatra) from 2020 to 2023. The field surveys were conducted following the free exploring method (Rugayah et al. 2004). The plant materials were preserved in the field using the Schweinfurt method, according to Bridson and Forman (1998). Thirteen voucher specimens used in this study were deposited in the Herbarium Bandungense (FIPIA), School of Life Sciences and Technology, Institut Teknologi Bandung (ITB), Indonesia. Further specimen examined was also conducted at Herbarium Bogoriense (BO), National Research and Innovation Agency (BRIN), Indonesia.

Taxonomic Treatment

Key to the tribe Eupatorieae in Kalimantan and Sumatra, according to Koster (1935) and Tjitrosoedirdjo (2000).

1	A	Appendages absent in the apex of anthers, pappus glandular…………………………………………………..…..*Adenostemma*
	B	Appendages present in the apex of anthers, pappus eglandular ……………………………………………………………... *2*
2	A	Vine, the head consists of 4 flowers, receptacle flat …………… ………………………………………….............. *Mikania*
	B	Herb to shrub, the head comprises of more than four flowers, receptacle convex to conical …..……………………..………… *3*
3	A	Phyllaries multi-seriate, receptacle without paleae, pappus more than 5 …………………………………………….. *4*
	B	Phyllaries 2-seriate, receptacle with paleae, pappus 5 ………… ……………………………...…………………… ……….*Ageratum*
4	A	Style base hairy……………………………….…....……… *5*
	B	Style base glabrous …..….. *6*

5	A	Carpopodia are well differentiated, anther appendages ovate-oblong……………………………..…… *Austroeupatorium*
	B	Carpopodia are slightly scarcely differentiated, anther appendages ovate-triangular………………….……..…… *Eupatorium*
6	A	Receptacle to convex, achene prismatic, 5-ribbed…………… 7
	B.	Receptacle conical, achene flattened, 3–4-ribbed…..…..*Praxelis*
7	A.	Shrub, corolla lobes densely papillose on the inner surface ……………………………………..………………… *Chromolaena*
	B.	Herb, corolla lobes glabrous on the inner surface…….. *Ayapana*

Praxelis clematidea (Hieron. ex Kuntze) R.M.King & H.Rob., Phytologia 20: 194 (1970). — TYPE: Argentina, Cordoba, 1819-1821, P.G. Lorentz 81 (lecto GOET!-Image seen [GOET001494], designated by Freire & Ariza Espinar, Flora Argentina 7 (1): 404. 2014; isolecto GOET! -Image seen [GOET001493]; syn GOET!-Image seen [GOET001492 & GOET001495]). – Figure 1 & 2.

Herb, erect, up to 75–78 cm tall, rooting at nodes, intensely aromatic. *Stem* angular, many-branched, green or purplish, hirsute. *Leaves* opposite; petioles 7–15 mm long, green, hirsute; lamina ovate, 1.2–5 × 1–3.5 cm, base attenuate, margin serrate, ciliate, apex acute, membranous, triplinerved, adaxial surface green, hirsute, uniseriate simple hairs present, abaxial surface pale green, densely hirsute, with simple uniseriate hairs and glandular hairs. *Capitulescence* of densely many-headed corymbiform cymes, terminal, discoid; peduncles 4–15 mm long, green, hirsute; receptacles conical, ca. 1.5 × 1 mm, apex acute, greenish white; phyllaries 18–20, 3–5-seriate, linear, 2.5–7 × 1–1.5 mm, green. *Paleae* absent. *Disc flowers* ca. 30–32, corolla ca. 5–6 mm long, purple, 5-merous; tube ca. 5 mm long, white; lobes triangular, ca. 1 mm long, papillose, purple; stamens 5, ca. 1 mm long; filaments free, filiform, white; anthers linear, ca. 3 mm long, connate, purplish; apical appendices ovate, ca. 0.5 mm long, purple, transparent; styles ca. 5 mm long, glabrous at the base, white; style arms 2, ca. 2–2.5 mm long, papillose, purplish blue. *Achenes* cylindric, ca. 2 mm long, black; *pappus* 1-seriate, numerous, ca. 40, 4–5 mm long, white.
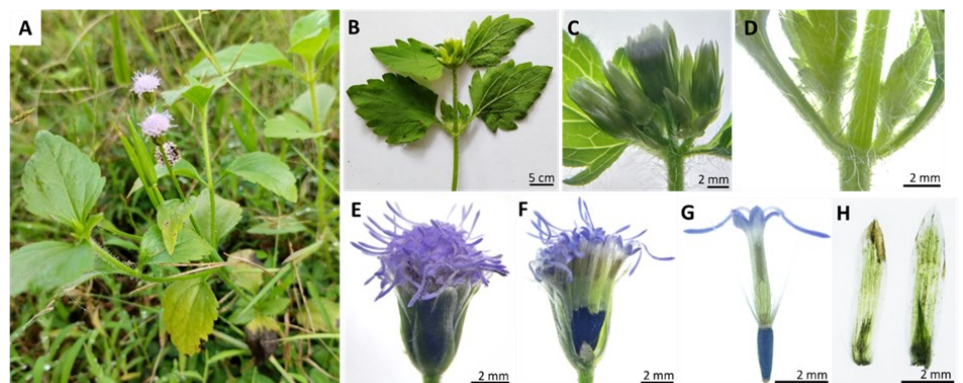
Figure 1. The morphological characteristics of *Praxelis clematidea* (Hieron. ex Kuntze) R.M.King & H.Rob. A. Habit; B. Opposite leaves; C. Capitulescence; D. Hirsute hairs on the stem; E-F. Head; G. Disc flower; H. Phyllaries.

Distribution: *Praxelis clematidea* is naturally distributed in Argentina, Bolivia, Brazil, Paraguay, and Peru (Veldkamp 1999; Salgado et al. 2022). It has become naturalized in Florida (Gardner & Williges 2015), China (Corlett & Shaw 1995; Veldkamp 1999; Wang et al. 2006a), Thailand (Intanon et al. 2020), Singapore (Chen et al. 2018), Java (Tjitrosoedirdjo

& Wahyuni 2018), and Northern Australia (Veldkamp 1999). Our study discovered the species in Kalimantan and Sumatra (Figure 2).

Habitat: *Praxelis clematidea* is mainly found in open areas, roadsides, ditches, peat swamps, and disturbed areas in Kalimantan and Sumatra. In Central Kalimantan, the species is often found growing at elevations between 11.41 and 23.55 m, while in Sumatra, it can be found at 20 to 530 m asl.

Specimens examined: INDONESIA: – **Kalimantan** • Central Kalimantan, Palangka Raya City, Jekan Raya Subdistrict, Menteng, G. Obos XVI, Cassadova Complex, 13.VI.2023, *RW Lestari 01* (FIPIA); Central Kalimantan, Palangka Raya City, Jekan Raya Subdistrict, Menteng, G. Obos XVI H, 13.VI.2023, *RW Lestari 02* (FIPIA); Central Kalimantan, Palangka Raya City, Jekan Raya Subdistrict, Menteng, Jl. Yos Sudarso 1, near the Merah Putih building, 13.VI.2023, *RW Lestari 03* (FIPIA); Central Kalimantan, Palangka Raya City, Jekan Raya Subdistrict, Palangka, Universitas Palangka Raya, around the Tunjung Nyaho Campus Forest, 13.VI.2023, *RW Lestari 04* (FIPIA); Central Kalimantan, Palangka Raya City, Jekan Raya Subdistrict, Palangka, Universitas Palangka Raya, near the library building, 13. VI.2023, *RW Lestari 05* (FIPIA); Central Kalimantan, Palangka Raya City, Jekan Raya Subdistrict, Palangka, Universitas Palangka Raya, near the LPPM building, Jl. Hendrik Timang, 13.VI.2023, *RW Lestari 06* (FIPIA). – **Sumatra** • Bangka Belitung Islands, Pangkal Pinang City, Bukitintan Subdistrict, Air Itam, Jl. Raya Pasir Padi, October 2020, *MR Hariri s.n.* (FIPIA); Bangka Belitung Islands, Belitung Regency, Membalong, Bantan, Jl. Serai Wangi, November 2020, *MR Hariri s.n.* (FIPIA); Jambi, Muaro Jambi Regency, Maro Sebo, Menapo Parit Duku Complex, Jl. Danau Lamo, August 2022, *MR Hariri s.n.* (FIPIA); Jambi, Muaro Jambi Regency, Maro Sebo, Candi Kotomahligai Complex, Jl. Danau Lamo, June 2021, *MR Hariri s.n.* (FIPIA); Sumatra Selatan, Ogan Komering Ulu Regency, Semidang Aji Subdistrict, Suka Merindu, Semidang Aji, Padang Bindu, June 2021, *MR Hariri s.n.* (FIPIA); Lampung, Tanggamus Regency, Semaka Subdistrict, Sedayu, Jl. Kota Agung-Bengkunat, 16.III.2023, *ASD Irsyam & The team of Tropical Forest Ecology Course TGGMS01-02* (FIPIA).
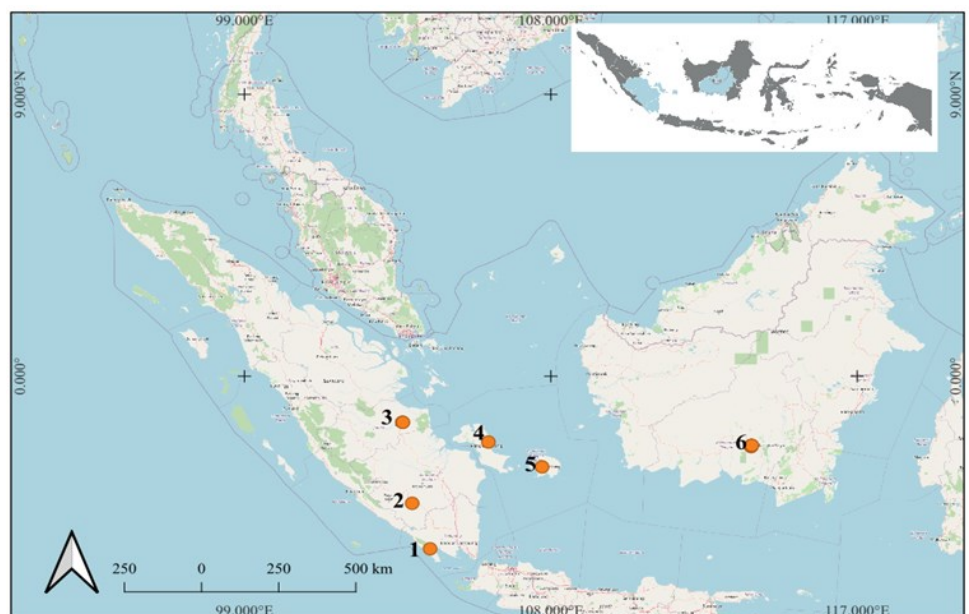
Figure 2. The Distributional map of *Praxelis clematidea* in Kalimantan and Sumatra. 1=Lampung, 2=South Sumatra, 3=Jambi, 4=Bangka, 5=Belitung, 6=Central Kalimantan.

Praxelis clematidea is a new addition to the exotic flora of Sumatra and Kalimantan. This species was reported for the first time in Indonesia in 2018 from Bogor, West Java (Tjitrosoedirdjo & Wahyuni 2018). Since then, it has expanded to several regions in West Java, including Sumedang Regency, Bandung City, and Bandung Regency. The genus *Praxelis* has not been recorded taxonomically in Kalimantan and Sumatra by previous botanists. Alien naturalised species are understudied in Sumatra and Kalimantan, Indonesia, because they tend to thrive in disturbed habitats less favourable to botanical research, according to Mustaqim and Putra (2020). As a result, many newly naturalised alien species will be discovered in the future.

Earlier botanists from the late 19th to the early 21st centuries addressed the taxonomical investigations on the Sumatran Asteraceae (Miquel 1861; Boerlage 1891; Koster 1935; Soerjani et al. 1987; Tjitrosoedirdjo 2002). As many as 133 species of Asteraceae, representing 74 genera, occur in Sumatra (Tjitrosoedirdjo 2002). Most of the members of Eupatorieae in Sumatra are introduced, such as *Ageratum* L, *Austroeupatorium* R.M.King & H.Rob., *Eupatorium* L, *Chromolaena* DC., and *Mikania* Willd. (Tjitrosoedirdjo 2002). The occurrence of *Praxelis* had never been reported in Sumatra at the beginning of the twenty-first century. On the other hand, the taxonomical information on the tribe Eupatorieae of Borneo was published by J.Th. Koster in 1935. There are four genera in Borneo: *Adenostemma* J.R.Forst. & G.Forst., *Ageratum*, *Eupatorium*, and *Mikania* (Koster 1935). It should be noted that the *Eupatorium* reported by Koster has since been split up into other genera, including *Austroeupatorium*, *Ageratina* Spach, *Ayapana* Spach, *Bartlettina* R.M.King & H.Rob., and *Chromolaena*. According to Koster (1935), *P. clematidea* is not mentioned as *Eupatorium* or *Praxelis*.

The introduction of *Praxelis* in Kalimantan and Sumatra may occur simultaneously. Its spontaneous populations are thought to have arisen due to naturalisation. According to a previous study, the species was intentionally introduced to Java as a contaminant (Tjitrosoedirdjo & Wahyuni 2018). A similar mechanism might develop in Kalimantan and Sumatra. *Praxelis clematidea* occupy many habitats, such as roadsides, ditches, open areas, and disturbed areas in Kalimantan and Sumatra. Surprisingly, it was also collected in peat swamps and sandy soils in Central Kalimantan, along with other weeds such as the families of Cyperaceae and Fabaceae. This species could spread widely throughout Kalimantan and Sumatra in the future.

Praxelis clematidea grows quickly and can produce numerous seeds and tiller stems. In general, small-seeded species can produce much more seeds than large ones. Seed traits include many seeds, a tiny seed size, and seed hair, which are crucial for alien species to propagate and settle in new locations successfully (Intanon et al. 2020). Its small achenes have bristly pappus, allowing the wind, animals, and farm equipment to spread them quickly (Veldkamp 1999; Salgado et al. 2020). Furthermore, since the species grows in ditches and peat swamp areas, the seeds may be transported by water in Central Kalimantan. *Praxelis clematidea* has invaded several countries worldwide over the past 40 years (Salgado et al. 2022). The species have been considered invasive alien species in China and Australia (Zhang et al. 2021; Simla et al. 2022). Previous studies revealed that its seeds could also generate allelopathy, promoting invasiveness in new locations (Wang et al. 2006b; Intanon et al. 2020). The species can establish dense stands in the wild that suffocate native species because it can produce many fertile seeds that will fall near the parent plant (Qin et al. 2008). Therefore, further research is required to compre-

hend the ecological implications of *P. clematidea* in Kalimantan and Sumatra.

Praxelis clematidea is frequently mistaken for other Eupatorieae species, such as *Ageratum conyzoides* L., due to direct visual observation (Corlett & Shaw 1995; Veldkamp 1999; Chen et al. 2018; Tjitrosoedirdjo & Wahyuni 2018). Mistakes in identifying *P. clematidea* impact inaccurate distribution maps and delays in eradication management, resulting in high control costs and low success rates (Marble et al. 2021). As the result, the distribution of *P. clematidea* in Kalimantan and Sumatra is underreported. Morphologically, the generative characters distinguish both species. Within the tribe Eupatorieae, *Ageratum* is classified in the subtribe Ageratinae Less., which is distinguished by its paleate receptacle, 2–3-seriate phyllaries, and 0–5 pappus (King & Robinson 1987; Robinson et al. 2007). On the other hand, *Praxelis* is grouped into the subtribe Praxelinae R.M.King & H.Rob. This genus has an epaleate receptacle, 3–4-seriate phyllaries, and numerous pappus (King & Robinson 1987).

Praxelis clematidea is commonly found in fields, forest edges, and abandoned land, where it disrupts the natural regeneration process, particularly in tropical regions. Khamare et al. (2020) mentioned that management of *P. clematidea* requires a strategic integration of manual and chemical control techniques. Mechanical removal techniques, including uprooting and cutting, are effective; however, they require ongoing follow-up to prevent regrowth. Chemical control, generally executed via targeted herbicide applications, effectively manages extensive infestations; however, it necessitates meticulous management to avert harm to native plants.

CONFLICT OF INTEREST
All authors declare no conflict of interests.

REFERENCES

Al Anshori, Z.A. et al., 2022. First Record of Naturalized *Acmella brachyglossa* and *Acmella radicans* (Asteraceae: Heliantheae) in Java, Indonesia. *Floribunda*, 7(1), pp.18-25. doi: 10.32556/floribunda.v7i1.2022.389.

Boerlage, J.G., 1891. *Handleiding tot de kennis der flora van Nederlandsch Indië,* Leiden: E.J. Brill.

Bridson, D.M. & Forman, L.L., 1998. *The Herbarium Handbook. 3rd ed.*, London: Kew Royal Botanic Gardens.

Chen, L.M.J. et al., 2018. Additions to the Flora of Singapore, new and overlooked records of naturalized plant species (1). *Gardens' Bulletin. Singapore*, 70(1), pp.91-101. doi: 10.26492/gbs70(1).2018-09

Corlett, R.T. & Shaw, J.C., 1995. *Praxelis clematidea*: yesterday South America, today Hong Kong, tomorrow the World?. *Memoirs of the Hong Kong Natural History Society*, 20, pp.235-236.

Funk, V.A. et al., 2007. Classification of Compositae. In *Systematics, Evolution, and Biogeography of Compositae*. Vienna: IAPT, pp.171–189.

Gardner, A.G. & Williges, K.A., 2015. *Praxelis clematidea* (Asteraceae): a new plant invader of Florida. *The Southeastern Naturalist*, 14, pp.N21–N27. doi: 10.1656/058.014.0111.

Grossi, M.A. et al., 2020. Providing tools for the reassessment of Eupatorieae (Asteraceae): Comparative and statistical analysis of reproductive characters in South American taxa. *Perspectives in Plant Ecology, Evolution and Systematics*, 46, 125566. doi: 10.1016/j.ppees.2020.125566.

Hind, D.J.N. & Robinson, H., 2007. Tribe Eupatorieae Cass. In *The Families and Genera of vascular plants 8*. Berlin: Springer, pp.510-574.

Holmes, R. et al., 2023. The naturalized vascular flora of Malesia. *Biological Invasions*, 25, pp.1339-1357. doi: 10.1007/s10530-022-02989-y.

Intanon, S., Wiengmoon, B. & Mallory-Smith, C.A., 2020. Seed morphology and allelopathy of invasive *Praxelis clematidea*. *Notulae Botanicae Horti Agrobotanici Cluj-Napoca*, 48(1), pp.261-272. doi: 10.15835/nbha48111831.

Irsyam, A.S.D. & Hariri, M.R., 2016. *Eupatorium capillifolium* (Lam.) Small ex Porter & Britton (Asteraceae: Eupatorieae), Rekaman baru untuk Flora Jawa. *Al-Kauniyah Journal of Biology*, 9(2), pp.80-86. doi: 10.15408/kauniyah.v9i2.3335.

Irsyam, A.S.D. & Irwanto, R.R., 2019. Nine additional cultivated species of Asteraceae from Java. *Jurnal Biodjati*, 4(2), pp.244-251. doi: 10.15575/biodjati.v4i2.4815.

Irsyam, A.S.D. et al., 2020a. Catatan marga *Pseudogynoxys* (Asteraceae) di Pulau Jawa. *Jurnal Biotika*, 18(1), pp.1-11. doi: 10.24198/biotika.v18i1.26539

Irsyam, A.S.D. et al., 2020b. Catatan marga *Centratherum* (Asteraceae: Vernonieae) di Pulau Jawa. *Al-Hayat: Journal of Biology and Applied Biology*, 3(2), pp.75-84. doi: 10.21580/ah.v3i2.6426.

Khamare, Y. et al., 2020. Biology and Management of Praxelis (*Praxelis clematidea*) in Ornamental Crop Production: ENH1321/EP585, 8/2020. *EDIS*, 2020(4). doi: 10.32473/edis-ep585-2020

King, R.M. & Robinson, H., 1970. Studies in the Eupatorieae (Compositae). XXVIII. the genus *Praxelis*. *Phytologia*, 20, pp.193-195.

King, R.M. & Robinson, H., 1987. The genera of the Eupatorieae (Asteraceae). *Monographs in Systematic Botany from the Missouri Botanical Garden*, 22, pp.1-581. doi: 10.5962/bhl.title.156613.

Koster, J., 1935. The Compositae of the Malay Archipelago. I. Vernonieae and Eupatorieae. *Blumea*, 1(3), pp.351-536.

Marble, S.C. & Brown, S.H., 2021. Invasive Plants with native lookalikes: how mistaken identities can lead to more significant plant invasions and delay management. *Hort Technology*, 31, pp.385-394. doi:10.21273/HORTTECH04821-21.

Miquel, F.A.W., 1861. *Flora van Nederlandsch Indie, Eerste bijvoegsel, Sumatra*, Amsterdam: C.g. van der Post.

Mustaqim, W.A. & Putra, H.F., 2020. *Melothria* (Cucurbitaceae): A new genus record of naturalized cucumber in Sumatra. *Floribunda*, 6(5), pp.183-187. doi: 10.32556/floribunda.v6i5.2020.318.

Qin, W. et al., 2008. Investigation and analysis on alien invasive plants in three national nature reserves in Hainan Province. *Journal of Plant Resources and Environment*, 17, pp.44-49.

Robinson, H., Schilling, E. & Panero, J.L., 2007. Eupatorieae. In *Systematics, Evolution, and Biogeography of Compositae*. Vienna: IAPT, pp.731-744.

Rugayah et al., 2004. Pengumpulan Data Taksonomi. In *Pedoman Pengumpulan Data Keanekaragaman Flora*. Bogor: Pusat Penelitian Biologi-LIPI, pp.5-42.

Salgado, V.G. et al., 2020. *Praxelis clematidea* (Asteraceae, Eupatorieae, Praxelinae) in Uruguay: First record of the genus and the species. *Darwiniana*, 8(2), pp.479-489. doi: 10.14522/darwiniana.2020.82.912.

Salgado, V.G. et al., 2022. Understanding *Praxelis* (Asteraceae, Eupatorieae): an updated taxonomy with lectotypifications and morphological and distributional clarifications. *Australian Systematic Botany*, 35(4), pp.198-218. doi: 10.1071/SB21027.

Simla, P. et al., 2022. Effect of Landscape Composition and Invasive Plants on Pollination Networks of Smallholder Orchards in Northeastern Thailand. *Plants*, 11(15), 1976.

Soerjani, M., Kostermans, A.J.G.H. & Tjitrosoepomo, G., 1987. *Weeds of Rice in Indonesia*, Jakarta: Balai Pustaka.

Tjitrosoedirdjo, S.S., 2000. *The Asteraceae of Sumatera*. Institut Pertanian Bogor.

Tjitrosoedirdjo, S.S., 2002. Notes on The Asteraceae of Sumatera. *Biotropia*, 19, pp.65-84.

Tjitrosoedirdjo, S.S. & Wahyuni, I., 2018. Rekor baru keberadaan *Praxelis clematidea* (Asteraceae) di Indonesia. *Prosiding Seminar Nasional XX Himpunan Gulma Indonesia*, pp.212-217.

van Steenis, C.G.G.J., 1987. *Checklist of Generic Names in Malesian Botany*, Leiden: Flora Malesiana Foundation.

Veldkamp, J.F., 1999. *Eupatorium catarium*, a new name for *Eupatorium clematideum* Griseb. non Sch.Bip (Compositae), a South American species naturalized and spreading in SE Asia and Queensland, Australia. *Gardens' Bulletin. Singapore*, 51, pp.119-124.

Wang, Z., An, F. & Chen, Q.B., 2006a. Praxelis (*Praxelis clematidea*): a new invasive exotic weed in China. *Journal of Tropical Agriculture*, 6, pp.33-37.

Wang, Z. et al., 2006b. Allelopathic potential and chemical constituents of volatile oil from *Praxelis clematidea*, *Allelopathy Journal*, 18, pp.225-235.

Zhang, Y. et al., 2021. Autonomous apomixis in *Praxelis clematidea* (Asteraceae: Eupatorieae), an invasive alien plant. *AoB Plants*, 13, plab007. doi: 10.1093/aobpla/plab007.

Short Communications

Morpho-Ecotype Characterization of Superior Local Durian (*Durio zibethinus* L.) in Jember Regency

Vega Kartika Sari[1]*, Halimatus Sa'diyah[1], Basuki[2]

1) Agronomy Study Program, Faculty of Agriculture, University of Jember, Jl. Kalimantan No.37 Kampus Tegalboto, Jember, East Java 68121
2) Soil Science Study Program, Faculty of Agriculture, University of Jember, Jl. Kalimantan No.37 Kampus Tegalboto, Jember, East Java 68121
* Corresponding author, email: vegakartikas@unej.ac.id

ABSTRACT

Panti and Sumberjambe Districs are known as durian centre in Jember Regency, it is necessary to characterise the main potential superior durian trees. The exploratory investigation was carried out between April - July 2023. Morphological characterisation and Ecological observations including topography, soil type and climate were carried out. Data were analysed in clusters and descriptively. The results showed that 10 local durian accessions from Panti District had 66% similarity. The highest similarity between Montong Belanda and Gendon durians (75%). Ten local durians from Sumberjambe showed 64% similarity. Si Sukun differed significantly, whereas LK 1 and LK 4 shared 85% similarity.

Indonesia is one of the centres of durian diversity in the world (Belgis et al. 2016). Durian is known as the King of Fruit, an exotic tropical fruit with a unique taste and aroma. Durian fruit production in 2021 will reach 1.35 million tonnes, including the top five leading fruit commodities after bananas, pineapples, mangoes, and oranges (BPS 2021). East Java Province is one of the largest durians producing regions, with a total production of 276,426 tonnes (24.20%), followed by Central Java, West Java, North Sumatra, and other provinces.

Specific natural conditions in the surrounding of an area could led to the development of a distinctive flora, such as Besuki residential area in East Java that is surrounded by several mountains (Rusmiati et al. 2013). Some of these mountains are Mount Raung, Mount Argopuro, and Mount Ijen. Banyuwangi Regency, located on the slopes of Mount Ijen, has been known as an area with red durian fruit as its superior fruit (Basuki et al. 2022b). Jember Regency is located on the slopes of Mount Raung and Mount Argopuro, where several areas, such as Panti District and Sumberjambe District, are known as durian centres in Jember Regency.

Durian has various morphological characters (Sundari et al. 2015). The diversity of durian shows in the taste, aroma, texture, and colour of the fruit flesh as well as in the shape and size of the fruit (Belgis et al. 2016). Local durians on the slopes of Mount Raung and Mount Argopuro may have distinct advantages, both in morphological characteristics and

the chemical content of the fruit. Until 2019, 104 superior durian varieties had been registered at the Ministry of Agriculture, and there were still many candidates for varieties that had not been registered that had advantages (Directorate General of Horticulture 2019). Determination of superior varieties begins with morphological characterization.

The aim of this study was to explore local durians on the slopes of Mount Argopuro and Mount Raung. The superior potential of the local durians obtained will be characterized by their morphology and ecology. The morphological and ecological characteristics of each type of local durian fruit with superior potential will be an important source of information in the management of local durian fruit plants.

Exploratory research was conducted by survey method to Panti District and Sumberjambe District in Jember Regency, East Java Province, Indonesia. Panti District is on the slopes of Mount Argopuro, while Sumberjambe District is on the slopes of Mount Raung (Figure 1).
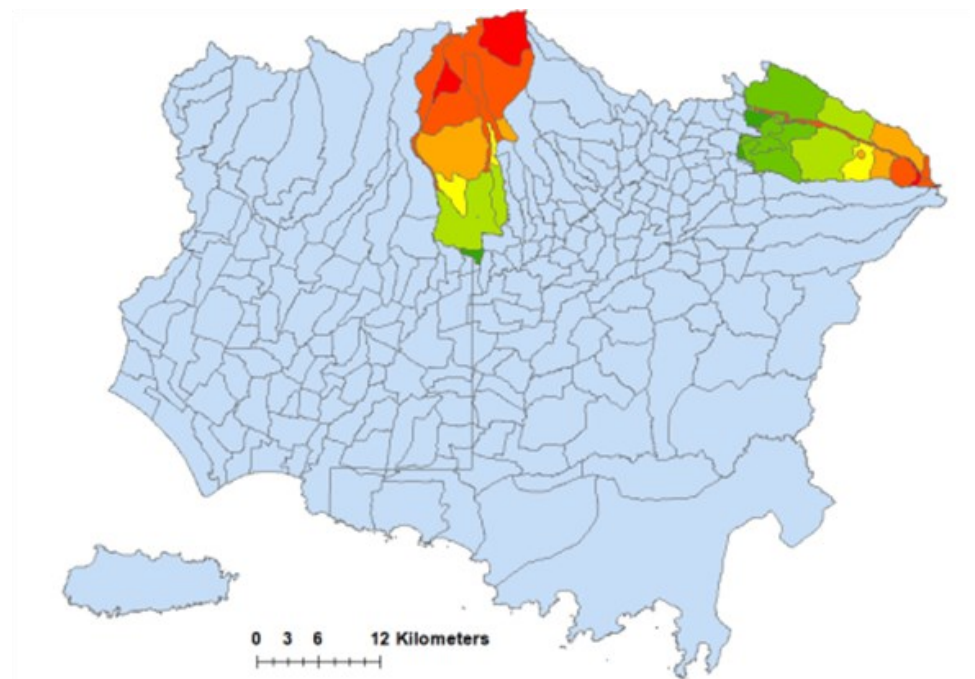
Figure 1. The Study Area of Durian Plants Used in Jember Regency, East Java, Indonesia.

Observation of land characteristics is divided into environment and soil. Observed environmental characteristics include slopes and rainfall. Slopes were analysed using DEM data analysis, while rainfall was analysed from several rainfall stations at the study site. Rainfall is taken from data for the last 10 years. The soil characteristics observed were previously taken from soil samples from the sampling results with a soil depth of 0-30 cm from the soil surface (Mustofa et al. 2024). Parameters observed included pH, C-Organic, total soil Nitrogen, Phosphate available (P_2O_5), Exchangeable potassium and Cation Exchange Capacity (CEC), and soil texture. The soil parameter analysis method is shown in Table 1.

The sampling technique used was purposive sampling. The selected durian trees are over 30 years old and are known for their high productivity and superior fruit quality, as reported by both durian tree owners and local residents. According to Sihaloho et al. (2021), the criteria for selecting durian plants for exploration and characterisation include those that are approximately 25 years old or older, have produced fruit multiple times, and possess desirable qualities that are valued by the communi-

Table 1. Parameters and methods of soil sample analysis.

No	Parameters	Methods	Reference
1	Soil pH	Sample and water ratio (1:5)	Zeraatpisheh et al. 2020; Basuki et al. 2023
2	C-Organic	Walkey & Black	Qureshi et al. 2012
3	Total soil Nitrogen	Kjeldahl	FAO 2021; Putra et al. 2021
4	Phosphate available (P_2O_5)	Olsen	Zhao et al. 2023
5	Exchangeable potassium	NH_4OAc 1 N pH 7	Shah et al. 2022
6	Cation exchange capacity (CEC)	NH_4OAc 1 N pH 7	Basuki et al. 2024
7	Soil Texture	pipette	Basuki et al. 2024

ty. The vegetative parts of the durian plant specifically the trees, branches, and leaves were examined using the Descriptors for Durio guidelines issued by Bioversity International (2007). The Global Positioning System (GPS) was utilized to gather location information. The morphological observations included ten traits of durian trees and eighteen traits of durian leaves. Additionally, ecological observations encompassed soil conditions, topography, and climate at the site. Microclimate data was collected from nearby weather stations.

Data were analysed by cluster using the Gower distance with average linkage program in statistic software. Cluster analysis resulting from morphological observations was also used in the study of Hariyono et al. (2022) to estimate morphological diversity in arrowroot plants resulting from exploration. The F test on statistics software is used to determine the effect of the environment on morphological characters. According to Neter et al. (1985), F test is often used to determine the variance of two groups.

A horticultural plant known as durian is categorized as an annual plant (Hafif 2014). The habitat in which it grows has a significant impact on the taste and fat content. The majority of durian plants are found on the sides of volcanic mountains, and there is a significant association between the appropriateness of the land and that level of suitability (correlation value: > 0.7) (Samsuri et al. 2019; Rahmawaty et al. 2020). There are 181 mountains in East Java that are more than 1,000 meters above sea level, and 7 of the mountains, including Mount Argopura, Mount Raung, Mount Baluran, Mount Ijen, Mount Lemongan, Mount Bromo, and Mount Semeru, are located in a horseshoe-shaped region.

The existence of adjacent mountains, and their environmental characteristics are not the same. In comparison to Mount Argopura, which is 3,088 meters above sea level, Mount Raung is 3,344 meters high (Basuki et al. 2022a). The topographic relief on the slopes of Argopura is topographically dominated by very steep topography (40-60%) with an area of 7,538.68 ha and sloping topography with an area dominating the second (3,759.95 ha) (Figure 2). On the slopes of Mount Argopura, there is 13.53 mm of rainfall each year on average. The research region is defined as having a C climatic type (wet), which has 4-5 dry months and 6-7 wet months, according to the Smith Ferguson climate classification. Mid-May to mid-October are the dry months (Figure 3). The soil formed on the slopes of Mount Argopura is dominated by the Inceptisol, Andisol, and Ultisol orders with seven great soil groups (Figure 4).

Seven reliefs (flat, slightly sloping, sloping, little hills, hilly, extremely steep, and steep) can be found on Mount Raung's slopes (Basuki et al. 2022b). The 5461.68 hectares of Mount Raung's slopes have a topographic gradient of 3–8% (Figure 2). The second dominant relief has an

area of 3884.04 ha and is gradually sloping (8–15%). The average annual rainfall is 2227.98 mm. The slopes of Mount Raung are classified by Smirt-Ferguson as having a mild climate with an average. There are 3–4 dry months and 8–9 wet months per year (Figure 3). The three orders—Andisols, Inceptisols, and Entisols—into which the soil types are subdivided are shown in Figure 4.

(a)   (b)
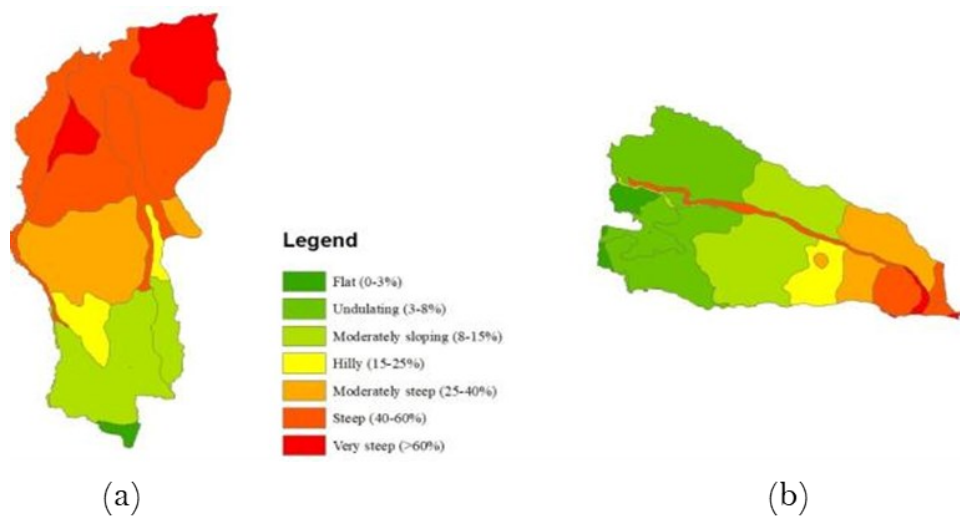
Figure 2. Geological formations (a) the southern slope of Mount Argopura, (b) the western slope of Mount Raung.
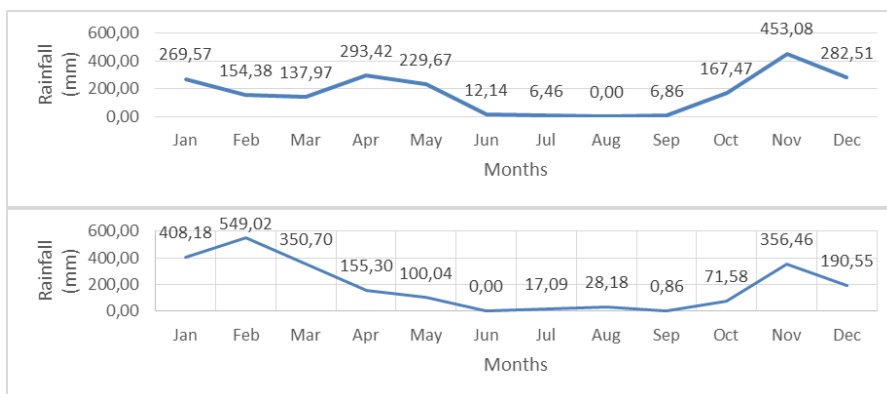
Figure 3. Distribution of annual rainfall on the slopes of Mount Argopura (top) and Mount Raung (bottom).

(a)   (b)
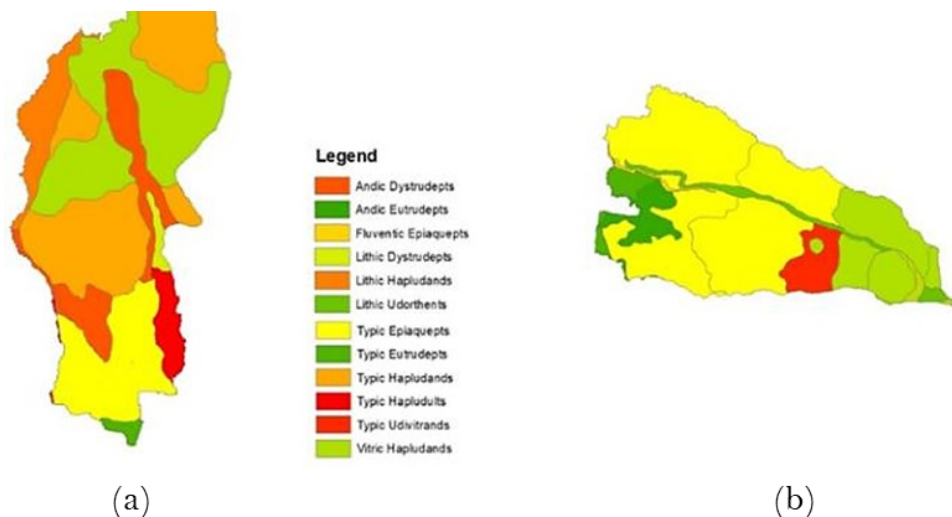
Figure 4. Soil type (a) the southern slope of Mount Argopura, (b) the western slope of Mount Raung.

The five variables that contribute to the formation of soil interact to create the features of soil (Neswati et al. 2019; Szalai et al. 2021; Bölscher et al. 2021). The soil characteristics, both physical and chemical, fluctuate depending on the topographical relief, altitude, rainfall, and type of soil generated at the study location (Table 2). The data in Table 2 demonstrates that the predominant soil texture is clay, which is made up of 20% sand, 40% silt, and 40% clay. The soil's volume weight on Mount Argopuro's slopes ranges from 1.03 to 1.05 g/cm3, with an average of 1.04 g/cm3. The hydrogen potential (pH) of soil is determined by the weathering effects of soil-forming elements (Da Costa et al. 2015; Zhong et al. 2019; Neswati et al. 2019; Alaboz et al. 2021). The results of weathering soil-forming materials result in soils with slightly acidic hydrogen potential (pH) (6.10), very low available phosphate (2.58 ppm), medium category exchangeable cations, particularly potassium (K), (0.42 Me/100g), and high Cation Exchange Capacity (CEC) of 32.38 Me/100g. On the slopes of Mount Argopura, the organic matter produced by the weathering of vegetation organic material is still low (1.94%) and inversely proportional to the total soil nitrogen value, which is moderate (0.28%). With a score of 6.93, the breakdown of organic matter on Mount Argopura's slopes falls into the low category. The amount of soil moisture, the type of litter, the nutrients that support the organic matter, and many other factors affect how quickly organic matter decomposes (Hajduk et al. 2015; Baskan et al. 2016; Wang et al. 2022; Soetriono et al. 2023).

The slopes of Mount Raung have a soil type that is dominated by inceptisol soil with a slightly acidic, pH value of 5.63 (Table 2). Other soil chemical characteristics that are formed, such as P_2O_5 is in the low category (5.05 ppm), potassium exchangeable is low (0.17 Me/100g), and CEC being in the very high category (40.05 Me/100g). The level of decomposition on the slopes of Mount Raung is in the high category with a C/N ratio of 33.3, where the C-Organic value is high (3.33%), and total soil nitrogen is in the low category (0.10%). The Raung slope is seen

Table 2. Soil characteristics of the slopes of Mount Argopuro and the slopes of Mount Raung.

No	Parameter	Unit	Value			
			The slopes of Mount Argopuro		The slopes of Mount Raung	
1	pH 1:5	–	6.10	Slightly acid	5.63	Slightly acid
2	C-Organic	%	1.94	Low	3.33	High
3	N Total	%	0.28	Mid	0.10	Low
4	P_2O_5	Ppm	3.58	Very low	5.06	Low
5	K	Me/100g	0.42	Mid	0.17	Low
6	CEC	Me/100g	32.38	High	40.05	Very high
8	C/N ratio	–	6.93	Low	33.3	Very high
9	BV	g/cm3	1.04	–	1.15	–
10	Texture					
	Sand	%	20	–	10	–
	Silt	%	40	–	50	–
	Clay	%	40	–	40	–
			Clay	–	Silty Clay	–

Note: Soil fertility assessment is based on the technical guidelines for soil water analysis of plant tissue issued by the Soil and Fertilizer Instrument Testing Center 2023.

from the physical characteristics of the soil, it is included in the silty clay soil texture category. Silty clay is a soil texture composed of 10% sand, 50% silt, and 40% clay, so the volume weight is 1.15 g/cm³.

The soil texture of the Mount Argopuro and Raung slopes contains clay, and silt and sand in equal proportions. According to Karim et al (2017), this soil texture is very suitable for durian plants. Soil pH from both locations is slightly acidic. According to Mansur (2007), the durian habitat studied also has a clay type with a slightly acidic pH.

The level of land suitability for durian plants on the slopes of Mount Argopura and the slopes of Mount Raung is in the moderately suitable class (S2) with available nutrient barrier factors. The limiting factor for durian plants on the slopes of Mount Argopura is the availability of phosphate nutrients. Phosphate nutrients on the slopes of Mount Argopura are in the low category. Thus, to increase them to highly suitable (S1), fertilization is needed in the amount of 1-2 kg/plant/year. Meanwhile, for durian plants on the slopes of Mount Raung, the level of land suitability is classified as moderately suitable (S2) with the limiting factors for available nutrients, including total soil nitrogen, available phosphate, and available potassium. Therefore, management requires balanced fertilization for these primary macronutrients.

Based on Figure 5, the morphological similarity of the 10 local durian varieties from Slope Mount Argopuro is 66%, or the level of dissimilarity is 34%. This indicates the great level of local durian diversity observed in Panti District on the slopes of Mount Argopuro. Two major groups were established from the dendogram analysis's findings: group I, which included eight varieties of durian, and group II, which included two varieties, Gendon and Montong Belanda (MB). In line with the research results of Mustikarini et al. (2017), the results of exploration and characterization of durian on South Bangka Island, from 27 accessions formed 5 clusters with a similarity level of 60%.
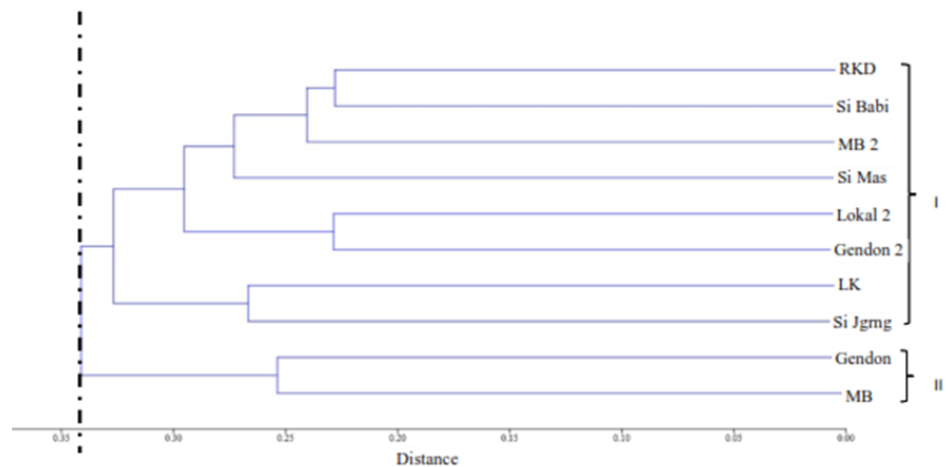
Figure 5. Dendogram of local durian plants from the slopes of Mount Argopuro.

Group I was made up of eight durian accessions that came from two distinct but nearby locales. The genotypes from the same region are not always in the same group, indicating that genotypes from various regions might also be in the same group (Susilawati & Sabran 2018; Sari et al. 2024). Meanwhile, in group II, the two local durian accessions had many morphological similarities compared to the other 8 types, and were in the same location, namely in Pakis Village. The degree of kinship depends on the degree of morphological similarity (Susilawati & Sabran 2018).

Local durians on the slopes of Mount Raung have a variety that is not too different from durians from the slopes of Mount ArgopuroMeanwhile, local durians in the District of Sumberjambe Slopes of Mount Raung shows high diversity. The dissimilarity of the 10 accessions based on the dendrogram formed was 36% or 64% similarity (Figure 6).
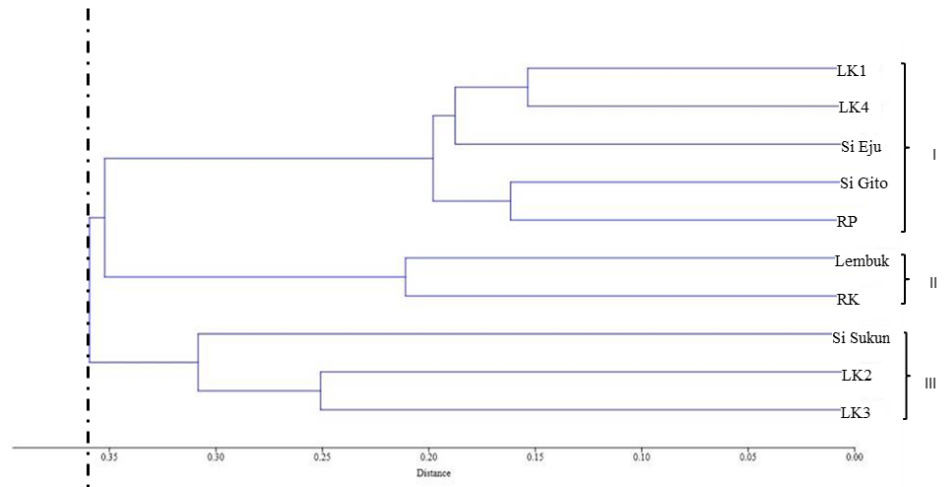
Figure 6. Dendogram of local durian plants from the slopes of Mount Raung.

Three major groups were established from the dendogram: group I, which included five varieties of durian, group II, which included two varieties (Lembuk and RK), and group III included three varieties (Si Sukun, LK 2, LK 3). According to Hu et al. (2014) and Pereira et al. (2015), the genetic diversity of a species in a population is a consequence of its sexual reproduction system. Handayani (2016) added that durian from Kalimantan has high genetic diversity because durian is a cross-pollinated and open plant that originates from random mating between other genotypes.

Seven quantitative morphological characteristics were observed, including stems, branches, and leaves. Among these, the height of the durian plant tended to vary depending on the ecotype, while the other six did not differ significantly (Table 3). Numerous genes regulate quantitative character. The growth characteristic of plant height is affected by numerous genes as well as environmental factors. The environment has a significant impact on how plants grow. In line with the findings of a study by Handayani and Ismadi (2018), which revealed variations in plant height between durian accessions in two separate sub-districts in the North Aceh District. Different planting timings and environmental factors like sunlight and soil qualities might contribute to variations in plant height. Yang et al. (2021) states beyond genetic effects, plant height is also influenced considerably by environmental conditions. Furthermore, Yang et al. (2021) describes that both agro-meteorological and soil properties influence plant height traits, but the agro-meteorological factors largely predominate.

Variations in the degree of similarity or dissimilarity caused by variations in the morphology of plants, including qualitative and quantita-

Table 3. F test on the morphological quantitative characters of local durian in 2 ecotypes in Jember Regency.

Quantitative Morphological Character	LHD	PHD	LTD	PTD	LB	TB	UT
F test	ns	ns	ns	ns	ns	*	ns

Notes: LHD: width of leaf blade; PHD: blade length; LTD: petiole width; PTD: petiole length; LB: leaf width; TB: stem height; UT: plant age; *: significantly different on the F test 0.05; ns: not significantly different.

tive characteristics, which are regulated by genetics and the environment. Plants require specific conditions in order to express their genetic potential (Handayani & Ismadi 2018). Weaknesses of morphological markers are affected by plant growth and environmental changes. It can be difficult to differentiate between genotypes since their morphology is similar even though they are distinct. Besides, due to self-incompatibility, durian plants have a high level of variety and undergo a significant amount of cross-pollination (Indriyani et al. 2012). Plant breeding activities are greatly enhanced by the availability of genetic resources (Lestari et al. 2016). This information on morphological variation may serve as the basis for future development and preservation.

The degree of similarity among the ten prospective superior local durians from Panti District, on the slopes of Mount Argopuro, is 66%, which is not significantly different from the level of similarity among the local durians from Sumberjambe, on the slopes of Mount Raung, at 64%. The most similar durians were Montong Belanda and Gendon from Panti District (75%), while those from Sumberjambe were closest to LK 1 and LK 4 durians (85%).

AUTHORS CONTRIBUTION
V.K.S. designed the research and supervised all the process, H.S. tabulated and analyzed the data morphology and wrote the interpretation, B. analysed the data of ecology and designed the maps.

CONFLICT OF INTEREST
The authors declare no conflict of interest.

REFERENCES

Alaboz, P. et al., 2021. Digital mapping of soil erodibility factors based on decision tree using geostatistical approaches in terrestrial ecosystem. *Catena*, 207, 105634. doi: 10.1016/j.catena.2021.105634.

Baskan, O., Dengiz, O. & Gunturk, A., 2016. Effects of toposequence and land use-land cover on the spatial distribution of soil properties. *Environmental Earth Sciences*, 75, 448. doi: 10.1007/s12665-016-5301-6.

Basuki, B. et al., 2022a. Evaluation of the suitability of a sugarcane plant in mount argopura's volcanic land using a geographic information system. *Jurnal Ilmiah Rekayasa Pertanian dan Biosistem*, 10(1), pp.145−160. doi: 10.29303/jrpb.v10i1.315.

Basuki, B. et al., 2022b. Soil Damage Potential Index Based on Weighting Scoring Analysis and Utilization of Geographical Information Systems. *Jurnal Teknik Pertanian Lampung*, 11(4), pp.601−616. doi: 10.23960/jtep-l.v11i4.601-616

Basuki, B. et al., 2023. The sensitivity level of landslide risk using Geographic Information System on the slopes of Mount Argopura, East Java, Indonesia. *Journal of Degraded and Mining Lands Management*, 11(1), pp.4949−4959. doi: 10.15243/jdmlm.2023.111.4949.

Basuki, B. et al., 2024. Soil classification and prediction model for critical land on the slopes of Mount Raung in Indonesia. *Journal of Degraded and Mining Lands Management*, 11(3), pp.5610–5621. doi: 10.15243/jdmlm.2024.113.5610.

Belgis, M. et al., 2016. Physichemical differences and sensory profiling of six lai (Durio kutejensis) and four durian (Durio zibethinus) cultivars indigenous Indonesia. *Inter. Food Research Journal* , 23(4), pp.1466-1473. doi: 10.5555/20163247220

Bioversity International, 2007, 'Descriptors for durian (Durio zibethinus Murr.)', in *Bioversity International*, viewed 27 January 2023, from https://cgspace.cgiar.org/items/523fcdb9-d840-4614-b6c5-c1b1ee69be3c

Bölscher, T. et al., 2021. Changes in pore networks and readily dispersible soil following structure liming of clay soils. *Geoderma*, 390, 114948. doi: 10.1016/j.geoderma.2021.114948.

BPS., 2021, 'Produksi Tanaman Buah-Buahan', in *Badan Pusat Statistik*, viewed 27 January 2023, from https://www.bps.go.id/indicator/55/62/1/produksi-tanaman-buah-buahan.html

Da Costa, P.Y.D. et al., 2015. Old landscapes, pre-weathered materials, and pedogenesis in tropical Africa: How can the time factor of soil formation be assessed in these regions? *Quaternary International*, 376, pp.47–74. doi: 10.1016/j.quaint.2014.04.062.

Directorate General of Horticulture., 2019, 'Surplus 735 ton, Durian Lokal Targetkan Ekspansi Ekspor', in *Direktorat Jenderal Hortikultura Kementerian Pertanian*, viewed 27 January 2023, from https://hortikultura.pertanian.go.id/?p=4131

Food and Agriculture Organization of the United Nations (FAO), 2021. *Standard operating procedure for soil nitrogen Kjeldahl.* Rome.

Hafif, B., 2014. Keragaan Lahan Sub-Optimal dan Perbaikan Produktivitas Melalui Kebijakan Daerah di Lampung. *Prosiding Seminar Nasional Pengembangan Teknologi Pertanian Politeknik Negeri Lampung 2014*, pp.7–16. doi: 10.25181/prosemnas.v0i0.364

Hajduk, E., Właśniewski, S. & Szpunar-Krok, E., 2015. Influence of legume crops on content of organic carbon in sandy soil. *Soil Science Annual*, 66(2), pp.52–56. doi: 10.1515/ssa-2015-0019.

Handayani, F., 2016. *Genetic diversity of Lai (Durio kutejensis [Hassk.] Becc.) based on morphological and inter-simple sequence repeat markers.* University of Gadjah Mada

Handayani, R.S. & Ismadi, 2018. Inventory and Morphological Characterization of Durian (Durio zibethinus) in Langkahan and Sawang Sub-District of North Aceh Indonesia. *Proceedings of MICoMS 2017*, 1, pp.601-608.

Hariyono, K. et al., 2022. Inventarisasi dan Identifikasi Morfologi Tanaman Garut (Maranta arundinaceus L.) di Kabupaten Jember. *Jurnal Penelitian Pertanian Terapan*, 22(3), pp.238-246. doi:10.25181/jppt.v22i3.2257

Hu, Y. et al., 2014. Genetic variation in cultivated Rheum tanguticum populations. *Genetics and Molecular Biology*, 37(3), pp.540–548. doi: 10.1590/S1415475720140004000010.

Indriyani, N.L.P. et al., 2012. Maternal and Paternal Effect on the Characters of durian (*Durio zibethinus* Murr.) Fruit from Cross-pollination. *Journal of Fruit and Ornamental Plant Research*, 20(2), pp.23–33. doi: 10.2478/v10290-012-0012-x

Karim, H., Zhiddiq, S. & Suprapta., 2017. Potential Land for Durian Plant (Durio zibethinus Murr) in Mungkajang Sub-District Palopo City. *UNM Geographic Journal.*, 1(1), pp.48-54.

Lestari, P. et al., 2016. Morphological Variability of Indonesian Rice Germplasm and the Associated SNP Markers. *Emirates Journal of Food and Agriculture*, 28(9), pp.660–670. doi: 10.9755/ejfa.2016-03-319

Mansur, M., 2007. Penelitian Ekologi Jenis Durian (Durio spp.) di Desa Intuh Lingau, Kalimantan Timur. *Jurnal Teknologi Lingkungan*, 8 (3). doi: 10.29122/jtl.v8i3.427

Mustikarini, E.D., Khodijah, N.S. & Yulistia, Y., 2017. Morphological Characterization and Yield Potency of Bangka Local Durian: Karakterisasi Morfologi dan Potensi Hasil Durian Lokal Bangka. *AGROSAINSTEK: Jurnal Ilmu dan Teknologi Pertanian*, 1(1), pp.1–9. doi: 10.33019/agrosainstek.v1i1.1.

Mustofa, A., Utami, S.N.H. & Purwanto, B.H., 2024. Soil quality index in some cropping systems in plot 17 of Wanagama forest, Gunungkidul, Yogyakarta, Indonesia. *Sains Tanah*, 21(1), pp.1–14. doi: 10.20961/stjssa.v21i1.65454.

Neswati, R., Lopulisa, C. & Adzima, A.F., 2019. Characterization and Classification of Soils from Different Topographic Positions under Sugarcane Plantation in South Sulawesi, Indonesia. *Journal of Tropical Soils*, 24(2), pp.93-100. doi: 10.5400/jts.2019.v24i2.93-100.

Neter, J., Wasserman, W. & Kutner, M.H., 1985. *Applied Linear Statistical Models*, Second Edition. Irwin, Inc

Pereira, D.A., Correa, R.X. & Oliveira, A.C., 2015. Molecular genetic diversity and differentiation of populations of somnus' passion fruit trees (Passiflora setacea DC): Implications for conservation and pre-breeding. *Biochemical Systematic and Ecology*, 59, pp.12–21. doi: 10.1016/j.bse.2014.12.020

Putra, B.T.W. et al., 2021. Comprehensive measurement and evaluation of modern paddy cultivation with a hydroganics system under different nutrient regimes using WSN and ground-based remote sensing. *Measurement: Journal of the International Measurement Confederation*, 178, 109420. doi: 10.1016/j.measurement.2021.109420.

Qureshi, A. et al., 2012. A review of protocols used for assessment of carbon stock in forested landscapes. *Environmental Science and Policy*, 16, pp.81–89. doi: 10.1016/j.envsci.2011.11.001.

Rahmawaty et al., 2020. GIS based: mapping of Multy Purpose Tree Species *(Durio zibethinus)* in Perkebunan Tambunan Village, Langkat District, North Sumatera Province, Indonesia. *IOP Conference Series: Earth and Environmental Science*, 454, 012147. doi: 10.1088/1755-1315/454/1/012147

Rusmiati, R. et al., 2013. Eksplorasi, Inventarisasi, dan Karakterisasi Durian Merah Banyuwangi. *Prosiding Semirata FMIPA Universitas Lampung*, pp.293-299.

Sari, V.K. et al., 2024. Genome identification and diversity analysis of banana (Musa spp.) from Jember based on morphological characters. *AGROMIX*, 15(1), pp.44-50. doi: 10.35891/agx.v15i1.4408

Sundari, E.L. et al., 2015. Exploration and Morphological Character Identification of Local Durian (Durio zibenthinus Murr.) from Tidore Island, North Maluku. *Proceeding of The 6th* ICGRC, pp.1-4.

Samsuri, S. et al., 2019. Evaluation of plant species suitability for lowland forest landscape restoration in Lepan watersheds, Langkat District, North Sumatra, Indonesia. *Biodiversitas Journal of Biological Diversity*, 20(10), pp.2903-2909. doi: 10.13057/biodiv/d201018

Shah, T.I. et al., 2022. Soil Quality Index as Affected by Integrated Nutrient Management in the Himalayan Foothills. *Agronomy*, 12(8), 1870. doi: 10.3390/agronomy12081870.

Sihaloho, M.A., et al., 2021. The phenotypic of durian plant (*Durio zibethinus* Murr.) in Tapanuli Tengah Regency, North Sumatra, Indonesia. *IOP Conf. Ser.: Earth Environ. Sci.*, 912, 012031. doi: 10.1088/1755-1315/912/1/012031

Soetriono, S. et al., 2023. The effectiveness of giving organic matter to the productivity of tomato plants The Effectiveness Of Giving Organic Matter To The Productivity Of Tomato Plants. *AIP Conference Proceedings*, 2583, 020014.

Susilawati & Sabran, M., 2018. Karakterisasi Morfologi Durian (Durio zibethinus) Lokal Asal Kabupaten Katingan. *Bul.Plasma Nutfah*, 24 (2), pp.107-114.

Szalai, Z. et al., 2021. Accelerated soil development due to seasonal water -saturation under hydric conditions. *Geoderma*, 401, 115328. doi: 10.1016/j.geoderma.2021.115328.

Wang, Q. et al., 2022. Runoff and nutrient losses in alfalfa (Medicago sativa L) production with tied-ridge-furrow rainwater harvesting on sloping land. *International Soil and Water Conservation Research*, 10 (2), pp.308–323. doi: 10.1016/j.iswcr.2021.09.005.

Yang, Q. et al., 2021. Environmental and genetic regulation of plant height in soybean. *BMC Plant Biol*, 21, 63. doi: 10.1186/s 12870-021-02836-7

Zeraatpisheh, M. et al., 2020. Assessing the effects of deforestation and intensive agriculture on the soil quality through digital soil mapping. *Geoderma*, 363, 114139. doi: 10.1016/j.geoderma.2019.114139.

Zhao, F. et al., 2023. An increase in intercropped species richness improves plant water use but weakens the nutrient status of both intercropped plants and soil in rubber–tea agroforestry systems. *Agricultural Water Management*, 284, 108353. doi: 10.1016/j.agwat.2023.108353.

Zhong, Q. et al., 2019. The influence of climate, topography, parent material and vegetation on soil nitrogen fractions. *Catena*, 175, pp.329–338. doi: 10.1016/j.catena.2018.12.027.

Research Article

Daily Activity and Honey Production Patterns of *Tetragonula laeviceps* Smith (Hymenoptera: Apidae) During the Wet and Dry Seasons

Andi Gita Maulidyah Indraswari Suhri[1], Bambang Retnoaji[2]*, Yusdar Mustamin[3], Sih Kahono[4]

1) Department of Biology, Faculty of Mathematics and Natural Sciences, Universitas Hasanuddin, Makassar City, South Sulawesi, Indonesia, 90245.
2) Faculty of Biology, Universitas Gadjah Mada, Jl. Teknika Selatan, Sleman, Yogyakarta, Indonesia, 55281.
3) Graduate School of Life Sciences, Tohoku University, 2-1-1 Katahira, Aoba-Ku, Sendai, Japan, 980-8588.
4) Research Center for Applied Zoology, National Research, and Innovation Agency (BRIN), Cibinong, Bogor, West Java, Indonesia, 16911.
* Corresponding author, email: bambang.retnoaji@ugm.ac.id

ABSTRACT

Honey production by stingless bees is closely related to the foraging activities of worker bees, particularly nectar foraging. The urgency of this study stems from the community's need for adequate understanding and information on honey production which can vary due to various factors, such as forage and season. The purpose of this study was to determine the extent to which foraging activity affects the amount of honey produced by *T. laeviceps* during the rainy and dry seasons. The focal sampling method was used to observe foraging behaviour and the acetolysis method was used to observe pollen. The abiotic factors were measured through direct observation. Honey production was observed as a result of foraging behaviour and variations in abiotic factors. In SPSS v27 software, data from foraging behaviour observations were analysed using one-way ANOVA followed by Tukey's test with 95% confidence level and interpreted in tables and figures. Multiple linear regressions and Pearson's correlations were used to test the relationship between abiotic variables and bee return to hive behaviour. All honey volume data were collected, averaged, and evaluated using bar charts. Based on these results, the amount of honey produced by *T. laeviceps* in the dry season was significantly higher than that produced during the wet season. This was because the number of bees actively foraging was also higher in the dry season (June-August) which was strongly influenced by temperature and light intensity ($p > 0.05$). In addition, the number of flowering plants available for harvest during the dry season was higher than that during the rainy season. The results of this study can be used as a reference by beekeepers to determine the appropriate time to harvest honey. Information on the types of forage plants identified in this study can provide information on bee preferences in making choices related to forage plants.

INTRODUCTION

Tetragonula laeviceps Smith is a type of social insect that only produces very small amounts of honey. Its small body size (2-3 mm) and honeypot diameter (1-2 mm) are some of the reasons why it produces very little honey. However, other factors, such as the availability of food sources,

flowering season, and abiotic factors, also influence stingless bee honey production. Stingless bees organise their lives into colonies and build their nests in the nooks and crannies of walls, logs, and stones (Gadhiya & Pastagia 2019). The utilisation of *T. laeviceps* has also been widely reported as a pollinator for various plants (Chuttong et al. 2022). *Tetragonula laeviceps* has the ability to visit a wide variety of flowers such as vegetable crops, fruit crops, oilseed crops, crops, fodder forage crops, weed crops, also ornamental and flower crops. In Indonesia, *T. laeviceps* has been widely recognised and cultivated for honey production and pollination. Various plant species such as *Citrus reticulata*, Family Bromeliaceae and Cyperaceae are favorite plants of *T. laeviceps* (Riendriasari & Rahayu 2022; Aldi et al. 2023). In general, beekeepers cultivate *T. laeviceps* around agroecosystem areas due to the compatibility between the morphology of agricultural crop flowers and the morphology of *T. laeviceps*. Both internal and external factors have been shown to affect the behaviour of bees during flight. It is possible that the flying activity that occurs during the intrinsic phase is related to the colony's reproductive phase. In the species *Plebeia* distant, worker bees gather more pollen in the summer and more nectar in the winter (Nunes-Silva et al. 2010; Nunes-Silva et al. 2013).

It has also been found that the activity level of stingless bees while they are in flight is related to the overall production of the colony. Honey production is an example of something that is heavily influenced by abiotic factors such as temperature, humidity, rainfall, light intensity, and wind speed. Honey production is also heavily influenced by the number of flowers that are available, as well as the amount of nectar that is collected by the worker bees (Agussalim et al. 2017; Agussalim et al. 2020). In addition to foraging activity, hive shape and size can also affect honey production, although it does not significantly affect it (Agussalim et al. 2023). The urgency of this research is the need for adequate understanding and information to the community regarding honey production that can change due to several factors, including feed and season. Because bees respond to climatic variables, studies of flight activity and resource collecting aid in understanding the ecological are niche of species. Temperature, relative humidity, light intensity, wind, and air pressure can all influence social insect flight activity. Foraging patterns can change seasonally in response to biological factors such as blossoming (Polatto et al. 2014). Most bee habitats have distinct seasons with variable climatic conditions; nonetheless, changing weather conditions can have a significant impact on bee activity. The objective of this study is to investigate the effect that the flying activity of *T. laeviceps* has on the amount of honey that is produced during both the wet and dry seasons. This research is expected to be a reference for the beekeepers of stingless bee *T. laeviceps* in determining the appropriate feed and treatment to obtain optimal honey production throughout the year.

MATERIALS AND METHODS
Materials
This research was conducted in the Indonesian provinces of Bantul, Purworejo, and Magelang during the wet season (December 2021–February 2022) and the dry season (June 2022–August 2022). At each study site, seven colonies were used in this study. The colonies employed during wet season observations were the same colonies used during the dry season.

Methods

Bee identification

First, collection, preservation, and species identification were carried out to confirm the observed bee species. Stingless bees were soaked in hot water for a few minutes to help them relax. This allows for better organisation of bee body sections. The stingless bees were then punctured with an insect size 00 needle (0.30 mm in diameter). The needle was then inserted in either the dorsal or lateral thorax. As a result, embedding has occurred. The puncturing method is designed to make it easier to observe under a microscope. Morphological features were studied and photographed with a stereomicroscope and Optilab 2.2. Observed morphological characteristics include the hind tibia, basitarsus, malar space, mandible, head, clypeus, propodeum, mesoscutum, mesoscutellum, antennae, eyes, gena, forewing, wing venation, hamuli, and body color (head, clypeus, thorax, abdomen, tegula, and wings). (Azizi et al. 2020). The identification was based on (Sakagami 1978).

Foraging behaviour

Foraging behaviour of *T. laeviceps* as well as honey production were the variables that were investigated for this study. Observation of foraging behaviour using focal sampling method (Martin & Bateson 1986). Ten days per month were spent at each site to observe the behavior of *T. laeviceps* returning to the nest. The foraging behavior of *T. laeviceps* was recorded by a CCTV camera installed at one meter from the nest. For fifteen minutes, at ten-minute intervals, a counter was used to count the number of worker bees that brought pollen back to the hive as well as the number of worker bees that did not. Observations continued until *T. laeviceps* stopped foraging.

Measurement of abiotic factors

Parameters measured included air temperature and humidity using a thermohygrometre, wind speed using an anemometre, light intensity using a luxmeter, elevation using an altimetre, and rainfall using an ombrometre. Measurement of abiotic factors was carried out during the bees' foraging activities. Measurement of these abiotic factors was carried out in conjunction with observations of foraging activities for ten days per month.

Measurement of honey volume

A measurement of honey production quantity was conducted to determine the fluctuation of honey volume produced by *T. laeviceps* during the rainy and dry seasons. The measurement of honey volume is carried out in accordance with the honey harvesting schedule by local farmers. At the time of honey volume measurement, the last honey harvest by the farmer was two months before the study took place.

Pollen collection, preservation, and identification

Pollen collection on *T. laeviceps* limbs was conducted in the morning for 3 days at each site. Pollen collection was done at 10-minute intervals during nest entry and exit observations. Pollen-carrying bees were captured at the nest entrance using an insect net. Pollen found on the limbs of worker bees was taken using tweezers and then put into an Eppendorf tube in dry conditions. After the pollen was collected, the bees were released again. The collected pollen was separated based on the location and time of sampling. Preparation and observation of pollen morphology were carried out on all collected pollen samples. Pollen preparation is

done using the acetolysis method (Erdtman 1972). The acetolysis stage is when the pollen is put into a 1.5-ml Eppendorf tube and acetyl anhydride is added: H2SO4 in a ratio of 9:1. The tube containing the pollen was heated using a water bath at a temperature of 80–90°C for 5 minutes. Next, the supernatant was discarded, 1 ml of distilled water was added, and the mixture was centrifuged at 12000 rpm for 2 minutes, then the supernatant was discarded and distilled water was added until the supernatant was clear. The supernatant was discarded, and then the sample was put into an oven at 60°C for one night with the Eppendorf lid open. After overnight, the samples were removed from the oven, and pollen preparations were made. On the dried samples, each was dripped with 1 ml of glycerine and then stirred. A drop of sample was taken using a drop pipette and dripped on a glass slide, then covered with a cover glass. The pollen preparations were observed using a compound microscope and an Optilab connected to a computer. The identification of pollen refers to the Pollen Flora of Taiwan (Huang 1972) and the Australian Pollen and Spores Atlas at http://apsa.anu.edu.au/ (APSA 2017).

Data analysis
Data from observations of foraging behaviour were analysed using a one-way ANOVA followed by a Tukey test with a 95% confidence level on SPSS v27 software and interpreted in tables and figures. Correlations between abiotic factors and bee return to hive behaviour were analysed using multiple linear regression and Pearson correlation. All honey volume data were combined, averaged, and interpreted in the form of bar charts.

RESULTS AND DISCUSSION
Foraging activity of *T. laeviceps*
Between the months of December and February, there was a decrease in the number of worker bees that are out collecting food in their natural habitat and older surroundings (the wet season). Nonetheless, there was a rise in foraging activity between June and August (the dry season).

In December 2021, the average number of bees carrying out foraging activities in Bantul was 257,991±60,902 individuals; in Purworejo there was 517,681±87,513 individuals; in Magelang there was 335,215±63,608 individuals (Figure 1).

In January 2022, the average number of bees carrying out foraging activities in Bantul was 519,742±87,531 individuals; in Purworejo there was 489,913±87,523 individuals; in Magelang there was 525,761±69,811 individuals (Figure 2).

In February 2022, the average number of bees carrying out foraging activities in Bantul was 506,827±69,235 individuals; in Purworejo there was 508,1193±62,113 individuals; in Magelang there was 477,138±54,108 individuals (Figure 3).

In June 2022, the average number of bees carrying out foraging activities in Bantul was 486,714±53,125 individuals; in Purworejo there was 586,991±56,218 individuals; in Magelang there was 708,423±49,106 individuals (Figure 4).

In July 2022, the average number of bees carrying out foraging activities in Bantul was 723,918±45,112 individuals; in Purworejo there was 612,68±45,521 individuals; in Magelang there was 603,308±39,515 individuals (Figure 5).

In July 2022, the average number of bees carrying out foraging activities in Bantul was 604,122±40,715 individuals; in Purworejo there was 765,131±39,143 individuals; in Magelang there was 695,724±36,311 individuals (Figure 6).
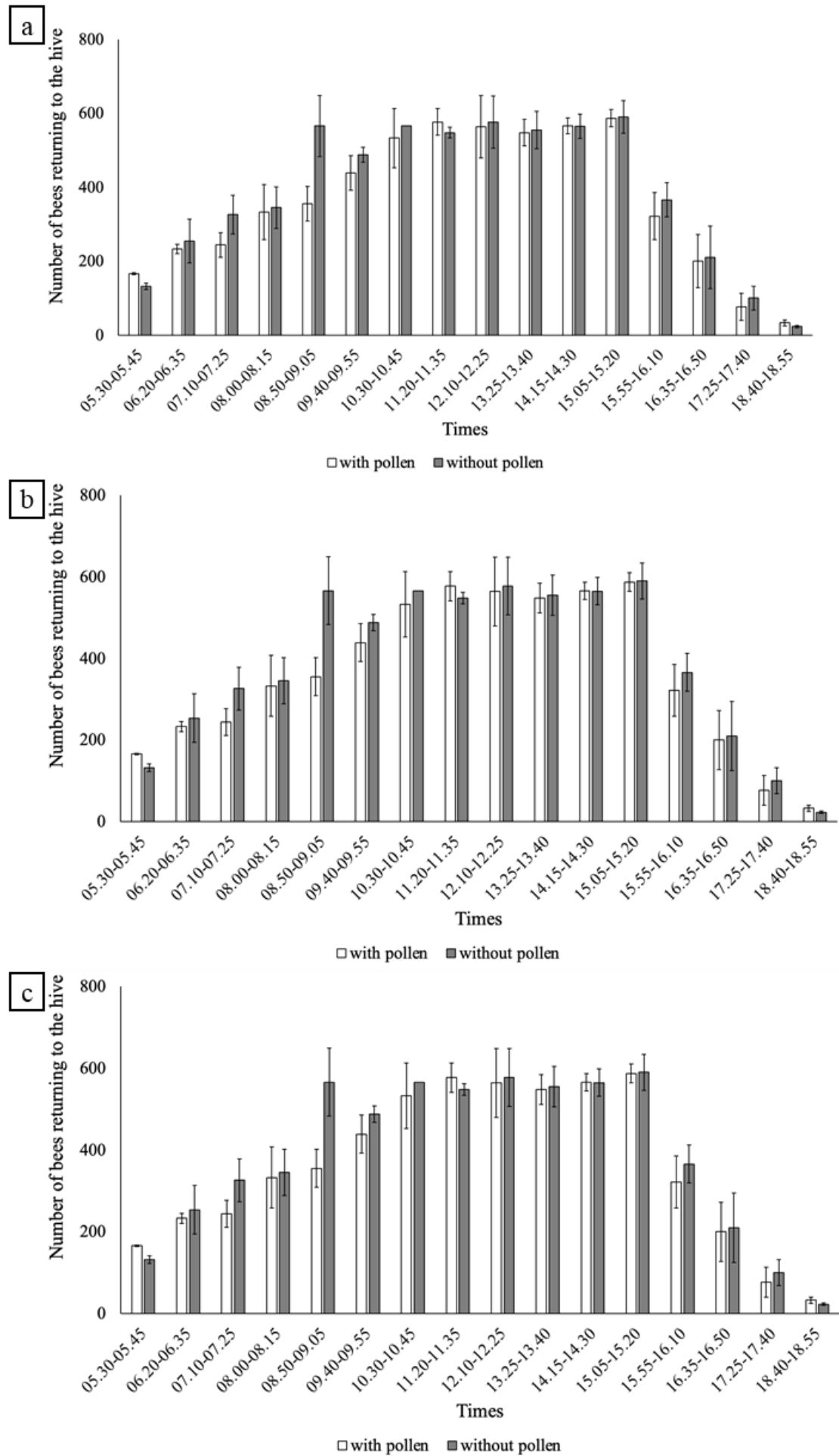
Figure 1. The number of *T. laeviceps* bees returning to the hive in December 2021 (wet season): a) Bantul, b) Purworejo, c) Magelang. Bars = standard deviation.
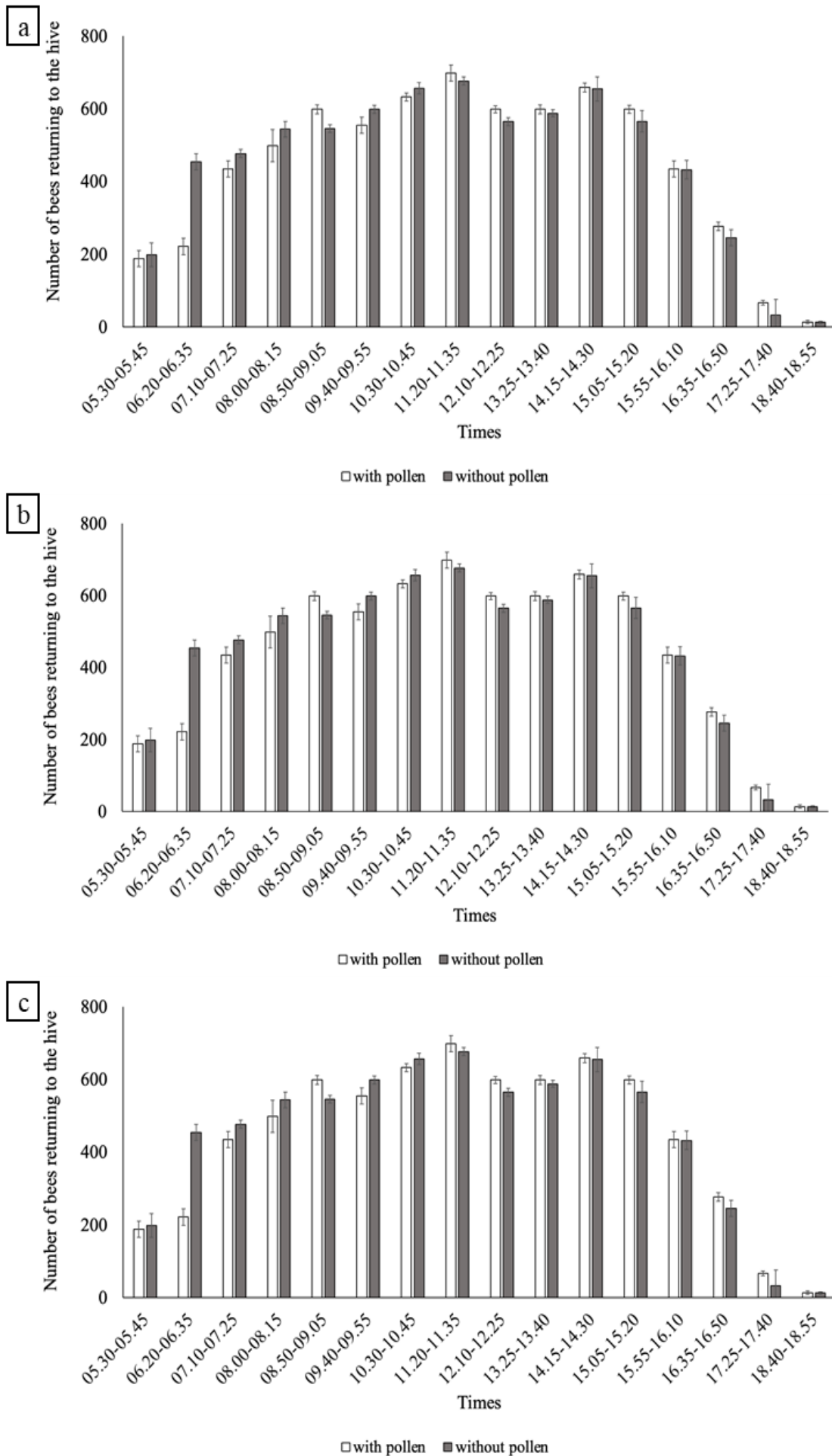
Figure 2. The number of *T. laeviceps* bees returning to the hive in January 2022 (wet season): a) Bantul, b) Purworejo, c) Magelang. Bars = standard deviation.
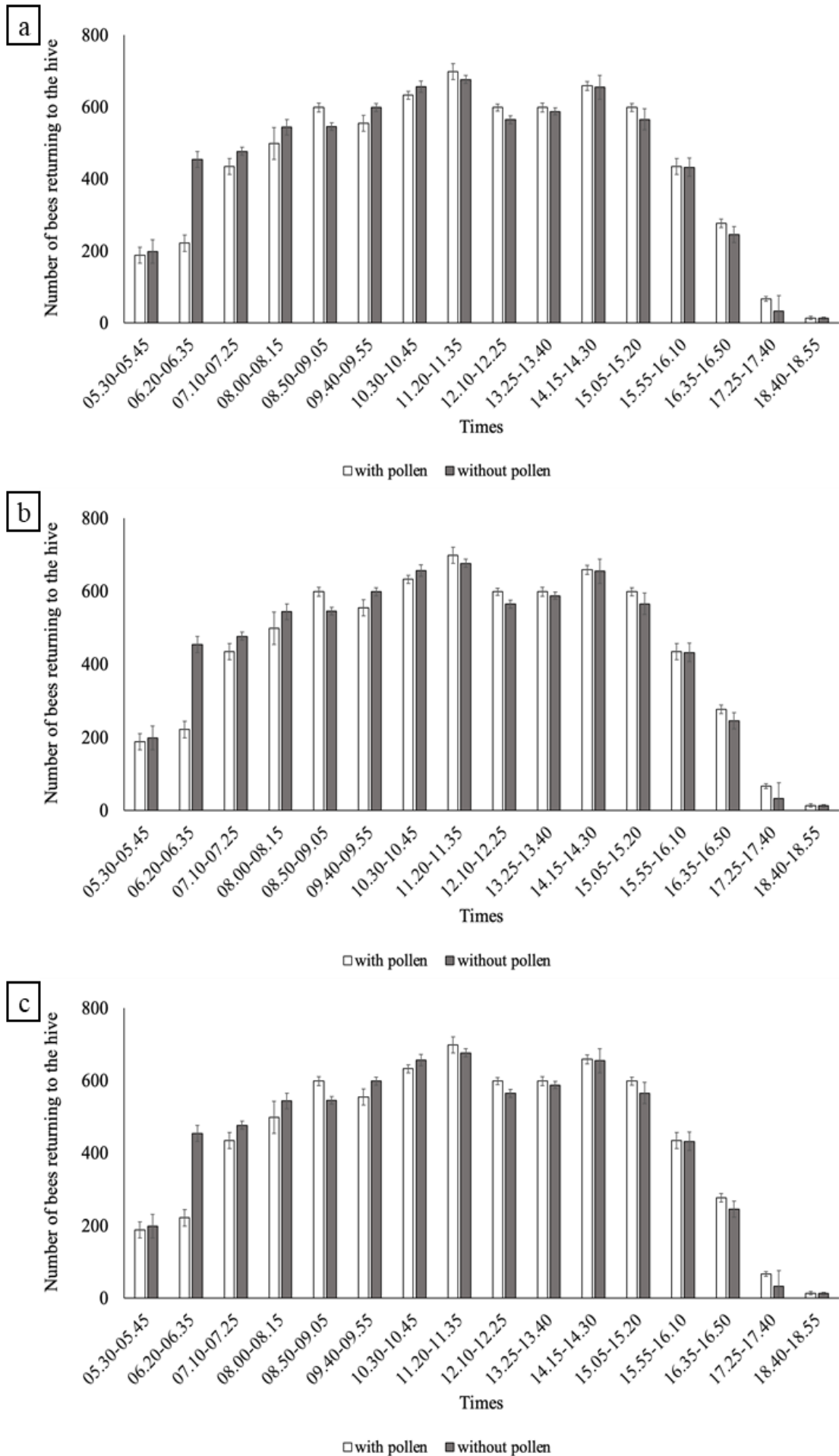
Figure 3. The number of *T. laeviceps* bees returning to the hive in February 2022 (wet season): a) Bantul, b) Purworejo, c) Magelang. Bars = standard deviation.
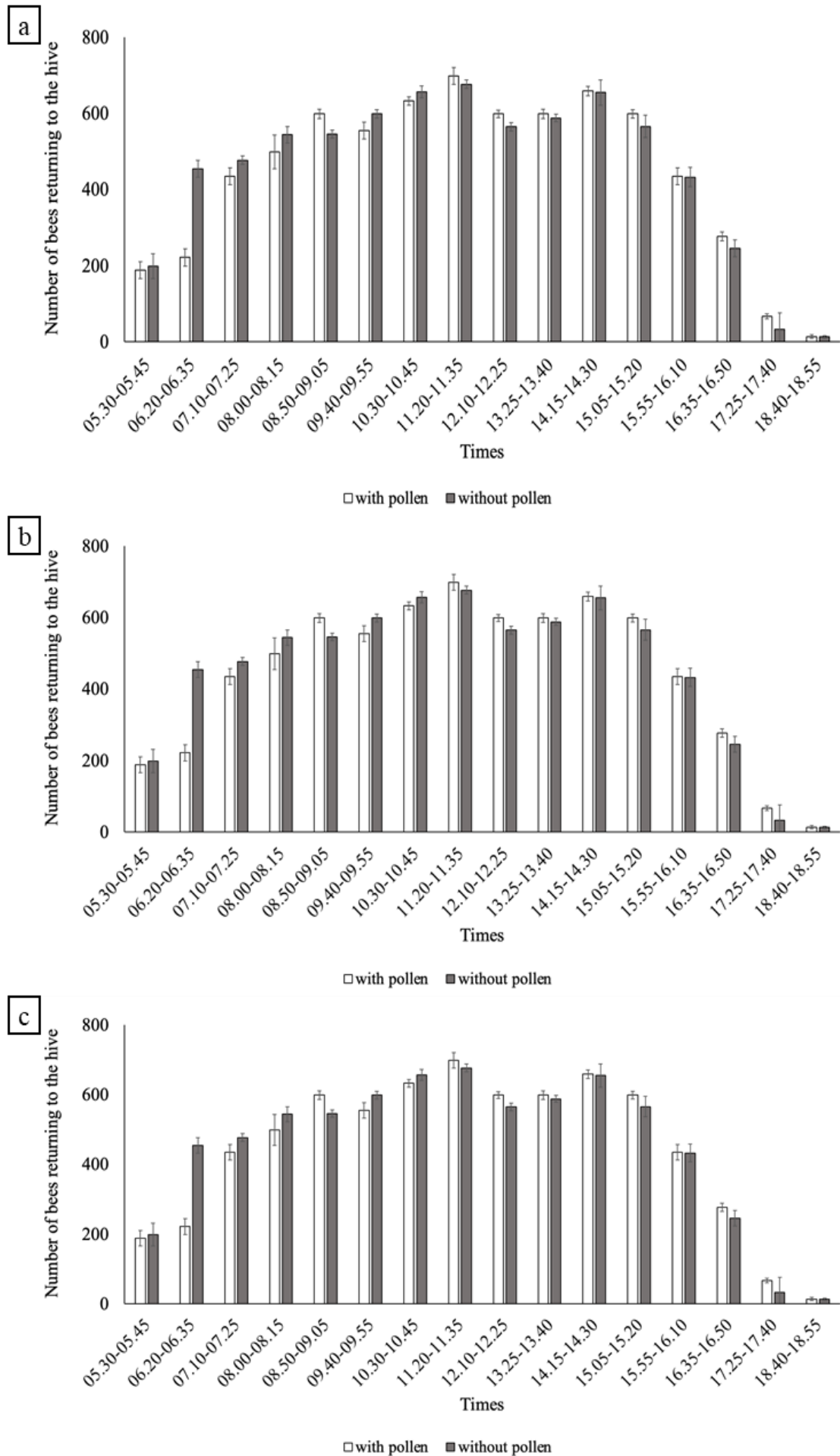
Figure 4. The number of *T. laeviceps* bees returning to the hive in June 2022 (dry season): a) Bantul, b) Purworejo, c) Magelang. Bars = standard deviation.
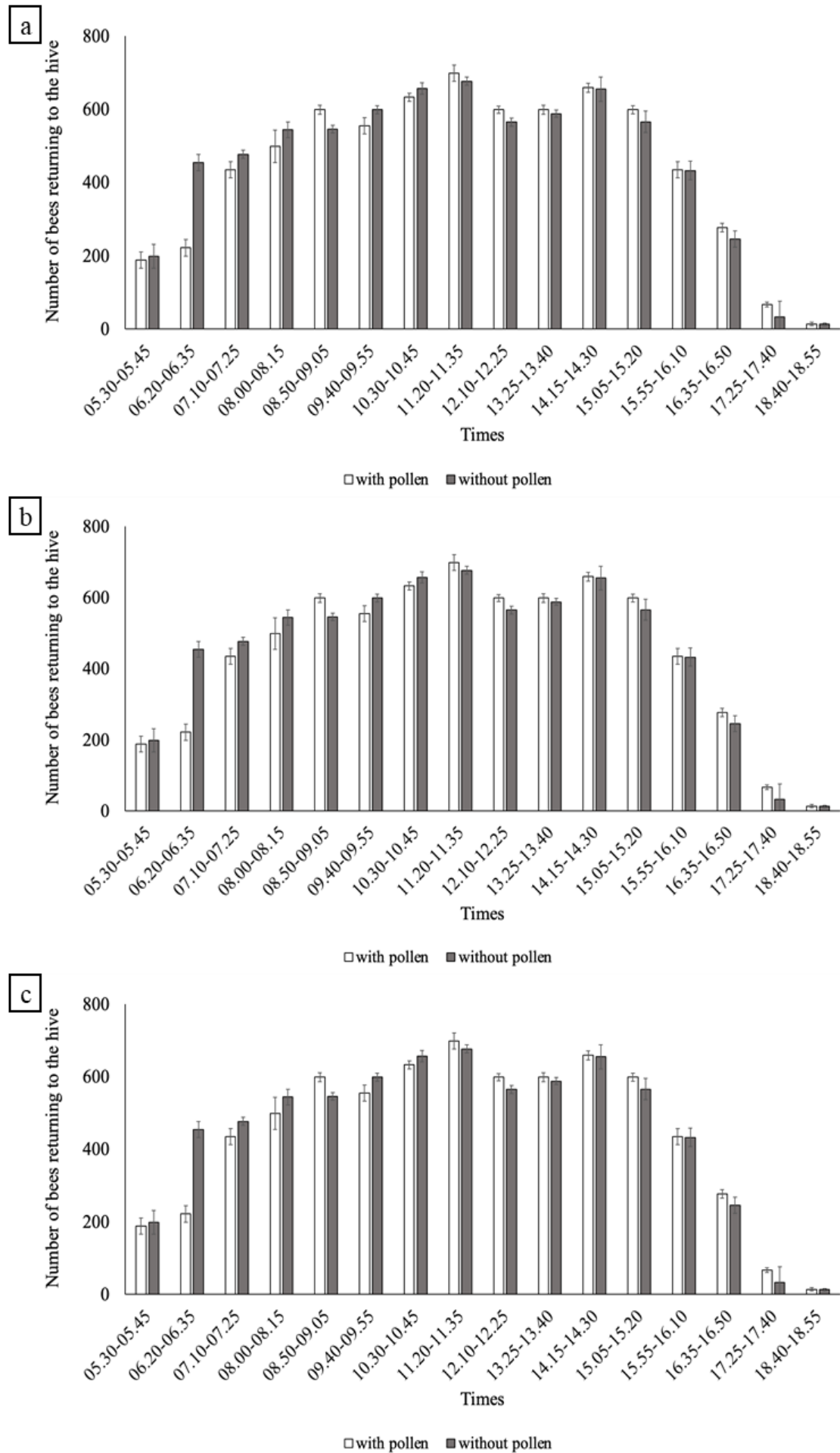
Figure 5. The number of *T. laeviceps* bees returning to the hive in July 2022 (dry season): a) Bantul, b) Purworejo, c) Magelang. Bars = standard deviation.
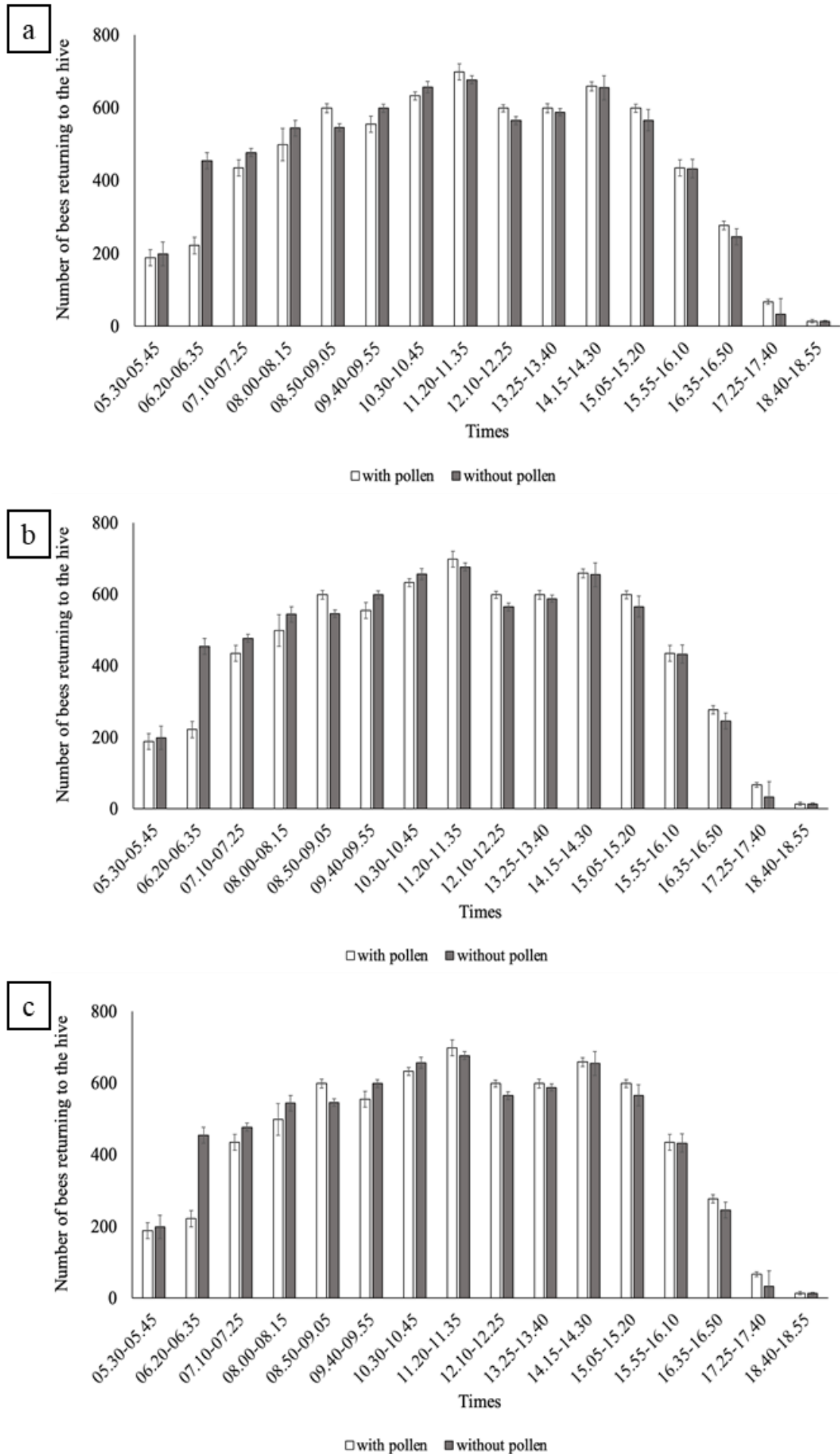
Figure 6. The number of *T. laeviceps* bees returning to the hive in August 2022 (dry season): a) Bantul, b) Purworejo, c) Magelang. Bars = standard deviation.

There was a possibility that the distance travelled by air was not directly proportionate to the distance covered by natural forage. The orientation of the feeding source could be the cause of the capacity to return to the nest after being displaced over a great distance. This extremely large gap between these bees' potential flight distance and their actual flight distance can be attributable to the quality of the resources and the spatial distribution of those resources (Westphal et al. 2006). Pollen is often the only resource that bees are choosy over, as opposed to nectar, hence foraging regions for these two resources may be different (Biesmeijer & Slaa 2004).

Correlation between abiotic factors and foraging activity of *T. laeviceps*

Foraging behaviour in social bees can be influenced not only by the demands of the colony but also by abiotic elements such as temperature, the amount of light present, and the speed of the wind. The geographic distribution of insects and other ectotherms can be partially explained by temperature, making temperature a significant aspect in this explanation (Wallace & Lee 2010).

Table 1. Correlation of abiotic factors with the activity of *T. laeviceps* in the new environment.

Abiotic factors	Significance value	Pearson correlation value	Adjusted R square	R square
Temperature	0,071	0,522		
Humidity	0,045	0,694		
Light intensity	0,054	0,528	0,227	0,810
Wind velocity	0,102	-0,421		
Rainfall	0,045	0,533		

There was a substantial connection between abiotic conditions and bees' ability to engage in foraging behaviour as shown by the fact that the number of bees that return to the hive has a correlation value of 0.81 with abiotic factors (Table 1). The coefficient of determination was 0.227 which indicated that abiotic factors impacted 22% of the foraging activity of *T. laeviceps* in the new environment, whereas biotic factors influenced 78% of the foraging activity. The significant effect of biotic factors on the number of bees that returned to the nest of *T. laeviceps* was known at the same time as the significance value of each abiotic factor was determined. There was no effect of any biotic component on the foraging behaviour of *T. laeviceps* in the new environment ($p > 0.05$).

There was an increase in the number of bees going in and out of the hive during the day with the light intensity varying from 1789 x 10 lux to 3282 x 100 lux, according to the observations that were made. Bees use the light to guide them as they look for food. The forager's visual acuity is improved, and the bee's body temperature is raised because of the increased light intensity (Heard & Hendrikz 1993; Polatto et al. 2014). On the other hand, activity dropped off significantly in the afternoon or when the weather was cloudy, and the light intensity was 1000 lux. This condition arises because of low levels of light intensity, which reduce the insects' capacity to see well enough to fly. In the morning, the temperature has a significant impact on the number of bees that leave the nest, whereas in the afternoon, the intensity of the light has the greatest bearing on this behaviour. In Batusangkar, West Sumatera, a study found that environmental factors such as temperature, light intensity, and hu-

midity collectively influenced the activity of *T. laeviceps* worker bees by 78%. The remaining 22% was believed to be influenced by unknown factors. These stingless bees were observed to be active from early morning when the temperature was 26°C, humidity was 87%, and light intensity was 720 Lux. The activity of the hive tended to increase as temperature and light intensity rose, while humidity decreased. Specifically, 11:00 am was recorded as the time with the highest average number of workers entering the nest (Puteri et al. 2022). The study conducted by Salatnaya et al. (2019) on *T. laviceps* in monoculture and polyculture gardens showed that the environment plays a crucial role in influencing the entry and exit activities of bees, which in turn affects propolis production. The highest level of bee activity was recorded when the temperature reached 26-28°C, humidity was between 55-71%, and light intensity was 46,875-91,347 lux. The environment also had an impact on the amount of propolis produced, with 27.79 g being produced in the monoculture garden and 48.80 g in the polyculture garden. The significant difference in propolis production was mainly attributed to environmental factors (Salatnaya et al. 2020).

It is possible for each species or group to have a unique reaction to the abiotic elements present, even when they are in the same environment. In addition, the same species can have very warious responses depending on the habitat in which it is living. A variety of abiotic elements, such as temperature, light intensity, humidity, wind speed, and rainfall, can influence the bee activity in a particular region. Because the bee's thoracic muscle needs to attain a particular temperature before it can fly, one of these factors can influence the outcome of the situation (Woods et al. 2005).
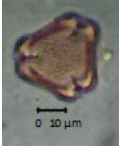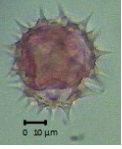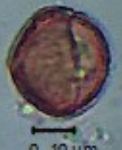
Pollen collected by *T. laeviceps* during the dry and wet seasons.

Tetragonula laeviceps bees collect more diverse pollen during the dry season than during the wet season. Pollen types identified based on identification results include *Xanthostemon chrysantus* (Myrtaceae), *Chromolaena odorata* (Asteraceae), *Picria felterrae* (Linderniaceae), *Zea mays* (Poaceae), *Portulaca oleracea* (Portulacaceae), *Antogonon leptopus* (Polygonaceae), *Euphorbia pulcherrima* (Euphorbiaceae), *Punica granatum* (Punicaceae), *Carica papaya* (Caricaceae) (Table 2).

Because illnesses are more prevalent in the environment during the wet season, there are less flowering plants than there are during the dry season. This is due to the fact that plants are more susceptible to attacks during the rainy season. In addition, precipitation of sufficient intensity causes pollen to be washed away and deteriorate, so it prevents reaching the stage of pollination (McLaren & McDonald 2005; Wijesinghe et al. 2020). Plant phenology is the outcome of the combination of biotic and climatic conditions which through the process of natural selection defines the optimal times for growth and reproduction. Because of the influence that seasonality has on patterns of seed generation, germination, seedling survival, and growth, the timing and duration of rainfall are two of the most important factors to consider when attempting to comprehend the dynamics of tropical dry forests (Khurana & Singh 2001; Borchert et al. 2004)

Honeybees collect two types of food besides water: nectar which is converted into honey and serves as a source of carbohydrates, and pollen which fulfilled the colony's need for proteins, minerals, and fats. Pollen is essential not only for the production of brood food but also for the development of tissues in newly emerged workers, such as the hypopharyngeal glands and fat bodies, which are necessary for brood rearing and winter-

Table 2. Types of pollen collected by *T. laeviceps* in the dry and wet seasons.

Pollen types	Family	Species	Seasons	
			Wet season	Dry season
	Myrtaceae	*Xanthostemon chrysantus*	√	√
	Asteraceae	*Chromolaena odorata*	√	√
	Linderniaceae	*Picria felterrae*		√
	Poaceae	*Zea mays*		√
	Portulacaceae	*Portulaca oleracea*	√	√
	Polygonaceae	*Antogonon leptopus*	√	√
	Euphorbiaceae	*Euphorbia pulcherrima*		√
	Punicaceae	*Punica granatum*		√
	Caricaceae	*Carica papaya*		√
	Passifloraceae	*Turnera subulata*	√	
	Asteraceae	*Ageratum conyzoides*	√	

ing (Hoover & Ovinge 2018). The consumption of pollen by adult workers depends on their age and the tasks they perform with nurse bees that are actively involved in brood rearing and feeding the queen consuming relatively large amounts of pollen. Although no direct correlation was observed between pollen and honey production, the type of pollen collected by bees may indicate the type of plants visited by worker bees. This is significant because it is difficult to identify the plants that bees visit to collect nectar.

Honey production in all locations during the wet and dry seasons

In Indonesia, beekeeping plays a significant role in the way of life of the country's rural population. Because of this, it is necessary to ensure that an adequate quantity of honey is produced. During the dry season, several different bee species, including *T. laeviceps,* can produce enormous quantities of honey. On the other hand, honey production drops significantly during the wet season. Honey production is affected by several factors, including the size of the colony, the kind and quantity of feed sources, and foraging activity (Abou-Shaara et al. 2017). Each worker bee in a colony of stingless bees is only capable of transporting a single food item when it goes out to forage (Fikru 2015; Hoover & Ovinge 2018). Honey production is directly proportional to the number of nectar-producing plants and foragers present in the area surrounding the hive.

Honey production in *T. laeviceps* was greater during the dry season which lasted from June to August, as opposed to the wet season which lasted from December to February (Figure 7). This was because there is a larger quantity of flowers available during the dry season, as well as a greater variety of those flowers, in comparison to the wet season. The decrease in the number of bees that returned to the nest during the rainy season was the indication that the foraging rate of *T. laeviceps* dropped during this time as well. Honey production by *T. laeviceps* rose across the board at all the research sites as a direct result of increased foraging activity during the dry season. The results of the pollen identification of *T. laeviceps* showed that the number of flowering plants that were available was lower during the rainy season. This was a factor that contributed to the reduction in honey production that took place between December and February. Research results related to *T. laeviceps* honey in Subang and Cileunyi Wetan showed that the color of honey could range from clear yellow to cloudy brown, which was influenced by the location where it was cultivated. Its taste can be sour, as indicated in many studies, due to a combination of honey, pollen, and fermentation that occurs during storage in the honey pot (Abduh et al. 2020). The flavour of honey was also influenced by the types of food and abiotic factors that were available to bees during their foraging activities.

The amount of honey produced by *T. laeviceps* in the wet and dry seasons was proportional to the number of pollen species collected. In the rainy season, there were fewer flowering plants, resulting in less honey production. During the dry season, the number and types of flowering plants were greater, resulting in increased honey production. Honey production by bees was the result of a series of interconnected factors. The conditions of abiotic factors were influenced by the season, and vice versa. Abiotic factors also influenced the foraging activities of worker bees. Foraging activity ultimately determined the quality and quantity of the material brought back to the hive.
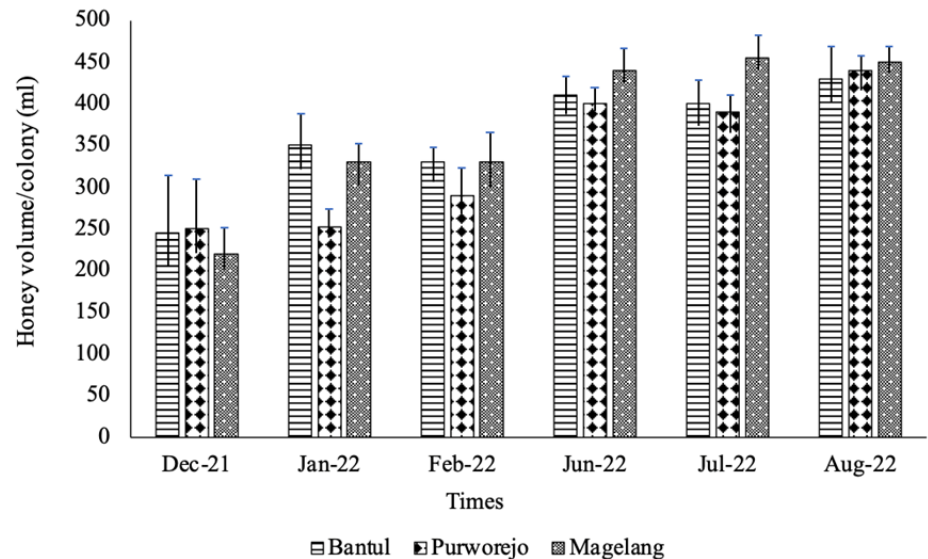
Figure 7. Honey volume per colony on *T. laeviceps* in the wet season (December -February) and dry season (June-August). Bars = standard deviation.

CONCLUSION
The variables that had a significant impact on the foraging activity of *T. laeviceps* were temperature and light intensity, whereas humidity and wind speed did not. Foraging activity of *T. laeviceps* was higher during the dry season than it was during the wet season. This was likely due to the possibility of a greater number of flowers being present during the dry season. As a result, there was a greater availability of pollen and nectar during the dry season. The foraging activity of worker bees influenced the amount of honey produced by the *T. laeviceps* species. *Tetragonula laeviceps* was seen to be more active in its nectar collection activities during the dry season as opposed to the wet season.

AUTHOR CONTRIBUTION
A.G.M.I. collected and analysed the data and wrote the manuscript. Y.M. analysed the data and wrote the manuscript. B.R. and S.K. designed the research and supervised all the process.

CONFLICT OF INTEREST
There is no conflict of interest regarding the research or the research funding.

REFERENCES

Abduh, M.Y. et al., 2020. Production of propolis and honey from *Tetragonula laeviceps* cultivated in Modular *Tetragonula* Hives. *Heliyon*, 6(11), e05405. doi: 10.1016/j.heliyon.2020.e05405.
Abou-Shaara, H.F. et al., 2017. A review of impacts of temperature and relative humidity on various activities of honey bees. *Insectes Sociaux*, 64(4), pp.455–463. doi: 10.1007/s00040-017-0573-8.

Agussalim et al., 2017. Variation of Honeybees Forages As Source of Nectar and Pollen Based on Altitude in Yogyakarta. *Buletin Peternakan*, 41(4), pp.448-460. doi: 10.21059/buletinpeternak.v41i4.13593.

Agussalim et al., 2020. The honey and propolis production from Indonesian stingless bee: *Tetragonula laeviceps*. *Livestock Research for Rural Development*, 32, 121.

Agussalim et al., 2023. The Effect of Daily Activities Stingless Bees of Trigona sp. on Honey Production. *The 7th International Seminar on Tropical Animal Production*, pp.223-227.

Aldi, N.M., Yusuf, A.M. & Permana, A.D., 2023. Effects of meliponiculture *Tetragonula laeviceps* on pollinator diversity and visitation rate and citrus productivity in West Java, Indonesia. *Biodiversitas*, 24 (10), pp.5757–5763. doi: 10.13057/biodiv/d241058.

APSA, 2017, 'Australasian pollen and spore atlas' in *Australasian pollen and spore atlas*, The Australian National University, viewed at 27 March 2023, from https://apsa.anu.edu.au/.

Azizi, M.G., Priawandiputra, W. & Raffiudin, R., 2020. Morphological identification of stingless bees from Belitung. *IOP Conference Series: Earth and Environmental Science*, 457, 012011. doi: 10.1088/1755-1315/457/1/012011.

Biesmeijer, J.C. & Slaa, E.J., 2004. Information flow and organization of stingless bee foraging. *Apidologie*, 35(2), pp.143–157. doi: 10.1051/apido:2004003.

Borchert, R. et. al., 2004. Environmental control of flowering periodicity in Costa Rican and Mexican tropical dry forests. *Global ecology and Biogeography*, 13(5), pp.409-425. doi.org/10.1111/j.1466-822X.2004.00111.x

Chuttong, B. et al., 2022. Foraging behavior and pollination efficiency of honey bees (*Apis mellifera* L.) and stingless bees (*Tetragonula laeviceps* species complex) on mango (*Mangifera indica* L., cv. Nam Dokmai) in Northern Thailand. *Journal of Ecology and Environment*, 46 (15), pp.1-7. doi: 10.5141/jee.22.012.

Erdtman, G., 1972. *Pollen morphology and plant taxonomy: an introduction to palynology*, Haffner publishing.

Fikru, S., 2015. Review of Honey Bee and Honey Production in Ethiopia. *Journal of Animal Science Advances*, 5(10), pp.1413-1421. doi: 10.5455/jasa.20151019083635.

Gadhiya, V. & Pastagia, J., 2019. Foraging behavior of stingless bees, *Tetragonula laeviceps* Smith in net house condition. *Journal of Entomology and Zoology Studies*, 7(6), pp.1005–1009.

Heard, T.A. & Hendrikz, J.K., 1993. Factors influencing flight activity of colonies of the stingless bee trigona carbonaria (Hymenoptera: Apidae). *Australian Journal of Zoology*, 41(4), pp.317–323. doi: 10.1071/ZO9930343.

Hoover, S.E. & Ovinge, L.P., 2018. Pollen collection, honey production, and pollination services: Managing honey bees in an agricultural setting. *Journal of Economic Entomology*, 111(4), pp.1509–1516. doi: 10.1093/jee/toy125.

Huang, T.C., 1972. *Pollen flora of Taiwan*, National Taiwan University, Botany Department Press.

Khurana, E. & Singh, J.S., 2001. Ecology of seed and seedling growth for conservation and restoration of tropical dry forest: A review. *Environmental Conservation*, 28(1), pp.39–52. doi: 10.1017/S0376892901000042.

Martin, P. & Bateson, P., 1986. *Measuring behaviour: An introductory guide*, Cambridge University Press.

McLaren, K. P. & McDonald, M. A., 2005. Seasonal patterns of flowering and fruiting in a dry tropical forest in Jamaica. *Biotropica*, 37(4), pp.584–590. doi: 10.1111/j.1744-7429.2005.00075.x.

Nunes-Silva, P. et al., 2010. Foraging activity in Plebeia remota, a stingless bees species, is influenced by the reproductive state of a colony. *Psyche: A Journal of Entomology*, 2010(1), 241204. doi: 10.1155/2010/241204.

Nunes-Silva, P. et al., 2013. The Behaviour of *Bombus Impatiens* (Apidae, Bombini) on Tomato (*Lycopersicon Esculentum* Mill., Solanaceae) Flowers: Pollination and Reward Perception. *Journal of Pollination Ecology*, 11, pp.33–40. doi: 10.26786/1920-7603(2013)3.

Polatto, L.P., Chaud-Netto, J. & Alves-Junior, V.V., 2014. Influence of Abiotic Factors and Floral Resource Availability on Daily Foraging Activity of Bees: Influence of Abiotic and Biotic Factors on Bees. *Journal of Insect Behavior*, 27(5), pp.593–612. doi: 10.1007/s10905-014-9452-6.

Puteri, G. et al., 2022. Foraging Activity of *Tetragonula laeviceps* Workers for Natural Resources and Nest Materials at a Polyculture Cropland in Batusangkar, Tanah Datar Regency, West Sumatra. *IOP Conference Series: Earth and Environmental Science*, 1059, 012086. doi: 10.1088/1755-1315/1059/1/012086.

Riendriasari, S.D. & Rahayu, A.A.D., 2022. The Foraging preference of stingless beekeeping in three types of land use at Lombok Island. *Jurnal Ilmu Kehutanan*, 16(2), pp.159–170. doi: 10.22146/jik.v16i2.3908.

Sakagami, S.F., 1978. Instructions for use *Tetragonula* Stingless Bees of the Continental Asia and Sri Lanka (Hymenoptera , Apidae) l) 2). *Journal of the Faculty of Science Hokkaido University, Zoology*, 21(2), pp.165–247.

Salatnaya, H. et al., 2020. The Influence of Environmental Factors on the Activity and Propolis Production of Tetragonula laeviceps. *Jurnal Ilmu Produksi dan Teknologi Hasil Peternakan*, 8(2), pp.67–71. doi: 10.29244/jipthp.8.2.67-71.

Wallace, H.M. & Lee, D.J., 2010. Resin-foraging by colonies of *Trigona sapiens* and *T. hockingsi* (Hymenoptera: Apidae, Meliponini) and consequent seed dispersal of *Corymbia torelliana* (Myrtaceae). *Apidologie*, 41(4), pp.428–435. doi: 10.1051/apido/2009074.

Westphal, C., Steffan-Dewenter, I. & Tscharntke, T. 2006. Foraging trip duration of bumblebees in relation to landscape-wide resource availability. *Ecological Entomology*, 31, pp.389–394.

Wijesinghe, S.A.E.C. et al., 2020. A global review of watermelon pollination biology and ecology: The increasing importance of seedless cultivars. *Scientia Horticulturae*, 271. doi: 10.1016/j.scienta.2020.109493.

Woods, W.A., Heinrich, B. & Stevenson, R.D., 2005. Honeybee flight metabolic rate: Does it depend upon air temperature? *Journal of Experimental Biology* 208(6), pp.1161–1173. doi: 10.1242/jeb.01510.

Research Article

Characterization of Lactic Acid Bacteria Isolated from Soymilk and Its Growth in Soymilk By-product Medium for the Application in Soymilk Fermentation

Faizah Diah Retnowati[1], Yekti Asih Purwestri[1]*, Yuni Sine[1]

1)Faculty of Biology, Universitas Gadjah Mada, Jalan Teknika Selatan, Sendowo, Sinduadi, Kec. Mlati, Kabupaten Sleman, Daerah Istimewa Yogyakarta 55281
* Corresponding author, email: yekti@ugm.ac.id

ABSTRACT

The separation phase of soy-product manufacturing, especially of soymilk production, involves using the liquid portion of soy while disposing primarily of the solid portion, known as soymilk by-product (SMB). The improper disposal of SMB can contribute to environmental concerns. As SMB contains many beneficial nutrients, this could serve as a valuable culture medium for lactic acid bacteria (LAB), especially considering the expense of the standard de Man, Rogosa, and Sharpe (MRS) medium. This study aimed to isolate and identify LAB from soymilk through 16S rRNA sequencing, assess the potential of SMB as a culture medium for LAB, and ferment soymilk with LAB cultured from SMB to demonstrate the probiotic capacity. The research identified a potential LAB as *Weissella confusa*. Effective cultivation of LAB was demonstrated at 2% SMB concentration, although LAB cultured with MRS medium yielded a higher colony count. Furthermore, fermentation of soymilk by the LAB isolates from SMB exhibited a positive probiotic ability, reaching 5.5×10^9 CFU/mL, with a lactic acid content of 0.27%.

INTRODUCTION

Soy is a staple food in many East Asian countries (Vanga & Raghavan 2018) and is widely consumed because of its versatility and nutritional value (Vanga & Raghavan 2018). Popular soy products include soymilk, tempeh, soy sauce, and various others that are enjoyed for their rich nutrient profiles. These products are favored for their abundance of proteins, dietary fiber-containing carbohydrates, vitamins, and minerals, all at a relatively low cost (Vanga & Raghavan 2018). With a protein content of up to 36.49% in its raw form, soy is one of the richest nonanimal sources of protein (Rizzo & Baroni 2018), making this a crucial dietary option for individuals adhering to vegan or vegetarian lifestyles.

Soymilk is one of the most successful soy-derived products and has been regularly consumed in most parts of the world as a replacement for dairy milk, often because of dietary preferences or intolerances. Lactose intolerance affects approximately 65% of the global population, according to Malik and Panuganti (2022), and is a prevalent issue with 75% to 100% of East Asian individuals experiencing lactose intolerance (Aydar et al. 2020).

However, the production of soy products, including soymilk, generates significant waste. During the processing of soybeans for products such as soymilk, the beans undergo soaking, grinding, separation, and pasteurization (Davy & Vuong 2022). During separation, the liquid soy portion is retained, whereas the solid by-product, known as soymilk by-product (SMB) or okara, is largely discarded (Davy & Vuong 2022).

Despite being discarded, SMB retains substantial nutrients, including proteins and carbohydrates, making this a potential resource for culturing lactic acid bacteria (LAB.) This is particularly valuable when considering the expense of standard culture media such as de Man, Ragosa, and Sharpe (MRS) medium (Hayek et al. 2019; Davy & Vuong 2022). Moreover, improper disposal of SMB poses environmental concerns because of decomposition processes, potentially impacting waterways during rainy weather.

Various studies, including those by Davy and Vuong (2022), Goda et al. (2011), and Kim (2019), have highlighted the potential of SMB as a culture medium for microorganisms such as *Pleurotus ostreatus* and *Phaeodactylum tricornutum*, yielding positive results. Aritonang et al. (2017) demonstrated the successful isolation of LAB from SMB, suggesting its suitability as a culture medium. The current study aims to explore the potential of using SMB for LAB culture media with a subsequent application in fermenting soymilk as a probiotic product to validate the probiotic efficacy of LAB cultured from SMB. Additionally, the study isolated LAB from fermented soymilk and applied 16S rRNA sequencing for their identification.

MATERIALS AND METHODS
Materials
For the preparation of soymilk and soymilk by-product (SMB), soybeans were sourced from Kranggan Traditional Market in the Special Region of Yogyakarta. For the isolation of LAB from soymilk, MRS broth medium and bacteriological grade agar powder was obtained from (HiMedia, Mumbai, India) and prepared using distilled water and saline as required.

For the morphological characterization of the isolated LAB, distilled water, crystal violet, iodine, 70% ethanol, safranin, microscope slides, and immersion oil were used for Gram staining. For the spore formation test, distilled water, filter paper, malachite green, safranin, microscope slides, and immersion oil were required. The motility test involved MRS broth, agar powder, and distilled water.

During the physiological and biochemical characterization, the catalase test required distilled water, microscope slides, and 3% hydrogen peroxide. Temperature and salt tolerance tests required MRS broth, NaCl, and distilled water.

The Bacteria DNA Isolation Kit by Geneaid was used for genomic DNA extraction. Electrophoresis required agarose, $1 \times$ Tris borate-EDTA buffer (TBE), FloroSafe DNA Stain (1st BASE), 1 Kb Plus DNA ladder, and loading dye. PCR used universal forward and reverse primers 27F (5′-AGAGTTTGATCCTGGCTCAG-3′) and 1427R (5′-GGTTACCTTGTTACGACTT-3′) and MyTaq™ HS Red Mix (Bioline).

Commercially used *Lactobacillus plantarum* was obtained from the Food and Nutrition Culture Collection in Universitas Gadjah Mada. For growing isolates and *L. plantarum* in SMB medium and MRS broth medium, materials included dried SMB, MRS broth medium, agar powder, saline solution, and disposable Petri dishes. During the soymilk fermentation by selected isolates and *L. plantarum*, materials such as MRS broth

medium, agar powder, universal indicator, saline solution, sterile diluent, disposable Petri dishes, phenolphthalein, and 0.1 N NaOH were used.

Methods

Preparation of soymilk and SMB

Soybeans were soaked for 24h to soften them, facilitating subsequent processes. After soaking, the soybeans were ground in a solution at a ratio of 8–10 parts water to 1 part beans. The resulting mixture was then separated using cheesecloth, with the liquid portion pasteurized and stored at 4°C. The solid portion, known as SMB, was dried in an oven at 100°C, being stirred every 15 min until a constant weight was achieved (Chun et al. 2007). The dried SMB was subsequently ground and sieved to achieve a consistent particle size (Malik et al. 2022), and finally stored in a cool, dry place until required.

Isolation of LAB from soymilk

Pasteurized soymilk (150 mL) was collected in an airtight container and left to ferment for 3 days. LAB isolation was conducted by serial dilutions of 1 mL of the fermented soymilk mixed with 9 mL of sterile saline solution. From this diluted sample, 0.1 mL was plated on MRS agar using the pour plate method (Sanders 2012). Plates were incubated at 37°C for 24–48 h. Macroscopic differences in colony morphologies were observed, and LAB growth was selected accordingly. Selected colonies were then streaked on MRS agar to obtain pure cultures. Pure cultures were preserved on MRS agar slants and recultured every 2 weeks throughout the research period.

Morphological characterization of isolated LAB

Morphological characterization of isolated LAB was performed via Gram staining as described by Tripathi and Sapra (2023), the spore formation test via the Schaeffer Fulton method as shown by Oktari et al. (2017), and the motility test from Rahayu and Setiadi (2023).

Physiological and biochemical characterization of isolated LAB

Physiological and biochemical characterization of isolated LAB was performed through the catalase test, temperature tolerance test at 4°C, 15°C, 37°C, and 45°C, and salt tolerance test at concentrations of 0%, 4%, and 6.5% NaCl as previously described (Ismail et al. 2018; Yudianti et al. 2020). The difference in optical density (OD) at 600 nm was observed after 48 h of incubation during the temperature and salt tolerance tests.

Genomic DNA extraction and identification by 16S rRNA

Before the extraction of genomic DNA from the isolates, selected isolates were subcultured in MRS broth at 37°C for 24 h. The selection of isolates for sequencing was based on the results of the morphological, physiological, and biochemical characterizations where isolates that showed the characteristics of LAB were selected.

Genomic DNA extraction was performed by using the Bacteria DNA Isolation Kit by Geneaid (Taiwan), according to the manufacturer's instructions. The extracted genomic DNA was assessed via electrophoresis with a 0.8% agarose gel. The resulting genomic DNA was amplified by universal forward and reverse primers 27F (5'-AGAGTTTGATCCTGGCTCAG-3') and 1427R (5'-GGTTACCTTGTTACGACTT-3') via PCR with an initial denaturation at 96°C for 4 min, denaturation at 94°C for 1 min, annealing at 52°C for 1 min and 30 s, extension at 68°C for 8 min, final extension at 68°C for 10 min, and cooling to 12°C for 10 min. Agarose gel electrophoresis

(1.8%) was then performed with $1 \times$ TBE at 100 V with FloroSafe DNA Stain (1st BASE). A 1 Kb Plus DNA ladder was added, where the target molecular weight for the PCR products was 1,500 bp. PCR products were sent to Laboratorium Penelitian dan Pengujian Terpadu in Yogyakarta for sequencing of the 16S rRNA gene. Generated sequences were aligned using BioEdit software and were subsequently analyzed by using the BLAST application for analysis of the NCBI gene bank database.

Growth of isolates and *L. plantarum* in SMB and MRS media

SMB medium was prepared by adding the appropriate amount of dried SMB into double-distilled water, into which 2% (w/v) or 3% (w/v) of SMB were added. MRS broth was prepared according to the manufacturer's instructions. All media was autoclaved at 121°C with a pressure of 1.02 kg/cm³ for 20 min.

Selected isolates and commercially bought *L. platantarum* were subcultured in MRS broth for 24 h at 37°C. Isolates were transferred to 24 mL of MRS broth and incubated in a shaking incubator until the OD reached 0.2 at a wavelength of 600 nm. Isolates (5%) from the previous media were then transferred into 30 mL of MRS broth. The culture was then incubated with shaking at 37°C until the OD reached 0.9 at 600 nm, which was equivalent to a viable cell population of approximately 10^7 colony-forming units (CFU)/mL (Chun et al. 2007). Isolates (5%) were added to the prepared medium, which included 2% SMB, 3% SMB, and MRS broth for comparison. All cultures were incubated with shaking at 37°C for 8 h. The number of viable cells was counted by performing a serial dilution with sterile saline solution, in which 1 mL was serially diluted in 9 mL of sterile saline solution that was then plated onto MRS agar via the spread plate method. Plates were incubated at 37°C for 48 h. A total plate count was performed, where plates containing between 25–250 colonies were counted and multiplied by the dilution factor to obtain the number of CFU/mL (Parseelan et al. 2019).

Soymilk fermentation by selected isolates and *L. plantarum*

The selected isolate and commercially bought *L. plantarum* from the Food and Nutrition Culture Collection in Universitas Gadjah Mada were recultured in MRS broth at 37°C for 24 h. A sample (1 mL) of the isolate and the commercially bought *L. plantarum* were transferred to 24 mL of MRS broth and was incubated in a shaking incubator until the OD reached 0.2 at a wavelength of 600 nm, which was then transferred into 30 mL MRS broth. Cultures were incubated with shaking at 37°C until the OD reached 0.9 at 600 nm (10^7 CFU/mL). The cultures were then centrifuged at 5,000 rpm for 15 min. Pelleted cells were washed twice with sterile diluent and resuspended and then used as the inoculum for soymilk fermentation. The inoculated soymilk was left to ferment for 6 h, and the pH of the fermentation was measured with a universal indicator every 2 h. The number of viable cells was analyzed through the plate count method with MRS agar, with serial dilutions in sterile saline solution. Plates were incubated at 37°C for 48 h. The total plate count was determined by counting the plates that had between 25–250 colonies and was multiplied by the dilution factor to obtain the number of CFU/mL (Parseelan et al. 2019). The total titratable acidity was determined by adding two drops of phenolphthalein indicator to 9 mL of the soymilk sample and then titrating with 0.1 N NaOH until a pink color was obtained.

Data analysis
Data were analyzed by using IBM SPSS Statistics 27. Means were analyzed by using the t-test with a significance level of $P < 0.05$. Furthermore, the method demonstrated by (Gunawan et al. 2021) was used to determine the total lactic acid percentage.

RESULTS AND DISCUSSION
Morphological characterization of isolated LAB
The morphological characterization of LAB was performed through macroscopic and microscopic observation of colonies. Fourteen isolates were initially obtained as described in Table 1.

The main differences between the isolates were observed from the colony shape, where isolates 1, 3, 4, 9, 10, 11, 12, and 14 had a circular colony shape, whereas isolates 2, 5, 6, 7, 8, and 13 had a punctiform colony shape. Furthermore, when observed macroscopically from the other parameters, all the colonies were quite similar and exhibited a colony arrangement of coccobacillus, were white in color, had a convex colony elevation, an entire colony margin, and a smooth colony surface. Thus, all isolates that were obtained had characteristics of LAB, whose colonies are either circular or punctiform in shape, with a colony arrangement of coccus, bacillus, or coccobacillus, white to yellow in color, with a convex colony elevation, entire colony margin, and smooth colony surface (Elbanna et al. 2018; Bayu et al. 2023; Rahayu & Setiadi 2023).

During the microscopic observation of the isolates, Gram staining and spore formation testing were performed, to visualize isolated cell shapes. Gram staining includes the performance of a staining process where four different reagents (crystal violet, iodine, 70% ethanol, and, safranin) are used to determine whether a bacterium is gram-positive or negative based on the thickness of the peptidoglycan layer in the bacterial cell walls (Rahayu & Setiadi 2023). The staining process works by adding crystal violet as the primary stain, followed by the addition of iodine, which causes the crystal violet stain to remain in the peptidoglycan layer of the bacterial cell wall. This is followed by the addition of 70% ethanol, which washes the stain from the peptidoglycan (Tripathi & Sapra 2023). Lastly, safranin is added as a counterstain to color the viable cells in the microscope slide. Through this process, gram-positive bacteria are stained purple because of the presence of a thick peptidoglycan layer,

Table 1. Morphological characterization of isolated LAB.

Isolate Code	Shape	Arrangement	Color	Elevation	Margin	Surface	Gram	Spore	Motility
1	Circular	Coccobacillus	White	Convex	Entire	Smooth	+	−	+
2	Punctiform	Coccobacillus	White	Convex	Entire	Smooth	+	−	−
3	Circular	Coccobacillus	White	Convex	Entire	Smooth	+	−	+
4	Circular	Coccobacillus	White	Convex	Entire	Smooth	+	−	−
5	Punctiform	Coccobacillus	White	Convex	Entire	Smooth	+	−	−
6	Punctiform	Coccobacillus	White	Convex	Entire	Smooth	+	−	+
7	Punctiform	Coccobacillus	White	Convex	Entire	Smooth	+	−	+
8	Punctiform	Coccobacillus	White	Convex	Entire	Smooth	+	−	−
9	Circular	Coccobacillus	White	Convex	Entire	Smooth	+	−	−
10	Circular	Coccobacillus	White	Convex	Entire	Smooth	+	−	+
11	Circular	Coccobacillus	White	Convex	Entire	Smooth	+	−	+
12	Circular	Coccobacillus	White	Convex	Entire	Smooth	+	−	+
13	Punctiform	Coccobacillus	White	Convex	Entire	Smooth	+	−	+
14	Circular	Coccobacillus	White	Convex	Entire	Smooth	+	−	+

whereas gram-negative bacteria are stained red as the peptidoglycan layer is thinner when compared with that of gram-positive bacteria (Tripathi & Sapra 2023).

The spore formation assay was performed using the Schaeffer Fulton method that uses malachite green stain and steam to enable the stain to enter the cells, penetrating the cell walls and the spores; safranin is used as a counterstain to stain the viable cells (Oktari et al. 2017). In this assay, spores are stained green while the viable cells are stained a red-pink color (Oktari et al. 2017).

All isolates had a negative result during the spore formation test (Table 1), indicating that the isolates did not contain spores, which agrees with the literature as LAB do not form spores (Rahayu & Setiadi 2023).
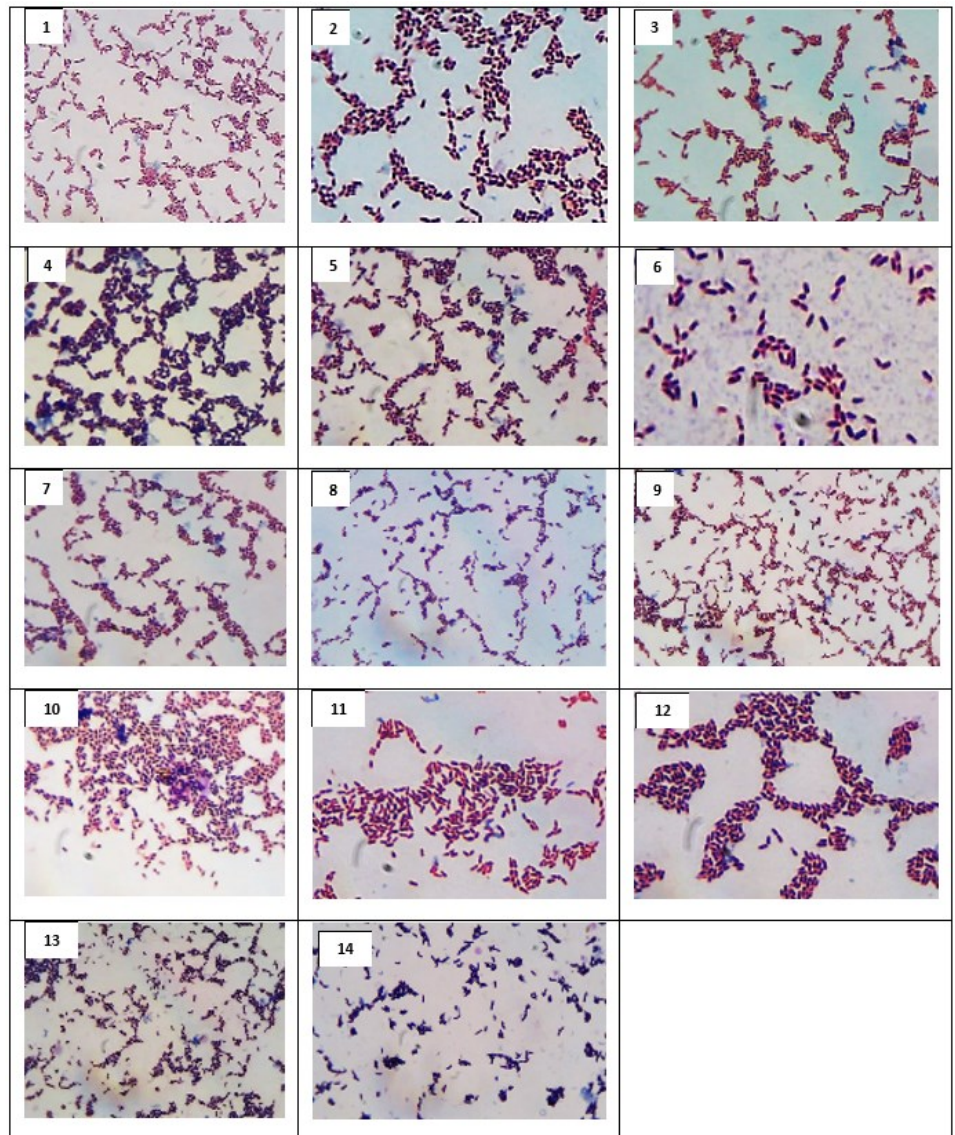
Figure 1. Colony morphology of isolated LAB as a result of Gram staining observed through a microscope with 1000× magnification.

The gram staining results are shown in Figure 1, which shows the colonies of the isolates after Gram staining with 1000× magnification. All isolates exhibited a purple stain, indicating that they were all gram positive bacteria. This result agrees with the literature that states that all LAB are gram positive bacteria (Bayu et al. 2023; Rahayu & Setiadi 2023).

The motility test determines if a bacterial isolate is motile or

nonmotile through the inoculation of the bacteria into a semisolid medium (Rahayu & Setiadi 2023). A positive result in the motility test is indicated by turbidity in the inoculated medium while a negative result is shown by the growth of the isolate along the streak line. The results of the motility test in Table 1 show that most isolates (1, 3, 6, 7, 10, 11, 12, 13, and 14) were motile. Generally, LAB are nonmotile as these lack structures such as flagella for motility (Rahayu & Setiadi 2023). Therefore, isolates 2, 4, 5, 8, and 9 that showed a negative result from the motility test were selected as potential LAB isolates while the rest of the isolates that showed a positive result were discarded.

Physiological and biochemical characterization of isolated LAB
The physiological and biochemical characterization of the isolated LAB included temperature tolerance, salt tolerance, and catalase tests to confirm the selected isolates as LAB.

The catalase test was performed to determine if the selected isolates could produce catalase, which changes hydrogen peroxide (H_2O_2) into water and oxygen (Ismail et al. 2018). A positive result of the catalase test is indicated by the production of bubbles when a drop of 3% H_2O_2 is added to the bacterial isolate, indicating the formation of oxygen gas, whereas a negative result is indicated by the absence of the formation of oxygen gas bubbles (Ismail et al. 2018). All isolates showed a negative result for the catalase test (Table 2), which agrees with the theory that indicates that LAB do not produce catalase (Ismail et al. 2018). This is because LAB are facultative anaerobic organisms that prefer anaerobic conditions to grow but can tolerate the presence of oxygen, unlike aerobic organisms that require the presence of oxygen to grow; therefore, H_2O_2 is created as a product of LAB metabolism and can be toxic, requiring catalase to breakdown the H_2O_2 into oxygen and water (Ismail et al. 2018).

Table 2. Physiological and biochemical characterization of isolated LAB.

Isolate Code	Temperature Tolerance (°C)				Catalase
	4	15	37	45	
2	+[a]	+	+	−	−[c]
4	−[b]	−	+	−	−
5	−	+	+	+	−
8	−	+	+	+	−
9	−	+	+	+	−

Note: a: Growth of isolate; b: death of isolate; c: negative reaction

The temperature tolerance test was performed to determine the growth ability of the isolates at different temperatures (4°C, 15°C, 37°C, and 45°C) over 48 h. LAB are generally known as mesophilic bacteria, with an optimum growth temperature from 25°C to 37°C (Bayu et al. 2023). However, some LAB can also grow and survive at temperatures lower or higher than the optimum temperature. Table 2 shows the ability of the isolates to grow at temperatures of 4°C, 15°C, 37°C, and 45°C, where the (+) symbol indicates the ability of the isolate to grow in the corresponding temperature while the (−) symbol indicates the inability of the isolate to grow in the corresponding temperature, which was determined by the obtaining the OD at 600 nm of the isolate at 0 and 48 h. Table 2 shows that all isolates could grow at 37°C, which confirms that they could potentially be LAB because of the mesophilic characteristic as described by Bayu et al. (2023). Furthermore, only isolate 2 could grow at 4°C while most of the isolates could grow at 15°C and 45°C.

Figure 2 shows the increase in the OD during the temperature tolerance test of selected isolates, which shows a trend where all isolates had an optimum growth temperature of 37°C. Furthermore, all isolates could grow well at 45°C, although not all the results exhibited a significant difference (Table 2). Testing for temperature tolerance is important for LAB, not only for the screening process but also to determine any probiotic potential of the isolated LAB. During the milk fermentation process, the milk is initially pasteurized, which requires high temperatures, and a temperature of 37°C is usually used for the fermentation process. Therefore, when selecting LAB for the fermentation process, not all LAB have the ability to survive high temperatures used for pasteurization (Ayo-Omogie & Okorie 2016).
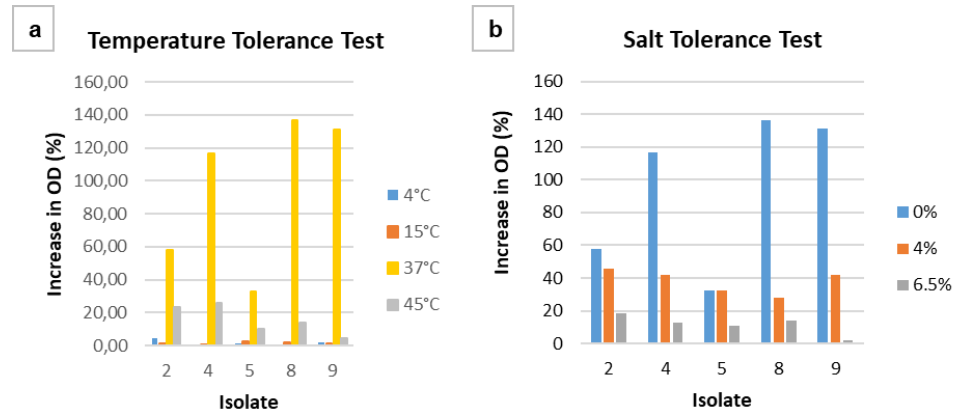
Figure 2. Increase in optical density (OD) during the (a) temperature tolerance test and (b) salt tolerance test of the isolated LAB.

The salt tolerance test determines the growth ability of selected isolates in different concentrations of salt, specifically at concentrations of 0%, 4%, and 6.5%, which is shown by Figure 2. This test was performed because some LAB are considered moderately halophilic bacteria, which means that they can withstand salt concentrations between 3% and 15% (Ismail et al. 2018; Karyantina et al. 2020). The salt tolerance test was conducted by inoculating the selected isolates into mediums with different salt concentrations (0%, 4%, and 6.5%) and comparing the OD at 0 h and after a 48-h incubation. Most of the isolated LAB thrived at 0% salt while 4% salt yielded a higher OD than that at 6.5%. This means that most of the bacteria could survive better at a salt concentration of 4% than at a salt concentration of 6.5%. The results obtained were in accordance with the theory stated by (Karyantina et al. 2020), where most of the isolated LAB can survive at salt concentrations from 2% to 6%, whereas a higher salt concentration resulted in a negative result, categorizing LAB as moderate halophiles. This test indicates that LAB have the potential to be used as a probiotic during the fermentation of salty food and beverages.

Genomic DNA extraction and identification by 16S rRNA sequencing

Genomic DNA was extracted from isolates 4 and 8 because of their supporting characteristics for use as a probiotic. Isolates 4 and 8 showed positive results during the temperature tolerance test at 45°C and showed positive results in tolerating different concentrations of salt during the salt tolerance test, which supports their potential for use as probiotic bacteria. The high-temperature tolerance indicates that the isolate can be used to create probiotic products as fermentation usually requires

an optimum temperature of 37°C (Ayo-Omogie & Okorie 2016). Furthermore, during the consumption of probiotic products, the temperature of the human gut can typically reach 37°C, which could affect the desired effect of the probiotic product if the probiotic bacteria lose viability before providing the effect for the consumer (Ayo-Omogie & Okorie 2016). A high salt tolerance is required for probiotic bacteria to ensure that the bacteria can survive the high salt condition created by the presence of bile salt in the body, where a lack of viability caused by the presence of salt prevents the delivery of the expected effect of the probiotic product (Ayo-Omogie & Okorie 2016).

Gel electrophoresis showed that the genomic DNA was successfully isolated from both isolates 4 and 8 (Figure 3). The DNA was then amplified as described in the Methods section.
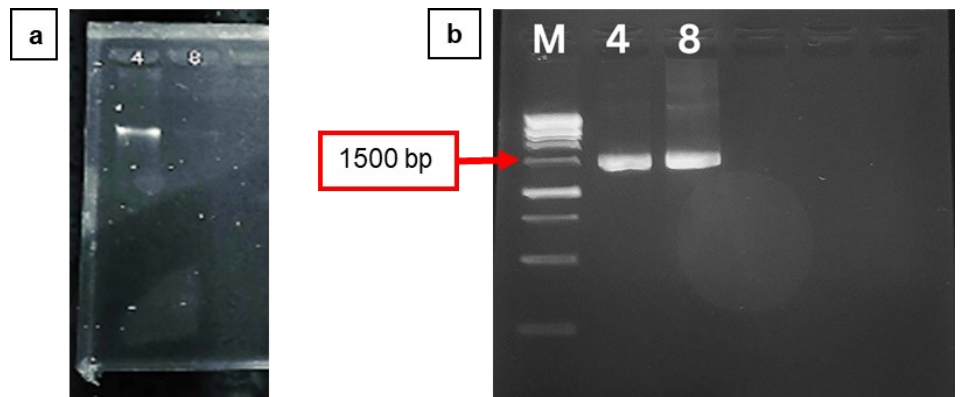
Figure 3. Electrophoresis result for the (a) DNA isolation of isolates 4 and 8 and (b) PCR product when amplified with 16S rRNA universal primers with 1 Kb plus marker (M).

Figure 3 shows the gel electrophoresis of the amplified PCR product from DNA extracted from isolates 4 and 8. A single band at 1,500 bp indicates that the DNA was successfully amplified with the primers. The PCR product was sequenced, and the sequencing results aligned to create a consensus sequence, which was then analyzed via BLAST to compare with sequences of species available in the NCBI GenBank database. From the BLAST results, isolate number 4 was identified as *Weisella confusa* strain NWAFU 8,001, with a percent identity of 99.71% and a query cover of 100% while isolate 8 was identified as *Weissella confusa* strain 3,273 with a percent identity of 100% and a query cover of 100%.

W. confusa is described as a gram-positive bacteria with a coccus colony shape that is facultatively anaerobic, nonmotile, and catalase-negative, has negative spore formation, and is considered a LAB (Fessard & Remize 2017; Spiegelhauer et al. 2020). Before recent classification, *W, confusa* used to be called *Lactobacillus confusus*; however, the *Weissella* genus was created in 1993 following 16S rRNA sequencing, and *L. confusus* was changed to *W. confusa* (Spiegelhauer et al. 2020). Macroscopically, *W. confusa* colonies can be observed as rods in pairs or chains. Physiologically, *W. confusa* is considered a facultative anaerobic bacteria, which means that *W. confusa* can live in either aerobic or anaerobic conditions and metabolize with or without the presence of oxygen (Fessard & Remize 2017). Fermentation occurs in the absence of oxygen, where lactic acid, carbon dioxide, ethanol, and acetic acid are produced as a final result of the fermentation process. *W. confusa* can grow in temperatures between 15°C to 37°C, and several strains can grow in temperatures up to 47°C (Fessard & Remize 2017). These results fully correspond to the morphological and physiological characteristics obtained for isolates 4 and 8.

W. confusa has been reportedly isolated from various sources, including fermented foods, such as fermented fruits, vegetables, dairy and meat products, indicating that the species can adjust to different growth conditions in different environments (Fessard & Remize 2017). Examples of reports of *W. confusa* isolated from fruit and vegetable sources include during the fermentation of Tuaw jaew, which is a type of fermented soybeans from Thailand, and during the fermentation of Korean leek (*Allium tuberosum* Rottler) (Yang et al. 2014). *W. confusa* has also been isolated from dairy products, including from Nono, a fermented skimmed milk from Nigeria, and from the surface of an Italian cheese (Di Cagno et al. 2007; Ayeni et al. 2011). Furthermore, *W. confusa* has been identified from clinical cases in humans, such as from the skin, gastrointestinal tract, and blood, where the disease-causing ability is still questioned (Fairfax et al. 2014; Spiegelhauer et al. 2020).

As *W. confusa* has been isolated from many fruit, vegetable, and dairy sources, the probiotic ability in fermented products has been explored. While most reports on the isolation of *W. confusa* were conducted using spontaneous fermentation, the use of *W. confusa* as a starter culture is being explored, especially as *W. confusa* can ferment many different types of food and beverages, supporting its ability to survive in different types of conditions. This is because when spontaneous fermentation occurs, it is challenging to control the microorganisms that grow in the product as this type of fermentation usually contains many different types of microorganisms, resulting in a product that can have different characteristics from one batch to another (Fessard & Remize 2017). However, when starters are used, the fermentation usually only contains one or a few types of microorganisms of known fermentation ability in suitable amounts, resulting in a product that has uniform characteristics (Fessard & Remize 2017).

Growth of isolates and *L. plantarum* in SMB and MRS media

The growth of isolates and *L. plantarum* in SMB and MRS media was conducted to compare the growth of isolates 4 and 8, and commercially bought *L. plantarum* in SMB as an alternative growth medium compared with their growth in the commercially available MRS medium. Generally, alternative mediums used as the standard or commercial medium can be expensive while alternative media are usually more low cost as the materials used are mainly from locally available food sources (Hayek et al. 2019; Malik et al. 2022).

Two different concentrations of SMB (2% and 3%) were used in this study, as pictureed in Figure 4. Visually, the SMB alternative medium appeared white in color while the SMB medium with a concentration of 3% had an opaque color. However, fully dissolving the SMB in the distilled water was difficult because of the high fiber content of soybeans; therefore, the SMB medium may be more appropriately used as a solid/agar medium than as a liquid/broth medium as the opaque color makes it difficult to observe bacterial growth in liquid culture.

To perform the growth comparison between the alternative SMB and standard MRS media, a similar number of viable bacterial cells were inoculated into the same amount of medium. The media was then incubated with shaking for 8 h, and the final CFU/mL of the media was calculated through serial dilution and the total plate count.

Figure 4c demonstrates that a similar trend was present in all isolates in the different types of media used. The highest CFU/mL count was observed in the MRS broth medium for all isolates, followed by 2% SMB, and then 3% SMB. The highest CFU/mL count was observed with

isolate 8 (*W. confusa*) in all media used when compared with the other isolates; *L. plantarum* has the second highest CFU/mL count followed by isolate 4 (also identified as *W. confusa*).
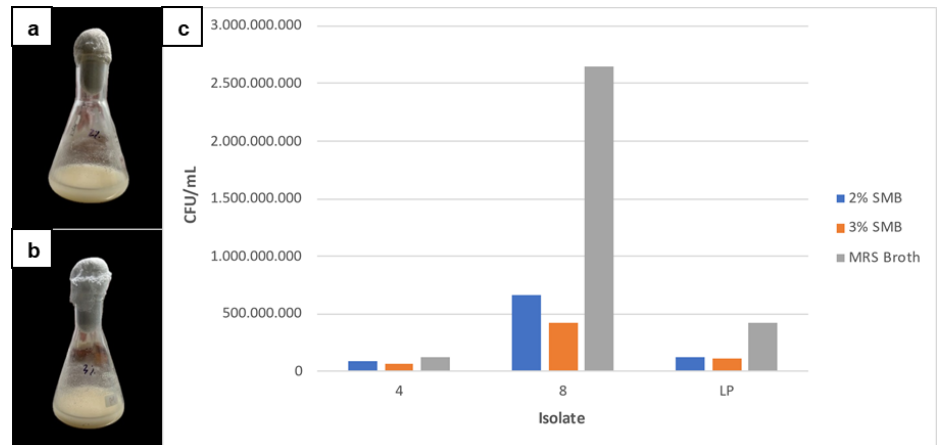
Figure 4. 2% (a) and 3% (b) SMB medium created to be inoculated with the selected isolates and *L. plantarum*; (c) Growth comparison through CFU/mL of isolates 4 and 8, and *L. plantarum* (LP) in 2% and 3% SMB (Okara) and MRS broth media after 8 h of incubation.

The CFU/mL count was highest with the use of MRS broth as this commercially made medium is considered a selective medium for LAB. This is because MRS contains all of the essential micro and micronutrients that are required for the growth of LAB and has been used as a standard medium for their cultivation for approximately 63 years (Hayek et al. 2019). Typical MRS medium usually contains high amounts of peptone that serves as a source of nitrogen content in the medium and can maintain an ideal pH level for LAB growth. However, a major limitation of the use of MRS medium is the expensive price, which can be an issue for research conducted in developing countries.

When compared between the different concentrations of the alternative SMB medium, between all the isolates, the 2% SMB medium had a higher CFU/mL count than that of the 3% SMB medium, although the differences between in the CFU/mL count between these media were not significant. First, soy is considered to contain high amounts of protein, which could serve as a nitrogen source for the growth of LAB as a high nitrogen content is required for its growth, supporting the use of soybeans or SMB for the use as an alternative media source. The differences between the results of the CFU/mL counts in the 2% and 3% SMB could be due to the higher water content that is available in the 2% SMB medium compared with that in the 3% SMB medium, which enables the nutrients that are available in the SMB to be more easily dissolved in the 2% medium, making the nutrients more readily available for the LAB to use (Alp & Bulantekin 2021).

Unfortunately, limited research has explored the use of SMB as a source of alternative medium, especially for LAB. Similar research used dried soybeans to make soybean flour as an alternative medium for the cultivation of microorganisms such as *Bacillus cereus* and evaluated different concentrations of soy flour along with different particle sizes (Utomo et al. 2022). A higher soy flour concentration with a smaller particle size was shown to increase the amount of *Bacillus* bacteria grown.

Soymilk fermentation with isolate 8 and *L. plantarum*

Soymilk fermentation was conducted by inoculating a similar number of viable cells from isolate 8 (*W. confusa*) and *L. plantarum* to compare their

fermentation ability and to determine the probiotic ability of the isolated bacteria when compared with a commercially available LAB.

The highest CFU/mL count was achieved with isolate 8 (5.5×10^9 CFU/mL) when compared with that of *L. plantarum* (3.27×10^9 CFU/mL) as shown by Figure 5. The higher CFU/mL count obtained with isolate 8 is because the isolate was isolated from soymilk, which means that the isolate may be adapted to the growth conditions in soymilk and could support a higher CFU/mL while the commercially bought *L. plantarum* was not fully adapted to these growth conditions. However, similar research conducted by Chun et al. (2007), which also used *W. confusa* and *L. plantarum* for the fermentation of soymilk for 9–12 h produced different results, where *L. plantarum* achieved a higher CFU/mL count than *W. confusa*. This difference may be caused by the difference in the strains of *Weissella* bacteria used. In this study, the *W. confusa* strain (isolate 8) was obtained by isolating the bacteria from soymilk and was better adapted to the growth conditions.
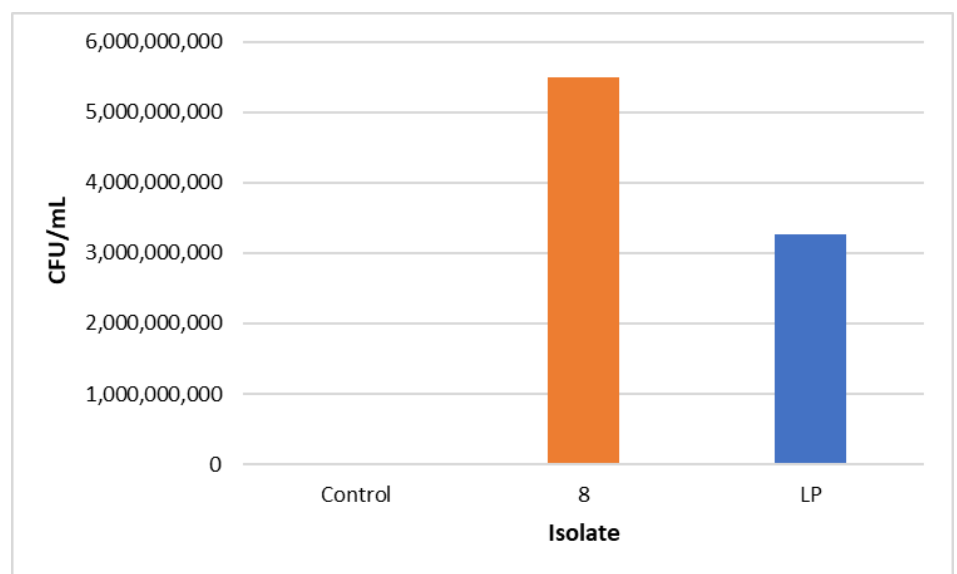
Figure 5. Comparison of CFU/mL of soymilk inoculated with 5% of isolate 8 and *L. plantarum* (LP) for 6 h at 37°C.

Furthermore, the results of the fermentation of soymilk with the isolated bacteria (isolate 8) showed that this isolate could successfully create a probiotic product as the final CFU/mL count was $>10^7$ CFU/mL, which is considered the minimum amount of bacteria required in probiotic products to provide a positive effect to the host (Teh et al. 2010).

During the soymilk fermentation process, the pH of the soymilk was determined by using a universal indicator every 2 h to understand the change in pH throughout the fermentation process, as shown by Figure 6. A drop in pH is usually a sign of the formation of lactic acid as a result of the metabolism by LAB present in the soymilk, showing that a continuous fermentation process is being performed (Liu et al. 2016). The largest drop in pH was produced in the isolate 8 culture (Figure 6a), where the pH of the milk decreased after 2 h of fermentation when compared with that in the *L. plantarum* and control cultures. The difference in the drop in pH between cultures of isolate 8 and *L. plantarum* could be due to the difference in the speed of the fermentation process of both isolates, where isolate 8 could be more well adapted to the growth conditions and has the ability to better ferment the soymilk than the commercially bought *L. plantarum* and produce more lactic acid to lower the pH

of the soymilk. A similar result was observed in a previous study (Chun et al. 2007), where the fermentation of soymilk with various strains of LAB, including *W. confusa* and *L. plantarum* reduced the pH to between 4.4. and 4.6 because of lactic acid production at 6 h of fermentation.

Titratable acidity is used to calculate the total lactic acid content of the fermented soymilk (Tyl & Sadler 2017; Gunawan et al. 2021). Figure 6b shows that the highest titratable acidity was achieved by isolate 8, followed by *L. plantarum,* and lastly by the control. This result corresponds to the final pH of the soymilk fermentation process, where the lowest pH was achieved in the same order. According to Chun et al. (2007), high titratable acidity is commonly achieved by strains that produce a lower pH during the fermentation process as a result of a higher acidity content. This result is reflected here as isolate 8 achieved the lowest pH while also achieving a higher titratable acidity.

Furthermore, the total lactic acid percentage (Figure 6c) was calculated as reported by Gunawan et al. (2021), which showed that the highest lactic acid percentage was achieved by isolate 8, followed by that achieved by the commercially bought *L. plantarum* and lastly by the control. The difference in the value of the total lactic acid percentage can be an indicator of the flavor that is created by the different isolates during soymilk fermentation. Furthermore, the higher the lactic acid content, the more difficult it is for the soymilk to spoil as the pH is lower, which therefore discourages the growth of spoilage bacteria in the product (Gunawan et al. 2021).
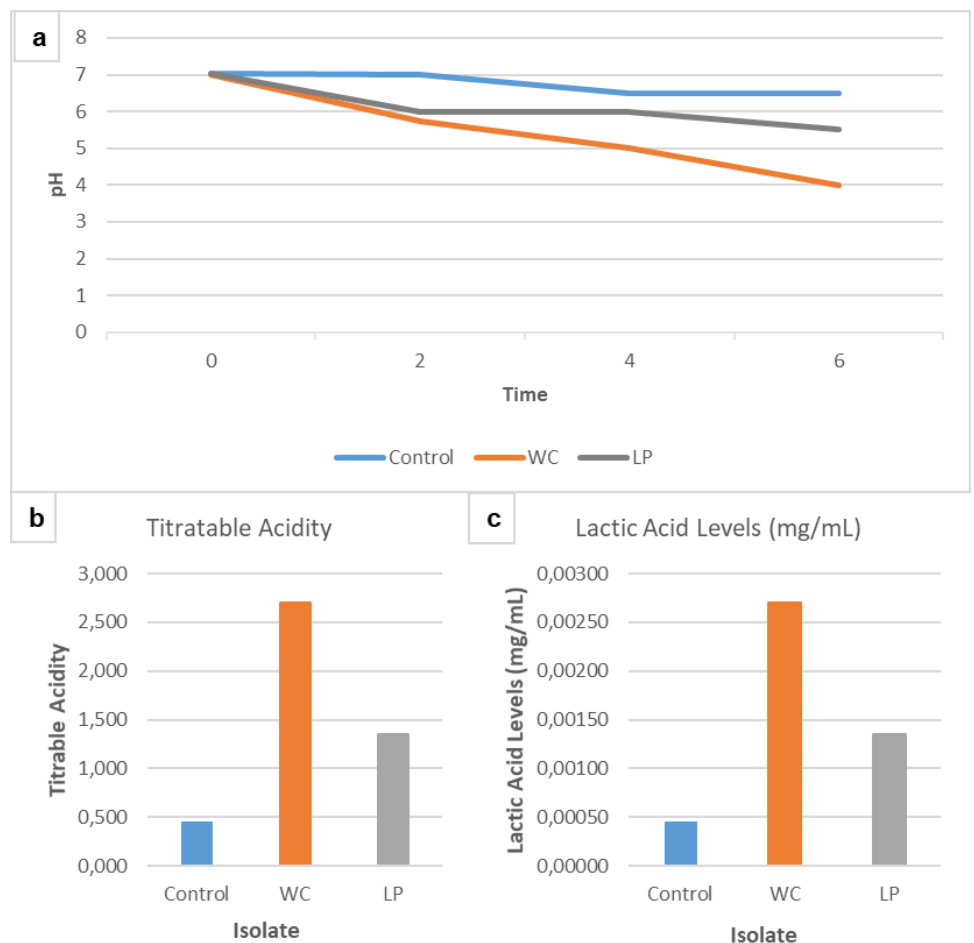
Figure 6. (a) pH of the fermented soymilk inoculated with 5% of isolate 8 and *L. plantarum* (LP) for 6 h at 37°C; (b) Titratable acidity and (c) total lactic acid content of soymilk fermented with isolate 8 and *L. plantarum* (LP).

CONCLUSIONS

This study showed that the isolates selected from fermented soymilk were both identified as *W. confusa* via sequencing of the 16S rRNA gene. *W. confusa* is considered an LAB that has been commonly isolated from many different sources, even forming spontaneous fermentations in foods and beverages. SMB could be used to culture LAB. The SMB was first dried until a constant weight was achieved, followed by grinding and sifting to obtain a uniform particle size. A concentration of 2% SMB was more effective in producing higher numbers of viable LAB colonies than that of 3%. LAB cultured from SMB can ferment soymilk, where the probiotic ability was demonstrated with a final CFU/mL count of 5.5×10^9 CFU/mL, which was higher than that of the commercially bought LAB isolate and reached the minimum standard of a probiotic product.

REFERENCES

Alp, D. & Bulantekin, Ö., 2021. The microbiological quality of various foods dried by applying different drying methods: a review. *European Food Research and Technology*, 247(6), pp.1333–1343. doi: 10.1007/s00217-021-03731-z.

Aritonang, S.N. et al., 2017. Isolation and Identification of Lactic Acid Bacteria from Okara and Evaluation of Their Potential as Candidate Probiotics. *Pakistan Journal of Nutrition*, 16(8), pp.618–628. doi: 10.3923/pjn.2017.618.628.

Aydar, E.F., Tutuncu, S. & Ozcelik, B., 2020. Plant-based milk substitutes: Bioactive compounds, conventional and novel processes, bioavailability studies, and health effects. *Journal of Functional Foods*, 70, 103975. doi: 10.1016/j.jff.2020.103975.

Ayeni, F.A. et al., 2011. Evaluation of the functional potential of Weissella and Lactobacillus isolates obtained from Nigerian traditional fermented foods and cow's intestine. *International Journal of Food Microbiology*, 147(2), pp.97–104. doi: 10.1016/j.ijfoodmicro.2011.03.014.

Ayo-Omogie, H. & Okorie, E., 2016. In vitro Probiotic Potential of Autochthonous Lactic Acid Bacteria and Microbiology of Kunu Made from Mixed Grains. *British Microbiology Research Journal*, 14(4), pp.1–10. doi: 10.9734/BMRJ/2016/25403.

Bayu, H.H. et al., 2023. Isolation and Identification of Lactic Bacteria from *Channa* sp. as Potential Probiotic. *Jurnal Pembelajaran dan Biologi Nukleus*, 9(1), pp.75–84. doi: 10.36987/jpbn.v9i1.3551.

Chun, J. et al., 2007. Conversion of Isoflavone Glucosides to Aglycones in Soymilk by Fermentation with Lactic Acid Bacteria. *Journal of Food Science*, 72(2). doi: 10.1111/j.1750-3841.2007.00276.x.

Davy, P. & Vuong, Q.V., 2022. Soy Milk By-product: Its Composition and Utilisation. *Food Reviews International*, 38(sup1), pp.147–169. doi: 10.1080/87559129.2020.1855191.

Di Cagno, R. et al., 2007. Characterization of Italian Cheeses Ripened Under Nonconventional Conditions. *Journal of Dairy Science*, 90(6), pp.2689–2704. doi: 10.3168/jds.2006-654.

Elbanna, K. et al., 2018. In vitro and in vivo evidences for innate immune stimulators lactic acid bacterial starters isolated from fermented camel dairy products. *Scientific Reports*, 8(1), 12553. doi: 10.1038/s41598-018-31006-3.

Fairfax, M.R., Lephart, P.R. & Salimnia, H., 2014. Weissella confusa: problems with identification of an opportunistic pathogen that has been found in fermented foods and proposed as a probiotic. *Frontiers in Microbiology*, 5. doi: 10.3389/fmicb.2014.00254.

Fessard, A. & Remize, F., 2017. Why Are Weissella spp. Not Used as Commercial Starter Cultures for Food Fermentation? *Fermentation*, 3(3), 38. doi: 10.3390/fermentation3030038.

Goda, H., Barakat, O. & Ali, M., 2011. Potential Exploitation of Okara as an Alternative Medium for Edible Pleurotus ostreatus Mycelium Production. *Arab Journal of Biotechnology*, 14, pp.139–153.

Gunawan, S. et al., 2021. Reaction kinetics of lactic acid fermentation from bitter cassava (Manihot glaziovii) starch by Lactobacillus casei. *Indonesian Journal of Biotechnology*, 26(1), 7. doi: 10.22146/ijbiotech.54119.

Hayek, S.A. et al., 2019. Cultivation media for lactic acid bacteria used in dairy products. *Journal of Dairy Research*, 86(4), pp.490–502. doi: 10.1017/S002202991900075X.

Ismail, Y., Yulvizar, C. & Mazhitov, B., 2018. Characterization of lactic acid bacteria from local cow´s milk kefir. *IOP Conference Series: Earth and Environmental Science*, 130, 012019. doi: 10.1088/1755-1315/130/1/012019.

Karyantina, M. et al., 2020. Moderate Halophilic Lactic Acid Bacteria from *Jambal roti*: A Traditional Fermented Fish of Central Java, Indonesia. *Journal of Aquatic Food Product Technology*, 29(10), pp.990–1000. doi: 10.1080/10498850.2020.1827112.

Kim, J., 2019. *Transforming okara into a microalgae culture medium*. Nanyang Technological University. doi: 10.32657/10220/49477.

Liu, Y. et al., 2016. Characterization of Lactobacillus pentosus as a starter culture for the fermentation of edible oyster mushrooms (Pleurotus spp.). *LWT - Food Science and Technology*, 68, pp.21–26. doi: 10.1016/j.lwt.2015.12.008.

Malik, N.H.A., Simarani, K. & Aziz, M.A., 2022. Soybean as an Alternative Nutrient Medium for *Bacillus subtilis* Growth. *Malaysian Applied Biology*, 51(4), pp.67–74. doi: 10.55230/mabjournal.v51i4.12.

Malik, T.F. & Panuganti, K.K., 2022. Lactose Intolerance. In *StatPearls*. Treasure Island (FL): StatPearls Publishing. http://www.ncbi.nlm.nih.gov/books/NBK532285/

Oktari, A. et al., 2017. The Bacterial Endospore Stain on Schaeffer Fulton using Variation of Methylene Blue Solution. *Journal of Physics: Conference Series*, 812, 012066. doi: 10.1088/1742-6596/812/1/012066.

Parseelan, A. et al., 2019. Aerobic Plate Count of Milk and Dairy Products Marketed in Different Zones of Chennai. *International Journal of Livestock Research*, 9(3). doi: 10.5455/ijlr.20180711104721.

Rahayu, H.M. & Setiadi, A.E., 2023. Isolation and Characterization of Indigenous Lactic Acid Bacteria from Pakatikng Rape, Dayak's Traditional Fermented Food. *Jurnal Penelitian Pendidikan IPA*, 9(2), pp.920–925. doi: 10.29303/jppipa.v9i2.2801.

Rizzo, G. & Baroni, L., 2018. Soy, Soy Foods and Their Role in Vegetarian Diets. *Nutrients*, 10(1), 43. doi: 10.3390/nu10010043.

Sanders, E.R., 2012. Aseptic Laboratory Techniques: Plating Methods. *Journal of Visualized Experiments*, (63), 3064. doi: 10.3791/3064.

Spiegelhauer, M.R. et al., 2020. A case report of polymicrobial bacteremia with Weissella confusa and comparison of previous treatment for successful recovery with a review of the literature. *Access Microbiology*, 2(5). doi: 10.1099/acmi.0.000119.

Teh, S. et al., 2010. Enhanced Growth of Lactobacilli in Soymilk upon Immobilization on Agrowastes. *Journal of Food Science*, 75(3). doi: 10.1111/j.1750-3841.2010.01538.x.

Tripathi, N. & Sapra, A., 2023. Gram Staining. In *StatPearls*. Treasure Island (FL): StatPearls Publishing.

Tyl, C. & Sadler, G.D., 2017. pH and Titratable Acidity. In *Food Analysis*. Food Science Text Series. Cham: Springer International Publishing, pp.389–406. doi: 10.1007/978-3-319-45776-5_22.

Utomo, A.S., Harismah, K. & Mulyaningtyas, A., 2022. Making *Bacillus cereus* Bacterial Growth Media from Soybeans (*Glycine max* (L.) Merril): In 4th International Conference Current Breakthrough in Pharmacy (ICB-Pharma 2022). Sukoharjo, Indonesia. doi: 10.2991/978-94-6463-050-3_26.

Vanga, S.K. & Raghavan, V., 2018. How well do plant based alternatives fare nutritionally compared to cow's milk? *Journal of Food Science and Technology*, 55(1), pp.10–20. doi: 10.1007/s13197-017-2915-y.

Yang, J. et al., 2014. Selection of functional lactic acid bacteria as starter cultures for the fermentation of Korean leek (Allium tuberosum Rottler ex Sprengel.). *International Journal of Food Microbiology*, 191, pp.164–171. doi: 10.1016/j.ijfoodmicro.2014.09.016.

Yudianti, N.F. et al., 2020. Isolation and Characterization of Lactic Acid Bacteria from Legume Soaking Water of Tempeh Productions. *Digital Press Life Sciences*, 2, 00003. doi: 10.29037/digitalpress.22328.

Research Article

Bioerosion in the Priabonian *Discocyclina javana* in Bayat Area, Indonesia: Implications for Paleoecology

Diana Rahmawati[1,3], Sugeng Sapto Surjono[2]*, Didit Hadi Barianto[2], Wartono Rahardjo[4]

1) Doctoral Program in Geological Engineering, Faculty of Engineering, Universitas Gadjah Mada, Jl. Grafika No. 2, Yogyakarta-55281, Indonesia
2) Department of Geological Engineering, Faculty of Engineering, Universitas Gadjah Mada, Jl. Grafika No. 2, Yogyakarta-55281, Indonesia.
3) Department of Geological Engineering, Faculty of Engineering, Universitas Mulawarman, Jl. Sambaliung No. 9, Samarinda, Kalimantan Timur-75119, Indonesia.
4) Independent Geologist, Yogyakarta, Indonesia.
* Corresponding author, email: sugengssurjono@ugm.ac.id

ABSTRACT

This paper discusses about the bioerosion discovered in carbonate tests of *Discocyclina javana* (Verbeek, 1891), a large benthic foraminifera from the Priabonian (Late Eocene). The study material was sampled from the Gamping beds in the Wungkal-Gamping Formation in Bayat, Indonesia. We discovered four bioerosional trace fossils from three different ichnogenera demonstrate bioerosion from the surface test analysis. *Oichnus simplex* and *Oichnus paraboloides* are ichnogenus *Oichnus* diagnostic drilling holes that are often found on the surface. *Caulostrepsis* isp. exhibits the presence of uncomplicated U-shaped borings. The observed formation of drill holes can be mostly linked to the predatory behaviour of gastropods, while other trace fossils are predominantly associated with the burrowing activities of worms. The occurrence of well-preserved individual tests exhibiting no signs of bioerosion is infrequently observed in *D. javana*. In addition, bioerosion occurs more frequently in the microspheric generation than in the megalospheric generation. This research also demonstrates for the first time in Indonesia that parrotfish bite marks have developed on individual tests of the microspheric generation of *D. javana*. The taphonomic characteristics exhibited by the bioeroded and encrusted *D. javana* specimens can serve as reliable paleoecological indicators for sediment deposition occurring at an intermediate to high sedimentation regime. The occurrence of larger foraminifera with some bioerosional trace fossil highly proficient at documenting shallow marine sclerobionts.

INTRODUCTION

Bioerosion is the process by which living organisms mechanically or chemically degrade hard substrates, including bones, shells, rocks, corals, wood, and also foraminifera test. This degradation can occur through various means, such as chemical dissolution facilitated by bacteria or fungi, as well as physical abrasion caused by animals like mollusks or echinoids (Hutchings et al. 2005; Tribollet et al. 2011; Wisshak & Tapanila 2008). The appearance and structure of these creatures can be greatly influenced by this phenomenon, hence offering valuable insights about environmental conditions and biodiversity. Bioerosional trace fossils, also

known as bioerosion traces or ichnofossils, are the result of various organisms' activities that cause the erosion or degradation of hard substrates such as rocks, shells, bones, and other mineral surfaces. These can include borings (holes drilled into the substrate), etchings (surface marks), gnawings (marks from chewing or biting), and other forms of physical alteration. Bioerosional trace fossils can provide valuable insights into paleoecological and paleoenvironmental conditions. Here are few key points about them: (1) Organism Interactions; (2) Environmental Indicators; (3) Substrate Preferences; (4) Temporal Distribution; (5) Biodiversity Indicators; and (6) Taphonomic Information (Wisshak & Tapanila 2008). In larger foraminifera tests, bioerosion can occur due to the activity of fungi, bacteria, and other microorganisms (Vohník 2021). The phenomenon of bioerosion in the large foraminifera, *Discocyclina javana* has not been well studied, and there is a lack of comprehensive investigation about the ichnofacies in the Wungkal-Gamping area. This research studied the carbonate individual test of *Discocyclina javana* (Verbeek), which was found in Desa Gamping, the east part of Jiwo Hills, Bayat, Indonesia. Bioerosion not only plays a significant role in shaping ecosystems and influencing biodiversity but also provides valuable information about past environments and climate change, especially in the Late Eocene-Priabonian stage (Hutchings et al. 2005). A previous study of bioerosion in the carbonate Eocene-nummulite test has been carried out by (Abdel-Fattah 2018), but this study concerned the Eocene-orthophragminid test for the first time. Bioerosion plays a significant role in shaping both modern and ancient ecosystems. It can influence the distribution and abundance of species, can contribute to the recycling of nutrients, and can affect the physical structure of habitats.

MATERIALS AND METHODS
Materials
Individual tests of the larger benthic foraminifers *Discocyclina javana* (Verbeek) were studied from the top of middle Eocene Wungkal-Gamping Formation, Southern Mountain, Bayat, Indonesia. The Wungkal Gamping Formation was divided into two rock units, they are Wungkal beds and Gamping beds (Bothe 1929; Sumarso & Ismoyowati 1975). Wungkal beds are characterised by the abundance of *Planocamerinoides* (=*Assilina*, of the older workers), representing Ta3 age (Lutetian-Bartonian stage) The individual tests of *D. javana* were collected from the Gamping beds. Although the outcrop at sampling location 1 is completely eroded, we were still able to find numerous loose individual specimens. In the sampling location 2, we observed small outcrops, with no loose-individual test. The coordinate location is S 07°46'33.8", E 110°40'24.0" for the first sampling location and S 07°45'44,2", E 110°40'33.0" for the second sampling location (see Figure 1-2). However, this remains a minority due to the scarcity of sedimentological information regarding the Gamping beds from the Late Eocene. It is hoped that this research will provide valuable insights into the sedimentation history of the Wungkal-Gamping Formation. The sole remaining geological data in the studied area consists of the loose-individual calcareous test.

Methods
The ichnotaxonomy of the documented boring was established upon the examination of over 100 samples gathered from the defined study sites. Around 75-80% (75-80 specimens) of the specimens that were obtained exhibit signs of encrustation and/or bioerosion. The specimens underwent a process of washing and drying in order to facilitate thorough thin
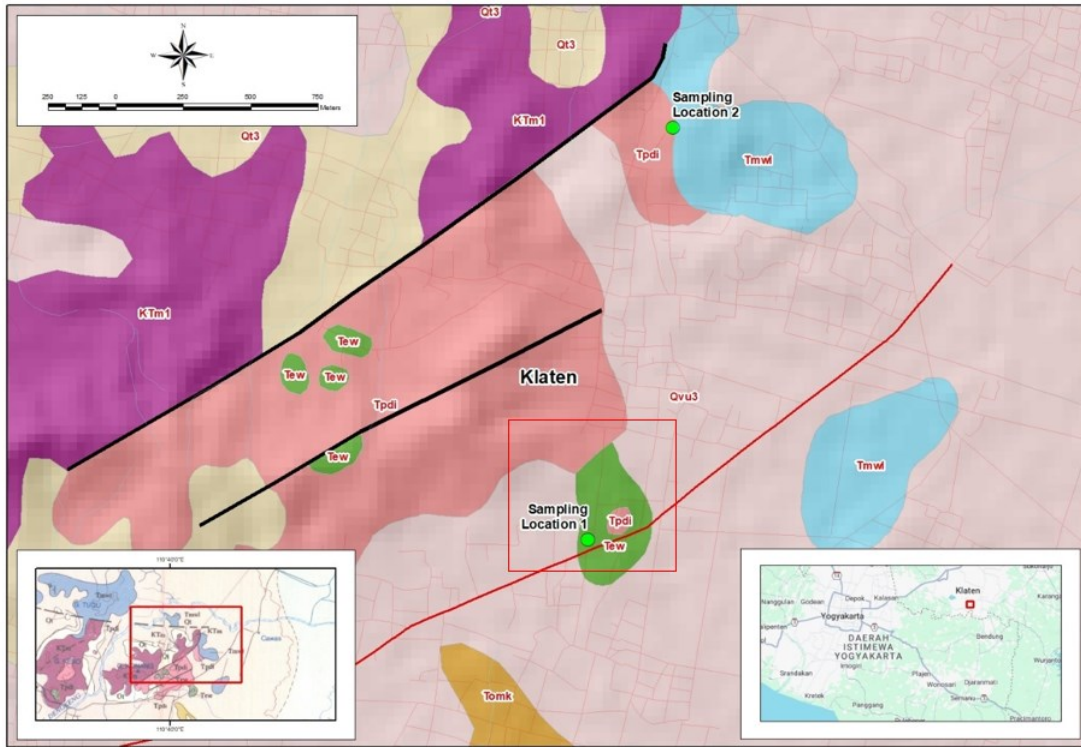
Figure 1. Geological map of the study area, red boxes show the studied sections (modified from Surono et al. 1992). At sampling location 1, the B-form of loose-individual *Discocyclina javana* test has sampled. At sampling location 2, the A-form occurs as small outcrops, without loose-individual test, therefore, preparing thin sections is necessary. Remarks: Tew = Wungkal-Gamping Formation; Tomk = Kebo-Butak Formation; Tms = Semilir Formation; Tmwl = Wonosari-Punung Formation; Tpdi = Pendul Diorite; Qvu = Merapi Volcanic Rocks; Qt: Older Alluvium; Qa = Alluvium; KTm = Metamorphic rocks.

section examinations using a polarised microscope-*Olympus* BX53M. A number of specimens were subjected to axial sectioning in order to facilitate comprehensive investigations (see Plate 3).

Figure 2. Outcrop situation at the sampling location 2, Eastern Jiwo, Bayat. The outcrop has a very limited lateral extent, just spotted. Most of the outcrop is eroded, leaving only a small, massive outcrop that is less than one meter in height. There were no observable sedimentary structures, and the grain orientation did not show any signs of imbrication.

RESULTS AND DISCUSSION

Introduction to Reproduction and Life Span of Foraminifera

Discocyclina javana (Verbeek) is one of cosmopolitan species of larger benthic foraminifera with a complex life cycle that produces two distinct generations, haploid and diploid (Hallock 1985; Hallock & Reymond 2022). Figure 3 explains the haploid generation, called 'gamonts,' has a single set of chromosomes and produces numerous gametes through multiple fission (Hohenegger 2011). These gametes, which are small and possess flagella, are isogametes, meaning they are identical in form. When two gametes fuse, they form a diploid zygote with a double set of chromosomes (Hohenegger 2011). The diploid generation, called 'agamonts,' reproduces asexually and can grow larger than the gamonts before reproduction (Hohenegger 2011; Beavington-Penney & Racey 2004). The agamonts form the megalospheric generation (also known as the A-form, see Figure 4), while the gamonts form the microspheric generation (B-form). This study reveals that bioerosion occurs more frequently in the microspheric generation (B-form).
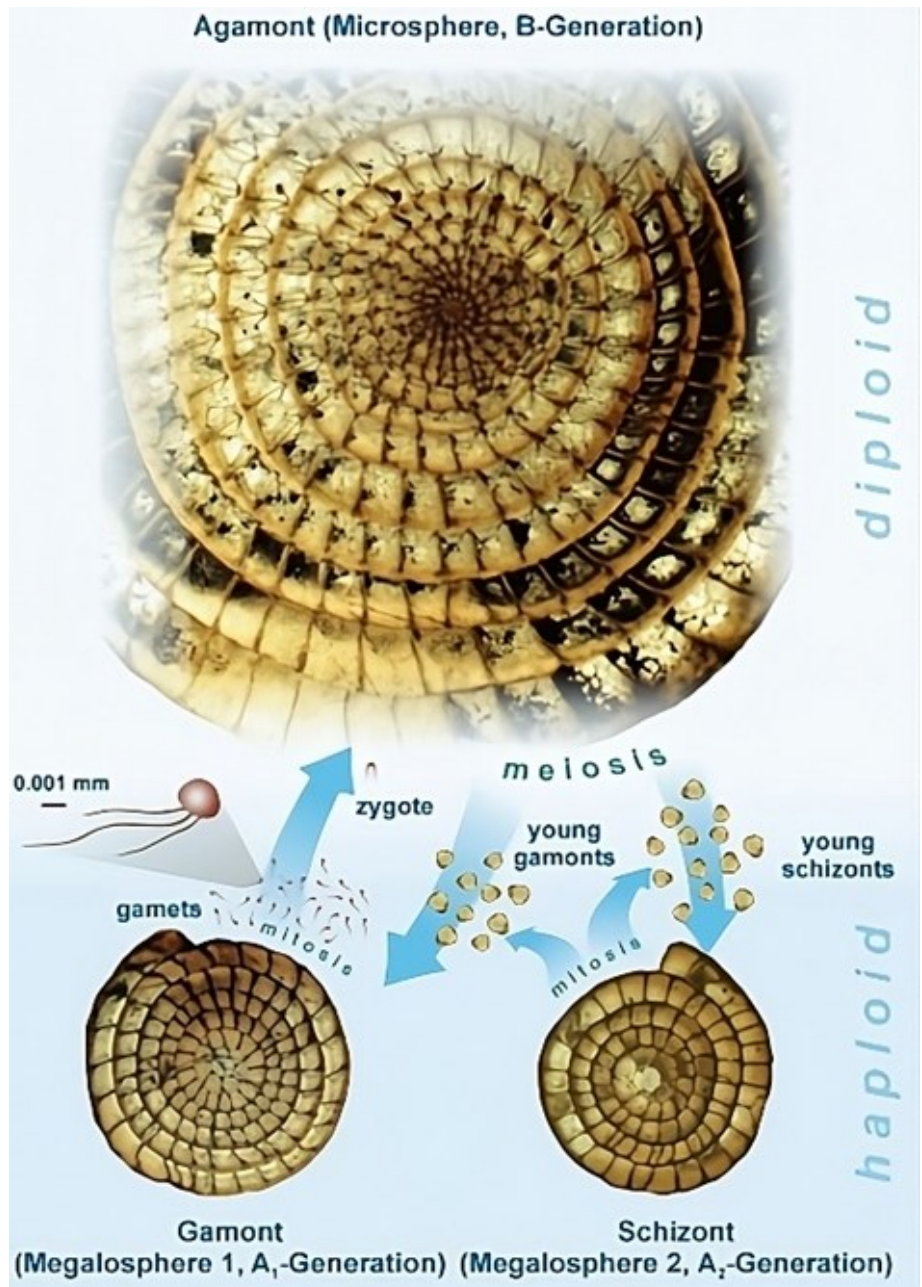
Figure 3. The life cycle of larger foraminifera, gamete seizes not to scale (Hohenegger 2011).

Bioerosion occurred more frequently in the microspheric generation, as our study showed that the megalospheric generation experiences less bioerosion (see Figure 4). Microspheric foraminifera, being larger, were more susceptible to bioerosion by marine organisms. Symbiotic organisms also preferred microspheric tests, increasing their vulnerability. These findings are aligned with previous research, indicating that organisms in sandy, medium to high-energy environments target microspheric generations. This selective bioerosion is important for paleoecological reconstructions and sedimentation rate assessments, highlighting differences in preservation potential between microspheric and megalospheric generations.
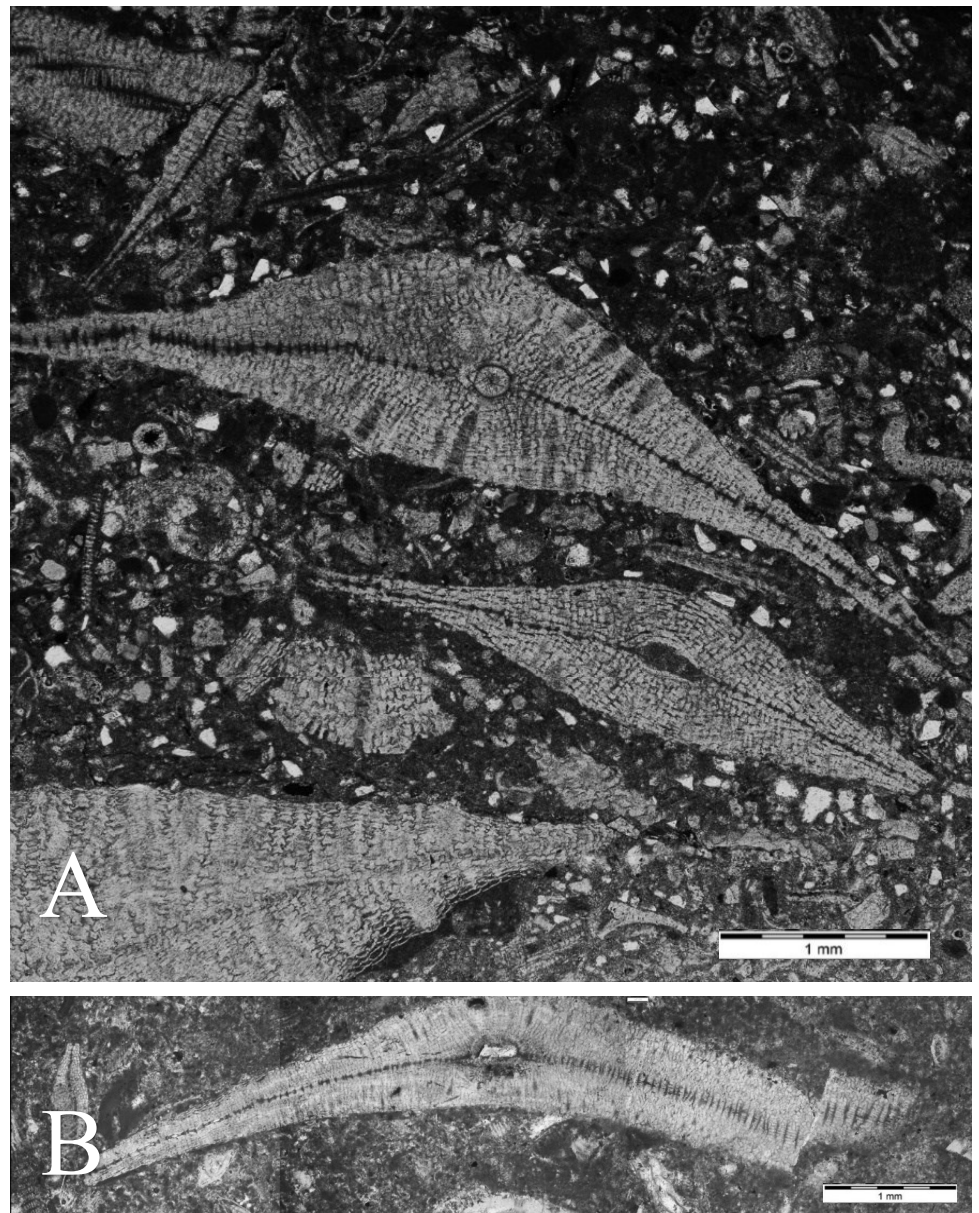
Figure 4. Photomicrographs showing megalospheric generation of *Discocyclina javana* (Verbeek). A) Thin section containing *D. javana* (A-form) sampled from location 2; B) Thin section containing *D. javana* (A-form) sampled from Wahau, North-east Kutai, Kalimantan (unpublished data). Both of them showing no sign of bioerosion penetrating into the test instead of any surface "shallow" bioerosion and/or abrasion indicates wave reworking during sedimentation. Scale bar = 1 mm.

Bioerosion Type
As illustrated in Figure 5, a detailed analysis of bioerosion on *Discocyclina javana* demonstrates the relationships between marine organisms and

their substrates during the Late Eocene. The shapes of the borings and spaces seen in this study are linked to four different ichnospecies that are grouped into three different ichnogenera and "unique" parrotfish bitemark. Those ichnogenera are *Oichnus* Bromley, 1981, *Caulostrepsis* Clarke, 1908, and *Helminthoidichnites* Fitch, 1850.
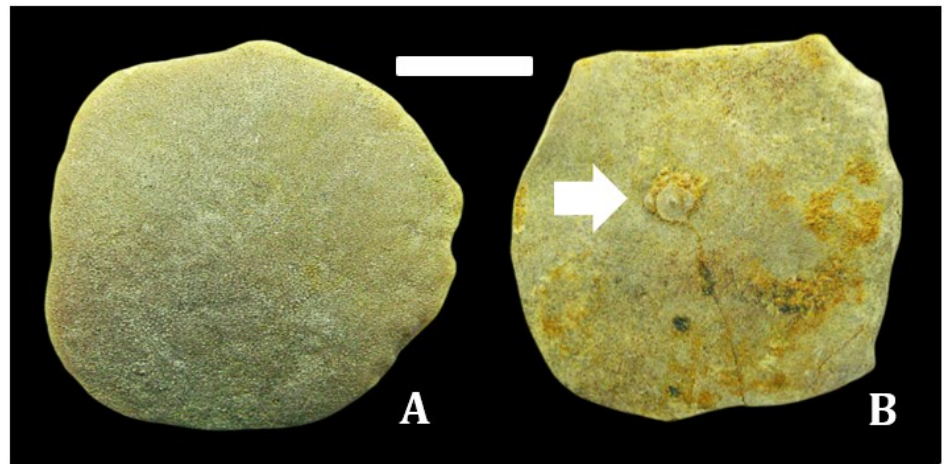
Figure 5. A) Well-preserved *Discocyclina javana* (Verbeek, 1891) without notable drilling and encrustations. B) A test of *Discocyclina javana* (Verbeek, 1891) showing encrustations (white arrow). Scale bar = 1 cm.

Ichnogenus: *Oichnus* Bromley, 1981

The ichnogenus *Oichnus* refers to bioerosive penetrations in calcareous skeletal substrates, which can be complete or incomplete (Wisshak et al. 2015). The trace fossils subject to examination exhibit round to subcircular perforations that are of biogenic nature, resulting from the drilling activity on rigid or calcareous skeletal surfaces (Bromley 1981) . *Oichnus* ichnogenera are morphologically identical to *Tremichnus* ichnogenera (Wisshak et al. 2015). Originally, *Oichnus* was exclusively established for bioerosion traces and interpreted as a result of predatory drilling. Meanwhile, *Tremichnus* specifically refers to shallow parabolic holes passing through echinoderm skeletons and is interpreted as *Domichnia* or *Fixichnia* (Wisshak et al. 2015). Two *Oichnus* ichnospecies were identified herein from the Priabonian *Discocyclina javana* Verbeek in Bayat, Indonesia, which are *Oichnus simplex* and *Oichnus paraboloides*.

a.   *Oichnus simplex* Bromley, 1981 (Plate 1A, 1B)
     Ichnofossil group   :   Bioerosional trace fossils
     Family   :   *Oichnidae*
     Ichnogenera   :   *Oichnus*
     Species   :   *simplex*

     Description: *Oichnus simplex* is characterised by small cylindrical to sub-cylindrical borehole with sharp border (Wisshak et al. 2015). The drill holes exhibit a diameter range spanning from 0.1 mm to 0.5 mm, with an average diameter of 0.3 mm. The boreholes are typically spherical or subspherical in shape and more or less perpendicular to the substrate surface. The walls of the borehole are typically smooth, and there is no surrounding debris or excavation halo. The hole itself is often similar in size throughout its depth, without significant tapering. These characteristics differentiate *Oichnus simplex* from other types of trace fossils which might have different shapes, sizes or patterns of penetration into the substrate.

Remarks: *Oichnus simplex* is a frequent form of boring commonly observed in *Discocyclina javana*, characterised by its comparatively diminutive size and simple vertical perforations. Cylindrical tiny round holes, known as *O. simplex* Bromley (1981), are frequently generated by predatory muricid gastropods, however similar structures can also be produced by other invertebrate species, including cephalopods or annelids (Donovan 2017). The size of the drill holes observed in the examinations of larger benthic foraminifers are very substantial, typically measured in millimetres. These holes can be effectively linked to the species *O. Simplex* (Abdel-Fattah 2018). *O. simplex* borings have been found in various fossils, such as *Hemipneustes striatoradiatus* (Echinoidea) from the Maastrichtian type area (Donovan & Jagt 2020). The dimensions and surface features of the ichnogenus in inquiry are not essential to its ichnotaxonomy (Bromley 1981). The stratigraphic age of this cosmopolitan ichnogenus ranges from Neoproterozoic to Holocene (Abdel-Fattah 2018). As with other ichnofossils, *O. simplex* can provide valuable information about past ecological interactions - for instance, they might represent evidence of predation or parasitism on the organism that once inhabited the substrate where these traces are found in different environments throughout geological history.

b. *Oichnus paraboloides* Bromley, 1981 (Plate 1C, 1D)
    Ichnofossil group   :   Biorosional trace fossils
    Family   :   *Oichnidae*
    Ichnogenera   :   *Oichnus*
    Ichospecies   :   *paraboloides*

Description: This ichnospecies is characterised by a spherical paraboloid form. The drill holes exhibit a diameter variation spanning from 0.8 mm to 2.2 mm, with a mean diameter of 1.5 mm. The boring is perpendicular from the opening. Sometimes the boring is not penetrative which has a slightly raised central boss. In *Discocyclina javana*, outer opening is enlarged by local bevelling. The wall of the boring is commonly ornamented by etching patterns reflecting the ultrastructure of the substrate (Bromley 1981).

Remarks: *Oichnus paraboloides* is more common boring than *O. simplex* in the studied *Discocyclina javana* tests from the Wungkal-Gamping Priabonian deposit. The stratigraphic range of this ichnospecies extended from the Cambrian to Holocene (Abdel-Fattah 2018). They are characterised by circular to subcircular holes of biogenic origin bored into hard substrates, such as foraminiferal tests and shells. *O. paraboloides* is an ichnospecies that has been interpreted as boring traces produced by predatory gastropods, particularly naticid gastropods (Kong et al. 2015). The ecological impact of *O. paraboloides* being found on a greater variety of foraminiferal tests can be attributed to the following factors: (1) The wide occurrence of *O. paraboloides* on the samples of foraminifera suggests that predation and parasitism of benthic foraminiferans are common phenomena in both contemporary and ancient marine ecosystems (Svensson Nielsen et al. 2003), (2) This suggests that the organisms responsible for creating *O. paraboloides* traces played a significant role in shaping the ecology of these environments. Bioerosion traces, such as those created by *O. paraboloides*, can have a direct impact on the foraminiferal tests, potentially affecting their structural integrity and can lead to changes in the distribution and abundance of foraminiferal species in the affected environments

(Svensson Nielsen et al. 2003; Kong et al. 2015; Abdel-Fattah 2018), (3) The presence of *O. paraboloides* on a greater variety of foraminiferal tests implies that the trace makers had a broader range of prey preferences, which can provide insights into the ecological interactions between predators and prey in ancient marine environments. In summary, the ecological impact of *O. paraboloides* being found on a greater variety of foraminiferal tests can be attributed to its role in predation and parasitism, bioerosion, ecological interactions, and environmental parameters. Studying the distribution and abundance of these ichnospecies can help researchers understand the environmental factors that influenced the distribution of foraminiferal species and their predators in shaping the structure and dynamics of ancient marine ecosystems.

Ichnogenus: Caulostrepsis Clarke, 1908

Caulostrepsis is a genus of trace fossil associated with bioerosion, which refers to the biological activity of organisms in excavating or modifying hard substrates such as rocks, shells, or wood (Santos et al. 2011). The morphology of *Caulostrepsis* can vary depending on the specific species and environmental conditions, but typically exhibits multiple small, circular to subcircular external openings on the substrate surface. These openings can be arranged in irregular clusters or scattered individually. The size and shape of *Caulostrepsis* can vary depending on the species and growth stage. They can range from millimetres to centimetres in diameter, and their overall shape may be elongated, irregular, or branching.

a. *Caulostrepsis* isp. (Plate 1E, 1F)

   Description: The length of this simple and cylindrical boring ranges from 3.3 mm to 7.7 mm with an average length 4.9 mm. The width ranges from 0.5 mm to 1.5 mm with an average width 1.0 mm. It is generally attributed to the work of spionid polychaetes.

   Remarks: Common borings found in *Discocyclina javana*. These particular borings are not designated to a specific ichnospecies within this context due to their inadequate preservation. The boring's morphological characters show similarity to *Caulostrepsis taeniola* Clarke, 1908. Rocky shorelines, with their reduction or lack of sedimentation, offer exceptional conditions for these organisms (Lopes 2011). For instance, it is often found in association with other organisms in hard-substrate biota, which is less well known than that of soft-bottom communities (Gibert et al. 1998). The presence of *Caulostrepsis* indicates conditions favourable for colonisation by boring and encrusting organisms. *Caulostrepsis* is widely distributed in shallow marine environments, and is produced by polychaetes, a group of marine worms, but is rarely known from polar regions (Hanken et al. 2012).

Ichnogenus: *Helminthoidichnites* Fitch, 1850

Helminthoidichnites is a type of trace fossil, which are geological records of biological activity. This ichnogenus displays only occasional loops, which distinguishes it from Gordia, where loops are a more characteristic feature. There is a single known ichnospecies of *Helminthoidichnites*, named *Helminthoidichnites* tenuis, but the morphological features found in study area is differ from H. tenuis. *Helminthoidichnites* represents a singular ichnotaxon that has been identified in both marine and non-marine sedimentary deposits spanning from the Precambrian to the Quaternary period (Lima et al. 2017).

a. *Helminthoidichnites* isp. (Plate 2A, 2B, 2E, 2E)
    Description: This ichnospecies is characterised by simple and straight to slightly curved trail, unbranched. *Helminthoidichnites* are horizontal trace fossils that are straight or curved, and more rarely, circular. The length of the unary ichnospecies measures 23 mm, while the length of the trail is 0.5 mm. This probably the grazing or feeding structures produced by mobile and sessile deposit and detritus feeding organism. It has a slightly wide opening.
    Remarks: Rarely found in this individual fossil test of *Discocyclina javana*. Grazing and feeding structures produced by mobile and sessile deposit- and detritus-feeding organisms (Knaust & Bromley 2012). *Helminthoidichnites* is a type of trace fossil, which are geological records of biological activity. The presence of *Helminthoidichnites* suggests mobility associated with significant sediment displacement, implying muscular mobility in the organisms that produced these traces (Evans et al. 2020).

Parrotfish bite mark (Plate 2C, 2D)

This paper is also aims to be the first to record parrotfish bite mark on the *Discocyclina javana* test in Indonesia after being first reported by Syed & Sengupta (2019). Their work focused on the discovery of parrotfish bite marks on larger foraminifera (*Assilina exponens*) fossils from the Middle Eocene period in Kutch, Gujarat, India, which are attributed to necto-benthic parrotfish (class *Actinopterygii*, family *Scaridae*) (Syed & Sengupta 2019). There is a similarity between what happens to the bioerosion in Discocyclina javana in Indonesia and *Assilina exponens* in India. The observations suggested that the bite marks are predominantly found on large microspheric specimens of both species. The comparison of the bioerosion patterns with those of extant parrotfish suggests that the ancient parrotfish belonged to the excavator category or the scraper–excavator category.

Paleoecology significance
Tracemaker ethology and biological affinities

Ethology, as a branch of biology, is the scientific study of animal behaviour. It includes both the behaviour under natural conditions and also under controlled conditions. In advanced ethology, the focus is often on more complex aspects of animal behaviour and its interpretation. In the other hand. bioerosion can also be related to paleoproductivity, as shown by a significant correlation between bioerosion rates and paleoproductivity estimates (Frozza et al. 2020). Bioerosion in the Priabonian *Discocyclina javana* exhibits encrustation and predation scars in may imply commensalism, mutualism, parasitism, or scavenging. Nematodes bore holes into foraminiferal tests to feed on their soft tissues (Sliter 1971). Neoichnological investigations indicated the tracemakers of numerous trace fossils, although bioeroders of various fossil borings are difficult to determine (Abdel-Fattah 2018). The drilling holes of the ichnogenus *Oichnus* are typically caused by gastropod predation, while the borings of *Caulostrepsis* and *Helminthoidichnites* are caused by polychaete worms. Parrotfish bite marks are typically indicative of coral reef environments. Parrotfish are known for their distinctive feeding behaviour, which involves scraping algae and small organisms off coral reefs using their beak-like teeth. Therefore, parrotfish bite marks are commonly employed as indicators of the vitality and activity of coral reef ecosystems.

Paleoenvironmental and larger foraminifera assemblages

The Eocene deposits found in Bayat, Indonesia primarily consist of shallow open marine sediments that were deposited in melange tectonic settings inside the Jiwo Hills, which are a component of the southern mountain range (Bothe 1929; Sumosusastro 1956; Sumarso & Ismoyowati 1975). The biofacies study from Wungkal-Gamping Formation can be classified as foreslope biofacies which dominantly show the fair to good imbrications of *Planocamerinoides* sp., *Nummulites javanus* Verbeek, 1891, *Palaeonummulites variolarius* (Caudri, 1934), and *Discocyclina.javana* during Late Eocene − Priabonian stage (Choiriyah et al. 2006; Rahmawati et al. 2012). The biometrical study based on the larger benthic foraminifera accumulation in Wungkal-Gamping Formation shows that conducive paleoecological conditions to reproduce compared to the Wungkal-Gamping formation which are shallow, warm and full of nutrients (Rahmawati, unpublished work). The distribution of larger foraminifera in carbonate deposits can provide a graphic indication of paleoenvironment (Hallock & Glenn 1986). Additionally, the biostratigraphy and facies of larger foraminifera can provide insights into sedimentary cover and paleoenvironmental conditions (Consorti & Köroğlu 2019). Therefore, bioerosion in larger foraminifera tests can provide valuable information about past environmental conditions and paleoecology. The search results suggested that there is a relationship between paleoenvironment and larger foraminifera accumulation. Larger foraminifera can be used as a tool for paleoenvironmental analysis of carbonate depositional facies (Hallock & Glenn 1986).

Paleoproductivity estimates and bioerosion rates show a significant correlation, suggesting that bioerosion is more frequent in eutrophic environments (Frozza et al. 2020). Additionally, bioerosion in larger foraminifera tests can be used as a tool for paleoenvironmental analysis (Beavington-Penney & Racey 2004). The effects of external influences on test size, shape, and distribution for some calcareous-walled foraminifera have been studied. This result show consistency with the bioerosion observed in the nummulitid group reported by Abdel-Fattah (2018).

CONCLUSIONS

1. *Discocyclina javana* (Verbeek) demonstrated evident bioerosion and most of them occur in microspheric generation, which was distinguished by a varied collection of four ichnospecies from three ichnogenera. The boreholes that are linked to the predation of gastropods can be classified as *Oichnus simplex* and *Oichnus paraboloides*, *Caulostrepsis* isp., and *Helminthoidichnites* isp.

2. *Oichnus* was found on commonly on *Discocyclina javana* test, it might suggest that there were drilling predators in that environment. In some cases, these holes are not made by predators but by parasites attaching to their hosts. Changes in size or shape patterns across geological timescales might also reveal evolutionary trends among both prey (e.g., shell thickness or hardness) and predators (e.g., drilling mechanism). A high concentration of bioerosion may suggest favourable conditions for predators or a high population density, or vice versa.

3. The bite marks on the individual microspheric *Discocyclina javana* test indicated that the parrotfish were herbivorous, feeding on algae that grew on the foraminiferal test as bioclasts, same as those of Middle Eocene deposit in India (Syed & Sengupta 2019). This information adds to the knowledge of the feeding habits of ancient parrotfish species.

4. The presence of larger foraminifera, which are excellent recorders of shallow marine sclerobionts, suggested that the depositional environment during Priabonian in Bayat was a shallow marine carbonate setting with medium to high sedimentation regimes.

AUTHOR CONTRIBUTION

ACKNOWLEDGEMENTS

CONFLICT OF INTEREST
The authors of this paper declare that they are free from any ties or financial conflicts of interest that may have seemed to impact their work.

REFERENCES

Abdel-Fattah, Z.A., 2018. Bioerosion in the middle Eocene larger foraminifer Nummulites in the Fayum depression, Egypt. *Proceedings of the Geologists' Association*, 129(6), pp.774–781. doi: 10.1016/j.pgeola.2018.08.003.

Beavington-Penney, S.J. & Racey, A., 2004. Ecology of extant nummulitids and other larger benthic foraminifera: Applications in palaeoenvironmental analysis. *Earth-Science Reviews*, 67(3–4), pp.219–265. doi: 10.1016/j.earscirev.2004.02.005.

Bothe, A.C.D., 1929. The Geology of The Hills Near Djiwo and The Southern Range. In *Proceeding of the Fourth Pacific Science Congress*. pp. 1–15.

Briguglio, A. & Hohenegger, J., 2011. How to react to shallow water hydrodynamics: The larger benthic foraminifera solution. *Marine Micropaleontology*, 81(1–2), pp.63–76. doi: 10.1016/j.marmicro.2011.07.004.

Bromley, R., 1981. Concepts in ichnotaxonomy illustrated by small round holes in shells. *Acta Geologica Hispanica*, 16(1), pp.55–64.

Choiriyah, S.U. et al., 2006. Foraminifera Besar pada Satuan Batugamping Formasi Gamping-Wungkal, di Sekarbolo, Perbukitan Jiwo, Bayat-Klaten. *Jurnal Ilmu Kebumian Teknologi Mineral*, 19(1), pp.1–8.

Consorti, L. & Köroğlu, F., 2019. Maastrichtian-Paleocene larger Foraminifera biostratigraphy and facies of the Şahinkaya Member (NE Sakarya Zone, Turkey): Insights into the Eastern Pontides arc sedimentary cover. *Journal of Asian Earth Sciences*, 183(April). doi: 10.1016/j.jseaes.2019.103965.

Donovan, S.K., 2017. A plea not to ignore ichnotaxonomy: recognizing and recording Oichnus Bromley. *Swiss Journal of Palaeontology*, 136 (2), pp.369–372. doi: 10.1007/s13358-017-0134-9.

Donovan, S.K. & Jagt, J.W.M., 2020. Oichnus simplex Bromley infesting Hemipneustes striatoradiatus (Leske) (Echinoidea) from the Maastrichtian type area (Upper Cretaceous, The Netherlands). *Ichnos:an International Journal of Plant and Animal*, 27(1), pp.64–69. doi: 10.1080/10420940.2019.1584561.

Evans, S.D. et al., 2020. Discovery of the oldest bilaterian from the Ediacaran of South Australia. *Proceedings of the National Academy of Sciences of the United States of America*, 117(14), pp.7845–7850. doi: 10.1073/pnas.2001045117.

Frozza, C.F. et al., 2020. Bioerosion on Late Quaternary Planktonic Foraminifera Related to Paleoproductivity in the Western South Atlantic. *Paleoceanography and Paleoclimatology*, 35(8), pp.1–16. doi: 10.1029/2020PA003865.

Gibert, J.M. De, Martinell, J. & Domènech, R., 1998. Entobia Ichnofacies in Fossil Rocky Shores, Lower Pliocene , Northwestern Mediterranean. , 13(5), pp.476–487.

Hallock, P., 1985. Why are Larger Foraminifera Large? *Paleobiology*, 11 (2), pp.195–208. https://www.jstor.org/stable/2400527.

Hallock, P. & Glenn, E.C., 1986. Larger Foraminifera : A Tool for Paleoenvironmental Analysis of Cenozoic Carbonate Depositional Facies. *PALAIOS*, 1(1), pp.55–64. https://www.jstor.org/stable/3514459%0A.

Hallock, P. & Reymond, C.E., 2022. Contributions of Trimorphic Life Cycles to Dispersal and Evolutionary Trends in Large Benthic Foraminifers. *Journal of Earth Science*, 33(6), pp.1425–1433. doi: 10.1007/s12583-022-1707-0.

Hanken, N.M., Uchman, A. & Jakobsen, S.L., 2012. Late Pleistocene-early Holocene polychaete borings in NE Spitsbergen and their palaeoecological and climatic implications: An example from the Basissletta area. *Boreas*, 41(1), pp.42–55. doi: 10.1111/j.1502-3885.2011.00223.x.

Hohenegger, J., 2011. *Large Foraminifera: Greenhouse Constructions and Gardeners in the Oceanic Microcosm*, Kagoshima: The Kagoshima University Museum.

Hutchings, P., Peyrot-Clausade, M. & Osnorno, A., 2005. Influence of land runoff on rates and agents of bioerosion of coral substrates. *Marine Pollution Bulletin*, 51(1–4), pp.438–447. doi: 10.1016/j.marpolbul.2004.10.044.

Knaust, D. & Bromley, R., 2012. *Fossils as Indicators of Sedimentary Environments. Developments in Sedimentology*, Elsevier. doi: 10.1017/S0016756813001118.

Kong, D.Y., Lee, M.H. & Lee, S.J., 2015. Traces (ichnospecies Oichnus paraboloides) of predatory gastropods on bivalve shells from the Seogwipo Formation, Jejudo, Korea. *Journal of Asia-Pacific Biodiversity*, 8(4), pp.330–336. doi: 10.1016/j.japb.2015.10.013.

Lima, J.H.D., Minter, N.J. & Netto, R.G., 2017. Insights from functional morphology and neoichnology for determining tracemakers: a case study of the reconstruction of an ancient glacial arthropod-dominated fauna. *Lethaia*, 50(4), pp.576–590. doi: 10.1111/let.12214.

Lopes, R., 2011. Ichnology of fossil oysters (Bivalvia, Ostreidae) from the southern Brazilian coast. *Gaea - Journal of Geoscience*, 7(2), pp.94–103. doi: 10.4013/gaea.2011.72.02.

Rahmawati, D., Novian, M.I. & Rahardjo, W., 2012. Studi Biostratigrafi dan Analisis Mikrofasies Batugamping , Formasi Wungkal-Gamping, Jalur Pengukuran Padasan, Gunung Gajah, Bayat, Klaten, Jawa Tengah. *41st IAGI Annual Convention and Exhibition Yogyakarta.* Yogyakarta: Ikatan Ahli Geologi Indonesia, pp. 3–6.

Santos, A., Mayoral, E. & Bromley, R.G., 2011. Bioerosive structures from Miocene marine mobile-substrate communities in southern Spain, and description of a new sponge boring. *Palaeontology*, 54(3), pp.535–545. doi: 10.1111/j.1475-4983.2011.01040.x.

Sliter, W.V., 1971. Predation on benthic foraminifers. *Journal of Foraminiferal Research*, 1, pp.20–29.

Sumarso & Ismoyowati, T., 1975. Contribution to the Stratigraphy of the Jiwo Hills and their Southern Surroundings (Central Java). *Proceedings Indonesian Petroleum Association, Fourth Annual Convention.* Indonesian Petroleum Association.

Sumosusastro, S., 1956. *A contribution to the Geology of the Eastern Djiwo hills and the Southern Range in Central Java.* Dept. Geol. Faclt. Scie., University of Indonesia.

Surono, Toha, B. & Sudarno, I., 1992. *Geological Map of The Surakarta - Giritontro Quadrangles, Java*, Bandung, Indonesia.

Svensson Nielsen, K.S., Nielsen, J.K. & Granville Bromley, R., 2003. Palaeoecological and ichnological significance of microborings in quaternary foraminifera. *Palaeontologia Electronica*, 6(1), pp.1–13.

Syed, R. & Sengupta, S., 2019. First record of parrotfish bite mark on larger foraminifera from the Middle Eocene of Kutch, Gujarat, India. *Current Science*, 116(3), pp.363–365.

Tribollet, A., Radtke, G. & Golubic, S., 2011. Bioerosion. In *Encyclopedia of Geobiology. Encyclopedia of Earth Sciences Series.* Dordrecht: Springer, pp. 117–134. doi: 10.1007/978-1-4020-9212-1_25.

Vohník, M., 2021. Bioerosion and fungal colonization of the invasive foraminiferan Amphistegina lobifera in a Mediterranean seagrass meadow. *Biogeosciences*, 18(8), pp.2777–2790. doi: 10.5194/bg-18-2777-2021.

Wisshak, M. et al., 2015. In defence of an iconic ichnogenus - Oichnus Bromley, 1981. *Annales Societatis Geologorum Poloniae*, 85(3). doi: 10.14241/asgp.2015.029.

Wisshak, M. & Tapanila, L., 2008. *Current Developments in Bioerosion* Erlangen E., Berlin, Heidelberg: Springer Berlin Heidelberg. doi: 10.1007/978-3-540-77598-0.

APPENDICES
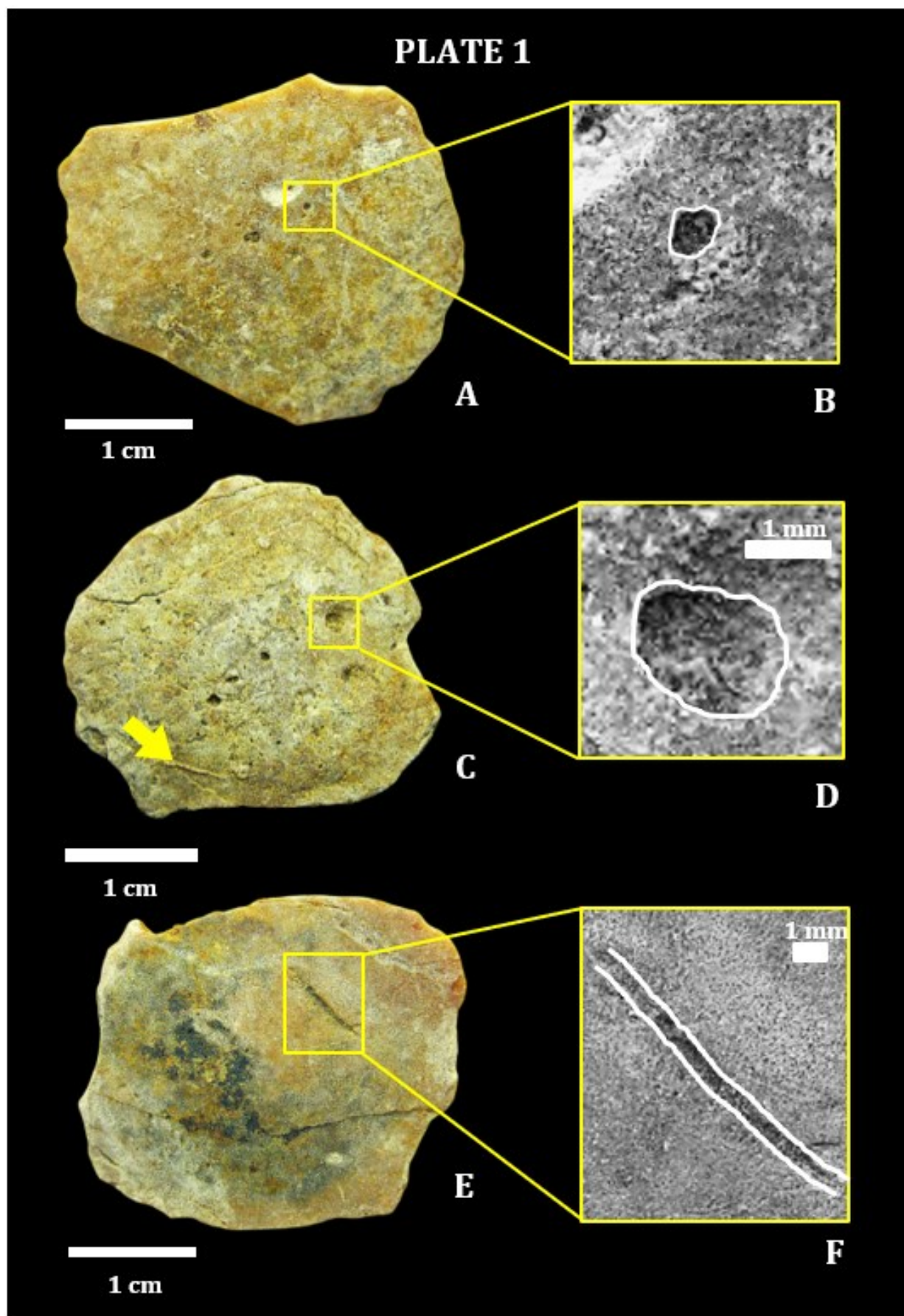
PLATE 1
A, C, E: External view on individual microspheric test of *Discocyclina javana* (Verbeek, 1891);
B, D, F: Closer zoom view showing the bioerosional trace fossil.
(A – B) *Oichnus simplex*; (C – D) *Oichnus paraboloides*; (E – F) *Caulostrepsis* isp. Scale bar = 1 cm
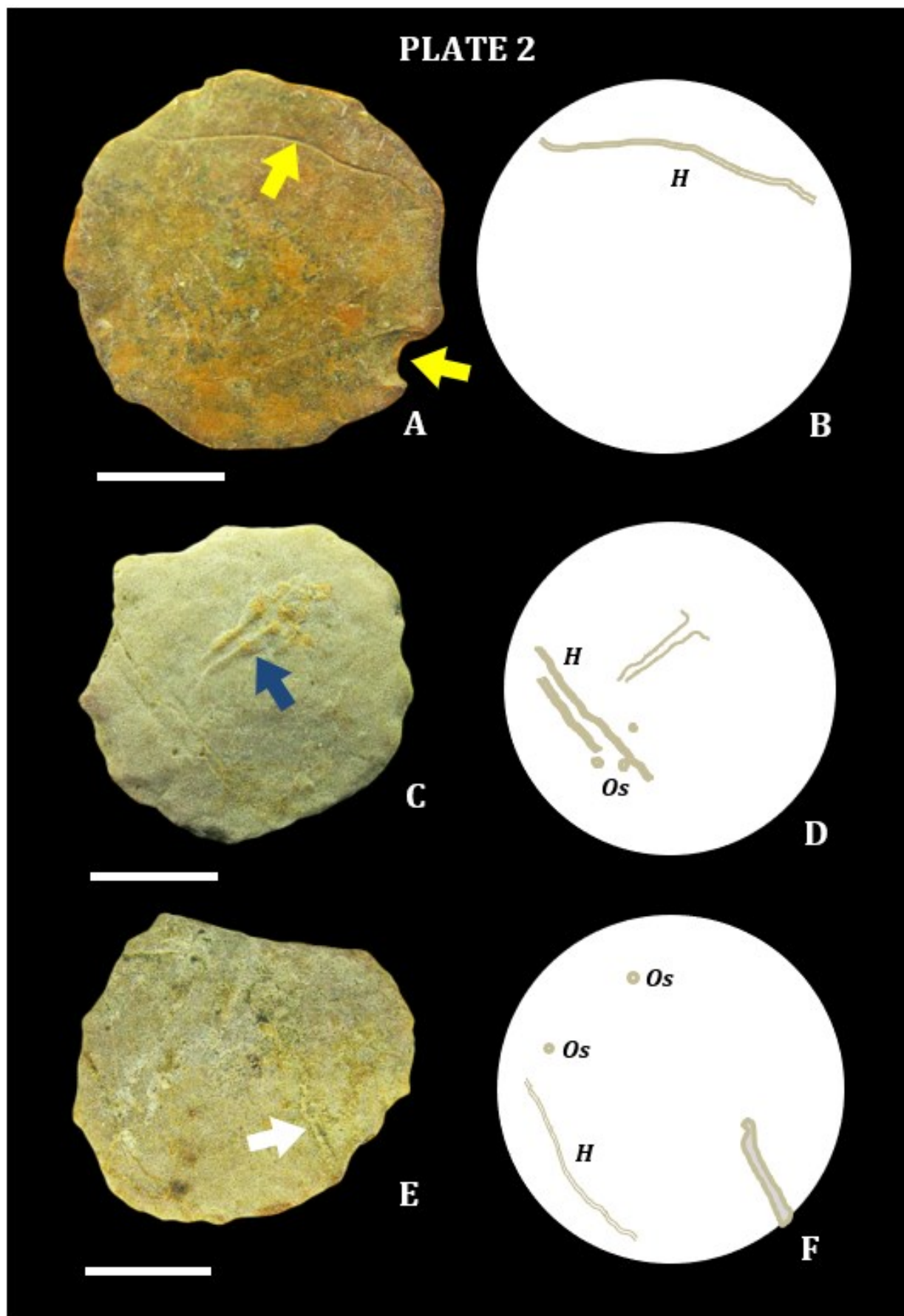
PLATE 2

A, C, E: External view on individual microspheric test of *Discocyclina javana* (Verbeek, 1891)
B, D, F: Closer zoom view showing the bioerosional trace fossil. (A – B) *Helminthoidichnites* isp (yellow arrow); (C – D) *Oichnus simplex, Helminthoidichnites* isp, parrotfish bitemark (yellow arrow); (E – F) *Oichnus simplex, Helminthoidichnites* isp, and some algae-symbiont traces (white arrow). Scale bar = 1 cm.
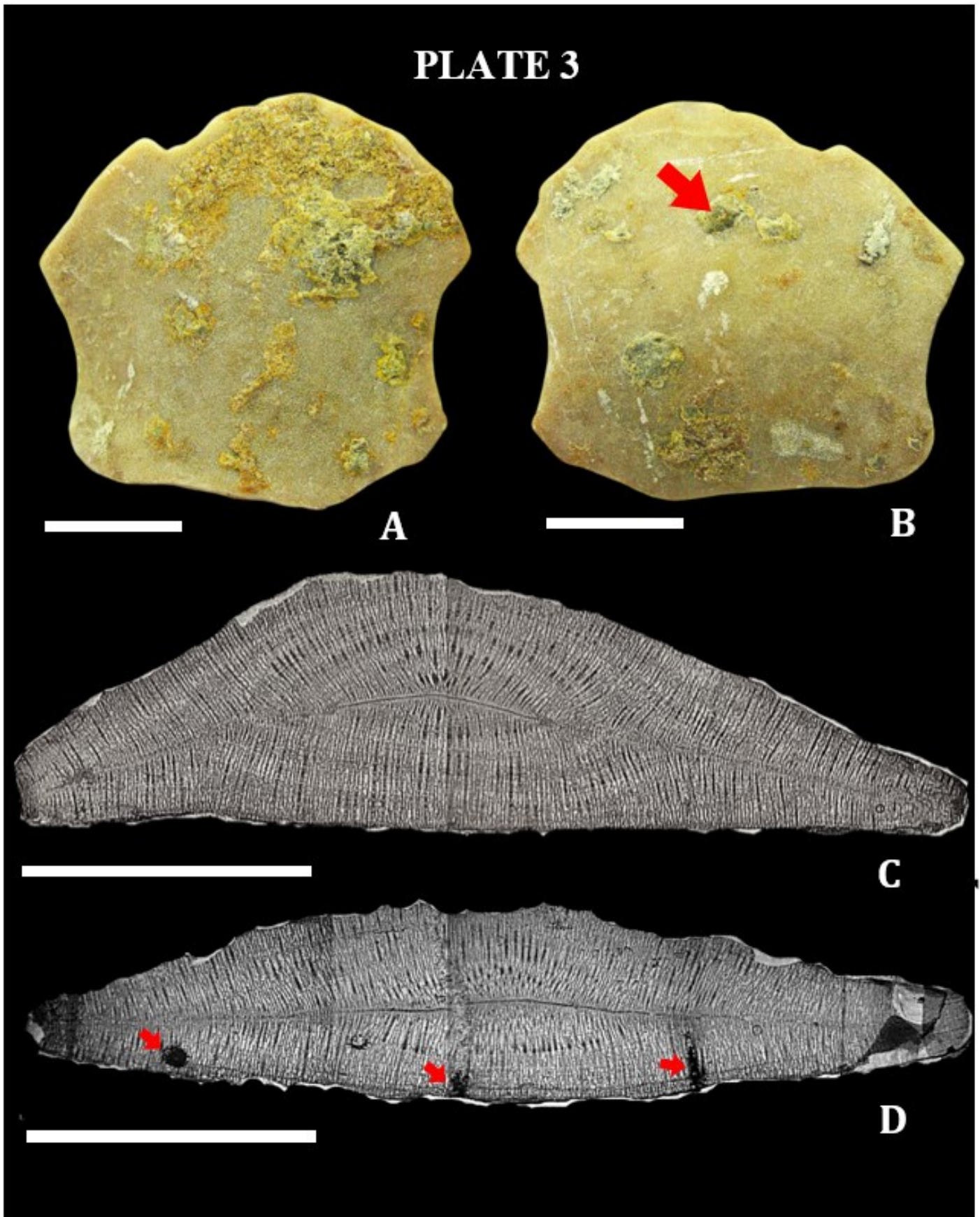
PLATE 3
A − B: External view on individual B-form of *Discocyclina javana* (Verbeek, 1891)
C − D: Axial section of internal B-form of *Discocyclina javana* (Verbeek, 1891)

Research Article

Inventory of Macrofungi in Area of Taman Hutan Raya (TAHURA) Ir. H. Djuanda Bandung

Yani Suryani[1], Tri Cahyanto[1], Rahmat Taufiq Mustahiq Akbar[1]*, Dicky[2], Pameila Qaulan Tsaqila Madani[1], Rindi Meldania[1], Sophia Eka Tisnawati[1], Adisty Virakawugi Darniwa[1], Musa'adah[1], Ita Fitriyyah[1], Siska Tridesianti[1], Ayuni Adawiyah[1]

1)Department of Biology, Faculty of Science and Technology, Universitas Islam Negeri Sunan Gunung Djati Bandung, Jl. A.H. Nasution, No. 105, Cibiru, Bandung 40614, West Java, Indonesia.
2)Taman Huta Raya (TAHURA), Jl. Ir. H. Juanda, No. 99, Ciburial, Cimenyan, Kabupaten Bandung 40198, West Java, Indonesia.
* Corresponding author, email: rahmattaufiq@uinsgd.ac.id.

ABSTRACT

Taman Hutan Raya (TAHURA) Ir. H. Djuanda Bandung is an integrated conservation area in which there are secondary natural forests that have various kinds of flora and fauna. Macrofungi are fungi whose fruiting bodies can be seen directly without the aid of a microscope, heterotrophic, and ecologically act as decomposers of organic matter (decomposers) and as biological control agents. Data related to research results on macrofungi in the Tahura area is still limited and need more comprehensive research. This study aimed to inventory, determine the growth factors, and potential utilization of macroscopic fungi. Observations were carried out during the period of November 2021 – April 2022 using exploration method. Sampling was done by purposive sampling method. Macrofungi identification process was carried out based on morphological characters such as cap, stalk, and lamella, The environmental factors observed included air humidity, soil pH, temperature, and type of substrate. The results showed that as many as 83 species were found in the Protection block, 50 species were found in the Collection block, and 99 species were identified in the Utilization block from the phyla Basidiomycota and Ascomycota. The macrofungi found have potential as biodegradation agents, food ingredients, non-food ingredients, drugs, antimicrobials, antioxidants, anticancer, and anti-inflammatory.

INTRODUCTION

Indonesia is known as a country with abundant biodiversity or more known as a mega-biodiversity country. This is because Indonesia's tropical climate makes it suitable as a habitat for various living things, both flora and fauna (Nur et al. 2021). Forests whose natural level is still maintained and have diverse and varied ecosystem components. Biological components that play an important role and have not been fully utilized properly are decomposers, for example, fungi. Fungi that benefits the ecosystem are macrofungi (Kinge et al. 2017).

Macrofungi are fungi whose fruiting bodies can be seen directly, without the aid of a microscope. Most are from the division Basidiomycota, Ascomycota, and some are from the division Zygomycota (Mueller et al. 2007). Macrofungi play an important role in forest

ecosystems (Suharno et al. 2018). From the ecological perspective, macrofungi act as decomposers and biological controllers by supporting biogeochemical cycles (Arini et al. 2019). Macrofungi are one of the biological components that are present in all types of ecosystems. Macrofungi are widely spread because their large spores are easy to spread (Proborini 2012).

Taman Hutan Raya (TAHURA) Ir. H. Djuanda Bandung is a secondary natural forest area and has quite various flora with an area of approximately 546.28 ha which is divided into three blocks namely the Protection block, Utilization block, and Collection block and two areas which stretches between Maribaya and Pakar areas. TAHURA Bandung is located in the north of Bandung City, more precisely in Kampung Pakar, Ciburial Village, Cimenyan District, Bandung, West Java. The forest type in this area is mixed vegetation forest where there are approximately 40 families and 112 plant species (Ihsan 2012). From these data, there are several types of higher plants, including pine, resin, cinnamon, banyan, cypress, kigelia, and also Rafflesia flower. Different geographical conditions in the TAHURA Ir. H. Djuanda Bandung cause many unidentified macrofungi.

Studies of macrofungi in the TAHURA Ir. H. Djuanda Bandung have not much been done. The activities carried out can determine the macroscopic mushrooms potential and classify toxic and non-toxic mushrooms. In addition, some people do not know the role of mushrooms as one of the biodiversity which is very rich in benefits, including being used as food, industry, health, cosmetics and their role in the environment. Besides that, the big role that mushrooms have will help in efforts to manage conservation and control the life cycle of an ecosystem in one area sustainably (Prasetyo et al. 2009).

MATERIALS AND METHODS

Field research was carried out using the exploration method in three blocks of TAHURA Ir. H. Djuanda which included the blocks of Protection, Collection, and Utilization (Figure 1). Sampling was carried out twice with the range time from November 2021 to April 2022. The samples found from the searching results were then preserved in wet or dry conditions and identified until the species stage. The results of the preservation that had been made were then stored in the Laboratory of Universitas Islam Negeri Sunan Gunung Djati Bandung as collections.

The research was carried out in a descriptive exploratory method in which the activities of this research included collecting specimens, identifying, classifying, describing, and inventorying samples of the macrofungi found. The sampling technique used was purposive sampling, namely a sampling technique by determining certain criteria (Mukhsin et al. 2017). According to Arikunto (2003), the method is also called a data collection method which is not specific to a particular area but focuses on the purpose of the data collection process itself. Sampling with this method was used to collect species and the data were analyzed descriptively.

Identification of macrofungi was carried out based on morphological characters of the cap (pileus), gills (lamella), and stalk (stipe), as well as other characteristics of the fruiting body. The data obtained was then matched with macrofungi identification books (Moore & Sullivan 2013), the Mycokey 4.1 application, and the Book on Macrofungi (Smith et al. 1988). Additionally, the identification process is aided by mushroom experts, field guides, and local communities. During field observations and mushroom tracking, data collection also involves recording abiotic factors or environmental conditions including altitude,
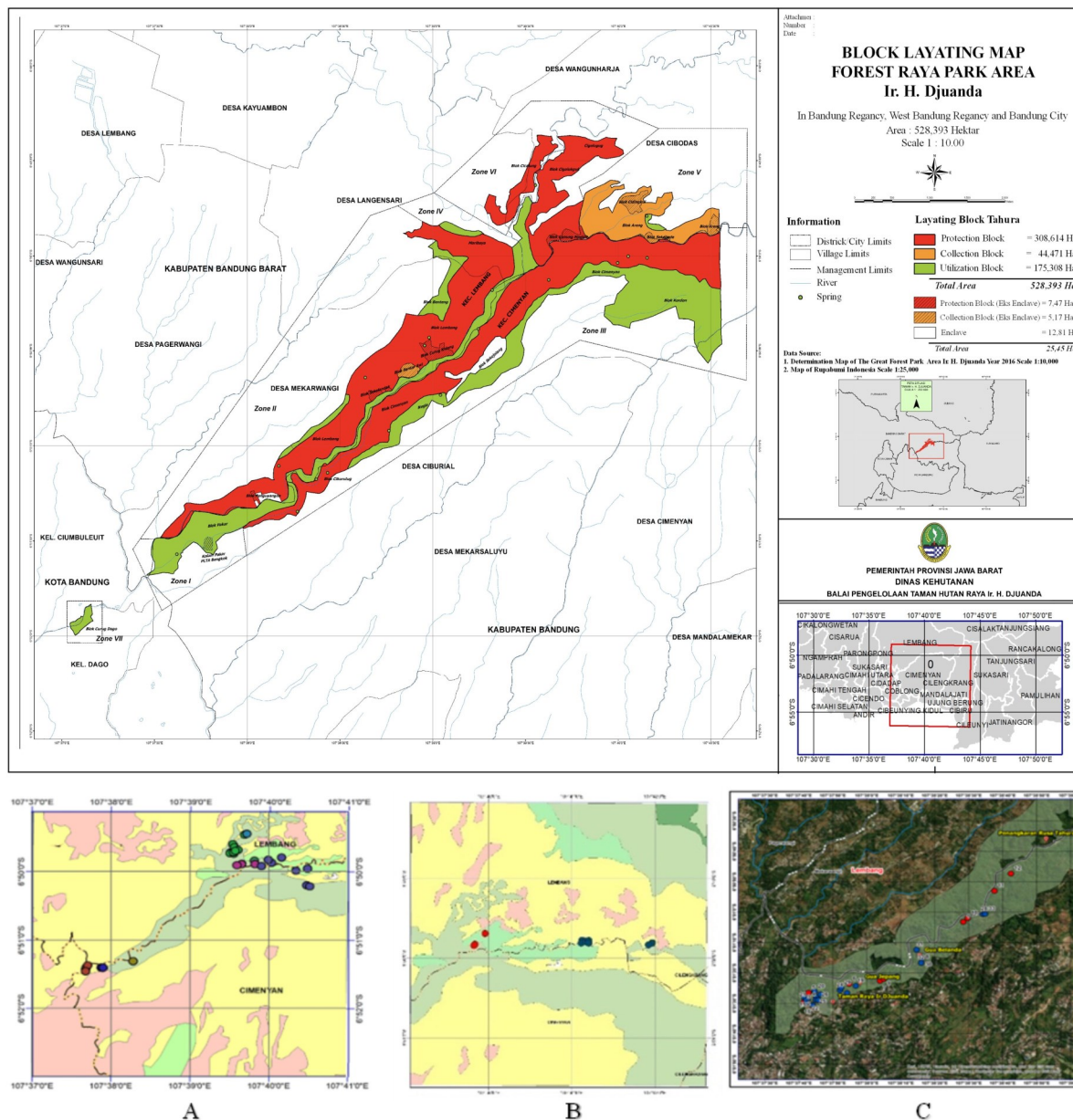
Figure 1. Location of TAHURA Ir. H. Djuanda Bandung (A= blocks of Protection, B= blocks of Collection, and C= blocks of Utilization

coordinate positions, measurement of environmental factors such as soil pH (using a soil tester), air humidity and temperature (using a thermo-hygrometer), and mushroom habitat.

RESULTS AND DISCUSSION
Types of Macrofungi
Based on the exploration results, 83 macrofungi species were found in the Protection block (Table 1), 50 in the Collection block (table 2), and 99 in the Utilization block (Table 3). In the Protection block, 83 macrofungi species were identified across two divisions, nine orders, and 29 families. November 2021 sampling discovered 40 species (22 in Tonjong Sawah, 9 in Cibingkul, 8 in Pakar (1), and 1 in Goa Belanda), while February 2022 sampling found 57 species (25 in Cibodas, 10 in Gunung Masigit, 10 in Seke Gede, and 12 in Pakar 2). Agaricales, with 15 families, dominated the Protection block, showing high adaptability. Polyporaceae family dominated the macrofungi in the Pakar (2) route due to the abundance of rotted wood in TAHURA, attributed to the order Polyporales, known for its various fruiting body shapes, colours, and sizes, particularly in the

genus Ganoderma.

Based on Table 2 (attachment), the Collection block harbou red 50 macrofungi species across all lines (*comprising two divisions, eight orders and twenty three families*), with 56 species from Basidiomycota and only one from Ascomycota. November 2021 sampling yielded 23 species (across eighteen families and two divisions), with 15 species in the Percoba Areng line. Basidiomycota dominated with ten families, while Ascomycota had one order, Xylariales. Gunung Masigit line had eight Basidiomycota species across seven families. January 2022 sampling found 34 species (across eighteen families and one division, Basidiomycota), with 26 species in the Percoba Areng line and eight in the Gunung Masigit line. The Collection block was dominated by Basidiomycota, particularly the Polyporaceae family, with 11 species. According to Khastini et al. (2019) the Polyporaceae family has good adaptability in various places at different altitudes with high humidity. Macrofungi collection during the rainy season (January) yielded higher numbers compared to the dry season (November). Macrofungi occurrence and diversity are greatly influenced by vegetation, geography, seasons, and succession stages. Optimal fruiting occurs in winter or the rainy season due to favourable humidity levels. Higher humidity in the rainy season promotes spore germination and growth. Macrofungi absorb nutrients from the environment through enzymatic breakdown of organic matter into simple molecules, which are then absorbed by hyphae.

Based on Table 3 (attachment), 99 macrofungi species were found in the Utilization block during January and April 2022. In January, 63 species were discovered, with Basidiomycota dominating (eight orders, 23 families), while Ascomycota had five species from two orders and three families. Agaricaceae was the most common family with 12 species. Macrofungi sampling in April found 24 species with Basidiomycota more prevalent. Polyporaceae was the most common family with 11 species.

The Utilization block's dense canopy provided stable temperatures, allowing macrofungi growth even in the dry season. Its proximity to a tourist route led to the discovery of macrofungi mainly from Agaricaceae and Polyporaceae families due to inorganic waste promoting their growth. Macrofungi depend on weathering wood for nutrients, thriving in places rich in carbohydrates, cellulose, and lignin, like leaf litter, tree branches, and rotted wood (Annissa et al. 2017). Some fungi are difficult to identify to the species level because some fungal samples are found in damaged conditions.

The Russulales order is an order that belongs to the class Agaricomycetes, according to Kirk et al. (2008), the order consists of 13 families and there are at least 3,060 species found. This order was previously included in the order Agaricales, but currently the order Russulales is a unitary order of several families that have different characters from the order Agaricales (Mishra 2005). Most Russulales have a cap that is convex to funnel-shaped above a stipe or stalk with no ring or volva. Some genera, such as Russula and *Lactarius*, do not have flexible fruit flesh, so when handled it is very brittle like soft chalk (Mishra 2005). The difference from each genus found is that the *Lactarius* genus has a fruiting body covered by latex while the Russula does not, even though their shape is similar. Meanwhile, *Sterum* has no stalks but hard fruiting bodies.

The order Geastrales has hygroscopic fruiting bodies where in dry weather the calyx-shaped parts of the fungus dry and curl around the soft spore sac to protect it. In this state, often the entire mushroom is

Table 1. Macrofungi found in the protection line/block.

No	Species	Genus	Family	Ordo	Line							
					TS	CB	PK1	GB	CBD	GM	SG	PK2
1	*Agaricus augustus* Fr.	*Agaricus*	Agaricacea	Agaricales	√	-	-	-	-	-	-	-
2	*Agaricus cf trisulphurata* Berk.	*Agaricus*	Agaricacea	Agaricales	-	-	√	-	-	-	-	-
3	*Agaricus silvicola* var. *silvicola* (Vittad.) Peck	*Agaricus*	Agaricacea	Agaricales	√	√	-	-	-	-	-	-
4	*Agaricus subrutilescens* (Kauffman) Hotson & D.E. Stuntz, (1938)	*Agaricus*	Agaricacea	Agaricales	√	-	-	-	-	-	-	-
5	*Amanita* cf. *hemibapha* (Berk. & Broome) Sacc.	*Amanita*	Amanitaceae	Agaricales	√	-	-	-	√	-	-	-
6	*Amanita sect. lepidella*	*Amanita*	Amanitaceae	Agaricales	-	-	-	-	-	-	-	-
7	*Amanita sect. vaginata* (Bull.:Fr.) *Vittadini*	*Amanita*	Amanitaceae	Agaricales	-	-	√	-	√	-	-	-
8	*Amauroderma rugosum* (Blume & TNees) Torrend	*Amauroderma*	Ganodermataceae	Polyporales	-	-	-	-	-	-	-	√
9	*Auricularia auricula-judae* (Bull.: Fr.) Wettstein	*Auricularia*	Auriculariaceae	Auriculares	-	-	-	-	√	√	-	-
10	*Auricularia delicata* (Mont. ex Fr.) Henn.	*Auricularia*	Auriculariaceae	Auriculares	-	-	-	-	√	√	√	-
11	*Baespora mysosura* Singer	*Baespora*	Marasmiaceae	Agaricales	√	-	-	-	-	-	√	-
12	*Bovista plumbea* Pers.	*Bovista*	Agaricacea	Agaricales	√	-	-	-	-	-	-	-
13	*Calvatia cyathiformis* (Bosc) *Morgan, J.*	*Calvatia*	Agaricacea	Agaricales	√	-	-	-	-	-	-	-
14	*Calvatia rugosa* (Berk. & M.A.Curtis) D.A. Reid	*Calvatia*	Agaricacea	Agaricales	√	-	-	-	√	-	-	-
15	*Candolleomyces eurysporus*	*Candolleomyces*	Crepidotaceae	Agaricales	-	-	-	-	√	-	-	√
16	*Collybia eucalyptorum* Cleland	*Collybia*	Tricholomataceae	Agaricales	√	-	-	-	√	-	-	-
17	*Coprinellus curtus* (Kalchbr.) Vilgalys, Hopple & Jacq.Johnson	*Coprinellus*	Psathyrellaceae	Agaricales	-	-	-	-	√	√	-	-
18	*Coprinopsis* sec. *atrsmentaria* (Bull.)	*Coprinopsis*	Psathyrellaceae	Agaricales	√	-	-	-	-	-	-	-
19	*Coprinopsis sect invei*	*Coprinopsis*	Psathyrellaceae	Agaricales	√	-	-	-	√	√	-	-
20	*Crepidotus applanatus* (Pers.) Kummer	*Crepidotus*	Crepidotaceae	Agaricales	-	-	-	-	√	-	-	-
21	*Crepidotus variabilis* (Pers.: Fr.) Kumme	*Crepidotus*	Crepidotaceae	Agaricales	-	-	-	-	√	-	-	-
22	*Cymatoderma* cf. *elegans* Jungh.	*Cymatoderma*	Meruliaceae	Polyporales	-	-	-	-	-	-	-	√
23	*Dacryopinax spathularia* (Schwein.) G.W. Martin	*Dacryopinax*	Dacrymycetaceae	Dacrymycetales	-	√	-	-	-	-	-	-
24	*Filoboletus manipularis* (Berk.) Teng	*Filoboletus*	Mycenaceae	Agaricales	√	-	-	-	-	-	-	√
25	*Favolus tenuiculus* P. Beauv.	*Favolus*	Polyporaceae	Polyporales	-	-	-	-	-	-	-	√
26	*Fistulina hepatica* (J.C. Sch. Fr.) Withering	*Fistulina*	Fistulinaceae	Agaricales	√	-	-	-	-	-	-	-
27	*Ganoderma applanatum* (Pers.) Pat.	*Ganoderma*	Ganodermataceae	Polyporales	-	-	√	-	√	-	-	√
28	*Geastrum fimbriatum* Fr.	*Geastrum*	Geastraceae	Geastrales	-	-	-	-	-	-	-	-
29	*Geastrum sessile* (Sow.) Pouzar	*Geastrum*	Geastraceae	Geastrales	-	-	-	-	√	√	-	-
30	*Geastrum triplex* Junghuhn	*Geastrum*	Geastraceae	Geastrales	-	-	-	-	-	-	-	-
31	*Gymnopilus sapineus* (Fr.: Fr.) Murrill	*Gymnopilus*	Cortinariaceae	Agaricales	√	-	-	-	-	-	√	-
32	*Gymnopus dichrous* (Berk. & M. A Curtis) Halling	*Gymnopus*	Omphallotaceae	Agaricales	√	-	-	-	-	-	-	-
33	*Gymnopus dryophilus* (Bull.) Murrill	*Gymnopus*	Omphallotaceae	Agaricales	-	√	-	-	-	-	-	-
34	*Heterobasidion amosum* (Fr Fr.) Brefeld	*Heterobasidion*	Bondarwiaceae	Russulales	-	-	√	-	-	-	-	-
35	*Heterobasidion* cf. *parviporum* Niemelä & Korhone	*Heterobasidion*	Bondarwiaceae	Russulales	-	-	-	-	-	-	√	-
36	*Hexagonia tenuis* (Fr.) Fr.	*Hexagonia*	Polyoraceae	Polyporales	-	-	-	-	√	-	-	-
37	*Inocybe cincinnata* (Fr.) Quélet	*Inocybe*	Inocybaceae	Agaricales	-	-	-	-	-	-	√	-
38	*Laccaria laccata* (Scop. Fr.) Cooke	*Laccaria*	Hydnagiaceae	Agaricales	√	-	-	-	-	-	-	-
39	*Lactarius* cf. *rubidus* (Hesler & A.H.Sm.) Methven	*Lactarius*	Russulaceae	Russulales	-	-	-	-	√	-	-	-
40	*Lactarius queticolor* Romagnesi	*Lactarius*	Russulaceae	Russulales	-	√	-	-	-	-	-	-
41	*Lamicella glischra* (Morgan) Murril	*Lamicella*	Amanitaceae	Agaricales	√	-	-	-	-	-	-	-

Table 1. Contd.

No	Species	Genus	Family	Ordo	TS	CB	PK1	GB	CBD	GM	SG	PK2
								Line				
42	*Lentinus arcularius* (Batsch: Fr.) Fr.	*Lentinus*	Polyporaceae	Polyporales	√	-	-	-	√	-	-	√
43	*Lentinus sajor-caju* (Fr.) Fr.	*Lentinus*	Polyporaceae	Polyporales	√	-	-	-	-	-	-	√
44	*Lentinus tricholoma* (Mont.) Zmitr.	*Lentinus*	Polyporaceae	Polyporales	-	-	-	-	√	-	-	-
45	*Lepiota Castanea*	*Lepiota*	Agaricaceae	Agaricales	-	-	-	-	√	-	-	-
46	*LeucoAgaricus croceovelutinus* (M. Bon & Boiffard) M. Bon & Boiffard	*LeucoAgaricus*	Agaricaceae	Agaricales	√	-	-	-	√	-	-	√
47	*Leucocoprinus fragilissimus* (Ravenel) Pat.	*Leucocoprinus*	Agaricaceae	Agaricales	√	-	-	-	-	-	-	-
48	*Lycoperdon perlatum* Pers.	*Lycoperdon*	Agaricaceae	Agaricales	√	√	-	-	-	-	-	-
49	*Lycoperdon umbrinum* Persoon	*Lycoperdon*	Agaricaceae	Agaricales	√	√	-	-	√	-	-	-
50	*Marasmiellus candidus* (Bolt.) Singer	*Marasmiellus*	Marasmieceae	Agaricales	-	√	-	-	-	√	-	-
51	*Marasmiellus villosipes* (Cleand) J. S OLiveira	*Marasmiellus*	Marasmiaceae	Agaricales	-	√	-	-	-	-	-	-
52	*Marasmius calhouniae* Singer	*Marasmius*	Marasmiaceae	Agaricales	-	-	-	-	-	-	-	-
53	*Microporus cf.affinis* (Blume & T.Nees) Kuntze	*Microporus*	Polyporaceae	Polyporales	√	-	-	-	√	√	-	-
54	*Mycena capillaripes* Peck	*Mycena*	Mycenaceae	Agaricales	√	-	-	-	-	-	-	-
55	*Mycena cf. hiemalis* (Osbeck) Quélet	*Mycena*	Mycenaceae	Agaricales	√	-	-	-	-	√	-	√
56	*Mycena galericulata* var. albida (Pers.) Gillet	*Mycena*	Mycenaceae	Agaricales	-	-	-	-	√	-	-	-
57	*Mycena holoporphyra* (Berl. & M. A. Cutis) Singer	*Mycena*	Mycenaceae	Agaricales	√	-	-	-	-	√	-	-
58	*Mycena leptocephala* (Pers. : Fr.) Gillet	*Mycena*	Mycenaceae	Agaricales	-	-	-	-	√	-	-	-
59	*Mycena stylobates* (Pers. : Fr.) Kummer	*Mycena*	Mycenaceae	Agaricales	-	-	-	-	-	-	√	-
60	*Nigroporus vinosus* (Berk.) Murrill	*Nigroporus*	Polyporaceae	Polyporales	-	-	-	-	-	-	√	√
61	*Oudemansiella canarii* (Jungh.) Hohn.	*Oudemansiella*	Physalacriaceae	Agaricales	-	-	-	-	√	-	-	-
62	*Parasola plicatilis* (Curt. : Fr.) Fr.	*Parasola*	Psathyrellaceae	Agaricales	-	-	-	-	√	-	-	√-
63	*Phillipsia domingensis* Berk.	*Phillipsia*	Sarcoscyaceae	Pezizales	-	-	√	-	-	-	-	-
64	*Pleurotus aff.djamor* (Rumph. Ex Fr.) Boedijn	*Pleurotus*	Pleurotaceae	Agaricales	-	-	-	-	-	-	√	-
65	*Polyporus grammocephalus* Berk.	*Polyporus*	Polyporaceae	Polyporales	-	-	-	-	√	-	√	-
66	*Psathyrella bipellis* (Quélet) A.H. Smith	*Psathyrella*	Psathyrellaceae	Agaricales	√	-	√	-	√	-	√	-
67	*Psathyrella corrugis* (Pers. : Fr.) Konrad & Maublanc	*Psathyrella*	Psathyrellaceae	Agaricales	-	-	-	-	√	-	√	-
68	*Pseudomerulius curtisii* (Berk.) Redhead & Ginns	*Pseudomerulius*	Tapinellaceae	Boletales	-	-	-	-	-	-	√	-
69	*Ramariopsis kunzei* (Fr. : Fr.) Corner	*Ramariopsis*	Clavariaceae	Agaricales	-	-	-	-	-	-	-	-
70	*Russula emetica* (J.C. Sch. : Fr.) Pers.	*Russula.*	Russulaceae	Russulales	√	-	√	-	√	√	-	-
71	*Russula zonatula* Ebbesen & Jul. Schaff	*Russula*	Russulaceae	Russulales	-	-	-	-	√	-	-	-
72	*Scutellinia aff. Scutellata* (L.) Lambote	*Scutellinia*	Pyronemataceae	Pezizales	-	-	-	-	-	-	-	-
73	*Stereum cf.hirsutum* (Willdenow : Fr.) S.F. Gray	*Stereum*	Stereceae	Russulales	-	√	√	-	-	-	√	-
74	*Stereum ostrea* (Blume & T.Nees) Fr.	*Stereum*	Stereceae	Russulales	-	√	-	-	√	-	√	√
75	*Suillus bovinus* (L. : Fr.) Roussel	*Suillus*	Suillaceae	Boletales	-	-	-	-	-	-	√	-
76	*Suillus granulatus* (L. : Fr.) Roussel	*Suillus*	Suillaceae	Boletales	-	√	-	-	-	-	√	-
77	*Suillus placidus* (Bonord.) Singer	*Suillus*	Suillaceae	Boletales	-	√	-	-	-	-	-	-
78	*Suillus spraguei* (Berk. & M.A.Curtis) Kuntze	*Suillus*	Suillaceae	Boletales	-	-	√	-	-	-	-	-
79	*Tapinella panuoides* (Fr. : Fr.) E.-J. Gilbert	*Tapinella*	Tapinella	Boletales	-	-	-	-	√	-	-	-
80	*Trametes ochracea* (Pers.) Gilbertson & Ryvarden	*Trametes*	Polyporaceae	Polyporales	-	√	-	-	√	-	-	-
81	*Tricholoma sulphureum* (Bull. : Fr.) Kummer	*Tricholoma*	Tricolomataceae	Agaricales	-	-	-	-	-	√	-	-
82	*Xylaria sp.*	*Xylaria*	Xylariaceae	Xylariales	-	-	-	-	-	-	-	√
83	*Xylaria longipes Nitschke*	*Xylaria*	Xylariaceae	Xylariales	-	-	-	-	-	√	-	√

Note: TS: Tonjong Sawah,   CB: Cibingkul, PK1: Pakar 1, GB: Goa Belanda, CBD: Cibodas, GM: Gunung Masigit, SG: Seke Gede, PK2: Pakar 2

Table 2. Macrofungi found in the collection line/block.

No	Species	Genus	Family	Ordo	Line Percoba Areng	Line Gunung Masigit
1	*Xylaria* sp.	*Xylaria*	Xylariaceae	Xylariales	√	-
2	*Mycena* sp.1	*Mycena*	Mycenaceae	Agaricales	√	-
3	*Mycena* sp.2	*Mycena*	Mycenaceae	Agaricales	√	-
4	*Mycena* sp.3	*Mycena*	Mycenaceae	Agaricales	√	-
5	*Favolaschia* sp.1	*Favolaschia*	Mycenaceae	Agaricales	√	√
6	*Favolaschia* sp.2	*Favolaschia*	Mycenaceae	Agaricales	√	√
7	*Marasmiellus* sp.1	*Marasmiellus*	Marasmiaceae	Agaricales	√	-
8	*Marasmiellus* sp.2	*Marasmiellus*	Marasmiaceae	Agaricales	√	-
9	*Marasmiellus* sp.3	*Marasmiellus*	Marasmiaceae	Agaricales	√	-
10	*Marasmiellus* sp.4	*Marasmiellus*	Marasmiaceae	Agaricales	√	-
11	*Gerronema* sp.	*Gerronema .*	Marasmiaceae	Agaricales	√	-
12	*Hygrocybe* sp.	*Hygrocybe*	Hygrophoraceae	Agaricales	√	√
13	*Parasola* sp.	*Parasola*	Psathyrellaceae	Agaricales	√	-
14	*Coprinellus* sp.1	*Coprinellus*	Psathyrellaceae	Agaricales	√	-
15	*Coprinellus* sp.2	*Coprinellus*	Psathyrellaceae	Agaricales	√	-
16	*Coprinellus* sp.3	*Coprinellus*	Psathyrellaceae	Agaricales	√	-
17	*Coprinellus* sp.4	*Coprinellus*	Psathyrellaceae	Agaricales	-	√
18	*Tricholomopsis* sp.	*Tricholomopsis*	Tricholomataceae	Agaricales	√	-
19	*Oudemansiella* sp.	*Oudemansiella*	Physalacriaceae	Agaricales	√	-
20	*Cyptotrama* sp.	*Cyptotrama*	Physalacriaceae	Agaricales	-	√
21	*Schizophyllum commune* Fr.	*Schizophyllum*	Schizophyllaceae	Agaricales	√	-
22	*Clavaria* sp.	*Clavaria*	Clavariaceae	Agaricales	√	-
23	*Gymnopus* sp.1	*Gymnopus*	Omphalotaceae	Agaricales	√	-
24	*Gymnopus* sp.2	*Gymnopus*	Omphalotaceae	Agaricales	-	√
25	*Gymnopilus* sp.	*Gymnopilus*	Cortinariaceae	Agaricales	-	√
26	*Lepista sordida* (Schumach.) Singer	*Lepista*	Tricholomataceae	Agaricales	-	√
27	*Entoloma* sp.	*Entoloma*	Entolomaceae	Agaricales	-	√
28	*Auricularia auricula-judae* (Bull.: Fr.) Wettstein	*Auricularia*	Auriculariaceae	Auriculariales	√	√
29	*Auricularia delicata* (Mont. Ex Fr.) Henn.	*Auricularia.*	Auriculariaceae	Auriculariales	√	√
30	*Microporus* sp.	*Microporus*	Polyporaceae	Polyporales	√	√
31	*Polyporus* sp.1	*Polyporus*	Polyporaceae	Polyporales	√	-
32	*Polyporus* sp.2	*Polyporus*	Polyporaceae	Polyporales	√	-
33	*Favolus* sp.	*Favolus*	Polyporaceae	Polyporales	√	-
34	*Cerioporus* sp.	*Cerioporus*	Polyporaceae	Polyporales	√	-
35	*Hexagonia* sp.	*Hexagonia*	Polyporaceae	Polyporales	√	-
36	*Poria* sp.	*Poria*	Polyporaceae	Polyporales	-	√
37	*Trametes* sp.1	*Trametes*	Polyporaceae	Polyporales	-	√
38	*Trametes* sp.2	*Trametes*	Polyporaceae	Polyporales	-	√
39	*Trametes* sp.3	*Trametes*	Polyporaceae	Polyporales	-	√
40	*Cymatoderma* sp.	*Cymatoderma*	Meruliaceae	Polyporales	√	-
41	*Nigroporus* sp.	*Nigroporus*	Steccherinaceae	Polyporales	-	√
42	*Rigidoporus* sp.	*Rigidoporus*	Meripilaceae	Polyporales	-	√
43	*Russula* sp.1	*Russula*	Russulaceae	Russulales	√	√
44	*Russula* sp.2	*Russula*	Russulaceae	Russulales	√	-
45	*Lactarius* sp.	*Lactarius*	Russulaceae	Russulales	-	√
46	*Stereum* sp.	*Stereum*	Stereaceae	Russulales	√	-
47	*Aseroe rubra* Labill.	*Aseroe*	Phallaceae	Phallales	-	√
48	*Phallus indusiatus* Vent.	*Phallus*	Phallaceae	Phallales	-	√
49	*Tremella* sp.	*Tremella*	Tremellaceae	Tremellales	√	-
50	*Suillus* sp.	*Suillus*	Suillaceae	Boletales	√	-

Table 3. Macrofungi found in the Utilization line/block.

No	Species	Genus	Family	Ordo	Line Pakar	Line Maribaya
1	*Phillipsia* cf. *subpurpurea* Berk. & Broome	*Phillipsia*	Sarcoscyphaceae	Pezizales	-	√
2	*Gymnopilus* sp.	*Gymnopilus*	Cortinariaceae	Agaricales	√	-
3	*Irpex* sp.	*Irpex*	Meruliaceae	Polyporales	-	√
4	*Meiorganum curtisii* (Berk.) Singer, J.García & L.D.Gómez	*Meiorganum*	Paxillaceae	Boletales	-	√
5	*Inocybe* cf. *haemacta* (Berk. & Cooke) Sacc.	*Inocybe*	Inocybaceae	Agaricales	-	√
6	*Conocybe* sp.	*Conocybe*	Bolbitiaceae	Agaricales	√	√
7	*Schizophyllum commune* Fr.	*Schizophyllum*	Scizophyllaceae	Agaricales	√	-
8	*Pleurotus columbinus* Quél.	*Pleurotus*	Pleurotaceae	Agaricales	√	-
9	*Candolleomyces* sp.	*Candolleomyces*	Psathyrellaceae	Agaricales	-	√
10	*Auricularia polytricha* (Mont.) Sacc.	*Auricularia*	Auriculariaceae	Auricurales	-	√
11	*Trogia* sp.	*Trogia*	Marasmiaceae	Agaricales	√	-
12	*Ganoderma* cf.*lobatum* (Cooke) G.F.Atk	*Ganoderma*	Ganodermataceae	Polyporales	-	√
13	*Tricholoma sulphureum* (Bull.) P.Kumm	*Tricholoma*	Tricholomataceae	Agaricales	√	-
14	*Stereum* sp.1	*Stereum*	Stereaceae	Russulales	-	√
15	*Stereum* sp.2	*Stereum*	Stereaceae	Russulales	√	-
16	*Geastrum* cf. *saccatum* Fr.	*Geastrum*	Geastraceae	Geastrales	-	√
17	*Geastrum hirsutum* Baseia & Calonge	*Geastrum*	Geastraceae	Geastrales	√	-
18	*Agaricus* aff. *Mangaoensis* M.Q.He &R.L.Zhao	*Agaricus*	Agaricaeae	Agaricales	-	√
19	*Cystolepiota seminude* (Lasch) Bon	*Cystolepiota*	Agaricaeae	Agaricales	-	√
20	*Lactarius* sp.	*Lactarius*	Russulaceae	Russulales	-	√
21	*Russula* cf. *Rosea* Pers.	*Russula*	Russulaceae	Russulales	√	√
22	*Marasmiellus* aff. *Candidus* (Fr.) Singer	*Marasmiellus*	Omphalotaceae	Agaricales	-	√
23	*Gymnopus* aff. *Ramealis* (Bull.) Gray	*Gymnopus*	Omphalotaceae	Agaricales	√	-
24	*Marasmiellus* sp.	*Marasmiellus*	Omphalotaceae	Agaricales	√	-
25	*Mycena* sp. 1	*Mycena*	Mycenaceae	Agaricales	-	√
26	*Mycena* sp. 2	*Mycena*	Mycenaceae	Agaricales	-	√
27	*Mycena* aff. *leptocephala* (Pers.) Gilllet	*Mycena*	Mycenaceae	Agaricales	-	√
28	*Lentinus tricholoma* (Mont.) Zmitr	*Lentinus*	Polyporaceae	Polyporales	-	√
29	*Tyromyces* sp.1	*Tyromyces*	Polyporaceae	Polyporales	-	√
30	*Polyporus* sp.1	*Polyporus*	Polyporaceae	Polyporales	-	√
31	*Polyporus* sp. 2	*Polyporus*	Polyporaceae	Polyporales	-	√
32	*Trametes* cf. *ochracea* (Pers.) Gilb. & Ryvarden	*Trametes*	Polyporaceae	Polyporales	-	√
33	*Lentinus arcularius* (Batsch) Zmitr.	*Lentinus*	Polyporaceae	Polyporales	-	√
34	*Tyromyces* sp.2	*Tyromyces*	Polyporaceae	Polyporales	-	√
35	*Trichaptum biforme* (Fr.) Ryvarden	*Trichaptum*	Polyporaceae	Polyporales	√	-
36	*Microporellus* sp.	*Microporellus*	Polyporaceae	Polyporales	√	-
37	*Favolus grammocephalus* (Berk.) Imazeki	*Favolus*	Polyporaceae	Polyporales	√	-
38	*Tyromyces* sp.3	*Tyromyces*	Polyporaceae	Polyporales	√	-
39	*Dacryopinax spathularia* (Schwein.) G.W.Martin	*Dacryopinax*	Dacrymycetaceae	Dacrymycetales	-	√
40	*Phallus indusiatus* Vent.	*Phallus*	Phallaceae	Phallales	√	-
41	*Auricularia auricula-judae*	*Auricularia*	Auriculariaceae	Auricurales	√	-
42	*Suillus* cf. *granulatus* (L.) Roussel	*Suillus*	Suillaceae	Boletales	-	√
43	*Tapinella panuoides* (Fr.) E.-J.Gilbert.	*Tapinella*	Tapinellaceae	Boletales	√	-
44	*Laccaria* cf. *ochropurpurea* (Berk.) Peck	*Laccaria*	Hydnangiaceae	Agaricales	-	√
45	*Oudemansiella* sp.	*Oudemansiella*	Physalacriaceae	Agaricales	√	-
46	*Panaeolus* cf. *antillarum* (Fr.) Dennis	*Panaeolus*	Bolbitiaceae	Agaricales	√	-
47	*Geastrum triplex* Jungh.	*Geastrum*	Geastraceae	Geastrales	√	-
48	*Daldinia concentrica* (Bolton) Ces. & De Not.	*Daldinia*	Hypoxylaceae	Xylariales	√	-
49	*Phillipsia domingensis* (Berk.) Berk. ex Denison	*Phillipsia*	Sarcoscyphaceae	Pezizales	√	-
50	*Clymacocystis* sp.	*Clymacocystis*	Fomitopsidaceae	Polyporales		√

Table 3. Contd.

No	Species	Genus	Family	Ordo	Line Pakar	Line Maribaya
51	*Daedalea dochmia* (Berk. & Broome) T.Hatt.	*Daedalea*	Fomitopsidaceae	Polyporales	√	-
52	*Crepidotus* sp.	*Crepidotus*	Inocybaceae	Agaricales	√	-
53	*Crepidotus applanatum* (Pers.) P.Kumm.	*Crepidotus*	Inocybaceae	Agaricales	√	-
54	*Russula* sp.	*Russula*	Russulaceae	Russulales	√	-
55	*Stereum* sp.3	*Stereum*	Stereaceae	Russulales	√	-
56	*Stereum* cf. *ostrea* (Blume & T.Nees) Fr.	*Stereum*	Stereaceae	Russulales	√	-
57	*Scleroderma columnare* Berk. & Broome	*Scleroderma*	Sclerodermataceae	Boletales	-	√
58	*Sclerodema* sp.	*Sclerodema*	Sclerodermataceae	Boletales	√	-
59	*Clitocybe fragrans* (With.) P.Kumm.	*Clitocybe*	Tricholomataceae	Agaricales	√	-
60	*Collybia* aff. *cirrhata* (Schumach.) Quél.	*Collybia*	Tricholomataceae	Agaricales	√	-
61	*Favolaschia manipularis* (Berk.) Teng	*Favolaschia*	Mycenaceae	Agaricales	√	-
62	*Mycena leaiana* (Berk.) Sacc.	*Mycena*	Mycenaceae	Agaricales	√	-
63	*Ganoderma* sp.	*Ganoderma*	Ganodermataceae	Polyporales	√	-
64	*Ganoderma applanatum* (Pers.) Pat.	*Ganoderma*	Ganodermataceae	Polyporales	√	-
65	*Marasmius* sp.1	*Marasmius*	Marasmiaceae	Agaricales	√	-
66	*Gerronema strombodes* (Berk. & Mont.) Singer	*Gerronema*	Marasmiaceae	Agaricales	√	-
67	*Marasmius* sp.2	*Marasmius*	Marasmiaceae	Agaricales	√	-
68	*Xylaria* cf. *cubensis* (Mont.) Fr.	*Xylaria*	Xylariaceae	Xylariales	√	-
69	*Xylaria polymorpha* (Pers.) Grev.	*Xylaria*	Xylariaceae	Xylariales	√	-
70	*Xylaria Hypoxylon* (L.) Grev.	*Xylaria*	Xylariaceae	Xylariales	√	-
71	*Coprinellus* aff. *disseminates* (Pers.) J.E.Lange	*Coprinellus*	Psathyrellaceae	Agaricales	-	√
72	*Parasola plicatilis* (Curtis) Redhead, Vilgalys & Hopple	*Parasola*	Psathyrellaceae	Agaricales	√	-
73	*Psathyrella* sp.	*Psathyrella*	Psathyrellaceae	Agaricales	√	-
74	*Parasola* sp.	*Parasola*	Psathyrellaceae	Agaricales	√	-
75	*Coprinopsis* sp.	*Coprinopsis*	Psathyrellaceae	Agaricales	√	-
76	*Gymnopus* sp.1	*Gymnopus*	Omphalotaceae	Agaricales	-	√
77	*Gymnopus* sp.2	*Gymnopus*	Omphalotaceae	Agaricales	√	-
78	*Marasmiellus* sp.	*Marasmiellus*	Omphalotaceae	Agaricales	√	-
79	*Gymnopus* sp.3	*Gymnopus*	Omphalotaceae	Agaricales	√	-
80	*Gymnopus* cf. *dryophilus* (Bull.) Murrill	*Gymnopus*	Omphalotaceae	Agaricales	√	-
81	*Gymnopus* sp.4	*Gymnopus*	Omphalotaceae	Agaricales	√	-
82	*Hexagonia* sp.1	*Hexagonia*	Polyporaceae	Polyporales	√	-
83	*Nigroporus* sp.	*Nigroporus*	Polyporaceae	Polyporales	√	-
84	*Hexagonia* sp.2	*Hexagonia*	Polyporaceae	Polyporales	√	-
85	*Trametes* sp.	*Trametes*	Polyporaceae	Polyporales	√	-
86	*Polyporus* sp.3	*Polyporus*	Polyporaceae	Polyporales	√	-
87	*Earliella scabrosa* (Pers.) Gilb. & Ryvarden	*Earliella*	Polyporaceae	Polyporales	√	-
88	*Agaricus* cf. *vinosobrunneofumidus* Kerrigan	*Agaricus*	Agaricaceae	Agaricales	-	√
89	*Agaricus* sp.1	*Agaricus*	Agaricaceae	Agaricales	-	√
90	*Lepiota rubrotinctoides* Murrill.	*Lepiota*	Agaricaceae	Agaricales	√	-
91	*Cyathus striatus* (Huds.) Willd.	*Cyathus*	Agaricaceae	Agaricales	√	-
92	*Calvatia rugosa* (Berk. & M.A.Curtis) D.A.Reid	*Calvatia*	Agaricaceae	Agaricales	√	-
93	*Agaricus trisulphuratus* Berk.	*Agaricus*	Agaricaceae	Agaricales	√	-
94	*Agaricus* sp.2	*Agaricus*	Agaricaceae	Agaricales	√	-
95	*Agaricus* sp.3	*Agaricus*	Agaricaceae	Agaricales	√	-
96	*Leucocoprinus fagilissimus* (Ravenel ex Berk. & M.A.Curtis) Pat.	*Leucocoprinus*	Agaricaceae	Agaricales	√	-
97	*Agaricus* sp. 4	*Agaricus*	Agaricaceae	Agaricales	√	-
98	*Cystoderma* sp.	*Cystoderma*	Agaricaceae	Agaricales	√	-
99	*Agaricus* sp.5	*Agaricus*	Agaricaceae	Agaricales	√	-

detached from the soil and may roll around. Upon maturity, their exoperidium splits into a number of varying colors, which gives the order a distinct star shape. The exoperidia exist to protect the endoperidial body and regulate spore dispersal. In wetter weather these petals become moist and do not curl, some even curl back lifting the spore sac upwards. This allows rain or animals to hit the spore sac, releasing the spores when there is sufficient moisture for them to reproduce (Kuhar et al. 2013).

The order Agaricales is the most familiar mushroom known to the public, where the term mushroom refers to this type. This mushroom is easy to be recognized because of its soft fruiting body characteristic, generally their shapes were like an umbrella with the bottom of the hood resembling a sheet (gills). Agaricales is considered a cosmopolitan mushroom that can easily grow in various habitats (Kusuma et al. 2021). The diversity of habitats and substrates occupied by these fungi indicates that the group of Agaricales includes saprophytic, symbiotic, and parasitic species in various of shapes, sizes, and colours. The order Agaricales includes 33 families (mainly the genus *Agaricus*), 413 genera, and more than 13,200 described species, together with six extinct genera known only from the fossil record (Kirk et al. 2008).

The order Pezizales has at least 16 families, 199 genera, and 1638 species. This order is characterized by the original which is usually open and broken so that the body is shaped like a bowl or plate. The fungi have ascospores that are single-celled, bilaterally or bipolar in shape. Several types of fungi in this order have their ascospores modified into ornaments that are visible on the surface such as warts or thorns (Hansen & Pfister 2006).

Phallales is an order of fungi in the subclass Phallomycetidae. Where in 2019, it was recorded that this order has two families, 39 genera, and 173 species. The most prominent family in this order is the Phallaceae and commonly referred to as the stinkhorn mushrooms. The most striking feature in this order is that they have a pseudo stalk which is hollow and usually the spores are present in a slime-like form. Ripe fruit bodies usually often smell like carrion. Most of this order grows in soil and leaf litter (Yakar et al. 2019).

The Xylariales order is the largest order in the Sordariomycetes class, the largest species in this order comes from the Xylariaceae family which until now consists of several genera including *Daldinia*, *Hypoxylon* and *Xylaria* which have striking fruit body shapes (Helaly et al. 2018). Xylariales is a large order of fungi from the division Ascomycota which contains more than 92 genera and 795 species (Smith et al. 2003).

It is known that two families in this order, Xylariaceae and Hypoxylaceae, represent one of the several lineages in this order that can produce the most productive secondary metabolites, like several other types of fungi, this order is also known to show quite varied diversity when living in the tropics. Several discoveries that have been made show that mycelium cultures of this order are often isolated and proven as materials for drug development (Becker & Stadler 2021).

The order Auriculariales includes all fungi with fruiting bodies that are simple to cobweb-shaped, do not have heminium (spores associated with the lining of certain fungi), and their bodies are also easily distinguishable. The characteristic of this order is that it has a fruiting body that is soft and supple, usually shaped like an earlobe (Hasibuan 2019). Auriculariales is also a typical order of the division Basidiomycota which has septate basidia that are elongated or transverse (Li et al. 2022).

According to Kirk et al. (2008), Boletales consists of 17 families, 96

genera, and 1316 species with various types of fruiting bodies. Boletes is the most well-known genus of this order, and until recently, Boletales was thought to consist of only one genus, *Boletes*. This order also includes several gilled mushrooms, in the families of Gomphidiaceae, Serpulaceae, Tapinellaceae, Hygrophoropsidaceae, and Paxillaceae, which often have a fleshy texture similiar to Boletes.

Taxonomic studies using secondary metabolites and molecular phylogenetic evidence then included several physically distinct groups within the Boletales, including Sclerodermataceae (earth globe) and Rhizopogonaceae (false truffles) (Wu et al. 2014). Fungi from this order usually live in the soil and most often act as ectomycorrhizae in woody higher plants (Mishra 2005).

Dacrymycetales is an order of the class Dacrymycetes which was identified in 2001, which is placed in the subphylum Agaricomycotina and phylum Basidiomycota. Fungi of this order are characterized by the presence of bifurcate basidia (shaped like branched fork) which have a gelatinous or cartilage-like consistency and vary in color from yellow, orange to brown with a variety of shapes (Castro-Santiuste et al. 2020). The order Dacrymycetales usually inhabits dead trees, fallen trunks, and branches of gymnosperms or angiosperms (Lian et al. 2022).

The order Polyporales is a group originating from the division Basidiomycetes which includes more than 1800 species from 216 genera and 13 families. Polyporales is said to have porous lamellae, large fruiting bodies that can live for years, and are fleshy when alive. The order Polyporales can live in fairly dry extreme conditions. The texture is usually hard like wood. The cells in the hyphae are usually thick-walled. Most of the spores are white, cream, or purple (Mishra 2005). Several genera in the order Polyporales include *Hexagonia*, *Tyromyces*, and *Polyporus*. All three have different characteristics, namely *Hexagonia* has a hexagon-shaped pore, *Tyromyces* has a fruiting body like cheese or styrofoam, while *Polyporus* has a small fruiting body in most of its species.

Factors Influencing Macrofungi Growth

Macrofungi have different adaptation abilities in a habitat, several factors can affect the growth of mushrooms, including the substrate or habitat where the fungus grows. In addition to the substrate, factors that can affect the growth of fungi are conditions, such as soil acidity (pH), air humidity, and temperature.

The higher the humidity in a place, it will affect the humidity of macroscopic fungi that grow in a place (Hiola 2014). Table 4 shows that altitude affects air temperature. Higher air temperatures are found at altitudes of more than 1000 meters above sea level. This is in accordance with the statement of Warisno and Dahana (2013) which states that altitude can affect the growth of macrofungi indirectly, where temperature and rainfall are several factors that can be affected by altitude so that they can affect fungal growth.

According to Purwantara (2018), the low or high of earth's surface air temperature is determined by the altitude of the place, the higher the altitude, the lower the temperature, because the air pressure is getting smaller. The farther a place from the center of the earth, the weaker the gravitational force, which causes the pressure and air to get smaller, this thin air content causes the air temperature to be colder than on the beach. However, the altitude also affects the amount of sunlight that hits the earth's surface, this will affect the expected density of vegetation in an area.

According to Roosheroe et al. (2006), the high pH can affect the

Table 4. Influence of Abiotic Parameters on Altitudinal Distribution of Macrofungi.

| Block | Time | Line | Altitude (m asl) | Abiotic Factors | | |
				Temperature (°C)	Air Humidity (%)	Soil pH
Protection	November 2021	Tonjong Sawah	$1077 - 1141$	$24 - 27$	$67 - 72$	$3.5 - 5.5$
		Cibingkul	$1092 - 1124$	$23.4 - 29.3$	$54 - 67$	$3.5 - 6$
		Pakar 1	$976 - 987$	$23.1 - 27.3$	$65 - 78$	$4 - 5.5$
		Goa Belanda	$873 - 896$	$23.3 - 27$	$53 - 64$	$3 - 5$
	February 2022	Cibodas	$1056 - 1090$	$22.7 - 26.1$	$71 - 90$	$3.5 - 4$
		Gunung Masigit	$1057 - 1076$	$24 - 26.9$	$63 - 82$	$3.5 - 4$
		Seke Gede	$1102 - 1121$	$23.1 - 27.3$	$80 - 92$	$3.5 - 5$
		Pakar 2	$860 - 879$	$21.5 - 24.5$	$70 - 91$	$3.5 - 5$
Collection	November 2021	Percoba Areng	$1216 - 1296$	$23.4 - 28.1$	$61 - 81$	$3.5 - 5$
		Gunung Masigit	$1158 - 1227$	$23.6 - 25$	$73 - 87$	$3.5 - 6$
	January 2022	Percoba Areng	$1109 - 1224$	$20.9 - 30.2$	$61 - 92$	$3.5 - 5$
		Gunung Masigit	$1067 - 1166$	$25.3 - 26.5$	$65 - 81$	$3.5 - 5$
Utilization	January 2022	Pakar	$929 - 956$	$20.4 - 25.8$	$64 - 87$	$5 - 7$
		Maribaya	$1047 - 1149$	$22.1 - 26.3$	$75 - 86$	$4.5 - 6.2$
	April 2022	Pakar	$923 - 987$	$22.6 - 24.5$	$61 - 71$	$4 - 5.1$
		Maribaya	$1138 - 1388$	$22.4 - 30.1$	$61 - 75$	$3.5 - 6.2$

growth of fungi indirectly; the high pH will affect the availability of nutrients needed by macrofungi. In general, fungi can live at a fairly wide range of pH, namely $3 - 7$, but the optimum pH for fungal growth is $6 - 7$ where the nutrients used by macrofungi to grow are mostly available at this pH (Gardner et al. 1991). Macrofungi can also grow with a fairly wide temperature range between $20 - 40$°C with the optimum temperature between $20 - 30$°C. The amount of humidity affects the availability of water in the environment, humidity can affect the ability of fungi to maintain water levels in cells which can function as nutrient transport (Wati et al. 2019).

Macrofungi Growth Subtance

Macrofungi from the divisions of Ascomycota and Basidiomycota can thrive in places that contain lots of carbohydrates, cellulose and lignin, these materials are commonly found in piles of leaf litter, tree branches, and weathered wood (Suhardiman 1995). Based on Figure 2 and Figure 3, macrofungi from the order Agaricales which grow a lot in the Protection and Utilization blocks mostly grow on soil substrates. These results are in accordance with Yunida et al. (2014) that Agaricales can grow well in areas with high humidity because it has a soft umbrella-like

Russulales   Geastrales   Agaricales   Pezizales   Phallales

Xylariales   Polyporales   Boletales   Dacrymycetales   Auriculariales

Figure 2. Some of the Macrofungi found in the TAHURA Ir. H. Djuanda Area.

fruiting body that rarely tolerates dry conditions.

The Collection block was dominated by macrofungi from the order Polyporales which grow mostly on wood stumps. The order Polyporales is a type of fungus whose habitat is mostly on wood stumps or dead wood. This order type has special characteristics in the form of a hard basidiocarp in the shape of planks and has a high tolerance to the environment so that this fungus can survive in various seasons including the dry season (Wibowo et al. 2021). According to Annissa et al. (2017) most types of Polyporaceae are macrofungi that act as decomposers in the environment, therefore, these types of macrofungi are found mostly on dead wood stump and generally saprophytic. Sudirman (1995) also mentioned that in its growth, macrofungi often depend on the weathering of wood, where macrofungi utilize it as food sources whether weathered wood or still weathering wood.
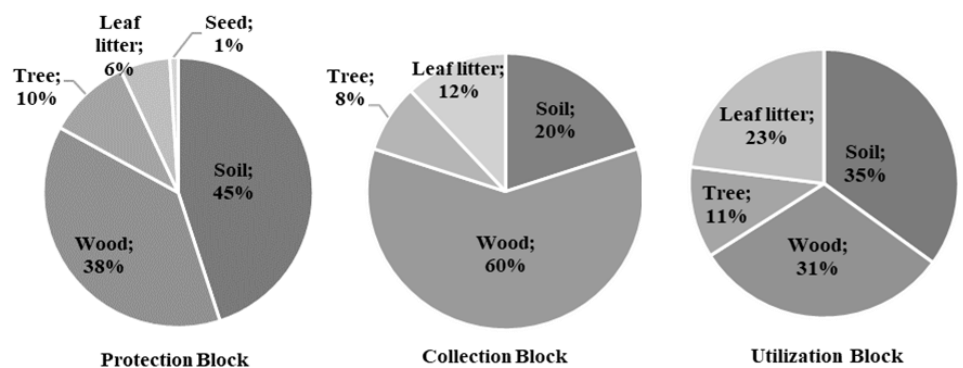
Figure 3. The Ecological Substrate Preferences of Macrofungi in The TAHURA Ir. H. Djuanda area.

Potential Utilization of Macrofungi

The existence of macrofungi in ecosystems is very important to support the organisms life in the environment. Macrofungi have an important role in the environment, namely as decomposers by breaking down complex compounds into simple forms. The main content of macrofungi are fats, proteins, minerals, vitamins, water and fiber. However, there are some mushrooms that cannot be eaten because they are poisonous. In symbiont macrofungi, namely mycorrhizae, their presence is necessary for plantsin the area. Especially in woody plants, macrofungi can help absorb water and minerals from the soil. Macrofungi can also be used as a source of food and medicinal raw materials (Suryani & Cahyanto 2022).

Based on Figure 4, the potential utilization of macrofungi from each block shows that the collection block is most commonly used as an anti-microbial, the protection block is more frequently used as food, while the utilization block is primarily used for medicinal purposes. Macrofungi from the Ascomycota division have potential as food and medicine. The genus *Xylaria* is a key source of antioxidants with antibacterial and anti-fungal properties (Saridogan et al. 2021). while the genus Daldinia is known for relieving cramps, treating umbilical hernias, and possessing antibacterial, antifungal, and antimicrobial properties (Boua et al. 2019).

Mushrooms from the genus *Ganoderma* contain triterpenoids and polysaccharides, which serve as antioxidants, antibacterials, and protect against cell damage from radicals. These compounds have potential as bioactives for treating cancer, tumors, and boosting the immune system (Surahmaida 2017). Additionally, mycelium from the genus *Stereum* shows activity against *S. aureus* bacteria when tested with acetone, etha-nol, and aqueous extracts. Researchers has proven that these fungi have the potential to inhibit the growth of gram positive and negative bacteria

(Ferreira Silva et al. 2017).
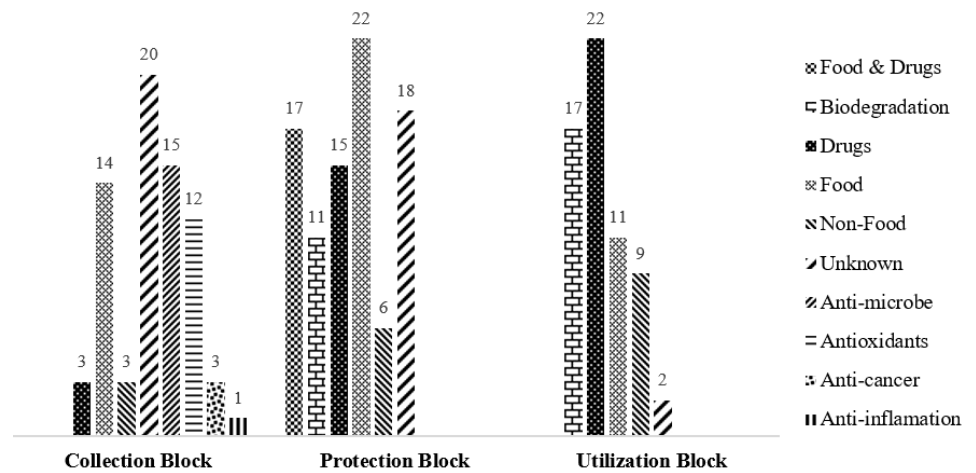
Figure 4. Potential Utilization of Macrofungi.

Scizophyllum is often used in food ingredients such as soup, it is known that some mushrooms from this order can function as a leucorrhoea medicine also has antitumor properties (Susan & Retnowati 2017). The genera *Auricularia* has the ability as an antibacterial and antioxidant so this fungus is known to be able to inhibit the growth of *E. coli* bacteria (Elfirta & Saskiawan 2020), besides its potential as a medicine, many Indonesian people consume one type of mushroom from this genus, namely *Auricularia auricular-judae* (Susan & Retnowati 2017). Mushroom species from several genera *Inocybe* and *Conocybe* are poisonous, although these mushrooms are proven to be ectomycorrhizal fungi, they are known to contain amanitin, psilocybin, psilocin, and baeocystin which can cause quite severe hallucinations. structurally similar to neurotransmitters (Annissa et al. 2017; Diaz 2018; Patocka et al. 2021).

The genus *Agaricus* has been used as an analgesic or pain reliever, several types of mushrooms from this genus are also known to contain fiber, protein, micronutrients, vitamins, carbohydrates, and have a low fat content so they are good for consumption. The genus *Pleurotus*, also known as oyster mushroom, has long been known to have high nutritional value and palatability. *Pelurotus ostreatus* type has tumor inhibitory properties, antibacterial activity, and cholesterol lowering. In addition, this mushroom can also control blood pressure against hypertension (Varghese et al. 2019). The genus *Phallus* was consumed by the people of ancient China because of its nutritional content besides having benefits for the eyes and tonic for the cardiovascular system, medicinal effects such as mental calming, antitumor and having the seven essential amino acids, calcium and high content of vitamin E (Ker et al. 2011). Based on the analysis results, the potential of macrofungi found in Ir. H. Djuanda Grand Forest Park in Bandung is dominated by fungi that can be utilized for medicinal and food purposes, such as one of them found in the genus *Marasmiellus*.

CONCLUSION

Based on the results of the research, 83 species of macrofungi were found in the Protection block, 50 species were found in the Collection block, and 99 species were identified in the Utilization block from the Basidiomycota and Ascomycota phyla. The macrofungi found have the potential to act as biodegradation agents, food ingredients, non-food

ingredients, medicines, antimicrobials, antioxidants, anticancer and anti-inflammatory.

REFERENCES

Annissa, I. et al., 2017. Keanekaragaman Jenis Jamur Makroskopis di *Arboretum sylva* Universitas Tanjungpura. *Jurnal Hutan Lestari*, 5 (4), pp.969–977. doi: 10.26418/jhl.v5i4.22874.

Arikunto, S., 2003. *Prosedur Penelitian Suatu Pendekatan Praktik*, Jakarta: Rineka Cipta.

Arini, D.I.D. et al., 2019. The Macrofungi Diversity and Their Potential Utilization in Tangale Nature Reserve Gorontalo Province. *Berita Biologi*, 18(1), pp.109–115. doi: 10.14203/beritabiologi.v18i1.3379

Becker, K. & Stadler, M., 2021. Recent progress in biodiversity research on the Xylariales and their secondary metabolism. *Journal of Antibiotics*, 74(1), pp.1–23. doi: 10.1038/s41429-020-00376-0.

Boua, B. et al., 2019. Chemical Composition and Anticancer Activity of *Daldinia Concentrica* (Xylariaceae). *World Journal of Pharmaceutical Research*, 8(1), pp.257–264. doi: 10.20959/wjpr20191-13874.

Castro-Santiuste, S. et al., 2020. Dacryopinax (Fungi: Dacrymycetales) in Mexico. *Phytotaxa*, 446(1), pp.6–22. doi: 10.11646/PHYTOTAXA.446.1.2

Diaz, J.H., 2018. Amatoxin-Containing Mushroom Poisonings: Species, Toxidromes, Treatments, and Outcomes. *Wilderness and Environmental Medicine*, 29(1), pp.111–118. doi: 10.1016/j.wem.2017.10.002.

Elfirta, R.R. & Saskiawan, I., 2020. The Functional Character of *Auricularia auricula* Crude Polysaccharides: Antioxidant and Antibacterial Activity. *Berita Biologi*, 19(3B), pp.433–440. doi: 10.14203/beritabiologi.v19i3b.3988

Ferreira Silva, V. et al., 2017. Antibacterial activity of ethyl acetate extract of agaricomycetes collected in Northeast Brazil. *Current Research in Environmental and Applied Mycology*, 7(4), pp.267–274. doi: 10.5943/cream/7/4/3

Gardner, F.P. et al., 1991. *Fisiologi Tanaman Budidaya*. Jakarta: UI-Press.

Hansen, K. & Pfister, D.H., 2006. Systematics of the pezizomycetes - The operculate discomycetes. *Mycologia*, 98(6), pp.1029-1040. doi: 10.3852/mycologia.98.6.1029.

Hasibuan, Z. I., 2019. *Inventarisasi Jamur Makroskopis Di Kawasan Taman Hutan Raya Bukit Barisan Kabupaten Karo Sumatera Utara*. Universitas Islam Negeri Sumatera Utara.

Helaly, S.E. et al., 2018. Diversity of biologically active secondary metabolites from endophytic and saprotrophic fungi of the ascomycete order Xylariales. *Natural Product Reports*, 35(9), pp.992–1014. doi: 10.1039/c8np00010g.

Hiola, S.F., 2014. Keanekaragaman Jamur Basidiomycota Di kawasan Gunung Bawakaraeng (Studi Kasus: Kawasan Sekitar Desa Lembanna Kecamatan Tinggi Moncong Kabupaten Gowa). *Bionature*, 12(2), pp.93–100. doi: 10.35580/bionature.v12i2.1402.

Ihsan, F.M., 2012. *Prosedur Pembuatan Database Untuk Spesies Di Taman Hutan Raya Ir. H. Djuanda Bandung*. Bandung.

Izati, N. et al., 2020. Keanekaragaman jamur makroskopis dan potensi pemanfaatannya di Cagar Alam Gunung Picis dan Cagar Alam Gunung Sigogor, Jawa Timur Diversity of macrofungi and their potential utilization in Mount Picis Nature Reserve and Mount Sigogor Nature Reserve, East J. *Prosiding Seminar Nasional Masyarakat Biodiversitas Indonesia*, 6(1), pp.484–492. doi: 10.13057/psnmbi/m060102.

Ker, Y.B. et al., 2011. Structural characteristics and antioxidative capability of the soluble polysaccharides present in dictyophora indusiata (Vent. Ex Pers.) fish phallaceae. *Evidence Based Complementary and Alternative Medicine*, 2011, 396013. doi: 10.1093/ecam/neq041.

Khastini, R.O. et al., 2019. Inventory and Utilization of Macrofungi Species for Food in Cikartawana Inner Baduy Banten. *Biodidaktika: Jurnal Biologi Dan Pembelajarannya*, 14(1), 7–13. doi: 10.30870/biodidaktika.v14i1.4838.

Kinge, T.R. et al., 2017. Species Richness and Traditional Knowledge of Macrofungi (Mushrooms) in the Awing Forest Reserve and Communities, Northwest Region, Cameroon. *Journal of Mycology*, 2809239. doi: 10.1155/2017/2809239.

Kirk, P.M. et al., 2008. *Dictionary of the Fungi* (10th ed.), Wallingford, UK: CAB International.

Kuhar, F. et al., 2013. *Geastrum* species of the La Rioja province, Argentina. *Mycotaxon*, 122(1), pp.145–156. doi: 10.5248/122.145.

Kusuma, H.I. et al., 2021. Agaricales: the most dominated macroscopic fungi in Tahura Pocut Meurah Intan Forest Park. *Journal of Physics: Conference Series*, 1882, 012096. doi: 10.1088/1742-6596/1882/1/012096.

Li, Q.Z. et al., 2022. Redelimitation of *Heteroradulum* (Auriculariales, Basidiomycota) with *H.australiense* sp. nov. *MycoKeys*, 86, pp.87–101. doi: 10.3897/MYCOKEYS.86.76425.

Lian, Y.-P. et al., 2022. Two New Species of Dacrymyces (Dacrymycetales, Basidiomycota) from Southwestern China. *Diversity*, 14(5), 379. doi: 10.3390/d14050379.

Mishra, S.R. 2005. *Morphology of Fungi*, New Delhi: Discovery Publishing House.

Moore, S. & O'Sullivan, P., 2013. *A guide to common fungi of the Hunter-Central Rivers region*, Hunter-Central Rivers Catchment Management Authority.

Mueller, G.M. et al., 2007. Global diversity and distribution of macrofungi. *Biodiversity and Conservation*, 16(1), pp.37–48. doi: 10.1007/s10531-006-9108-8.

Mukhsin, R. et al., 2017. Pengaruh Orientasi Kewirausahaan Terhadap Daya Tahan Hidup Usaha Mikro Kecil dan Menengah Pengolahan Hasil Perikanan di Kota Makassar. *Jurnal Analisis*, 6(2), pp.188–193.

Nur, I.F. et al., 2021. Keanekaragaman makrofungi di hutan kota Srengseng dan Pesanggrahan Sangga Buana Jakarta. *Proceeding of Biology Education*, 4(1), pp.89–108. doi: 10.21009/pbe.4-1.9.

Patocka, J. et al., 2021. Chemistry and toxicology of major bioactive substances in inocybe mushrooms. *International Journal of Molecular Sciences*, 22(4), 2218. doi: 10.3390/ijms22042218.

Prasetyo, L.B. et al., 2009. Spatial model approach on deforestation of Java Island, Indonesia. *Journal of Integrated Field Science*, 6, pp.37–44. doi: 10.4018/978-1-60960-619-0.ch018.

Proborini, M.W., 2012. Eksplorasi dan identifikasi jenis - jenis jamur klas basidiomycetes di kawasan bukit jimbaran bali. *Jurnal Biologi*, 16(2), pp.45–47.

Purwantara, S., 2018. Studi Temperatur Udara Terkini di Wilayah di Jawa Tengah dan DIY. *Geomedia: Majalah Ilmiah Dan Informasi Kegeografian*, 13(1), pp.41–52. doi: 10.21831/gm.v13i1.4476

Roosheroe, I.G. et al., 2006. *Mikologi: Dasar dan Terapan*, Jakarta: Yayasan Pustaka Obor Indonesia.

Saridogan, B.G.O. et al., 2021. Antioxidant antimicrobial oxidant and elements contents of *xylaria polymorpha* and x *Hypoxylon (xylariaceae)*. *Fresenius Environmental Bulletin*, 30(5), pp.5400–5404.

Smith, G.J.D. et al., 2003. The Xylariales: A monophyletic order containing 7 families. *Fungal Diversity*, 13, pp.185–218.

Sudirman, L.A.M.I., 1995. Pemanfaatan *Lentinus* spp dalam Menunjang Industri Farmasi dan Pertanian. *Agrotek*, 2(2), pp.55–59.

Suhardiman, P., 1995. *Jamur Kayu* (6th ed.), Jakarta: Penebar Swadaya.

Suharno, S., et al., 2018. Keragaman Makrofungi di Distrik Warmare Kabupaten Manokwari, Papua Barat. *Jurnal Biologi Papua*, 6(1), pp.38–46. doi: 10.31957/jbp.451.

Surahmaida, S., 2017. Review: Potensi Berbagai Spesies *Ganoderma* Sebagai Tanaman Obat. *Journal of Pharmacy and Science*, 2(1), pp.17–21. doi: 10.53342/pharmasci.v2i1.61.

Suryani, Y. & Cahyanto, T. 2022. *Pengantar Jamur Makroskopis*, Bandung: Gunung Djati Publishing.

Susan, D. & Retnowati, A., 2017. Notes on Some Macro Fungi From Enggano Island: Diversity and its Potency. *Berita Biologi*, 16(3), pp.243–256.

Varghese, R. et al., 2019. Historical and current perspectives on therapeutic potential of higher basidiomycetes: an overview. *3 Biotech*, 9(10), 362. doi: 10.1007/s13205-019-1886-2.

Warisno & Dahana, K., 2013. *Tiram : menabur jamur menuai rupiah*, Jakarta: Gramedia Pustaka Utama.

Wati, R. et al., 2019. Keanekaragaman Jamur Makroskopis Di Beberapa Habitat Kawasan Taman Nasional Baluran. *Al-Kauniyah: Jurnal Biologi*, 12(2), pp.171–180. doi: 10.15408/kauniyah.v12i2.10363

Wibowo, S.G. et al., 2021. Eksplorasi dan Identifikasi Jenis Jamur Tingkat Tinggi di Kawasan Hutan Lindung Kota Langsa. *Jurnal Biologica Samudra*, 3(1), pp.1–13. doi: 10.33059/jbs.v2i1.3197.

Wu, G. et al., 2014. Molecular phylogenetic analyses redefine seven major clades and reveal 22 new generic clades in the fungal family Boletaceae. *Fungal Diversity*, 69(1), pp.93–115. doi: 10.1007/s13225-014-0283-8

Yakar, S. et al., 2019. Contributions to the distribution of Phallales in Turkey. *Anatolian Journal of Botany*, 3(2), pp.51–58. doi: 10.30616/ajb.593692

Yunida, N. et al., 2014. Inventarisasi Jamur Di Gunung Senujuh Kabupaten Sambas Dan Implementasinya Dalam Pembuatan Flash Card. *Jurnal Pendidikan Dan Pembelajaran*, 3(10), pp.1–18. doi: 10.26418/jppk.v3i10.7502

Research Article

Expression, Characterisation and Structural Homology Modelling of Recombinant Mercuric Reductase of *Streptomyces* sp. AS2

Anis Uswatun Khasanah[1], Wahyu Aristyaning Putri[2], Hanum Mukti Rahayu[3], Langkah Sembiring[4], Yekti Asih Purwestri[5,6]*

1) Microbiology Laboratory, Department of Biology, Science Faculty, State Islamic University of Sultan Maulana Hasanuddin Banten. Jl. Jalan Jendral Sudirman No. 30 Panancangan Cipocok Jaya, Serang, Banten 42118, Indonesia.
2) Biotechnology Laboratory, Department of Tropical Biology, Universitas Gadjah Mada. Jl. Teknika Selatan, Sekip Utara, Bulaksumur Yogyakarta 55281, Indonesia
3) Program of Biology Education, Faculty of Teacher Training and Education, Universitas Muhammadiyah Pontianak. Jl. Ahmad Yani No. 111 Pontianak 78124, West Kalimantan, Indonesia.
4) Microbiology Laboratory, Department of Tropical Biology, Universitas Gadjah Mada. Jl. Teknika Selatan, Sekip Utara, Bulaksumur Yogyakarta 55281, Indonesia.
5) Biochemistry Laboratory, Department of Tropical Biology, Universitas Gadjah Mada. Jl. Teknika Selatan, Sekip Utara, Bulaksumur Yogyakarta 55281, Indonesia.
6) Research Center for Biotechnology, Universitas Gadjah Mada, Yogyakarta, Indonesia.
* Corresponding author, email: yekti@ugm.ac.id

ABSTRACT

Mercury pollution poses a significant environmental challenge worldwide, prompting extensive efforts over the past two decades to combat its detrimental effects. Cloning *merA* from *Streptomyces* sp. AS2 (Accession numbers LC026157) into the expression vector pET-28c (+) marks a critical advancement in this field, necessitating further investigation into the expression and structural analysis of the resulting recombinant mercuric reductase protein. This study aimed to optimise the expression and characterise the structural MerA protein. The study involved the expression of *merA* from AS2 isolate in the host *Escherichia coli* BL21 and the measurement of mercuric reductase using SDS-PAGE. Induction of *E. coli* BL21 was optimized by adding IPTG concentration and incubation time. Purification of mercuric reductase was attempted using ammonium sulphate precipitation, dialysis, and column chromatography. Protein structural characterisation was conducted using computational modelling tools Swiss-Model and Phyre2. Expression of *merA* from AS2 isolate was successfully performed *in E. coli* BL21, with SDS-PAGE showing a dominant band in the 55-70 kDa range using IPTG concentration 1 and 1,2 mM and 18-hour incubation time. The specific activity of mercuric reductase was obtained at an enzyme concentration of 294.07 Unit/mg. Protein structural characterisation revealed homology with *Lysinibacillus sphaericus* (Swiss-Model) and similar folding to c5c1Yc, a known mercuric reductase from the same species using Phyre2. The successful expression of recombinant pET-*merA* in *E. coli* BL21 offers new opportunities for bioremediation efforts targeting mercury contamination.

INTRODUCTION
Bioremediation is a biotechnological strategy that employs live organisms (plants, bacteria, fungi, or algae) or components of living organisms

to eliminate pollutants and mitigate their environmental impact (Barkay et al. 2010; Bharagava et al. 2017). *Actinomycetes* are a stimulating group of microorganisms that are integral members of the microbial community in soil. These microorganisms exhibit excellent metabolic variety and specific growth features (Cuozzo et al. 2018). Therefore, they are very suitable for the biological decomposition of environmental pollutants (Cuozzo et al. 2018). *Streptomyces* spp. can degrade the mercury in the environment because they harbour the *merA* (Putri et al. 2021). It could be utilized to address the issue of biological mercury exposure with its detoxification ability by *Streptomyces* spp. Detoxification primarily involves the conversion of toxic heavy metal ions into non-toxic ions (Mello et al. 2020; Rahayu et al. 2021).

Mercuric reductase (EC.1.16.1.1) is an oxidizing enzyme and *Flavin Adenine Dinucleotide* (FAD) is required for the conversion of mercury from Hg^{2+} to non-toxic Hg^0 (Bafana et al. 2017). As a result of elemental mercury's high vapor pressure, Hg^{2+} readily volatilizes and changes into Hg^0, which causes the atmosphere to become mercury-free (Bafana et al. 2017). Mercury has a high vapor pressure and low solubility, allowing it to escape into the atmosphere freely. In addition, Hg^{2+} is a non-biodegradable element that can persist in the atmosphere for several years (Dash et al. 2017). Furthermore, the *merA* commonly present in bacteria and archaea is likely to survive at high mercury concentrations. Adenine Dinucleotide Phosphate (NADPH) and *merA*-FAD compounds are critical in mercury volatilization and subsequent binding (Singh & Kumar 2020).

The homology structure of mercuric reductase, elucidated through comparative modeling techniques, reveals conserved motifs and structural features across different bacterial species, highlighting its evolutionary significance and functional conservation (Bafana et al. 2017). Beyond its fundamental catalytic role, mercuric reductase finds diverse applications in environmental bioremediation, where engineered microbial systems utilise the enzyme to mitigate mercury contamination in soil, water, and industrial effluents (Bharagava et al. 2017). Additionally, the enzyme's ability to selectively bind and reduce mercury ions has garnered interest in biotechnological applications, including biosensors for mercury detection and novel approaches for mercury recovery from waste streams (Dash et al. 2017). These multifaceted applications underscore the importance of understanding both the catalytic mechanism and structural characteristics of mercuric reductase in addressing environmental and industrial challenges associated with mercury pollution.

Rahayu et al. (2021) purified and characterised mercuric reductase from four strains of *Streptomyces* spp. isolated from a mercury-contaminated site in Indonesia (Rahayu et al. 2021). These strains, namely *Streptomyces* spp. AS1, AS2, AS6, and BR28, exhibited varying resistance activities to $HgCl_2$, with *Streptomyces* sp. AS6 demonstrates the highest resistance. Mercuric reductase from *Lysinibacillus sphaericus* has been previously characterised, with a molecular weight of approximately 60 kDa, Km of 32 μM HgCl2, and Vmax of 18 units/mg (Bafana et al. 2017). Cloning of the *merA* from *Streptomyces* sp. AS2 was successfully achieved (Putri et al. 2021), revealing a gene length of 1456 bp and similarities with *Streptomyces lividans*. The AS2 has received an accession number from the DNA Data Bank of Japan (DDBJ) with code LC026157 for AS2 clone 2. However, research on *merA* transformation from *Streptomyces* sp. AS2 into *E. coli* BL 21 is important to assess protein expression, activity, and structural characterization. This study aims to

optimise recombinant protein expression and structural homology characterization of *Streptomyces* sp. AS2.

MATERIALS AND METHODS
Materials
A plasmid pET-28c (+) containing the *merA*, and competent *E. coli* BL21 cells used for transformation of the *merA* into *E. coli* BL21. Inoue buffer was used to transform *E. coli* using the pET-*merA* plasmid. Inoue buffer consists of 55 mM $MnCl_2.4H_2O$, and 15 mM $CaCl_2$. $2H_2O$, 250 Mm KCl, and 10 mM PIPES with pH 6.7 (Green & Sambrook 2020). Liquid Luria Bertani (LB) medium is used as a medium for the growth of *E. coli* BL21. The components of the Luria Bertani liquid medium are 10 g NaCl, 5 g yeast extract, 10 g tryptone, and 1 litre of distilled water. The pH of the solution is made to 7.0 (Sezonov et al. 2007). Iso Propyl Thio D-Galactoside (IPTG) is used to optimize the expression of mercuric reductase. The *Nicotinamide Adenine Dinucleotide Phosphate* (NADPH), Mercuric Reductase Assay (MRA) solution, PBS solution, $MgCl_2$, EDTA, β-mercaptoethanol, and $HgCl_2$ are used for determining the specific activity of mercuric reductase. Bradford reagent is used for quantification of protein concentration. Protease inhibitor, and DEAE Sepharose anion column chromatography are used for protein purification. A retained protein marker 180 kDa is used as a marker to determine protein molecular weight.

Methods
E. coli BL21 transformation using pET-*merA*
E. coli BL21 transformation using pET- *merA* into was carried out using the heat shock method (Sambrook & Russell 2001). A 3 μL volume of plasmid pET-28c(+) containing the *merA* from previous study (Putri et al. 2021) was added to 100 μL of competent *E. coli* BL21 cells. The mixture was then incubated on ice for 30 minutes, followed by a 52-second incubation at 42°C. After 52 seconds, the mixture was promptly transferred back to ice bath and further incubated for 3 minutes. Subsequently, 900 μL of SOC medium consists of 2% tryptone, 0.5% yeast extract, 10 mM NaCl, 2.5 mM KCl, 10 mM $MgCl_2$, and 20 mM glucose (Cold Spring Harbor Laboratory Press 2012) was added to the suspension and incubated in a 37°C shaker for 1 hour. The suspension was then centrifuged at 8000 rpm for 1 minute, and the supernatant (1100 μL) was discarded, leaving 100-200 μL for plating on LB medium supplemented with 20 μg/mL kanamycin. The plated cells were then incubated at 37°C for 24 hours.

Confirming and optimising mercuric reductase expression involved varying IPTG concentration and incubation time
The *E. coli* BL21 carrying pET-*merA* plasmid was inoculated in 5 mL of liquid Luria Bertani (LB) containing 20 μg/mL kanamycin and incubated for 3 hours. The study used IPTG as an inducer with concentrations of 1 and 1.2 mM and also 4 hours and 18 hours incubation time. The various treatments are IPTG 1 mM with an incubation time of 4 hours, IPTG 1 mM with an incubation time of 18 hours, IPTG 1,2 mM with an incubation time of 4 hours, and IPTG 1.2 mM with an incubation time of 18 hours. The cell culture was centrifuged at 6000 rpm for 30 minutes. The supernatant was discarded, and the pellet was washed twice with PBS, pH 7.2. The obtained pellets were broken down using sonication for 30 seconds, with 3 repetitions, each followed by a 10-second rest. The supernatant was directly analysed for expression of mercury reductase by SDS

PAGE or stored frozen at 80°C.

Mercuric Reductase Enzyme Activity Assay

Mercuric reductase enzyme activity was determined by measuring $NADPH_2$ oxidation at λ 340 nm. The method involved adding 17 µL of the enzyme extract to 83 µL of Mercuric Reductase Assay (MRA) solution, which comprised 50 mM PBS solution (pH 7), 100 µM $NADPH_2$, 0.2 mM $MgCl_2$, 0.5 mM EDTA, 0.1% (vol/vol) β-mercaptoethanol, and 200 µM $HgCl_2$. Incubation occurred for 60 minutes at 37°C in darkness. Spectrophotometric measurements at 340 nm λ were conducted before and after incubation to determine initial and final $NADPH_2$ concentrations, enabling calculation of oxidized $NADPH_2$ quantity using the $NADPH_2$ standard curve equation $y = ax + b$. Activity was expressed as units of oxidised $NADPH_2$ per mg of protein per minute (µM $NADPH_2$/mg protein/min). Protein concentration was determined using the raw protein curve's regression line $y = ax + b$. The activity of mercuric reductase was measured by determining the concentration of oxidized Nicotinamide Adenine Dinucleotide Phosphate ($NADPH_2$) per milligram of protein per minute (M NADPH/mg protein/min) using the equation of the regression line $y = ax + b$ of the NADPH standard curve.

Quantification of Protein Concentrations Using Bradford Assay

The standard curve was initially generated. Protein concentration testing was conducted using the Coomassie Blue (Bradford Assay) method. Crude enzyme samples (8 µL) were combined with 200 µL of Bradford reagent and incubated for 2 minutes at room temperature. Absorbance was then measured at a wavelength of λ 595 nm. Protein concentration (mg/mL) was determined using the regression equation of the standard protein curve.

Resistance test of *E. coli* BL21 to $HgCl_2$

The resistance tests were carried out using the paper disk method. A 100 µL volume of *E. coli* BL21 pET-*merA* suspension which has been added IPTG was grown on the surface of a petri dish containing LB medium. A 6 mm paper disk was placed on top of the medium, and a drop of 8 µL of 1 mM $HgCl_2$ solution was added. The media was incubated at 37°C for 24 hours, and the diameter of the inhibition zone was measured.

Production and Purification of MerA Recombinant

The optimized IPTG induction and incubation time results were utilised as standard cell culture conditions for optimal mercuric reductase production. *E. coli* BL21 pellets were added with protease inhibitor then sonicated to disrupt the cells. Sonication, performed in three 30-second cycles with a 10-second rest between each, was supplemented with a protease inhibitor (1 tablet per 50 mL cell culture). A supernatant and pellet solution were obtained, with the supernatant collected for analysis due to the solubility of mercuric reductase. This supernatant constituted the crude enzyme extract, which could be directly analysed with SDS-PAGE or stored at -20°C. The purification process involved three stages: precipitation with ammonium sulphate at a saturation level of 20-70%, dialysis, and DEAE Sepharose anion column chromatography.

Characterisation of MerA Recombinant using SDS-PAGE

Protein analysis was conducted using SDS-PAGE with the Pre-stained

Protein Marker 180 kDa. 4% stacking gel and 12% resolving gel were used for SDS PAGE. Enzyme samples (10 µL) were mixed with sample buffer and heated at 100°C for 2 minutes, followed by a 10-minute incubation in an ice bath. Samples and protein markers were loaded into the wells of the electrophoresis gel, and electrophoresis was run for 1.5 hours at 100 volts using a running buffer. The gel was stained with Coomassie Brilliant Blue and destained to remove the background colour.

Protein Modelling, Prediction, and Structural Analysis
Tertiary protein structure prediction techniques can be divided into homology modelling, fold recognition, and *ab initio* prediction. Homology modelling was predicted using the Swiss model (Biasini et al. 2014) whereas modeling based on fold recognition using Phyre2 (Kelley et al. 2015). The protein prediction template was sourced from the Protein Data Bank (PDB) dataset.

Phylogenetic Tree of Amino Acid Sequences
The reference protein was downloaded from the PDB ID (Protein Data Bank). Reconstruction and analysis of phylogenetic trees based on mercuric reductase protein sequences were performed using MEGA11 (Zeyaullah et al. 2010).

RESULTS AND DISCUSSION
Transformation of *E. coli* BL21 using pET-*merA*
The successful expression and characterisation of recombinant MerA from *Streptomyces* sp. AS2 underscores its potential for mercury detoxification applications, confirming its functionality as a mercuric reductase enzyme involved in bacterial mercury resistance mechanisms. *Streptomyces* sp. AS2 isolates demonstrated successful transformation, as evidenced by their growth in selective medium. Approximately 40 colonies were observed, indicating the effective transcriptional activity of the pET-28c (+) plasmid with a strong promoter for target protein production (Figure 1).
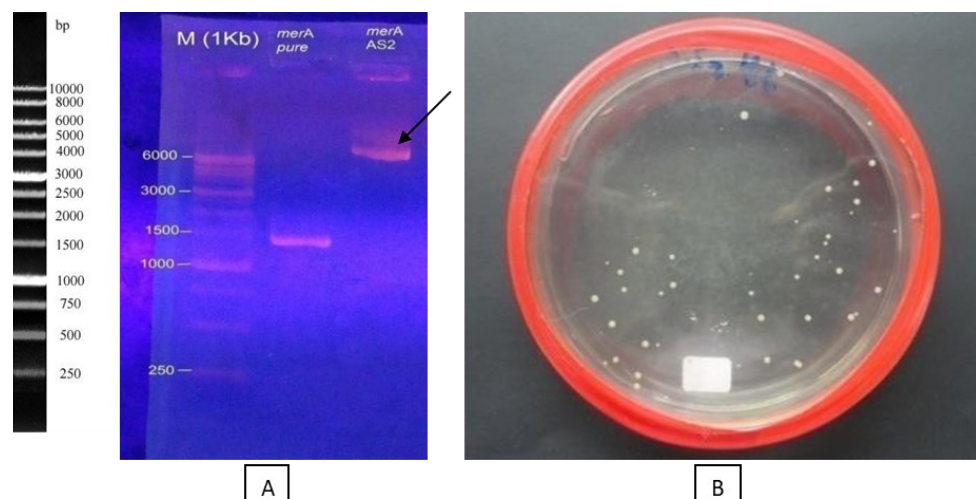
Figure 1. (A) Confirmation of *merA* after transformation; (B) *E. coli* BL21 recombinant inserted pET-*merA*.

Optimisation of Mercuric Reductase Expression and Measurement of Molecular Weight
Heterologous expression of mercuric reductase was confirmed by specific protein bands appearing at 55–70 kDa on SDS-PAGE (Figure 2). The

study used IPTG concentrations of 1 and 1.2 mM, with an optimal incubation time of 18 hours. Our findings demonstrate successful expression of mercuric reductase from *Streptomyces* sp. AS2 upon IPTG induction in *E. coli* BL21. The results of this study are in line with of Zeyaullah et al. (2010), who obtained a plasmid containing *merA* (1695 bp) from *E. coli* isolated from a mercury-contaminated site and expressed it in the pQE-30U/A vector, resulting in the expression of a 66.2 kDa mercuric reductase protein (Zeyaullah et al. 2010).
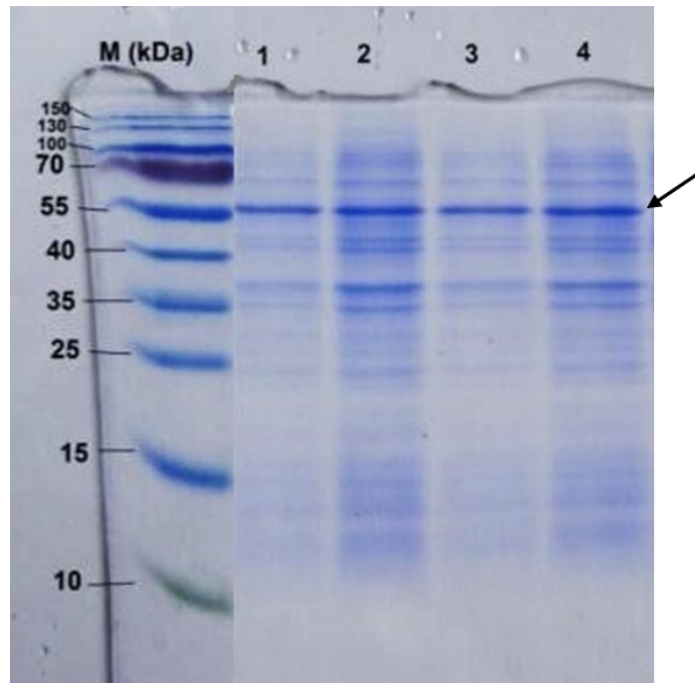
Figure 2. Expression of mercuric reductase *Streptomyces* sp. AS2 after induction IPTG 1 mM (1,2) & 1.2 mM (3,4) with 18 hours incubation (two replicates).

The observed size of the mercuric reductase aligns with findings from prior research. Gene expression analysis using *E. coli* BL21 (DE3) as the host revealed a mercuric reductase size of 66.2 kDa, consistent with reports on mercuric reductase expression from *Zymomonas mobilis*, which had a size of 65 kDa (Jones et al. 1992). These findings are attributed to the presence of a pET-28c (+) plasmid containing a robust T7 promoter, facilitating more efficient transcription of mercuric reductase compared to other proteins. Activation of T7 RNA polymerase occurs upon induction with IPTG, a lac operon inducer (Ogunseitan 1998).

Resistance test of *E. coli* BL21 against HgCl₂

The resistance test conducted in *E. coli* BL21 aims to evaluate its resistance level to 1 mM $HgCl_2$. Figure 3 depicts a 5.65 mm inhibitory diameter in *E. coli* BL21 carrying the *merA* isolate AS2 against 1 mM $HgCl_2$ (3 replications). The inhibitory diameter of *E. coli* BL21 against 1 mM HgCl2 was measured at 5.65 mm. Rahayu et al. (2021) conducted a similar test with *Streptomyces* sp. The inhibitory diameter produced by *Streptomyces* sp. AS2 is 9.6 mm (Rahayu et al. 2021). Comparison before and after transformation revealed that the resistant activity of *E. coli* BL21 surpassed the endogenous inhibitory activity of *Streptomyces* sp. AS2. The increase in mercuric reductase resistance is characterised by a decrease in the diameter of the resistance. The greater resistance activity may be due to the high quantity of mercuric reductase in the cell, resulting from the strong T7 promoter, compared with the quantity of mercuric reductase from endogenous *Streptomyces*.

Protein Extraction and Purification

In this study, the specific activity of recombinant mercuric reductase crude enzyme was higher than that of precipitation with ammonium sulphate, dialysis, and DEAE sepharose anion column chromatography (294.07 Unit / mg protein), and the lowest specific activity was found in dialysis results (29.22 Units / mg protein) (Table 1). Recovery of purified enzymes is also quite low. This less optimal result can be caused by several factors, including inclusion body, incubation time after less optimal induction of IPTG, ineffective lysis method, and purification method not specific for recombinant protein (Paul et al. 2020). So, another purification method for recombinant protein still needs to be performed for further study (Zeroual et al. 2003).

Protein Modelling, Prediction, and Analysis

To understand the structural properties of mercuric reductase, protein modelling, and prediction techniques were employed. Swiss-Model and Phyre2 were utilised for homology modelling and fold recognition, respectively. The resulting three-dimensional structure provided insights into the protein's architecture and spatial arrangement of amino acid residues. The search result shows several proteins similar to the query sequence based on the alignment of sequence pairs (Figure 4). The mercuric reductase protein in *Streptomyces* sp. AS2 shares a high homology with *Lysinibacillus sphaericus*. The query of mercuric reductase was submitted in Phyre2 using standard mode. The summary showed that a single template could model 97% of the query sequences. Figure 4 illustrates the three-dimensional structure of mercuric reductase generated by the Swiss-Model (Figure 4A), the results of a reference structure search (Figure 4B), and the phyre2 prediction results (Figure 4C). These computational modelling approaches enhance our understanding of AS2 mercuric reductase structural features and facilitate further biochemical investigations.

The structure of a protein is more evolutionarily conserved than its amino acid sequence, and the sequence of the desired protein (target) can be pretty accurately modelled using a very distant sequence of known structure (substrate), as long as the relationship between the target and the model can be distinguished by the association of sequences (Tamura et al. 2021). The *Streptomyces* sp. AS2 mercuric reductase protein has a sequence length of 466 amino acids and a globular protein. Characterisation and modelling of proteins using the Swiss model for homology view and Phyre2 for folding view.

Protein modelling using the Swiss model showed that the mercuric reductase protein in *Streptomyces* sp. AS2 shares high homology with

Table 1. Purification of Mercury Reductase of *E. coli* BL21 as the result of transformation.

		Protein		Mercury Activity			Purification	
Stage	Volume (mL)	Concentration of Protein (mg/mL)	Total Protein (mg)	Activity of Enzyme (Unit)	Total Activity	Specific Activity (Unit/mg protein)	Purification Factor	Results (%)
Crude Enzyme	80	0.2518	20.1405	74.05	5923.69	294.07	1	100
Precipitation Am. Sulphate	18	0.3052	5.4941	68.94	1240.96	228.01	0.7754	20.95
Dialysis	6	1.306	7.8361	38.15	228.92	29.22	0.1282	3.86
DEAE sepharose anion column chromatography	4	0,3454	1,3871	40.91	118.32	163.65	5.6006	2.00
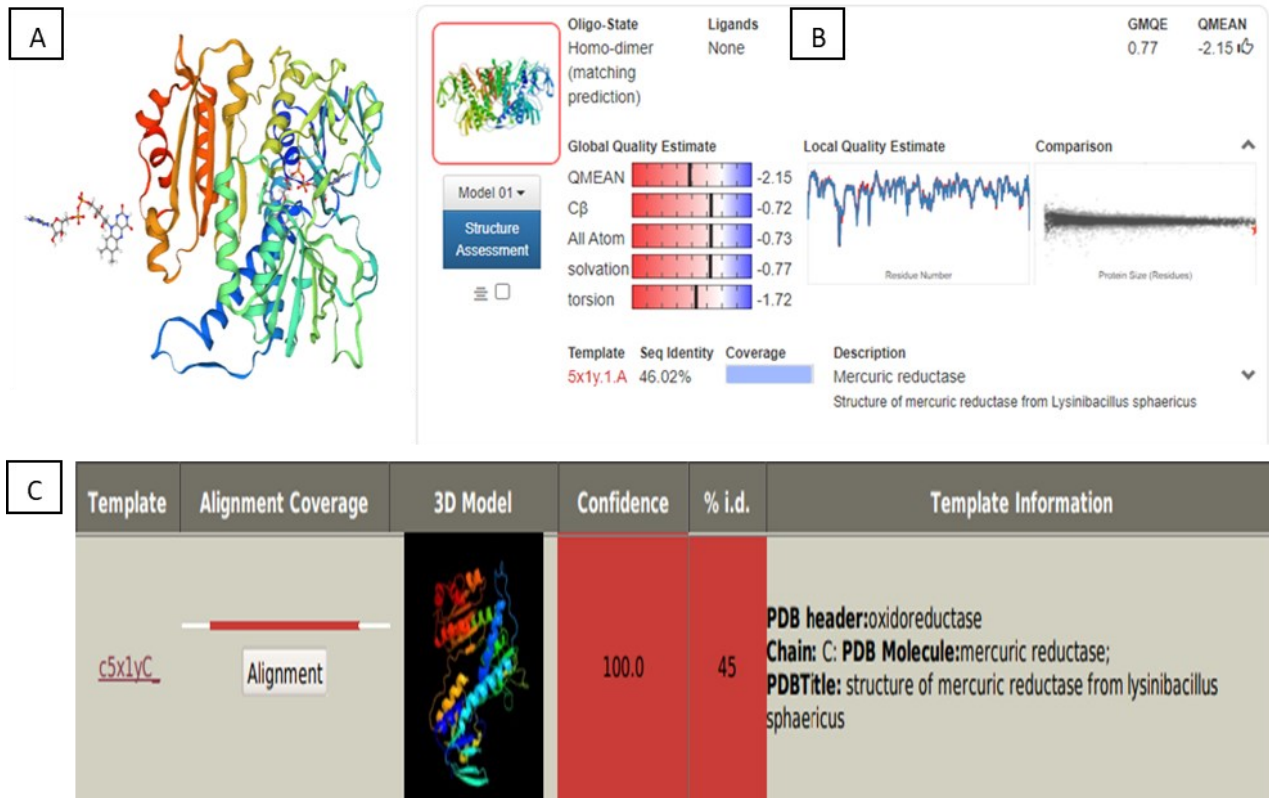
Figure 4. Image of the three-dimensional structure of the mercuric reductase protein; (A) Modelling the 3D structure result using Swiss-Model; (B) Results of a reference structure search using mercuric reductase *Streptomyces* AS2 protein sequence query; (C) Display of phyre2 prediction results with the best reference structure.

Lysinibacillus sphaericus. The query mercuric reductase protein *Streptomyces* sp. AS2 has the best GMQE and QMEAN scores among the three structures (Mercuric reductase Crystal Structure of TN501 MerA, Mercuric reductase Crystal Structure of the C136, and Mercuric reductase Crystal Structure of C558). The thumb symbol pointing up to the right of the QMEAN score indicates that the reference structure is sufficient to represent the query protein structure.

Protein modeling using Phyre2 reported that a protein with code c5c1Yc from *Lysinibacillus sphaericus* is the best reference structure among other predictive reference structures for mercuric reductase *Streptomyces* sp. AS2. The code is a Phyre2 accession code adopted from the SCOP database. The letter "c" at the beginning indicates that the entire protein chain is used as the reference structure if "d" shows only certain domains. The code of c5c1Yc refers to mercuric reductase from *Lysinibacillus sphaericus.* Based on the confidence level of the predicted results, a total of 461 or 97% residues of the *Streptomyces* sp. AS2 mercuric reductase protein are estimated to have 100% structural similarity to the reference protein. The prediction of secondary structure mercuric reductase *Streptomyces* sp. AS2 using the phyre2 program showed that mercuric reductase *Streptomyces* sp. AS2 has 32% α-helix bonds, 30% β-strands, and 4% transmembrane helices.

Phylogenetic Tree of Amino Acid Sequences

The phylogenetic tree based on mercuric reductase amino acid sequences, depicted in Figure 5, illustrates the evolutionary relationships among various organisms. Our study identified a 100% similarity between *Streptomyces* sp. AS2 and *Streptomyces lividans* in terms of the mercuric reductase sequence. Mercuric reductase sequences were obtained from the alpha fold protein database, comprising 11 organisms, primarily from the
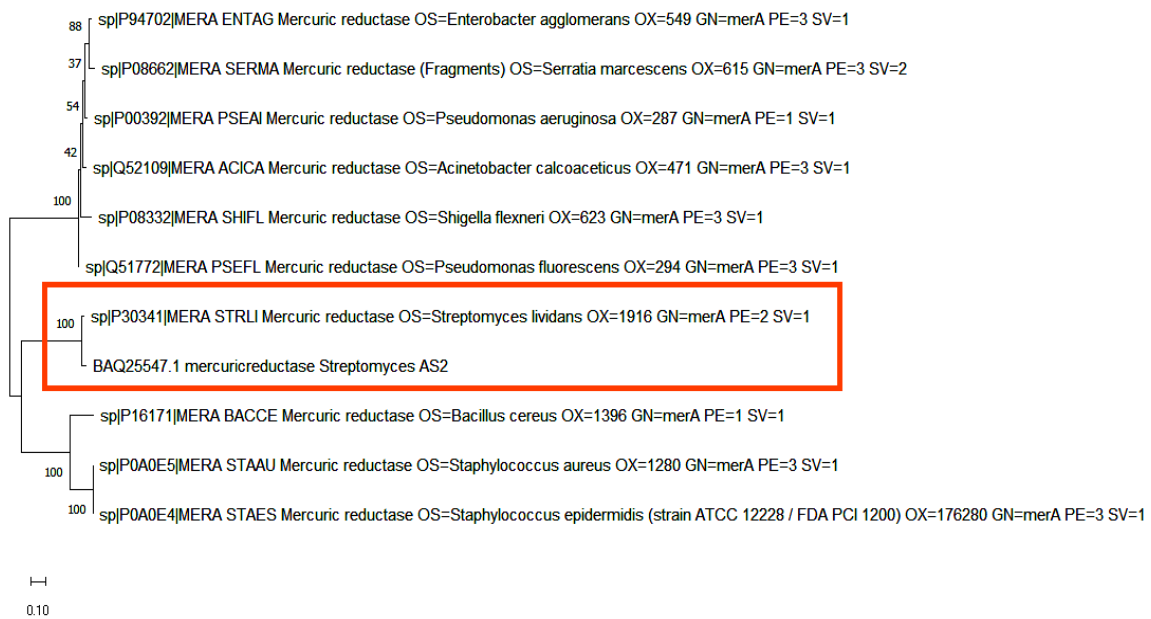
Figure 5. The results of the reconstruction of the phylogenetic tree using a MEGA11 program based on the mercuric reductase protein.

Streptomyces genus. Maximum likelihood estimation using the JTT matrix model was employed to infer the evolutionary history (Aprilyanto & Sembiring 2017), resulting in a tree with the highest logarithmic probability (3361.13). Branches on the tree indicate the percentage of trees supporting the clustering of related taxa. The tree, drawn to scale, reflects branch lengths denoted by the number of substitutions at each site. The analysis of the amino acid sequences of the 53 TNLs in roses and other Rosaceous species, with a bootstrap consensus tree derived from 500 iterations deemed representative of their evolutionary history (Terefe-Ayana et al. 2012). These analyses were conducted using MEGA11 (Tamura et al. 2021). Interestingly, a previous study based on the 16S rRNA gene suggested that *Streptomyces* sp. AS2 closely related *Streptomyces ardesiacus* NRRL B-1773. Our protein database (Alpha fold) analysis revealed *Streptomyces* sp. AS2 mercuric reductase its similarity to *Streptomyces lividans*. This investigation demonstrated of the tertiary structure of mercuric reductase protein in *Streptomyces.*

Reconstruction of the phylogenetic tree using the mercuric reductase protein database in several bacteria was intended to determine the similarity of mercuric reductase in *Streptomycetes* to other bacterial strains. Reconstruction of the tree using the phylogeny.fr program. The phylogenetic reconstruction in this program is arranged in the form of a pipeline, starting from the juxtaposition of multiple sequences, calculating the evolutionary distance, to the reconstruction of the tree itself. Tree reconstruction is done through a one-click menu (Dereeper et al. 2008). The mercuric reductase data base on various bacteria was obtained from the NCBI protein database. The phylogenetic tree shows the mercuric reductase protein *Streptomyces* sp. AS2 used in this study, has 60% similarity to *Lysinibacillus sphaericus.* These results are following the results of the reconstruction of the tertiary structure of 3D proteins using the Swiss-model and Phyre, both of which use mercuric reductase in *Lysinibacillus sphaericus* as a query and reference template. *Elizabethkingia anophelis* in the phylogenetic tree reconstruction was used as an outgroup due to the type of protein oxidoreductase but not mercuric reductase. *Elizabethkingia anophelis* is one of the species from

Elizabethkingia, a bacterial genus commonly found in soil and water. *Elizabethkingia anophelis* is a gram-negative bacteria and has been isolated from *Anopheles* mosquitoes (Centers for Disease Control and Prevention 2024). This bacteria was used as a comparison in the phylogenetic tree reconstruction.

CONCLUSION

In conclusion, our study represents a significant step forward in mercury bioremediation research, paving the way for innovative strategies to address environmental mercury contamination. The *mer*A gene isolated from *Streptomyces* sp. AS2 can be expressed in *E. coli* BL21 and was confirmed by specific protein bands appearing at 55–70 kDa. IPTG concentration 1 and 1.2 mM IPTG as inducer and 18-hour incubation time are optimal variations to determine the optimal expression of mercuric reductase. The specific activity of purified mercuric reductase on crude enzyme with a concentration of 294.07 units/mg Structural characterization of the *Streptomyces* sp. AS2 MerA protein has homology to *Lysinibacillus sphaericus* and has a similar fold to c5c1Yc. By elucidating MerA expression, enzymatic activity, and structural characteristics, we contribute to the development of advanced biotechnological interventions aimed at preserving ecological health and safeguarding human well-being.

AUTHORS CONTRIBUTION

A.U.K. designed and performed the experiments and wrote the manuscript. W.A.P. performed the experiments and edited the manuscript. H.M.R. performed the experiments and edited the manuscript. L.S. designed the experiments. Y.A.P. designed the experiments and edited the manuscript.

ACKNOWLEDGMENTS

CONFLICT OF INTEREST

The authors have no conflict of interest in participating in this research. The funder had no role in the study design, data collection, and analysis, decision to publish, or preparation of the manuscript.

REFERENCES

Aprilyanto, V. & Sembiring, L., 2017. *Bioinformatika*, Innosain.

Bafana, A., Khan, F. & Suguna, A., 2017. Structural and functional characterization of mercuric reductase from *Lysinibacillus sphaericus* strain G1. *Biometals*, 30(5), pp.809–819. doi: 10.1007/s10534-017-0050-x.

Barkay, T. et al., 2010. A thermophilic bacterial origin and subsequent constraints by redox, light and salinity on the evolution of the microbial mercuric reductase. *Environmental Microbiology*, 12(11), pp.2904–2917. doi: 10.1111/j.1462-2920.2010.02260.x.

Bharagava, R., Chowdhary, P. & Saxena, G., 2017. Bioremediation: An Eco-Sustainable Green Technology: Its Applications and Limitations. In *Environmental Pollutants and Their Bioremediation Approaches*. Florida, USA: CRC Press, pp.1–22. doi: 10.1201/9781315173351-2.

Biasini, M. et al., 2014. SWISS-MODEL: modelling protein tertiary and quaternary structure using evolutionary information. *Nucleic Acids Research*, 42(Web Server issue), pp.W252-W258. doi: 10.1093/nar/gku340.

Centers for Disease Control and Prevention, 2004, 'Elizabethkingia', in *Centers for Disease Control and Prevention*, viewed 19 June 2024, from https://www.cdc.gov/elizabethkingia/about/index.html.

Cold, S.H.P., 2012, 'SOC Medium for *E. coli* ', in *Cold Spring Harbor Laboratory Press*, viewed 13 June 2024, from https://cshprotocols.cshlp.org/content/2012/6/pdb.rec069732.short

Cuozzo, S.A. et al., 2018. *Streptomyces* sp. is a powerful biotechnological tool for the biodegradation of HCH isomers: biochemical and molecular basis. *Critical Reviews in Biotechnology*, 38(5), pp.719–728. doi: 10.1080/07388551.2017.1398133.

Dash, H.R. et al., 2017. Functional efficiency of MerA protein among diverse mercury resistant bacteria for efficient use in bioremediation of inorganic mercury. *Biochimie*, 142, pp.207–215. doi: 10.1016/j.biochi.2017.09.016.

Dereeper, A. et al., 2008. Phylogeny.fr: robust phylogenetic analysis for the non-specialist. *Nucleic Acids Research*, 36(Web Server), pp.W465–W469. doi: 10.1093/nar/gkn180.

Green, M.R. & Sambrook, J., 2020. The inoue method for preparation and transformation of competent *Escherichia coli*: Ultracompetent cells. *Cold Spring Harbor Protocols*, 2020(6), 101196. doi: 10.1101/pdb.prot101196.

Jones, D.T., Taylor, W.R. & Thornton, J.M., 1992. The rapid generation of mutation data matrices from protein sequences. *Computer applications in the biosciences: CABIOS*, 8(3), pp.275–282. doi: 10.1093/bioinformatics/8.3.275.

Kelley, L.A. et al., 2015. The Phyre2 web portal for protein modeling, prediction and analysis. *Nature Protocols*, 10(6), pp.845–858. doi: 10.1038/nprot.2015.053.

Mello, I.S. et al., 2020. Endophytic bacteria stimulate mercury phytoremediation by modulating its bioaccumulation and volatilization. *Ecotoxicology and Environmental Safety*, 202, 110818. doi: 10.1016/j.ecoenv.2020.110818.

Ogunseitan, O.A., 1998. Protein method for investigating mercuric reductase gene expression in aquatic environments. *Applied and Environmental Microbiology*, 64(2), pp.695–702. doi: 10.1128/AEM.64.2.695-702.1998.

Paul, T. et al., 2020. A comprehensive review on recent trends in production , purification , and applications of prodigiosin. *Biomass Conversion and Biorefinery*, 12, pp.1409-1431. doi: 10.1007/s13399-020-00928-2.

Putri, W.A. et al., 2021. Identification of mercury-resistant *Streptomyces* isolated from *Cyperus rotundus* L. rhizosphere and molecular cloning of mercury (II) reductase gene. *Indonesian Journal of Biotechnology*, 26(4), pp.206-213. doi: 10.22146/ijbiotech.65989.

Rahayu, H.M. et al., 2021. Indigeneous *Streptomyces* spp. isolated from *Cyperus rotundus* rhizosphere indicate high mercuric reductase activity as a potential bioremediation agent. *Biodiversitas Journal of Biological Diversity*, 22(3), pp.1519-1526. doi: 10.13057/biodiv/d220357.

Sambrook, J. & Russell, D.W., 2001. *Molecular Cloning: A Laboratory Manual*, Cold Spring Harbor Laboratory Press.

Sezonov, G., Joseleau-Petit, D. & D'Ari, R., 2007. *Escherichia coli* physiology in Luria-Bertani Broth. *Journal of Bacteriology,* 189(23), pp.8746-8749. doi: 10.1128/JB.01368-07.

Singh, S. & Kumar, V., 2020. Mercury detoxification by absorption, mercuric ion reductase, and exopolysaccharides: a comprehensive study. *Environmental Science and Pollution Research,* 27(22), pp.27181–27201. doi: 10.1007/s11356-019-04974-w.

Tamura, K., Stecher, G. & Kumar, S., 2021. MEGA11: molecular evolutionary genetics analysis version 11. *Molecular Biology and Evolution,* 38(7), pp.3022–3027. doi: 10.1093/molbev/msab120.

Terefe-Ayana, D. et al., 2012. Evolution of the Rdr1 TNL-cluster in roses and other Rosaceous species. *BMC Genomics,* 13, 409. doi: 10.1186/1471-2164-13-409.

Zeroual, Y. et al., 2003. Purification and characterization of cytosolic mercuric reductase from *Klebsiella pneumoniae. Annals of Microbiology,* 53, pp.149–160.

Zeyaullah, M et al., 2010. Molecular cloning and expression of bacterial mercuric reductase gene. *African Journal of Biotechnology,* 9(25), pp.3714-3718.

Research Article

The Application of Amino Acid Racemization Geochronology of *Tubipora* sp. in Marine Terraces of Manokwari Region, West Papua, Indonesia

Rahmadi Hidayat[1]*, Sukahar Eka Adi Saputra[2], Salahuddin Husein[1]
1)Department of Geological Engineering, Faculty of Engineering, Universitas Gadjah Mada, Yogyakarta, 55281, Indonesia.
2)Center for Geological Survey, Geological Agency of Indonesia, Bandung, 40122, Indonesia
* Corresponding author, email: rahmadihidayat@ugm.ac.id

ABSTRACT
The active neotectonics of northern West Papuan coastlines allow the formation of emergent marine terraces associated with Quaternary sea-level high stands. These terraces contain fossils from the coral assemblage, which are useful for geochronological assessments and further estimating uplift rates. Here, we report the applicability of amino acid racemization (AAR) of *Tubipora* sp. to discriminate different ages associated with stages of sea-level high stand, constrained by previous uranium-thorium (U/Th) series dating. The results from amino acid dating of three samples reveal two distinct extents of racemization corresponding to terraces developed during Marine Isotope Stage (MIS) 5 *sensu lato* and 1. However, AAR analysis could not further discriminate interstadial MIS 5a and 5c as determined by published radiometric dating. This indicates the low resolving power of amino acid dating to distinguish sub-sequences beyond the interglacial period. Nevertheless, the cost-effective and rapid analysis of AAR dating of *Tubipora* sp. can be used as preliminary results related to marine terraces formed in different interglacial events.

INTRODUCTION

The emergent coral reef terraces have been widely studied to infer the uplift rate of tectonically active sites such as Barbados (Bard et al. 1990; Schellmann & Radtke 2004), Haiti (Dodge et al. 1983; Dumas et al. 2006), and Huon Peninsula (Bloom et al. 1974). The crucial parameter for estimating the degree of uplift is a robust chronological method to assign palaeosea-level elevation based on calcium carbonate-bearing samples, mostly corals (Tomiak et al. 2016). In most cases, uranium-thorium (U/Th) dating has been applied to evaluate the age of common fossil corals inhabiting near water surfaces as a suitable indicator of the mean sea-level (Hibbert et al. 2016). In principle, U/Th geochronology is a radiometric dating technique focusing on the decay activity of Uranium-234 as parent to Thorium-230 as the daughter isotope contained in the calcium-carbonate fossils. Unlike uranium, thorium is characteristically insoluble in marine water; and thus, in an ideal environment, the abundance of Thorium-230 is considered the main result of radioactive decay from the coral skeleton (Chen et al. 2020). Moreover, the typically closed-system nature of corals, having a limited exchange of both

thorium and uranium uptakes associated with the environment, provides high age resolution and precision determined from the U/Th technique (Chutcharavan & Dutton 2020).

Despite its suitability in coral assemblages, some marine terrace sites present a challenge in establishing U/Th dating due to the introduction of reworked materials from older successions. The occurrence of reworked corals has been identified in several areas within the Pacific coastlines of the US due to the combined effect of vertical displacement and glacial-isostatic adjustment associated with the waxing and waning of the ice sheet (Muhs et al. 2012; Simms et al. 2016). In this case, the age assessment should be conducted carefully, especially when selecting samples that represent the actual age of coral reef terraces. This could be achieved by dating large subsets of coral to determine and remove the reworked fossils, although it may take longer time to complete and be considered costly.

In this case, an alternative dating method of fossils that is able to perform in high-density samples, such as amino acid racemization (AAR), is important to complement the primary geochronological tool. As opposed to U/Th dating, AAR focuses on measuring the degree of protein degradation by determining the ratio between left- and right-handed amino acids. In principle, the concentration of right-handed amino acids began to build up after the death of organisms, so the increasing ratio of left- and right-handed amino acids, namely DL ratios, are proportional to the longer time since death (Demarchi 2020). The current technology of reverse-phase high-performance liquid chromatography (RP-HPLC) and its detector has improved the capability of large amounts of analytical measurement, 2 hours each, with relatively small-sized fossils (Kaufman & Manley 1998; Hidayat et al. 2024). For example, Hidayat et al. (2023) have conducted as many as 472 analyses of individual minuscule fossils of foraminifera (~ 0.5 mm) to understand the nature of reworking in the development of carbonate-rich coastal deposits.

U/Th dating has been utilized to analyze fossil coral embedded in marine terraces to investigate the neotectonics of the Manokwari region, West Papua (Saputra et al. 2022). To determine the uplift rate in this area, Saputra et al. (2022) suggested using soft coral *Tubipora* sp. as specimens for dating. *Tubipora* sp. colonies are widely distributed across the west of Pacific, south of Japan, and the Red Sea, typically inhabiting shallow waters up to 20 meters deep (Ammar 2005). Alongside other coral assemblages such as *Acropora* and *Porites*, *Tubipora* sp. is commonly found in sheltered, low-energy zones rather than fore-reef environments (Manaa et al. 2016). The distinctive organ pipe-like structures and deep red coloration of this species are due to carotenoids in their aragonite skeleton (Ammar 2005). Given its specific habitat requirements, the abundance of *Tubipora* sp. is pertinent for conducting geochronological reconstructions to model vertical ground movements over geological timeframes (Saputra et al. 2022). Despite these valuable attributes, the application of amino acid racemization (AAR) for this species is currently limited, particularly in distinguishing ages related to sea-level highstands.

Here, we investigate the application of amino acid geochronology of fossil soft corals *Tubipora* sp. to determine different ages associated with interglacial sea-levels with references from previous U/Th dating from Saputra et al. (2022). The rapid and cost-effective AAR method for age determination may be valuable to provide large datasets to identify the potential age mixing or reworked fossils and further complement a more

expensive and time-consuming dating method, for example, U/Th series, in selecting the most appropriate sample set to analyze.

REGIONAL SETTING

Manokwari area is geologically situated in the Bird's Head terrane of West Papua (Figure 1), a region considered tectonically active due to oblique convergence of major tectonic plates (Pacific, Caroline and Australia) as evidenced by regional strike-slip faults such as Sorong, Yapen, and Ransiki (Gold et al. 2014). This intense neotectonic setting allows emergent Quaternary coral reef terraces to occur >150 m above the present sea-level (APSL), showing well-developed landforms with northwest-southeast directed escarpments (Saputra & Fergusson 2023). These terraces are characterized by massive and thick reefal limestone comprising calcirudite, calcarenite, conglomerate, and carbonate-rich breccia (Robinson & Ratman 1978). Saputra et al. (2022) documented varying uplift rates of these marine successions of up to 1.28 meter/kilo annum (m/ka) based on U/Th chronology from fossil corals, mainly *Porites* sp., coralline algae, and *Tubipora* sp. The latter specimen is the focus of conducting amino acid dating in this study.
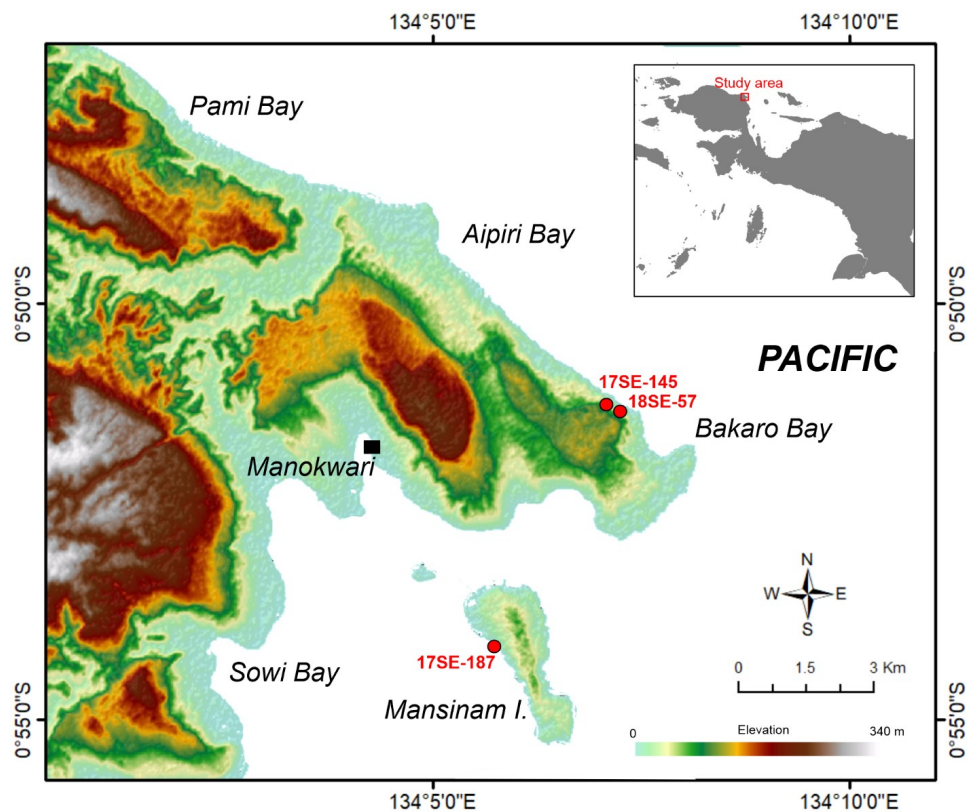
Figure 1. Location of sampling sites within Manokwari region; and an inset of the western part of New Guinea (a territory of Indonesia). The topographic dataset and inset map were retrieved from the Digital Elevation Model Nasional from Badan Informasi Geospasial (2018, https://tanahair.indonesia.go.id/demnas/#/).

MATERIALS AND METHODS
Sampling sites

Three samples previously collected by Saputra et al. (2022) from two different sites within the Manokwari region were used in this study (Figure 1). In Mansinam Island, a sample (coded 17SE-187, Figure 2a) was retrieved from a 150 m wide raised coral reef terrace at an elevation of 3 m APSL. Two remaining *Tubipora* sp. specimens were collected from the terraces of Bakaro Bay (Figure 1), around 6 km north of Mansinam

Island. In more detail, a sample (coded 17SE-145) was obtained from Suweni Terrace, around 77.5 m APSL (Figure 2b), typically comprising a back reef to reef crest facies (Saputra et al. 2022). To the southeast (~120 m), a sedimentary unit consisting of abundant *Tubipora* sp. (18SE-57) was sampled from different coral reef terrace, namely Suweni Dua, with an elevation of 62.5 m APSL (Figure 2c). The characteristics of this faunal assemblage are mostly preserved on the terraces of Bakaro Bay, exhibiting distinctive and unique organ pipe structures filled with sand-sized carbonate particles (Figure 2d).

Amino acid racemization

A suite of *Tubipora* sp. samples, 100 mg each, were initially cleaned with a brush and further immersed in a glass beaker with distilled water and sonicated for 10 min. Subsequently, stoichiometric acid etch (2 mol/L HCl) was applied to remove the outer surface with a potential diagenetic alteration. Following this, samples were treated using a 3% hydrogen peroxide (H_2O_2) solution, rinsed with distilled water five times and air-dried overnight. The dried samples were placed in designated glass tubes, demineralized with 8 mol/L HCl according to the remaining mass, filled with a stream of nitrogen gas and finally sealed. The small amount (50 µL) of samples were transferred to vials for analysis of the free amino acid (FAA) fraction prior to sealing, whereas to recover the free and total bound state of peptides, termed total hydrolyzable amino acids (THAA), the remaining solutions within glass tubes were hydrolyzed using an

a) Raised reef, Mansinam Island (17SE-187)

b) Suweni Terrace, Bakaro Bay (17SE-145)

c) Suweni Dua Terrace, Bakaro Bay (18SE-57)

d) Suweni Dua Terrace, Bakaro Bay (18SE-57)
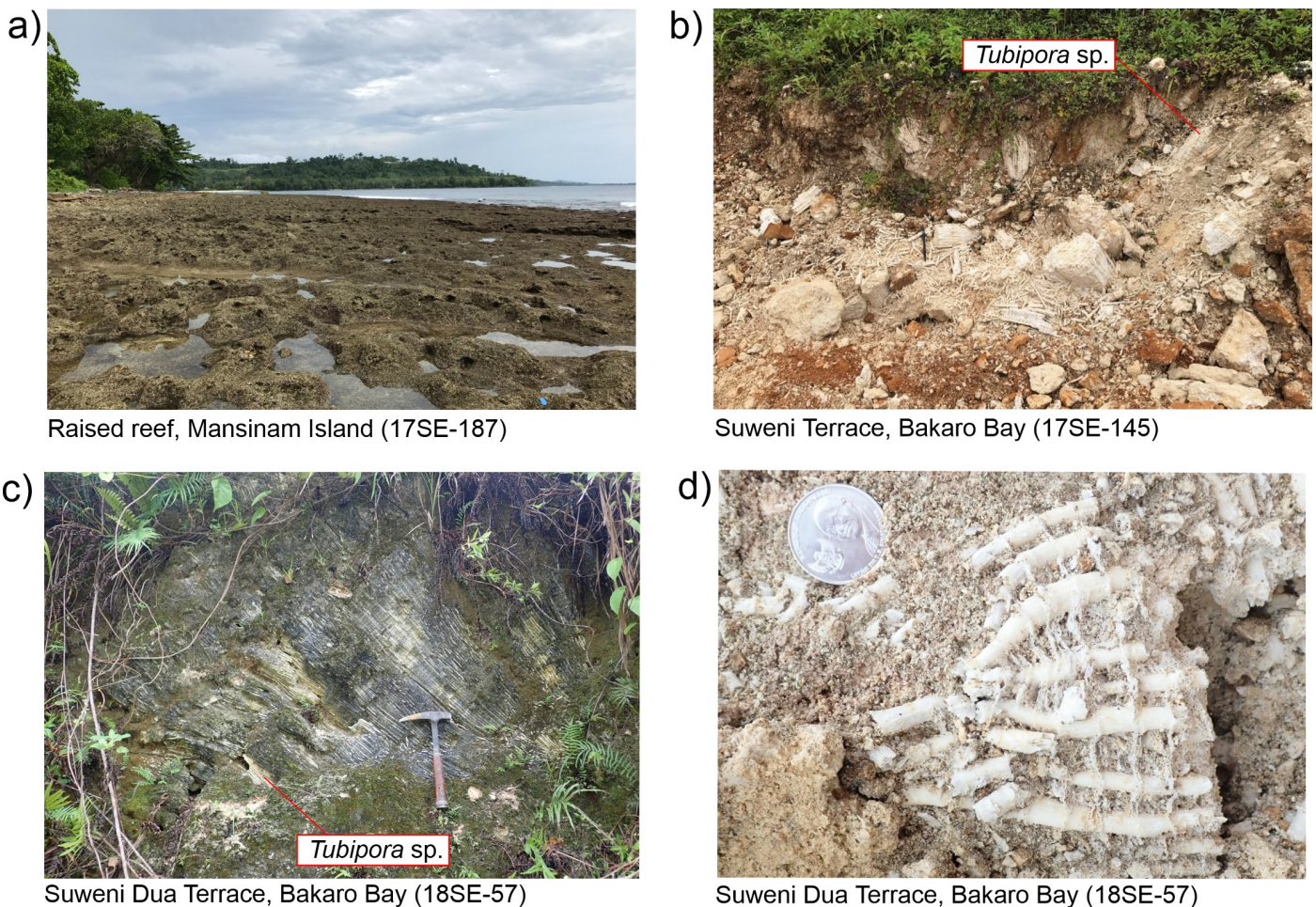
Figure 2. a) Coastal landscape of Mansinam Island (17SE-187) showing raised reef unit close to the present-day sea-level. b) Marine terrace with colonies of *Tubipora* sp. (17SE-145) at Suweni Terrace, Bakaro Bay. c) Organ pipe structures dominate the terrace outcrop of Suweni Dua, Bakaro Bay. d) Close-up of *Tubipora* sp. retrieved from Suweni Dua terrace.

oven for 22 h at 110 °C. After that, the solutions were placed in separate vials and evaporated to dryness via a vacuum desiccator. Finally, all samples were rehydrated using internal standard L-*Homo*-Argenine to estimate amino acid concentration.

The analytical procedure for RP-HPLC generally follows Kaufman and Manley (1998). Pre-column derivatization was performed using ophthaldialdehyde (OPA) and the chiral thiol N-isobutyryl-L-cysteine (IBLC). The instrument used to calculate the extent of racemization (defined by the ratio of D- and L-amino acids or DL ratio) was an Agilent 1100 equipped with a Hypersil BDS C18 column and a fluorescence detector, with mixture of solvents consisting of methanol, aqueous sodium acetate with minor ethylene-diamine-tetraacetic acid (EDTA), sodium azide, and acetonitrile. Inter-laboratory standards (ILC A to C) were used to monitor the instrument's analytical uncertainty. Four amino acids were selected for this study: aspartic acid (ASX), glutamic acid (GLX), valine (VAL), and isoleucine epimerization (A/I), as shown in Table 1. The total abundance of amino acids was calculated based on these three selected amino acids combined with serine (SER), glycine (GLY), alanine (ALA), phenylalanine (PHE), and isoleucine (ILE), as shown in Table 2.

RESULTS

A *Tubipora* sp. from exposed reef outcrop at Mansinam Island (17SE-187) showed the lowest racemization degree compared to other

Table 1. Results of the extent of racemization from *Tubipora* sp. in the Manokwari region's marine terraces with respective U/Th age from *Saputra et al. (2022). Both analyses of total hydrolyzable and free amino acids (in italics) are presented. UWGA: University of Wollongong sample code. ASX: aspartic acid, GLX: glutamic acid, VAL: valine and A/I: isoleucine epimerization.

Location	Code	UWGA (replicates)	U/Th age* (ka)	ASX	GLX	VAL	A/I
Mansinam I.	17SE-187	11407 (4)	2.7 ± 0.3	0.552 ± 0.005 *0.715 ± 0.005*	0.278 ± 0.013 *0.487 ± 0.033*	0.256 ± 0.023 *0.455 ± 0.023*	0.555 ± 0.033 *0.755 ± 0.083*
Suweni, Bakaro Bay	17SE-145	11404 (4)	90 ± 5.0	0.779 ± 0.008 *0.910 ± 0.008*	0.551 ± 0.010 *0.680 ± 0.008*	0.522 ± 0.021 *0.858 ± 0.059*	0.738 ± 0.029 *1.087 ± 0.076*
Suweni Dua, Bakaro Bay	18SE-57	11403 (4)	102 ± 1.5	0.765 ± 0.008 *0.910 ± 0.004*	0.544 ± 0.005 *0.665 ± 0.020*	0.503 ± 0.011 *0.834 ± 0.066*	0.705 ± 0.030 *0.947 ± 0.049*

Table 2. Results of the amino acid concentrations of *Tubipora* sp. in marine terraces of Manokwari region with respective U/Th age from *Saputra et al. (2022). Both analyses of total hydrolyzable and free amino acids (in italics) are presented. UWGA: University of Wollongong sample code. ASX: aspartic acid, GLX: glutamic acid, VAL: valine and ILE: isoleucine. Total amino acid concentrations are measured from aspartic acid, glutamic acid, valine, serine, glycine, alanine, phenylalanine and isoleucine.

Location	Code	UWGA (replicates)	U/Th age* (ka)	ASX (pmol/mg)	GLX (pmol/mg)	VAL (pmol/mg)	ILE (pmol/mg)	Total (pmol/mg)
Mansinam I.	17SE-187	11407 (4)	2.7 ± 0.3	972.2 ± 4.3 *50.6 ± 14.9*	608.6 ± 2.7 *23.2 ± 1.6*	470.7 ± 0.4 *12.8 ± 1.3*	328.6 ± 1.2 *6.0 ± 0.9*	4429.0 ± 1.2 *216.5 ± 22.7*
Suweni, Bakaro Bay	17SE-145	11404 (4)	90 ± 5.0	392.2 ± 7.8 *178.9 ± 0.6*	151.6 ± 7.0 *25.9 ± 0.4*	93.0 ± 8.6 *35.9 ± 1.0*	50.6 ± 1.2 *13.1 ± 0.4*	1152.4 ± 1.2 *473.3 ± 8.3*
Suweni Dua, Bakaro Bay	18SE-57	11403 (4)	102 ± 1.5	430.8 ± 6.1 *183.2 ± 1.4*	104.7 ± 1.8 *25.6 ± 0.2*	44.2 ± 0.7 *40.9 ± 2.1*	23.7 ± 0.8 *21.7 ± 0.8*	894.6 ± 0.8 *501.9 ± 8.8*

specimens with ASX and GLX DL ratios 0.552 ± 0.005 and 0.278 ± 0.013 respectively for THAA (Figure 3a). The AAR results based on THAA show a lower extent of racemization than FAA, which is expected as a result of the introduction of low amino acid racemization within bound state peptides that were broken down via hydrolysis (Wehmiller 1993) by exposing them to a temperature of 110 °C for 22 h. In this case, the results from FAA of *Tubipora* sp. at Mansinam Island (17SE-187) exhibit ASX and GLX DL ratios of 0.715 ± 0.005 and 0.478 ± 0.033 (Figure 3b). Similarly, these values are lower compared with two specimens obtained from Bakaro Bay.

The remaining samples collected from Bakaro Bay yielded a distinctly greater extent of ASX racemization at 0.779 ± 0.008 (17SE-145) and 0.765 ± 0.005 (18SE-57) for THAA (Figure 3a). Regarding GLX, the AAR results from Bakaro Bay samples consistently showed higher DL ratios at roughly twice that of the sample from Mansinam Island at 0.551 ± 0.010 (17SE-145) and 0.544 ± 0.005 (18SE-57) for THAA. The racemization extent of VAL from these specimens is also roughly twice greater than *Tubipora* sp. from Mansinam Island. The FAA analyses for two specimens of Bakaro Bay yielded almost racemic for ASX (~0.910), whereas for GLX, the DL ratios are within the range of 0.665 − 0.680 (Figure 3b).

Similarly, the ASX and GLX amino acid concentrations in the Mansinam Island sample (17SE-187) indicate limited protein degradation, with the highest values at 972.2 ± 4.3 pmol/mg and 608.6 ± 1.5 pmol/mg for THAA, respectively (Figure 4a). Overall, the sample from Mansinam Island yielded about 4429 ± 17.7 pmol/mg of measured THAA abundance. In contrast, two *Tubipora* sp. specimens from Bakaro Bay displayed significantly lower total amino acid abundance, approximately one-fourth of the sample from Mansinam Island. The ASX concentration in the Bakaro Bay samples ranged from 430 to 392 pmol/mg, while GLX contents were around 104 to 151 pmol/mg. For total amino acid abundance detected from the FAA pool, *Tubipora* sp. from Bakaro Bay yielded higher values (Figure 4b), particularly for ASX,
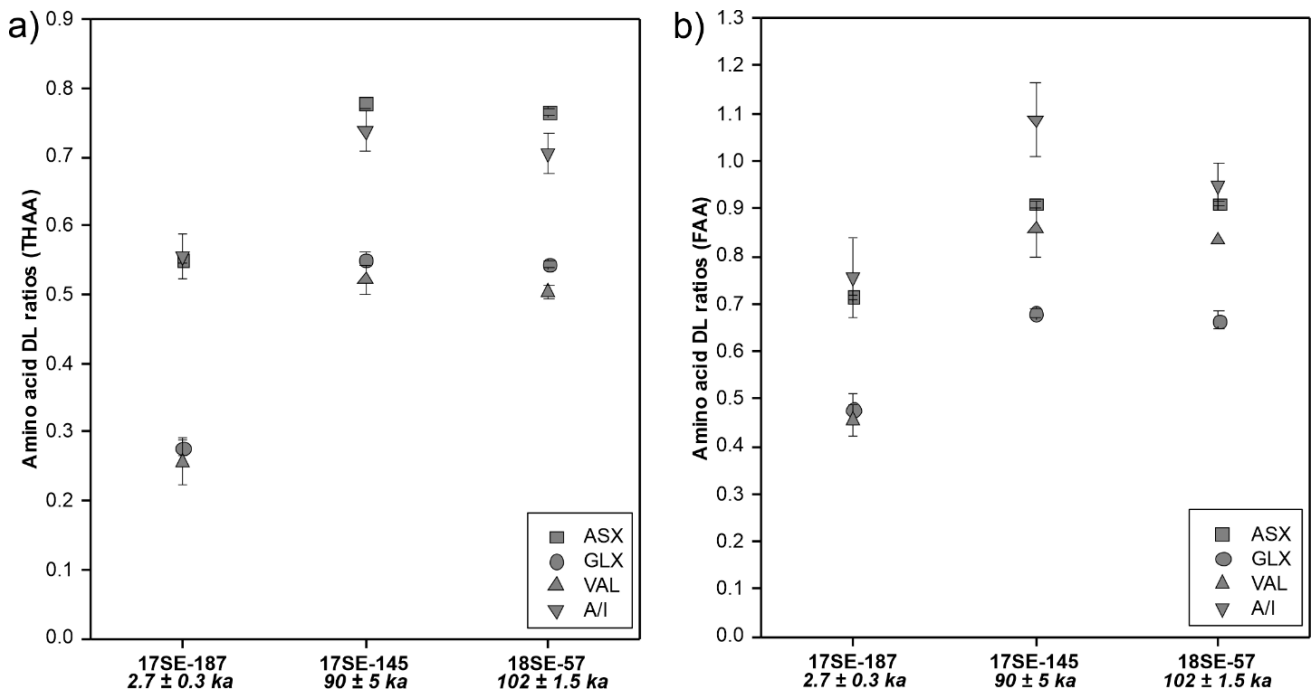
Figure 3. Amino acid DL ratios of three *Tubipora* sp. samples for a) THAA and b) FAA. Note that the MIS 1 sample from Mansinam Island (17SE-187) showed a substantially lower extent of amino acid racemization. Independent ages were reported by Saputra et al. (2022) from the U/Th series.
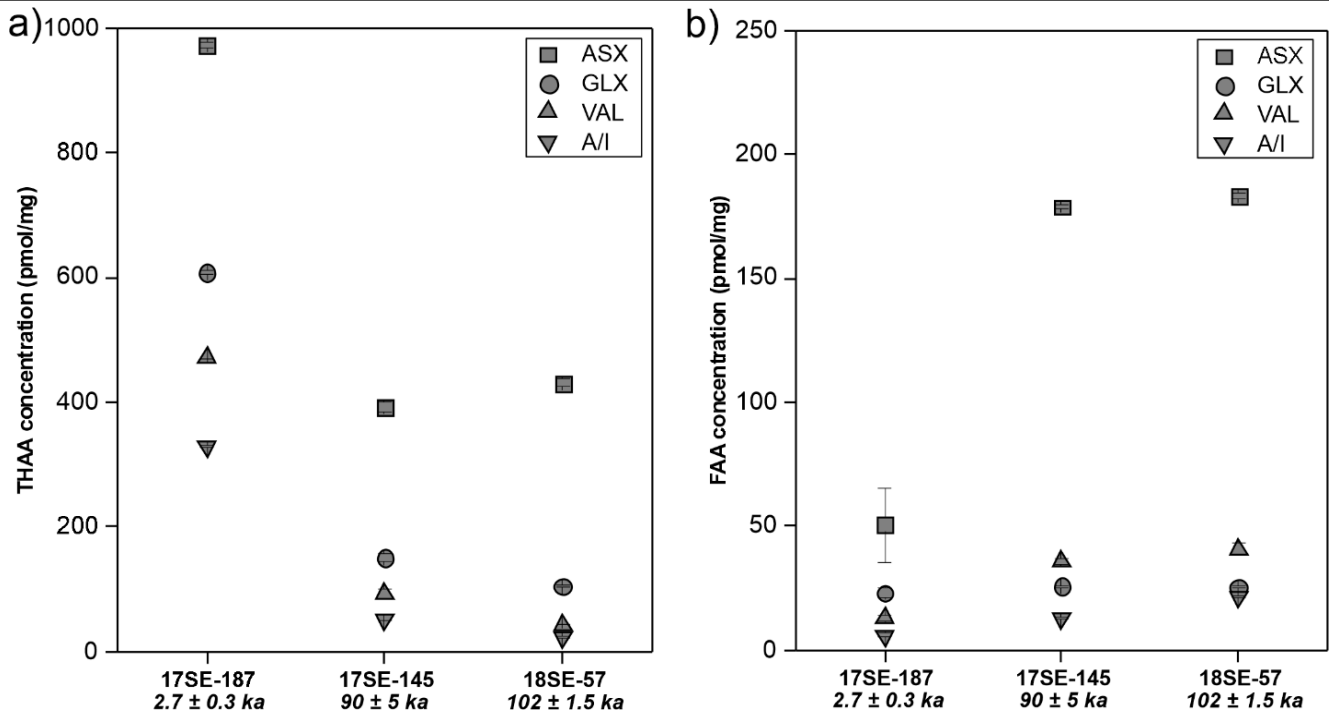
Figure 4. Selected amino acid concentration of three *Tubipora* sp. samples for a) THAA and b) FAA. Note that the MIS 1 specimen from Mansinam Island (17SE-187) yielded noticeably high amino acid contents for THAA. On the contrary, smaller amino acid concentrations are observed in the same sample for FAA, particularly ASX. Independent ages were reported by Saputra et al. (2022) from the U/Th series.

which ranged from 178 to 183 pmol/mg, compared to the sample from Mansinam Island (50.6 ± 14.9 pmol/mg). A slight decrease in amino acid abundance was also observed for both GLX and VAL in *Tubipora* sp. from Mansinam Island.

DISCUSSION

Three *Tubipora* sp. specimens analyzed in this paper show two distinct groups determined from AAR dating. A sample derived from Mansinam Island showed a typically low extent of racemization, suggesting a younger age. This supports the previous U/Th dating from *Porites* sp. within the same depositional unit, resulting in 2.7 ± 0.3 ka of age corresponding to the interval of Marine Isotope Stage (MIS) 1 sea-level highstand (Saputra et al. 2022). The extent of ASX racemization (DL ratio 0.552 ± 0.005), however, is relatively high for Holocene calcareous skeletons, most likely due to warm temperature within the region West Papua. AAR dating from the coral specimen of *Montastraea annularis*, dated 6.64 ka based on radiocarbon geochronology, also yielded a DL ratio of >0.5 at Glover Reef, Caribbean carbonate atoll with a mean annual temperature of 26 °C (Van Ee et al. 2012). Fossil coral *Favia* sp. from the Holocene marine terrace of New Guinea has also been dated using AAR with an extent of epimerisation (A/I) of 0.4 (Wehmiller et al. 1976). Here, the epimerisation extent of *Tubipora* sp. from Mansinam Island was recorded at 0.555 ± 0.033 for THAA (Figure 3a). Thus, despite the fact that different taxa affect the rate of racemization (Miller & Brigham-Grette 1989), the high racemization degree is generally found within coral assemblages from tropical climate regimes.

The amino acid DL ratios from two samples from Bakaro Bay are also consistent with older age representing MIS 5, especially sub-stages 5a and 5c, provided by U/Th dating studies by Saputra et al. (2022) with age 90 ± 5 ka (17SE-145) and 102 ± 1.5 ka (17SE-145). AAR results from both terraces showed a cluster of ASX and GLX DL ratios at >0.75

and >0.54, respectively. These are comparable to the Pleistocene-age corals (*Acropora* and *Montastraea*) dated in Glover Reef, showing >0.7 and >0.45 for ASX and GLX DL ratios, respectively (Van Ee et al. 2012).

AAR dating based on FAA shows two different clusters, as seen in the THAA analysis. The older cluster is represented by two samples from Bakaro Bay with ASX DL ratios close to the racemic point. However, AAR results based on the free amino acid pool are lacking from previous research, particularly in tandem with other independent ages. Despite different taxa, the specimens from Bakaro Bay also yielded A/I values around 1 for FAA, which is in good agreement with MIS 5a dated *Porites* sp. from New Guinea, yielding an extent of epimerization at 1.03 (Wehmiller et al. 1976).

The AAR dating conducted in this study could not separate sub-stages of MIS 5 as demonstrated by U/Th dating. Both samples show a relatively similar extent of ASX and GLX racemization, including the FAA analysis. Moreover, the ASX DL ratio for MIS 5a (0.779 ± 0.008) was recorded higher than MIS 5c (0.765 ± 0.005). This is also shown in GLX and VAL DL ratios where MIS 5c dated *Tubipora* sp. has lower values. These values are likely due to the lower resolution of AAR dating with an increasing extent of racemization. The inability of AAR dating of corals to discriminate sub-stages of MIS 5 in tropical climates has been shown in some sites. In Barbados, Wehmiller et al. (1976) noted the challenge of determining the age of MIS 5a (80 ka) and 5e (120 ka) due to the statistically similar GLX DL ratios.

In addition to the low precision of AAR dating, the warm temperature in tropical climate sites, such as the Middle Pleistocene and beyond, makes it difficult to assess older age. This is mainly due to the high sensitivity of racemization rates and diagenetic temperature history. The warmer temperature increases the racemization rate exponentially (Miller & Brigham-Grette 1989; Kaufman & Miller 1992). The exponential trend of racemization or epimerization rate has been shown from the collection of fossil mollusks of MIS 5e succession from temperate settings (e.g., southern Australia) towards tropical sites (e.g., Huon Peninsula, New Guinea) (Murray-Wallace 2000). For example, the extent of epimerization of the large mollusk *Tridacna maxima* was reported close to a racemic point beyond 125 ka (Hearty & Aharon 1988). In contrast, several 125 ka mollusks within a colder, temperate region of southern Australia yielded A/I around 0.4 (Murray-Wallace 2000).

CONCLUSION

The fossils of soft coral *Tubipora* sp. deposited in the uplifted marine terraces of the Manokwari area, West Papua, are considered a potential specimen for conducting amino acid geochronology. In this site, the aminozone or cluster associated with MIS 5 from a sample collected in Bakaro Bay can be confidently defined based on a greater extent of amino acid racemization than MIS 1-aged specimen from Mansinam Island. Significantly reduced total amino acid (THAA) concentrations are evident from those older *Tubipora* sp. samples, signifying the longer term of protein degradation. Moreover, the increasing abundance of total amino acid of FAA, ASX in particular, was observed within the MIS 5-aged specimens due to prolonged peptide breakdown that leads to enrichment of free amino acid pool. However, despite the warmer temperature in the West Papuan region, the resolution of AAR dating is deemed insufficient to discriminate sub-stages of MIS 5. In addition, the warm temperature of the West Papuan area substantially increases the racemization rates, particularly ASX and A/I, which likely reduce the

capability to date beyond the late Pleistocene age (>125 ka). Nonetheless, AAR dating may be complementary to establish along with an independent dating method (e.g., U/Th series or radiocarbon) to discriminate the Holocene from the late Pleistocene interglacial period due to rapid and cost-effective analysis.

AUTHORS CONTRIBUTION

R.H. made the research design, data analysis and original manuscript writing; S.E.A.S. did field data collection and manuscript writing; SH did the supervision and manuscript editing.

ACKNOWLEDGMENTS

CONFLICT OF INTEREST

The authors declare that there are no competing interests concerning the research or research funding.

REFERENCES

Ammar, M.S.A., 2005. An alarming threat to the red organ pipe coral Tubipora musica and suggested solutions. *Ecological Research*, 20(5), pp.529–535. doi: 10.1007/s11284-005-0064-7.

Badan Informasi Geospasial, 2018, 'DEMNAS: Seamless Digital Elevation Model dan Batimetri Nasional' in *DEMNAS*, viewed 15 January 2023, from https://tanahair.indonesia.go.id/demnas/#/

Bard, E., Hamelin, B. & Fairbanks, R.G., 1990. U-Th ages obtained by mass spectrometry in corals from Barbados: Sea level during the past 130,000 years. *Nature*, 346(6283), pp.456–458. doi: 10.1038/346456a0.

Bloom, A.L. et al., 1974. Quaternary sea level fluctuations on a tectonic coast: New 230Th234U dates from the Huon Peninsula, New Guinea. *Quaternary Research*, 4(2), pp.185–205. doi: 10.1016/0033-5894(74)90007-6.

Chen, C.Y. et al., 2020. U-Th dating of lake sediments: Lessons from the 700 ka sediment record of Lake Junín, Peru. *Quaternary Science Reviews*, 244, 106422. doi: 10.1016/j.quascirev.2020.106422

Chutcharavan, P.M. & Dutton, A., 2020. A global compilation of U-series dated fossil coral sea-level indicators for the Last Interglacial Period (MIS 5e). *Earth System Science Data*, 13(7), pp.3155-3178. doi: 10.5194/essd-2020-381.

Demarchi, B., 2020. *Amino acids and proteins in fossil biominerals: an Introduction for archaeologists and palaeontologists*, John Wiley & Sons.

Dodge, R.E. et al., 1983. Pleistocene sea levels from raised coral reefs of Haiti. *Science*, 219(4591), pp.1423–1425. doi: 10.1126/science.219.4591.1423.

Dumas, B., Hoang, C.T. & Raffy, J., 2006. Record of MIS 5 sea-level highstands based on U/Th dated coral terraces of Haiti. *Quaternary International*, 145–146, pp.106–118. doi: 10.1016/j.quaint.2005.07.010.

Gold, D. et al., 2014. The Biak Basin and its setting in the Bird's Head region of West Papua. *38th Annual Indonesian Petroleum Association Exhibition and Convention Proceedings*, pp.448-460.

Hearty, P.J. & Aharon, P., 1988. Amino acid chronostratigraphy of late Quaternary coral reefs: Huon Peninsula, New Guinea, and the Great Barrier Reef, Australia. *Geology*, 16(7), pp.579–583. doi: 10.1130/0091-7613(1988)016<0579:AACOLQ>2.3.CO;2.

Hibbert, F.D. et al., 2016. Coral indicators of past sea-level change: A global repository of U-series dated benchmarks. *Quaternary Science Reviews*, 145, pp.1–56. doi: 10.1016/j.quascirev.2016.04.019.

Hidayat, R. et al., 2024. Heating experiments on benthic foraminifera Ammonia sp. to assess the suitability of amino acid-based dating. *Indonesian Journal of Marine Sciences*, 29(3), pp.293-300. doi: 10.14710/ik.ijms.29.3.293-300.

Hidayat, R., Murray-Wallace, C.V. & Jacobs, Z., 2023. Late Pleistocene evolution of Robe Range, southern Australia–The timing and carbonate source dynamics of coastal dune development. *Marine Geology*, 456, 106987. doi: 10.1016/j.margeo.2022.106987.

Kaufman, D.S. & Manley, W.F., 1998. A new procedure for determining DL amino acid ratios in fossils using reverse phase liquid chromatography. *Quaternary Geochronology*, 17, pp.987–1000.

Kaufman, D.S. & Miller, G.H., 1992. Overview of amino acid geochronology. *Comparative Biochemistry and Physiology -- Part B*, 102(2), pp.199–204. doi: 10.1016/0305-0491(92)90110-D.

Manaa, A.A. et al., 2016. Dating Quaternary raised coral terraces along the Saudi Arabian Red Sea coast. *Marine Geology*, 374, pp.59–72. doi: 10.1016/j.margeo.2016.02.002.

Miller, G.H. & Brigham-Grette, J., 1989. Amino acid geochronology: Resolution and precision in carbonate fossils. *Quaternary International*, 1(C), pp.111–128. doi: 10.1016/1040-6182(89)90011-6.

Muhs, D.R. et al., 2012. Sea-level history during the Last Interglacial complex on San Nicolas Island, California: Implications for glacial isostatic adjustment processes, paleozoogeography and tectonics. *Quaternary Science Reviews*, 37, pp.1–25. doi: 10.1016/j.quascirev.2012.01.010.

Murray-Wallace, C.V., 2000. Quaternary coastal aminostratigraphy: Australian data in global. In *Perspectives in Amino Acid and Protein Geochemistry*. New York: Oxford University Press, pp.279–300.

Robinson, G.A. & Ratman, N., 1978. The stratigraphic and tectonic development of the Manokwari area, Irian Jaya. *Bureau of Mineral Resources Australia Journal*, 3, pp.19–24.

Saputra, S.E.A. et al., 2022. Late Quaternary neotectonics in the Bird's Head Peninsula (West Papua), Indonesia: Implications for plate motions in northwestern New Guinea, western Pacific. *Journal of Asian Earth Sciences*, 236, 105336. doi: 10.1016/j.jseaes.2022.105336.

Saputra, S.E.A., & Fergusson, C.L., 2023. Pacific-Gondwana Permo-Triassic Orogenic Belt with Lesser Overprinted Cenozoic Deformation, Eastern Bird Head Peninsula, West Papua, Indonesia. *Indonesian Journal on Geoscience*, 10(2), pp.119–138. doi: 10.17014/ijog.10.2.119-138

Schellmann, G. & Radtke, U., 2004. A revised morpho- and chronostratigraphy of the Late and Middle Pleistocene coral reef terraces on Southern Barbados (West Indies). *Earth-Science Reviews*, 64(3–4), pp.157–187. doi: 10.1016/S0012-8252(03)00043-6.

Simms, A.R., Rouby, H. & Lambeck, K., 2016. Marine terraces and rates of vertical tectonic motion: The importance of glacio-isostatic adjustment along the Pacific coast of central North America. *Bulletin of the Geological Society of America*, 128(1–2), pp.81–93. doi: 10.1130/B31299.1.

Tomiak, P.J. et al., 2016. The role of skeletal micro-architecture in diagenesis and dating of Acropora palmata. *Geochimica et Cosmochimica Acta*, 183, pp.153–175. doi: 10.1016/j.gca.2016.03.030.

Van Ee, N.J. et al., 2012. Evaluation of Amino Acid Racemization Variability in Quaternary Corals. *Proceedings of the 12th International Coral Reef Symposium.*

Wehmiller, J.F., 1993. Applications of organic geochemistry for Quaternary research: aminostratigraphy and aminochronology. In *Organic geochemistry: principles and applications, Topics in geobiology.* Springer Science and Business Media, pp.755–779.

Wehmiller, J.F., Hare, P.E. & Kujala, G.A., 1976. Amino acids in fossil corals: racemization (epimerization) reactions and their implications for diagenetic models and geochronological studies. *Geochimica et Cosmochimica Acta*, 40(7), pp.763–776. doi: 10.1016/0016-7037(76)90029-6.

Research Article

Biotransformation of *n*-butanol to Fruity-Like Bio-Flavour by Indonesian Lactic Acid Bacteria

Fitri Setiyoningrum[1]*, Deddy Triyono Nugroho Adi[2], Gunawan Priadi[1], Des Saputro Wibowo[1], Senlie Octaviana[1], Fifi Afiati[1], Rusli Fidriyanto[3], Doni Dwi Prasetyo[4], Abdul Rahman Siregar[4], Dharma Vincentlau[5]

1) Research Center for Applied Microbiology, National Research and Innovation Agency, Jl. Raya Bogor KM.46, Indonesia, 16911
2) Research Center for Biomass and Bioproduct, National Research and Innovation Agency, Jl. Raya Bogor KM.46, Indonesia, 16911
3) Research Center for Applied Zoology, National Research and Innovation Agency, Jl. Raya Bogor KM.46, Indonesia, 16911
4) Department of Tropical Biology, Faculty of Biology, Universitas Gadjah Mada, Yogyakarta, Indonesia, Jl. Teknika Selatan, Sekip Utara, Yogyakarta, 55281
5) Department of Chemistry, Faculty of Mathematics and Natural Sciences, Universitas Gadjah Mada, Sekip Utara, Bulaksumur, Yogyakarta, Indonesia 55281
* Corresponding author, email: fitr012@brin.go.id

ABSTRACT

Microbial production of aroma compounds is a promising alternative to extracting plants or chemical synthesis. In our research, the Indonesian lactic acid bacteria (LAB) have been utilised as producing fruity-like bio flavour by biotransformation approach using n-butanol as a precursor. The aims of our research are to identify LAB- secondary metabolites categorised fruity-like bio flavour and investigate the changes of glucose, mannitol, xylose, lactic acid and acetic acid in growth medium after fermentation. Our result research showed that n-butanol could be transformed to several fruity like bio flavour such as ethyl butyrate, butyl acetate, butyl formate, ethyl 2-methylbutanoate, ethyl 3-methylbutanoate, 2-heptanone, butyl propanoate, butyl propanoate, butyl 2-methylbutanoate, butyl isovalerate, butyl pentanoate, and butyl hexanoate. All of LABs consumed above 75% of glucose and only *Lactococcus lactis* KGB1 consumed all the mannitol on fermentation medium. In addition, *Lactococcus lactis* KGB1 produced the highest xylose, 11.87 g/L LABs produced. Based on the amount of fruity-like bio flavour compound generated, *Lactobacillus fermentum* WKS2, *Lactobacillus fermentum* KGL2, *Lactococcus lactis* KK4, *Lactobacillus fermentum* WKS3, *Lactococcus lactis* KGB1, and *Lactobacillus fermentum* KGL7 could be considered as agent fruity-like bio flavour by biotransformation approach.

INTRODUCTION

Flavour is an important component of food could improving organoleptic properties by giving satisfaction to consumers. Flavour ingredient is generally added to food in small amounts to impart a specific taste to a product or replace flavours lost during processing. In the food and beverage industry, flavours are needed to create new products, to introduce new products. and to change the taste of existing products. One type of flavour that is in demand in the food and beverage industry

is fruit flavour (Reshna et al. 2022). Worldwide demand of fruity flavor reaches a market valuation to US$ 1.23 billion by 2034 (Fact.MR 2024).

There are three kinds of flavour: synthetic, natural, and bio-flavour. Synthetic flavours can undergo lethal synthesis when introduced into the body's metabolic pathways because of toxic compounds which cause many complex chronic disorders. To reduce this risk, an alternative is the use of natural flavours (bio-flavor) obtained from natural sources such as animals, plants, and microorganisms. Plant-natural flavors have many disadvantages such as being expensive, weak, and not resistant to the rigors of food processing and storage. By biotechnology, bio-flavour could overcome the weakness of plant-natural flavour such as depends on seasonal and climatic, has low concentration, and improves ecological problem (Bicas et al. 2010). Bio-flavour utilises microbes that have many advantages such as resistance to temperature, gas, pH; and unstable gas during food processing. It is also beneficial for improving health (Roy & Kumar 2019).

Bio-flavor compounds can be produced in two ways, namely de novo synthetic pathways and biotransformation processes that involve the addition of precursors, as well as enzymes to help microbes convert a compound to other volatile compounds (Hosoglu et al. 2018). In our research, we used biotransformation methods to produce fruity-like flavour. Biotransformation is a method that has the ability to modify the structure of an organic compound with the help of microorganisms or the addition of enzymes. Some precursors require the presence of enzymes. For example, the precursor butanol and lipase enzyme with the aim of producing more specific bioflavor compound, namely butyl butyrate (Seo et al. 2017). The advantages of the biotransformation method compared to the de novo synthetic method are that it can produce bio-flavor compounds with certainty and it can produce more optimal bioflavor compounds (Shaaban et al. 2016).

LAB (lactic acid bacteria) can produce flavour compounds through biosynthetic pathways such as fermentation. During fermentation, carbohydrates, proteins, and fats are broken down by microbes to produce flavour compounds (Hosoglu et al. 2018). From research conducted by Nor et al. (2021). LAB of the genus *Lactobacillus* sp. is known to be able to produce bioflavor compounds of ester groups and their derivatives such as methyl esters with fragrance characteristics of fruits and flowers. *Lactiplantibacillus plantarum* is one of the LAB group bacteria known to be able to produce ester-derived compounds naturally in the form of butyric acid (Aiello et al. 2023). In our study, we employed LAB on producing fruity-like bio-flavour. The aims of this research are to analysed the volatile organic compounds (VOC) generated and the changes of sugar composition (glucose, mannitol, xylose) also organic acids (lactic acid and acetic acid) in fermentation medium. To triggers LAB in producing bioflavor compounds, *n*-butanol and lipase were added as a precursor and a as a catalyst for the esterification process.

MATERIALS AND METHODS
Materials
This research screened 18 LABs isolate, namely *Lactococcus lactis* KGP1, *Lactobacillus fermentum* KBP2, *Lactobacillus fermentum* IPEA, *Lactococcus lactis* KK4, *Lactobacillus fermentum* WKS3, *Lactococcus lactis* KGP2, *Lactococcus lactis* KGP3, *Lactobacillus fermentum* KGL7, *Lactococcus garvieae* SS3, *Lactobacillus kefiranofaciens* KK2, *Lactococcus garvieae* SS5, *Lactococcus lactis* KGB1, *Leuconostoc mesentroides* KGL2, *Lactococcus garvieae* SS4, *Lactobacillus fermentum* KGG3, *Lactobacillus kefiranofaciens* KK1, *Lactococcus lactis*

KGB3, *Lactobacillus fermentum* WKS2. All those isolates were private collection of our group research. The reagents used in this research were de Man Rogosa Broth (Merck, Germany). Bio-flavour synthesis- fermentation medium containing lipase (technical grade, as catalysing enzyme). *n*-butanol (Merck, Germany. as precursor), yeast extract (Himedia, India), glucose (Himidea, India), 0.5 g/L KH_2PO_4; 0.5 g/L K_2HPO_4; 2.2 g/L CH_3COONH_4; 0.2 g/L $MgSO_4.7H_2O$; 0.01 g/L $MnSO_4.H_2O$; 0.01 g/L $FeSO_4.7H_2O$; 0.01 g/L NaCl; 10 µg/L, biotin. All of those minerals are produced by Merck, Germany. Yeast and glucose solution were sterilised by autoclave at 121°C, 15 minutes and mineral solution was filtered by 0.45 µm membrane.

Methods

Fermentation process

The glycerol stock of LABs was cultured in de Man Rogosa Broth (MRSB) for 24 hours, 30°C, twice. The 10^8 colony forming unit (cfu)/ml -working culture was inoculated into medium fermentation and incubated at 30°C for 48 hours. After fermentation, all samples were harvested and centrifuged at 4°C, 10000 rpm, 10 minute. The supernatant was collected and stored at -20°C for further analysis.

Analysis of fermentation products

VOCs were obtained using headspace Gas Chromatography Mass Spectra (headspace-GC-MS) Shidmadzu QP 2020. 2 ml of the supernatants were placed in headspace vial and injected into GC-MS through headspace methods. The samples were equilibrated at 60°C for 20 minutes. 2000 µL of the sample's vapor was injected into GC-MS. The initial GC temperature was set at 40°C for 1 min with a ramp rate of 5 C/min to 70°C, increased at the rate of 10 C/min to 220°C, held for 1min. Samples were introduced into the split ratio 1:10 at 230°C at a pressure of 61.8 kPa with helium carrier gas. with a purge flow 2.3 mL/min. A RTx-5Sil-MS column (30-m length 0.25-mm i.d. 0.25-µm df) (Shimadzu) was used for all analyses. Purge time was set at 1 min. The MS transfer line was maintained at 250°C and ion source at 230°C. All samples were analysed using scan mode from 50 to 550 m/z.

Glucose, mannitol, lactic acid and acetic acid in the aqueous medium were quantified by a high-performance liquid chromatography (HPLC) (Shimadzu) system equipped with a refractive index detector (RID) using ICSep COREGEL-87H column (300 x 7.8 mm). The column was eluted with 5mM of H_2SO_4 at a flow rate of 0.6 mL/min at 30°C.

Statistical analysis

All results were expressed as a mean of two replicates. The changes in glucose, mannitol, lactic acid and acetic acid were analysed by descriptive analysis. Principle Component Analysis (PCA) was employed to investigate the sample groupings and correlations among volatile profiles of all isolates. The data was carried out using XLStat (Version 2019 v.2.2), and an add-in software package for Microsoft Excel (Addinsoft Corp., Paris, France).

RESULTS AND DISCUSSION

Principle Component Analysis (PCA) describes the relative location of volatile compounds in bio-flavour metabolites of LABs. The PCA biplot explained about 53.4% of the variability. Most of the variability 38.8%. was attributed to PC1, with PC2 (the vertical axis) accounting for just 14.6% of the total variability (Figure 1). Bio-flavour metabolites of KK1

and WKS2 were quite different compared with other isolates. The highest factor loading metabolite of PC1 was butyl methyl propanoate processed by WKS2. Meanwhile, ethyl 3-methyl butanoate was the highest in PC 2 generated by WKS3. These flavours have apple, pineapple and sour aroma. Figure 1 also explained that biosynthesis of ethyl 2-methyl butanoate had a negative correlation with butyl methanoate. It meant that the number of ethyl 2-methyl butanoate's biosynthesis was opposite with butyl methanoate. Butyl butyrate and butyl acetate as the main VCOs were present in KK4 and WKS2.
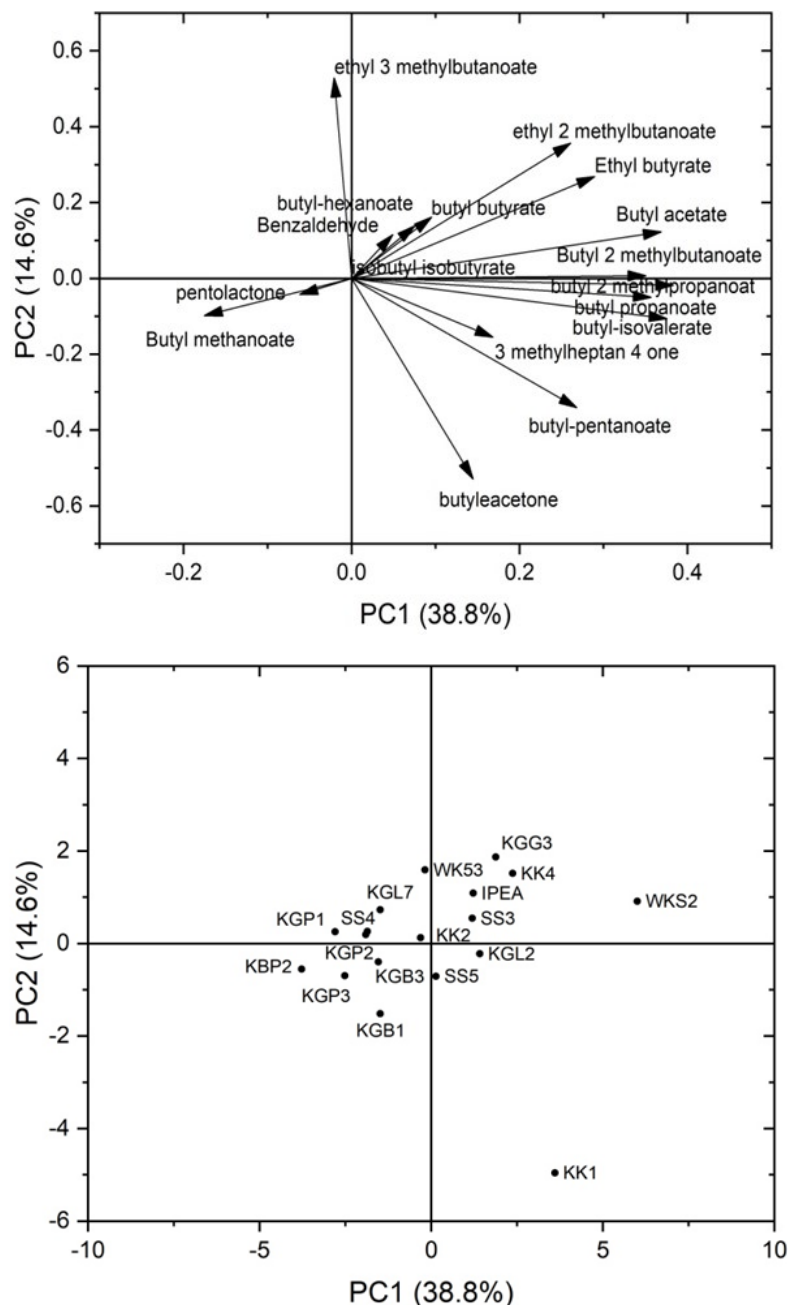
Figure 1. Principle component analysis biplot VCOs detected in LABs through *n*-butanol biotransformation.

Lactic Acid bacteria (LAB) naturally have been known to have the ability to synthesise some organic flavours such as ester and ketone that have been used in food production. Several studies showed that LAB can produce certain flavor compounds such as butyric acid (Gupta 2015), vanillin (Kaur et al. 2013), and diacetyl (Leroy & De Vuyst 2004). The bio-flavour produced by LABs was shown in Table 1. Among 17 compounds analysed, butyl acetate (BA) and butyl butyrate (BB) formation

were mostly produced among the isolates. The pathway was through alcohol acyltransferase (AAT). Both two compounds were derived from butanol; a precursor that was supplemented in the media. Butyryl-CoA was metabolically synthesised from glucose and mannitol (building block) and conducted a condensation reaction with butanol to form BB by AAT (Guo et al. 2023). The addition of other sugar like mannitol was to increase the amount of fructose-6-P in order to produce more pyruvate.

Analogous to BB, the synthesis of BA was also through AAT (Figure 2). Instead of butyryl-CoA, the acetyl-CoA was synthesised to form BA. Compared to butyryl-CoA synthesis, acetyl-CoA formation was simpler since it was less carbon and formed after the pyruvate step (Ku et al. 2022). In the same isolate, the amount of BA tended to be higher than BB. That might be caused by the pathway to form BA was shorter than the BB.
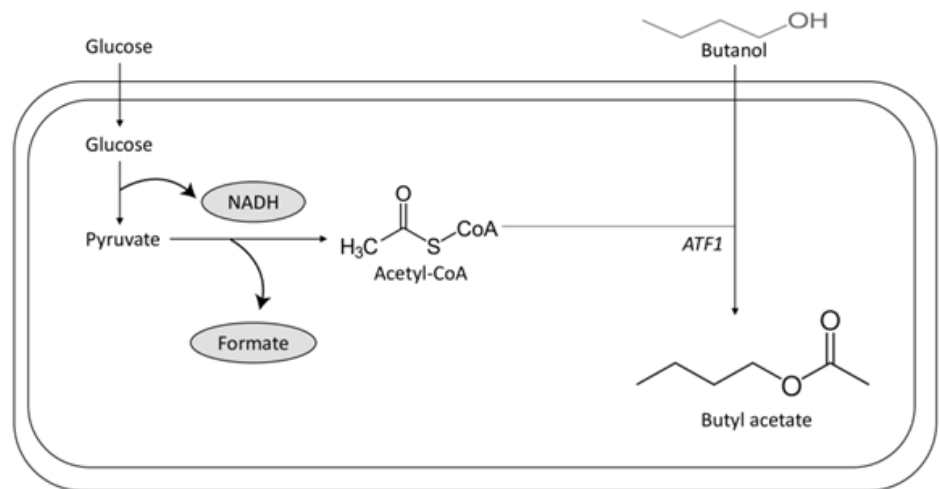
Figure 2. Butyl acetate pathway from glucose with butanol supplementation.

The three bacteria that produced the highest BA were *Lactobacillus fermentum* WKS2, KGL2, and *Lactococcus lactis* KK4 produce the highest BA with 79.30, 73.69 and 71.70% from the total bio-flavour produced respectively. On the other hand, the other bacteria that produced the highest BB were *Lactobacillus fermentum lactis* KGB1 and *Lactobacillus fermentum* KGL7 with 54.17, 52.17 and 50.41% from the total bio-flavour produced respectively (Table 1) Based on the sugar consumption,almost of isolate consumed 100% glucose in the fermentation media (compare against the media without fermentation) except for *Leuconostoc mesenteroides* KGL2 which only consume 75% of the glucose presence (Figure 3). These means that glucose was a carbon source that used to synthesise metabolites and energy carrier. Even though glucose in media had been consumed by all of isolates, the differences of concentration BB formation probably due to the differences in AAT activity in each isolate. ATT plays a role in condensation between butyryl-CoA and *n*-butanol (Noh et al. 2019).

In terms on mannitol consumption,only *Lactococcus lactis* KGB1 that consumed all the mannitol presence in the fermentation media, the second and the third highest were KGP2 and WKS3 with 60% mannitol consumption (Figure 3). Though many exception, mannitol is commonly fermented by LABs and produce lactate following path : mannitol à mannitol-1- P à fructose-6-P à 2 pyruvate à2 lactate (Liu 2003). Not many LABs have been reported be able to metabolise mannitol. *Lactobacillus plantarum* and *Lactobacillus casei* were reported can ferment mannitol to lactate and other metabolites, depends on the presences of oxygen (Liu

2003). The relatively high BB produced by *Lactococcus lactis* KGB1 might because it maximised the sugar consumption so that the amount of Acetyl Co-A was higher than other bacteria. Mannitol consumption was less than glucose because glucose prevents the use of other carbon sources. Furthermore,many bacteria prefer glucose as their carbon source including LAB. Mannitol was more reduced than glucose, thus it can form more NADHs (3 mol) than glucose (2 mol) (Fu et al. 2020). Glucose fermentation was not only synthesising the flavouring compound, but also producing another compound such as lactic acid, acetic acid, and xylose. These compounds were formed by different metabolism. Lactic acid, acetic acid, and xylose are produced via hetero-lactic metabolism (PK-pathway) and homo-lactic acid metabolism (PP-glycolytic pathway) (Abedi & Hashemi 2020).
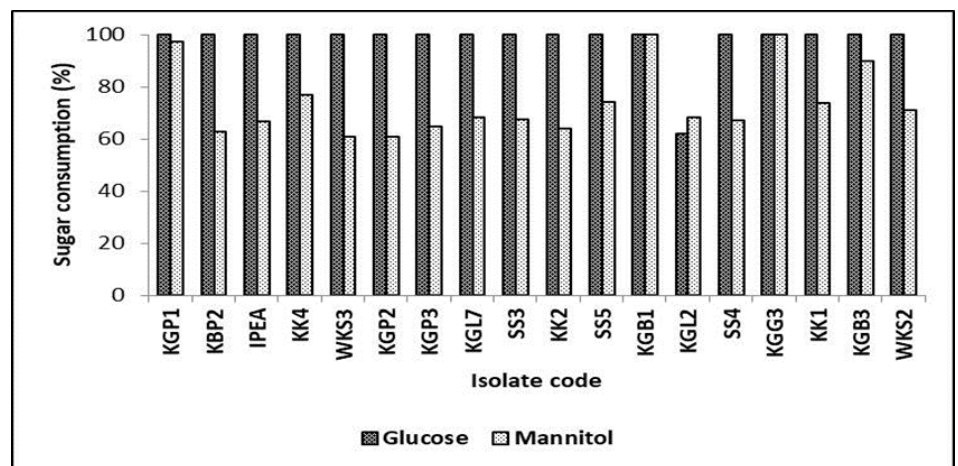
Figure 3. Glucose and mannitol consumption of LABs

Over 90% of lactic acid was produced through microbial fermentation (Rodrigues et al. 2015). Lactic acid can be produced both via PK-pathway and PP-glycolytic pathway. In both paths, the glucose was converted into glucose 6-P. Glucose 6-P was then converted into 6-Phospho-Gluconate in PK-pathway, while in PP-glycolytic pathway, it was converted into fructose 6-P. In the end, both of the substituent were converted into pyruvate and then they were formed lactic acid by oxidising the NADH into NAD⁺.

Lactobacillus kefiranofaciens KK1, *Lactobacillus fermentum* WKS2, and *Lactobacillus fermentum* KGL2 produced the highest lactic acid which were 16.34, 13.37. and 12.88 g/L respectively (Figure 4). Abedi et al. (2020) has reviewed some LAB producing lactic acid. It showed that *Lactococcus lactis* with glucose as a carbon source can produce lactic acid between 0.3 g/L to 39 g/L. In addition, *Lactobacillus fermentum* produced lactic acid between 5.19 to 31.11 g/L.

Acetic acid was only produced via PK-pathway. Acetic acid was produced after acetyl-P was formed. It can be from xylulose 5-P or from acetyl-CoA by phosphate transferase. Acetic acid was considered as a side product in lactic acid production. To some extent it was undesired product and also potentially inhibit the bacteria environment since the pH level would getting lower.

In the end of the fermentation, xylose was also produced as an intermediate sugar. It was begun to form when xylulose-5-P was formed. Xylose was equilibrium with xylulose-5-P and xylulose. Xylulose was formed by removing the phosphate group and bonding with ADP to form ATP. After that, the xylose was formed by the assist of xylose reductase and xylitol dehydrogenase (Abedi & Hashemi 2020). Figure 5 showed

Table 1. Fruity bio-flavour produced by LABs.

RT	Compound	Flavour description	KGP1	KBP2	IPEA	KK4	WKS3	KGP2	KGP3	KGL7	SS3	KK2	SS5	KGB1	KGL2	SS4	KGG3	KK1	KGB3	WKS2
											% area[BC]									
4.629	Ethyl butyrate	Apple. Pineapple. strawberry	nd	nd	3.10	2.57	nd	nd	nd	nd	nd	nd	nd	nd	nd	nd	2.92	nd	nd	3.41
4.900	Butyl acetate	Apple. banana	58.13	nd	69.99	71.7	27.79	61.31	nd	nd	70.28	63.41	64.77	nd	73.69	nd	68.86	63.38	46.35	79.3
4.913	Butyl formate	Fruity	nd	44.32	nd	Nd	nd	nd	42.39	nd	nd	nd	nd	nd	nd	nd	nd	nd	nd	nd
5.730	Ethyl 2-methylbutanoate	Apple. strawberry	nd	nd	0.22	0.29	0.79	nd	nd	1.85	0.33	0.7	0.65	nd	0.31	2.07	0.64	nd	nd	0.52
5.835	Ethyl 3-methylbutanoate	Apple. pineapple. sour	2.22	1.56	0.66	0.84	1.14	1.71	1.67	3.32	0.76	0.57	0.69	nd	0.29	3.54	0.89	0.24	1.58	0.24
6.760	Heptan-2-one	Nutty. Spices	nd	nd	nd	Nd	nd	nd	nd	nd	nd	nd	nd	nd	nd	nd	nd	0.18	nd	nd
7.240	Butyl propanoate	Strawberry	9.9	8.26	4.57	4.23	5.84	5.83	8.63	16.53	5.03	5.96	5.54	17.67	4.68	14.31	4.71	6.16	7.96	2.68
7.692	Butyl propyl ketone		nd	nd	0.19	0.16	nd	0.4	0.61	nd	0.17	nd	0.24	1.04	0.13	0.86	0.11	0.19	0.49	0.11
8.350	Butyl isobutyrate	Fruity	11.95	11.52	5.84	5.19	7.16	7.7	10.66	19.67	6.11	7.87	6.91	19.51	4.94	19.01	5.40	7.31	10.32	3.72
8.632	Benzaldehyde	Almond	nd	nd	0.12	Nd	nd	nd	nd	nd	nd	nd	nd	nd	nd	nd	nd	nd	nd	nd
9.333	Butyl butyrate	Apple. banana. pineapple	14.5	29.53	13.02	12.86	54.17	19.81	31.44	50.41	14.86	17.59	17.11	52.17	13.63	50.25	13.93	18.97	28.3	7.72
9.717	DL-pentolactone		nd	nd	nd	Nd	nd	nd	nd	nd	nd	nd	nd	nd	nd	nd	nd	nd	0.16	nd
10.30	Butyl 2-methylbutanoate	Fruity	nd	1.65	0.77	0.71	1.12	1.18	1.63	2.82	0.9	1.21	1.13	2.84	0.74	3.18	0.79	0.99	1.57	0.61
10.41	Butyl isovalerate	Fruity	3.3	3.17	1.52	1.39	1.99	2.05	2.97	5.4	1.55	2.68	2.81	6.76	1.58	6.78	1.75	2.64	3.27	1.71
11.32	Butyl pentanoate	Fruity	nd	nd	nd	0.07	nd	nd	nd	nd	nd	nd	0.15	nd	nd	nd	nd	0.17	nd	0.05
12.44	Butyl hexanoate	Fruity	nd	nd	nd	0.07	nd	nd	nd	nd	nd	nd	nd	nd	nd	nd	nd	nd	nd	nd

[A] Isolate code: *Lactococcus lactis* KGP1, *Lactobacillus fermentum* KBP2, *Lactobacillus fermentum* IPEA, *Lactococcus lactis* KK4, *Lactobacillus fermentum* WKS3, *Lactococcus lactis* KGP2, *Lactococcus lactis* KGP3, *Lactobacillus fermentum* KGL7, *Lactococcus garvieae* SS3, *Lactobacillus kefiranofaciens* KK2, *Lactococcus garvieae* SS5, *Lactococcus lactis* KGB1, *Leuconostoc mesentroides* KGL2, *Lactococcus garvieae* SS4, *Lactobacillus fermentum* KGG3, *Lactobacillus kefiranofaciens* KK1, *Lactococcus lactis* KGB3, *Lactobacillus fermentum* WKS2

[B] nd = not detected

[C] mean of two replicates

that all bacteria produced xylose less than 2 g/L except for *Lactococcus lactis* KGB1 which surprisingly produced 11.87 g/L of xylose. Xylose has fewer calories than table sugar so that it is used as a diabetic sweetener in food and beverage (Galvan et al. 2022).
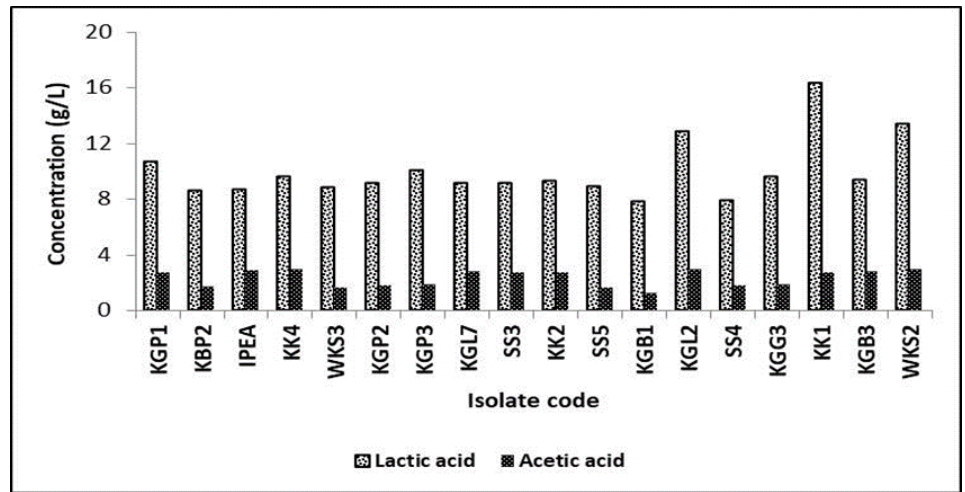
Figure 4. Lactic acid and acetic acid production of LABs.
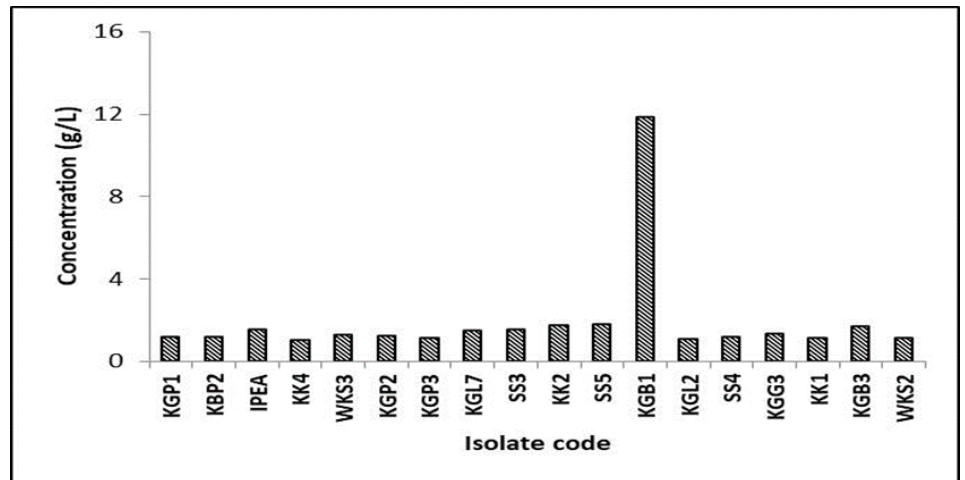
Figure 5. Xylose production from LAB.

CONCLUSIONS
All employed LABs generated fruity-like bio-flavour such as butyl acetate (BA), butyl butyrate (BB), ethyl 3-methylbutanoate, butyl propanoate, butyl 2-methylpropanoat and butyl isovalerate. The most VOCs resulted through *n*-butanol transformation were butyl acetate and butyl butyrate which have apple, banana, and pineapple aroma. The highest BA was produced by *Lactobacillus fermentum* WKS2, meanwhile the highest BB was *Lactobacillus fermentum* WKS3. Almost all LABs consumed 100% glucose in the fermentation media except *Leuconostoc mesenteroides* KGL2. There was only *Lactococcus lactis* KGB1 which consumed all mannitol presence in the media and produced above 10 g/L of xylose in media fermentation. In terms of organic acid, *Lactobacillus kefiranofaciens* KK1 produced the highest lactic acid and acetic among others.

AUTHOR CONTRIBUTION
F.S designed the research and supervised all the process; DTNA, GP, DSW, DDP, FA contributed on collecting data; SO, RF, ARS, DV analysed the data. All authors contributed on writing the manuscript.

CONFLICT OF INTEREST
There is not any conflict of interest regarding the research or the research funding.

REFERENCES

Abedi, E. & Hashemi, S.M.B., 2020. Lactic acid production – producing microorganisms and substrates sources-state of art. *Heliyon*, 6(10), e04974. doi: 10.1016/j.heliyon.2020.e04974.

Aiello, A. et al., 2023. Production of butyric acid by different strains of Lactobacillus plantarum (Lactiplantibacillus plantarum). *International Dairy Journal*, 140, 105589. doi: 10.1016/j.idairyj.2023.105589.

Bicas, J.L. et al., 2010. Biotechological production of bioflavor and functional sugars. *Food Science and Technology*, 30(1), pp.7–18. doi: 10.1590/S0101-20612010000100002.

Fact.MR, 2024, 'Food Flavor Market Outlook (2024-2034)' in *Fact.MR*, viewed from https://www.factmr.com/report/fruit-flavor-market

Fu, H. et al., 2020. High-selectivity butyric acid production from *Saccharina japonica* Hydrolysate by *Clostridium tyrobutyricum*. *Ind. Eng. Chem. Res.*, 59(39), pp.17147-17155. doi: 10.1021/acs.iecr.0c01279.

Galvan, S. et al., 2022. Regulation of transgene expression by the natural sweetener xylose. *Advanced Science*, 9(34), pp.1–10. doi: 10.1002/advs.202203193.

Guo, X. et al., 2023. De novo biosynthesis of butyl butyrate in engineered Clostridium tyrobutyricum. *Metabolic Engineering*, 77(2023), pp.64–75. doi: 10.1016/j.ymben.2023.03.009.

Gupta, C., 2015. A Biotechnological approach to microbial based perfumes and flavours. *Journal of Microbiology & Experimentation*, 2(1), pp.11–18. doi: 10.15406/jmen.2015.02.00034.

Hosoglu, M.I., Guneser, O. & Yuceer, Y.K., 2018. Different bioengineering approaches on production of bioflavor compounds. In *Handbook of Food Bioengineering: Role of Materials Science in Food Bioengineering*. Academic Press. doi: 10.1016/B978-0-12-811448-3.00002-4.

Kaur, B., Chakraborty, D. & Kumar, B., 2013. Phenolic biotransformations during conversion of ferulic acid to vanillin by lactic acid bacteria. *BioMed Research International*, 2013, pp.590359. doi: 10.1155/2013/590359.

Ku, J.T., Chen, A.Y. & Lan, E.I., 2022. Metabolic engineering of Escherichia coli for efficient biosynthesis of butyl acetate. *Microbial Cell Factories*, 21, 28. doi: 10.1186/s12934-022-01755-y.

Leroy, F. & De Vuyst, L., 2004. Lactic acid bacteria as functional starter cultures for the food fermentation industry. *Trends in Food Science and Technology*, 15(2), pp.67–78. doi: 10.1016/j.tifs.2003.09.004.

Liu, S.Q., 2003. Practical implications of lactate and pyruvate metabolism by lactic acid bacteria in food and beverage fermentations. *International Journal of Food Microbiology*, 83(2), pp.115–131. doi: 10.1016/S0168-1605(02)00366-5.

Noh, H.J., Lee, S.Y. & Jang, Y.S., 2019. Microbial production of butyl butyrate, a flavor and fragrance compound. *Applied Microbiology and Biotechnology*, 103(5), pp.2079–2086. doi: 10.1007/s00253-018-09603-z.

Nor, S.M., Yusof, N.N.M. & Ding, P., 2021. Volatile organic compound modification by lactic acid bacteria in fermented chilli mash using GC-MS headspace extraction. *IOP Conference Series: Earth and Environmental Science*, 765, 012043. doi: 10.1088/1755-1315/765/1/012043.

Reshna, K.R., Gopi, S. & Balakrishnan, P., 2022. Introduction to flavor and fragrance in food processing. In *Flavors and Fragrances in Food Processing: Preparation and Characterization Methods. ACS Symposium Series*, 1433, pp.1-19. doi: 10.1021/bk-2022-1433.ch001.

Rodrigues, A.K.O., Maia, D.L.H. & Fernandes, F.A.N., 2015. Production of lactic acid from glycerol by applying an alkaline hydrothermal process using homogeneous catalysts and high glycerol concentration. *Brazilian Journal of Chemical Engineering*, 32(3), pp.749–755. doi: 10.1590/0104-6632.20150323s00003356.

Roy, P. & Kumar, V., 2019. Production of bioflavour from microbial sources and its health benefits. *Indian Journal of Biochemistry and Biophysics*, 56(5), pp.352–357.

Seo, S.O. et al., 2017. Characterization of a Clostridium beijerinckii spo0A mutant and its application for butyl butyrate production. *Biotechnology and Bioengineering*, 114(1), pp.106–112. doi: 10.1002/bit.26057.

Shaaban, H.A. et al., 2016. Application of biotechnology to the production of natural flavor and fragrance chemicals. *Research Journal of Pharmaceutical, Biological and Chemical Sciences*, 7(6), pp.2670–2717. doi: 10.1021/bk-2005-0908.ch004.

Research Article

Planktonic Foraminifera Biostratigraphy of the Pliocene Kintom and Bongka Formations, Central Sulawesi, Indonesia

Moch. Indra Novian[1], Didit Hadi Barianto[1], Salahuddin Husein[1], Sugeng Sapto Surjono[1]*, Akmaluddin[1]

1)Geological Engineering Department, Universitas Gadjah Mada, Jl. Grafika Bulaksumur No.2, Senolowo, Sinduadi, Kec. Mlati, Kabupaten Sleman, Daerah Istimewa Yogyakarta, 55284
* Corresponding author, email: sugengssurjono@ugm.ac.id

ABSTRACT

The Pliocene sediments exposed in the Eastern Arm of Southern Sulawesi consist of Kintom and Bongka Formations, thought to be the result of collisions in the Middle Miocene. The research area is located along the Matindok – Ondoondolu road, Banggai Regency, Central Sulawesi Province. The aims of the research is to determine the rock units that developed in the Kintom and Bongka Formations and determine the chronological time frame based on planktonic foraminifera biostratigraphy. This research used stratigraphic measurement on a scale of 1:100 and Plio-Pleistocene planktonic foraminifera biostratigraphy. A lithological column along 315 meters divided into three rock units. The marl unit and calcareous sandstone unit show characteristics similar to flysch deposits from the collision and are part of the Kintom Formation. Intergrade conglomerate gravelly sandstone deposited unconformably on top of the previous unit is part of the Bongka Formation. This last unit shows characteristics similar to molasse deposits. In total of 46 rock samples were analyzed for foraminifera biostratigraphy. Seven foraminifera biozones showing the age of rock deposition from the Early Pliocene to the Late Pleistocene. The order of the foraminifera biozone is *Globorotalia tumida* Brady LOZ (PL1a; 5.59 - 4.45 Ma), *Globoturborotalita nepenthes* Todd CRZ (PL1b; 4.45 - 4.39 Ma), *Globotalia acostaensis* Blow PRZ (PL2a; 4.39 – 4.31 Ma), *Globotalia margaritae* Bolli HOZ (PL2b; 4.31 - 3.85 Ma), *Sphaeroidinellopsis seminulina* Schwager HOZ (PL 3-4; 3.85 – 3.20 Ma), *Globorotalia* (M) *miocenica* Palmer/ *Globorotalia miocenica* Palmer HOZ (PL5–6; 3.20 – 2.30 Ma), and *Pulleniatina praecursor* Banner & Blow HOZ (PL6–PT1a; 2.30 – 2.26 Ma).

INTRODUCTION

The collision between the Eastern Arm of Sulawesi and the Banggai Sula microcontinent led to the formation of post-orogenic clastic sediments included in the Kintom and Bongka Formations. Both formations are widely exposed in the southern part and, to a lesser extent, in the northwest of the eastern arm of Sulawesi. This collision event is estimated to have occurred during the Middle Miocene (Simandjuntak 1986), while the post-orogenic sediments are interpreted to have formed during the Middle Miocene or later.

The Kintom and Bongka Formations in the eastern section of the

study area display a slightly distinct rock configuration compared to those found in the western region. In the west, the Kintom Formation consists of fine-grained rocks such as sandy marl and sandstone, while in the east, it consists of conglomerate, sandstone, and limestone. The Bongka Formation, both in the western and eastern parts, consists of relatively similar rocks in the form of conglomerate, sandstone, marl, siltstone, and lignite. According to Simandjuntak (1986), Rusmana et al. (1993) and Surono et al. (1993), these two formations were deposited during the Late Miocene to Middle Pliocene. Recent research on post-orogenic sediments in Sulawesi (Nugraha et al. 2022) suggests that the Kintom Formation formed during the Early Pliocene and is unconformably overlained by the Bongka Formation, which ranges in age from the Late Pliocene to the Pleistocene.

The Matindok section is located along the Matindok – Ondo Ondolu road, Batui District, Banggai Regency, Central Sulawesi Province, displays rock layers known as the Kintom and Bongka Formations, according to the Regional Geological Map of the Batui Sheet (Surono et al. 1993). The Kintom Formation is present in the northwest part of the Matindok section, while the Bongka Formation is found in the southeast. Based on the dip of the rocks sloping towards the southeast, it is assumed that the Kintom Formation is younger than the Bongka Formation. The type and sequence of sedimentary rocks in the Matindok section slightly differed from other Kintom and Bongka Formation outcrops in various areas.

The differences in the rocks that make up the Kintom and Bongka Formations as well as the age of deposition of the rocks as well as the existence of the Matindok Section, which reveals the Kintom-Bongka Formation rocks well-encouraged researchers to carry out this research. This research has two objectives; the first is to determine the rock units that developed in the Kintom and Bongka Formations, and the second is to build a chronological time frame for the rock units that make up the Kintom and Bongka Formations through biostratigraphy of planktonic foraminifera. The location of the Matindok Section is illustrated in Figure 1.
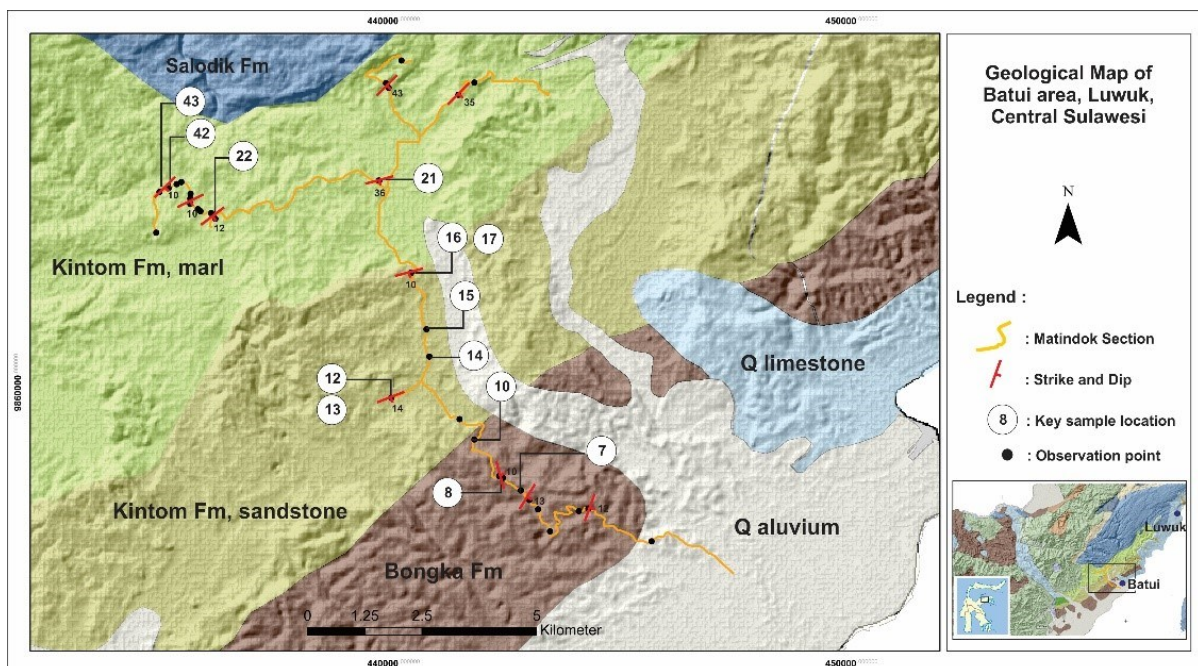
Figure 1. Geological Map of the research location (Surono et al. 1993) located in the southwest of the Eastern Arm of Sulawesi. The orange lines indicate the sections for collecting stratigraphic data, and the black dots indicate the observation locations with several sample numbers that are key to this study's division of foraminifera biozones.

Sedimentary rocks in the East Arm of Sulawesi are mostly distributed on the southern side, with a range of rock ages from the Mesozoic to the Quaternary. A small number of sedimentary rocks can be found in the western part (Martosuwito 2012). The outcrop of Pliocene sedimentary rocks at the surface forms the Kintom, Bongka, and Lonsio Formations (Rusmana et al. 1993; Surono et al. 1993). Rocks from the Bongka and Kintom Formations are considered as the result of the collision between the Eastern Arm of Sulawesi and the Banggai Sula Microcontinent, which has been occurring since the Middle Miocene (Simandjuntak 1986), with sedimentary material originating from the collision complex. This differs from the Lonsio Formation, which has sediment origins from volcanic highs. The Kintom and Bongka Formations are distributed in the southern and western parts of the Eastern Arm of Sulawesi, while the Lonsio Formation is spread in the northern part of Balantak Head and the Togian Islands.

GEOLOGICAL SETTING

The research is located within the Banggai Basin, a vessel-like, narrow in the north and widening towards the south. The research area in the north is bordered by Paleogene-Neogene limestone folded hills. To the south, the research area is bordered by the alluvial-coastal plain.

The northwestward movement of the Banggai Sula microcontinent in the early Miocene pushed it closer to the Asian plate, including the Sulawesi Island Arc, leading to a collision between continental plates (Garrard et al. 1988). Following the collision, rocks originating from the Bangai Sula and Sulawesi microcontinents undergo obduction towards the east, resulting in the forming of molasses deposits (Figure 2).
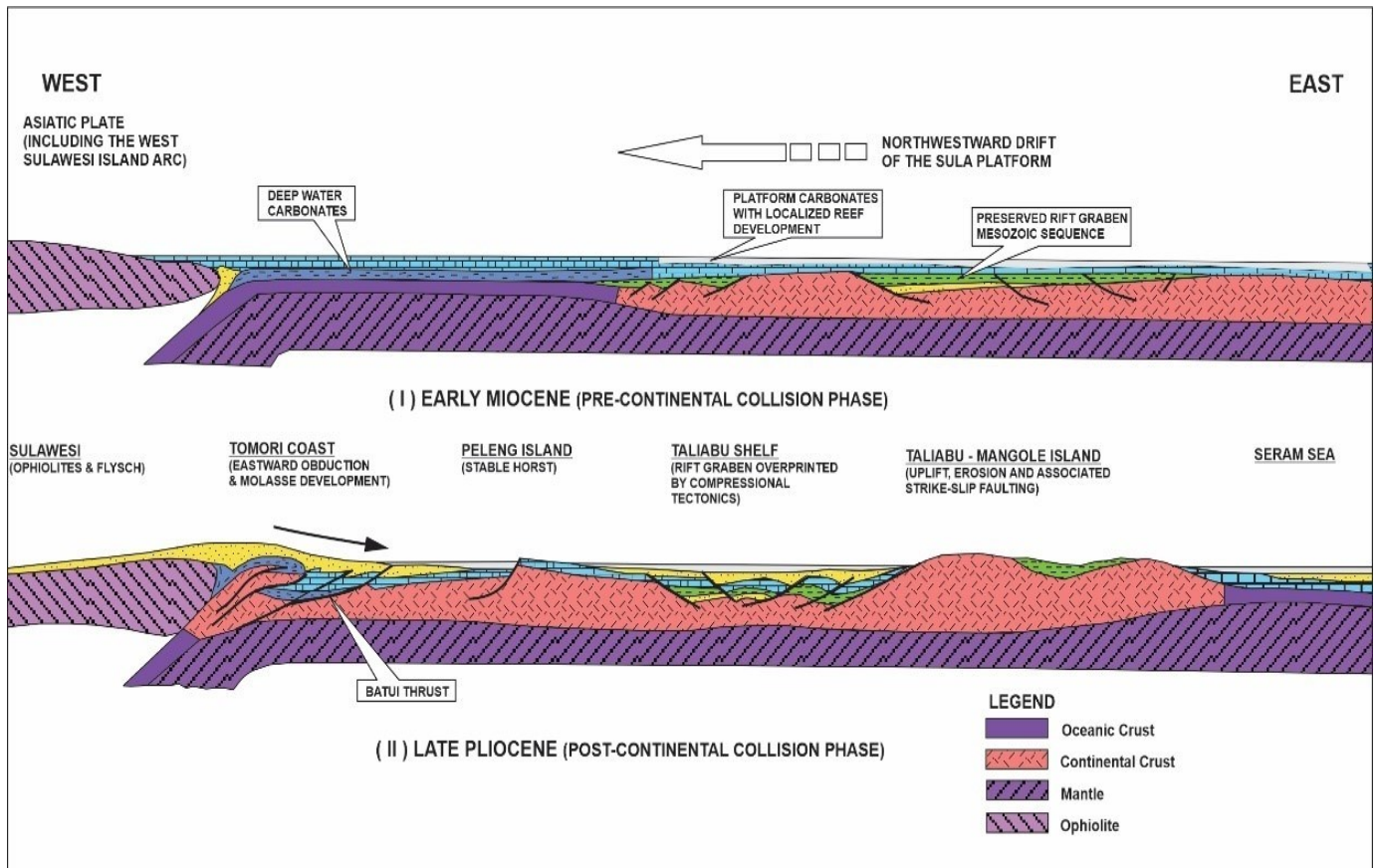
Figure 2. The movement of the Banggai Sula microcontinent towards the Asian plate (including the Sulawesi Island Arc) during the Early Miocene caused rocks formed initially on both plates to undergo eastward obduction, becoming the source material for the formation of flysch and molasse during the Late Pliocene (Garrard et al. 1988).

The rocks formed after the movement of the Banggai Sula microcontinent from the Early Miocene to the Holocene are divided into several formations, as seen in Figure 3 :

a. Bancuh Kolokolo

The "Bancuh Kolokolo" consists of of Mesozoic rock fragments; chert, schist, peridotite, gabbro, serpentinite, limestone, marl, and siltstone within a scaly clay and marl matrix. The age of the Bancuh Kolokolo, based on fossil content in limestone and marl fragments, is Oligocene to Miocene. The foraminifera fossil assemblage includes *Amphistegina* sp., *Orbulina universa* D'Orbigny, *Globigerina* sp., *Globigerinoides* sp., *Globorotalia menardii* D'Orbigny, *Globorotalia* sp., *Lepidocyclina* sp., and *Sphaeroidinellopsis subdehiscens* (Blow).

However, is based on the fossil content of planktonic foraminifera in the scaly mud and marl matrix, indicating the formation age from the Middle Miocene to Pliocene (Figure 3). The planktonic foraminifera fossils in this matrix includes *Globigerina venezuelana* Hedberg, *Globigerinoides immaturus* Broniman, *Globigerinoides obliquus* Bolli, *Globigerinoides sacculifer* Brady, *Globigerinoides trilobus* Reuss, *Globoquadrina altispira* Cushman & Jarvis, *Globorotalia cultrata*, *Globorotalia menardii* D'Orbigny, *Globorotalia scitula* Brady, *Globorotalia tumida*, *Orbulina universa* D'Orbigny, *Orbulina* sp., *Sphaeroidinella subdehiscens* Blow, and *Sphaeroidinellopsis seminulina* Schwager (Surono et al. 1993).
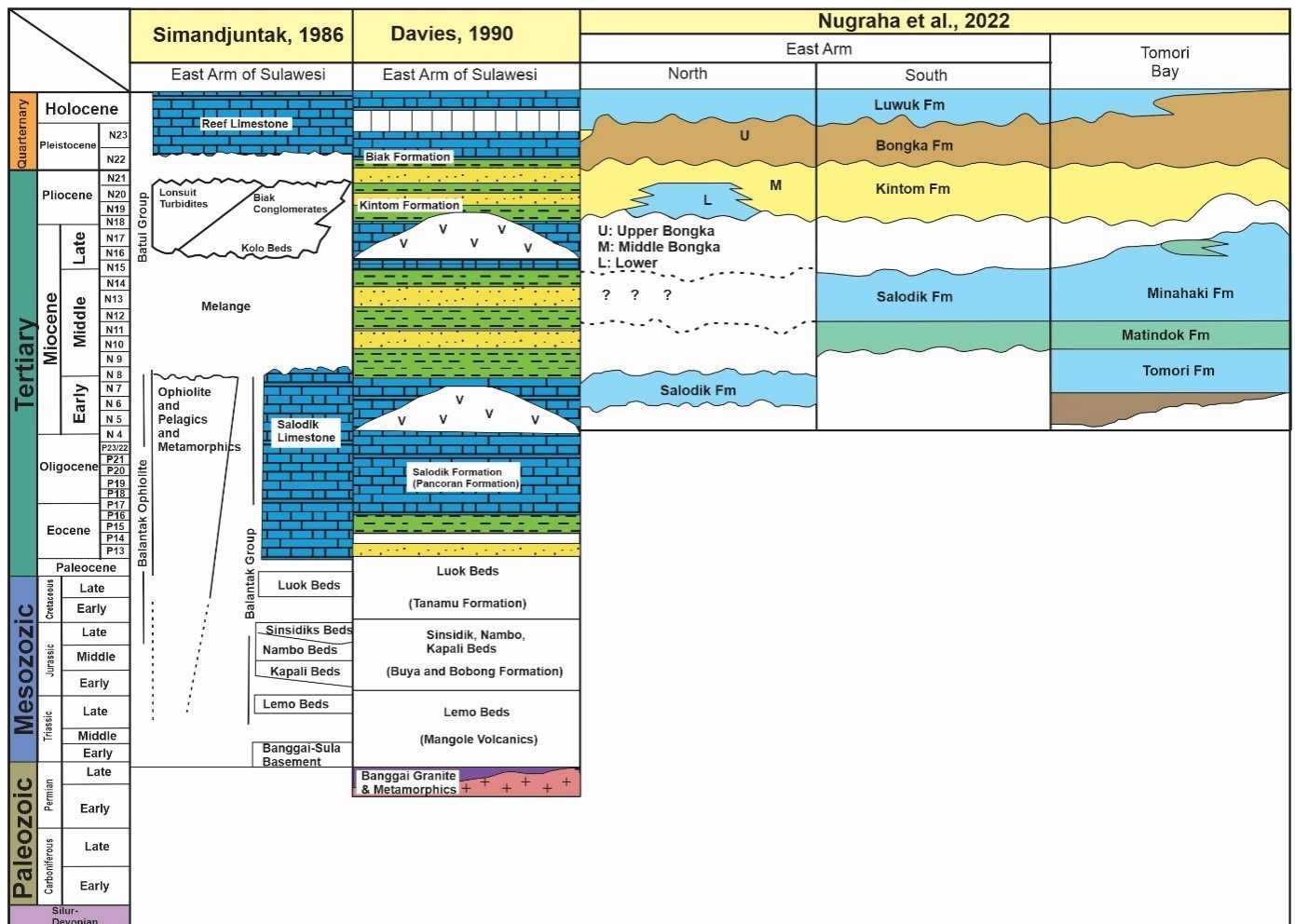
Figure 3. The stratigraphy of the study is based on several previous studies (Simandjuntak 1986; Davies 1990; Nugraha et al. 2022). Fine-grained sedimentary rocks are interpreted as part of the Kintom Formation formed during the Pliocene, while coarse-grained sedimentary rocks are included in the Bongka Formation (Nugraha et al. 2022) or Biak Formation (Simandjuntak 1986; Davies 1990). The red box represents the formation that is the focus of this study.

b. Salodik Formation

The Salodik Formation consists of bedded limestone with marl and sandstone intercalations. The abundant presence of large foraminifera indicates the age of the formation from the Middle Eocene to the Middle Miocene (Rusmana et al. 1993; Surono et al. 1993; Nugraha et al. 2022). The large foraminifera include *Amphistegina* sp., *Alveolinella* sp., *Cycloclypeus* sp., *Distichoplax biserialis* (Dietrich), *Heterostegina* sp., *Lepidocyclina* (*Eulepidina*) *ephipoides* Jones & Chapman, *Lepidocyclina* sp., *Nummulites* sp., *Operculina* sp., and *Spiroclypeus tindunganensis* Van Der Vlerk. The marl contains several species of small planktonic foraminifera, including *Globigerina boweri* Bolli, *Globigerinoides immaturus* Broniman, and *Globigerinoides trilobus* Reuss, *Globoquadrina altispira* Cushman & Jarvis, *Globorotalia acostaensis* Blow, *Globorotalia aragonensis* Nuttal, *Globorotalia menardii* D'Orbigny, *Globorotalia spinulosa* Cushman, *Orbulina universa* D'Orbigny, and *Sphaeroidinellopsis seminulina* Schwager (Rusmana et al. 1993; Surono et al. 1993).

In the Poh-Pagimana area, the age of the Salodik Group is slightly different, ranging from the Early Eocene to the Middle Miocene. The age determination is based on the planktonic foraminifera content; *Morozovella aragonensis* Nuttal, *Morozovella lehneri* Cushman & Jarvis, *Morozovella subbotinae* Morozova, *Morozovella caucasica* Glaessner, *Paragloborotalia peripheroacuta* Blow & Banner, and *Paragloborotalia peripheroronda* Blow & Banner (Fakhruddin & Kurniadi 2019). This formation extends from the eastern to western parts of the Eastern Arm of Sulawesi, forming folded hills in the central part. In the sub-surface, Tomori PSC, the Salodik Formation forms three rock formations, namely Matindok, Tomori, and Minahaki (Davies 1990; Nugraha et al. 2022).

c. Poh Formation

The Poh Formation consists of interbedded limestone with marl and some carbonate sandstone intercalations at its base. Similar to the Salodik Formation, Poh limestone is rich in large foraminifera such as *Amphistegina* sp., *Alveolinella* sp., *Cycloclypeus* sp., *Gypsina* sp., *Heterostegina* sp., *Lepidocyclina* (*Eulepidina*) sp., *Lepidocyclina ferreroi* Provale, *Miogypsina* sp., *Operculina* sp., and *Spiroclypeus tindunganensis* Van Der Vlerk, indicating an age from the Oligocene to the Late Miocene. The marl in the Poh Formation is rich in small foraminifera fossils such as *Globigerina naparimaensis* Bronniman, *Globigerinoides ruber* D'Orbigny, *Globigerinoides trilobus* Reuss, *Globorotalia acostaensis* Blow, *Globorotalia plesiotumida* Banner & Blow, *Globorotalia* sp., *Sphaeroidinella subdehiscens* Blow, and *Sphaeroidinellopsis seminulina* Schwager (Rusmana et al. 1993; Surono et al. 1993). The stratigraphic relationship between the Salodik and Poh Formations is interfingering. In the sub-surface, Tomori PSC, this formation is equivalent to the Mentawa Member (Davies 1990; Nugraha et al. 2022).

d. Kintom Formation

The Kintom Formation in the western part comprises fine-grained rocks such as sandy marl and sandstone (Surono et al. 1993), while the eastern part consists of conglomerate, sandstone, and limestone (Rusmana et al. 1993). In the sub-surface, Tomori PSC, the Kintom Formation consists of mudstone with intercalations of sandstone and limestone (Figure 3). The planktonic foraminifera content in the marl consist of *Globigerinoides immaturus* Broniman, *Globigerinoides obliquus* Bolli, *Globigerinoides sacculifer* Brady, *Globigerinoides trilobus* Reuss, *Globoquadrina altispira* Cushman & Jarvis, *Globoquadrina venezuelana* (Hedberg), *Globorotalia acostaensis* Blow, *Globorotalia flexuosa* (Koch),

Globorotalia menardii D'Orbigny, *Globorotalia multicamerata* Cushman & Jarvis, *Globorotalia plesiotumida* Banner & Blow, *Globorotalia tumida* Brady, *Hastigerina siphonifera* (D'Orbigny), *Orbulina universa* D'Orbigny, *Sphaeroidinella subdehiscens* Blow, and *Sphaeroidinellopsis seminulina* Schwager (Rusmana et al. 1993; Surono et al. 1993). This fossil assemblage indicates an age from the Late Miocene to the Pliocene.

e. Bongka Formation

The rocks forming the Bongka Formation consist of repetitive sequences of conglomerates with sandstone and mudstone, along with several lenses of limestone. Occasionally, in some locations, siltstone and lignite intercalations can be found. The age of the Bongka Formation is the same as that of Kintom, which is from the Late Miocene to the Pliocene (Surono et al. 1993; Rusmana et al. 1993). However, according to other researchers (Nugraha et al. 2022), the Bongka Formation has a Late Pliocene age and unconformably overlies the Kintom Formation, which has an Early Pliocene age (Figure 3). The foraminifera fossil assemblage, including *Candeina nitida* D'Orbigny, *Globigerina naparimaensis* Bronniman, *Globigerinoides extremus* Bolli & Bermudez, *Globigerinoides immaturus* Broniman, *Globigerinoides obliquus* Bolli, *Globigerinoides ruber* D'Orbigny, *Globoquadrina venezuelana* (Hedberg), *Globorotalia acostaensis* Blow, *Globorotalia crassaformis* Galloway & Wissler, *Globorotalia crassaformis* Blow, *Globorotalia menardii* D'Orbigny, *Globorotalia multicamerata* Cushman & Jarvis, *Globorotalia tumida* Brady, *Globorotalia tosaensis* Takayanagi & Saito, *Orbulina universa* D'Orbigny, *Pulleniatina obliquiloculata* Parker & Jones, *Pulleniatina primalis* Banner & Blow, and *Sphaeroidinella dehiscens* Parker & Jones, indicates an age from the Late Miocene to the Pliocene (Rusmana et al. 1993; Surono et al. 1993).

f. Quaternary Coral Reefs

The formation consists of coralline-reefal limestone with marl (Surono et al. 1993; Rusmana et al. 1993). In some places, such as on the road cut in the village of Bunga, reefal limestone cut by conglomerate layers is found. Nugraha et al. (2022) and Rusmana et al. (1993) refer to it as the Luwuk Formation. Based on the content of planktic foraminifera such as *Globorotalia tosaensis* Takayanagi & Saito, *Globorotalia truncatulinoides* D'Orbigny, *Globorotalia tumida* Brady, *Pulleniatina obliquiloculata* Parker & Jones, and *Pulleniatina primalis* Banner & Blow, the age of this formation is Pleistocene (Surono et al. 1993). The Luwuk Formation unconformably overlies the Kintom-Bongka Formation and is still forming today (Figure 3).

Previously, Rusmana et al. (1993) and Surono et al. (1993) have categorised the Kintom, Bongka, and Luwuk Formations as molasse-type sedimentary rocks. This study will only focus on the Kintom and Bongka Formations, while the Luwuk Formation will not be the subject of this research.

MATERIALS AND METHODS

The stratigraphic column of the Matindok Section was obtained by conducting a measured section around the Matindok – Ondoondolu road with a scale of 1:100. Measurements were taken on outcrops located on cliffs, riverbanks, and road cuts (Figure 4). Some outcrops had weathered rock conditions, necessitating a shift to other locations to obtain fresh outcrops or stratigraphic measurements were not performed (Figure 1). As a result, there are several points in the stratigraphic column where the column is empty. Based on the measured stratigraphy, a 315 m thick

stratigraphic column was produced (Figure 5).

A total of 46 rock samples were collected for the analysis of planktonic foraminifera content to determine the age of the rocks in this section. The prepared rocks mostly consisted of marl, but some rock samples were taken from calcareous sandstone and conglomerate matrix due to the absence of fine-grained rocks, especially in the sandstone and conglomerate units.

A 100-gram rock sample was crushed by pounding and soaked in hydrogen peroxide (H_2O_2) solution. After several hours, the hydrogen peroxide solution was discarded, and the sample is filtered under running water. The filters used employ mesh sizes of 50, 150, and 200. Before usage, the filters were soaked in a methylene blue solution to stain fossils from the previous filtration process that may have been missed on the mesh. After filtration, the samples were dried in an oven, and once dried, they were ready for observation under a binocular microscope. The identification of planktonic foraminifera was facilitated by referring to standard foraminifera identifications from Bolli et al. (1985), Ducassou et al. (2015), BouDagher-Fadel (2015), Berghuis et al. (2019), Badaro and Petri (2022), and Bown et al. (2024).

The foraminifera zonation followed the classification outlined by Wade et al. (2011) and van Gorsel et al. (2014). Wade et al. (2011) was chosen because it presented a calibration of Cenozoic planktonic foraminifera zones in low-latitude areas. The calibration has also been synthesised with the Cenozoic geomagnetic polarity time scale (GPTS) and the astronomical time scale (ATS). In general, the results of Wade et al. (2011) were in accordance with previous studies (ex. Bolli et al. 1985), but in some cases, there are several adjustments to the biochron duration. Van Gorsel et al. (2014) conducted a review of biostratigraphy and biofacies interpretation in Cenozoic basins in Indonesia and Southeast Asia. Several biodatums not found in Wade et al. (2011) can be found in van Gorsel et al. (2014).

RESULTS AND DISCUSSION
Rock Unit

From the stratigraphic measurements, three rock units were identified, from oldest to youngest, consisting of:

a. Marl unit consists of marl with intercalations of calcareous sandstone and breccia. The marl has a gray color and is massive, with grain size ranging from silt to very fine sand (Figure 4A), sub-angular grain shapes, open fabric, and the composition is lithic sedimentary and mafic igneous rocks, also rich in small foraminifera. The calcareous sandstone is light gray, generally massive (Figure 4B), but sometimes shows parallel sedimentary structures. It has fine sand grain size, sub-angular grain shapes, open fabric, and the composition is lithic fragments and small foraminifera. The breccia is gray, with a massive-channel sedimentary structure, the fragment sizes ranging from 4 mm to 6 cm, angular shapes, open fabric, with dominant fragment composition is lithic marl and calcareous sandstone fragments (Figure 4C).

b. Calcareous sandstone unit consists of calcareous sandstone with intercalations of claystone and siltstone. The calcareous sandstone is cream-colored with graded–bedded sedimentary structures, occasionally massive, fine – medium sand grain size, subangular to subrounded grain shapes, open fabric, and fragments composed of quartz, small foraminifera, serpentinite, and opaque minerals (Figure 4D). The claystone is dark gray, massive, with clay-sized grains, and a

thickness of 5 cm. The siltstone is gray and massive, with sub-angular grain shapes, open fabric, and a fragment composition consisting of small foraminifera, quartz, and lithic sedimentary and igneous rocks.

c. Intergrade conglomerate- gravelly sandstone unit. The conglomerate is gray, with a graded-bedded, channel to cross-beds structures (Figure 4E), fragment sizes ranging from 4 mm to 10 cm, rounded grain shapes, open fabric, and a composition of fragments including serpentinite, gabbro, peridotite, greenschist, claystone, and limestone (Figure 4F). The conglomerate matrix is sand-sized with a composition similar to the fragments, and sometimes small foraminifera can be found. The gravelly sandstone is light brown, exhibiting graded-bedded to cross-bed sedimentary structures, with coarse sand grain size and some gravel-sized fragments. The grain shapes are subrounded to rounded, with an open fabric. The fragment composition includes lithic rocks of ultramafic origin such as serpentinite, gabbro, peridotite, and green schist; as well as sedimentary rocks like claystone and limestone.
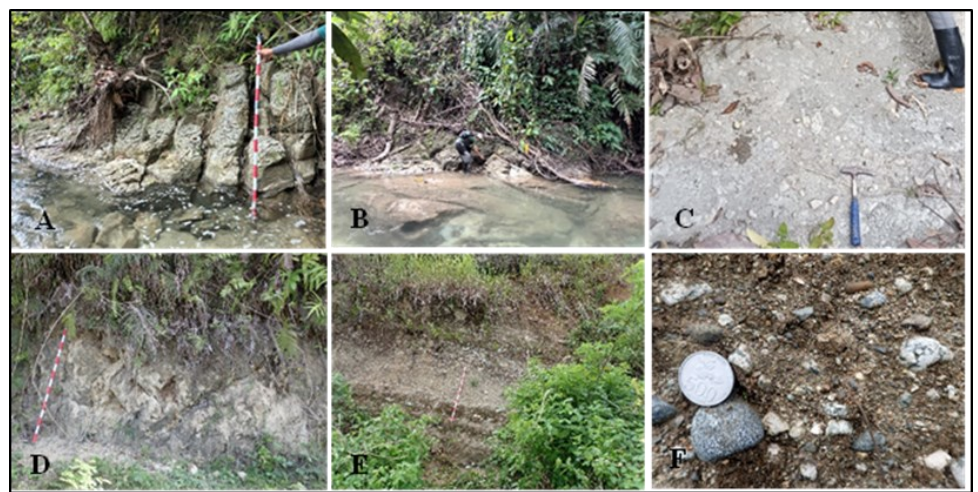
Figure 4. Rocks outcrops in the Matindok section. A. Marl from the marl unit with intercalations of calcareous sandstone and breccia. The marl is massive and often jointed. B. Intercalation of calcareous sandstone with parallel bedding sedimentary structures. C. Breccia intercalation with fragments of calcareous sandstone and marl. D. Layer of fine calcareous sandstone from the calcareous sandstone unit with claystone and tuffaceous rock intercalations. E. Graded conglomerate transitioning into gravelly sandstone. F. Conglomerate fragments consisting of lithic gabbro, basalt, serpentinite, and limestone.

Foraminiferal Biostratigraphy

From the 46 prepared samples, one sample was barren. The other samples contained small foraminifera, both planktonic and benthonic, with varying abundances. A total of 49 species of planktic foraminifera were successfully identified from the prepared samples. The significant abundance of foraminifera from the research results provided a fairly good division of foraminifera biostratigraphy. Seven foraminifera biozones during the Pliocene could be identified. Markers delimited the biozones used the first occurrence (FO) and last occurrence (LO) of a species as datum (Figure 5). The markers generally used the biozonation employed by Wade et al. (2011) and van Gorsel et al. (2014). The names of the biozones referred to 5 types of biozones based on stratigraphic presence, namely Lowest Occurrence Zone (LOZ), Highest Occurrence Zone (HOZ), Taxon Range Zone (TRZ), Concurrent Range Zone (CRZ), and Partial Range Zone (PRZ) (Wade et al. 2011). Seven biozones generated, from the oldest to the youngest, are:
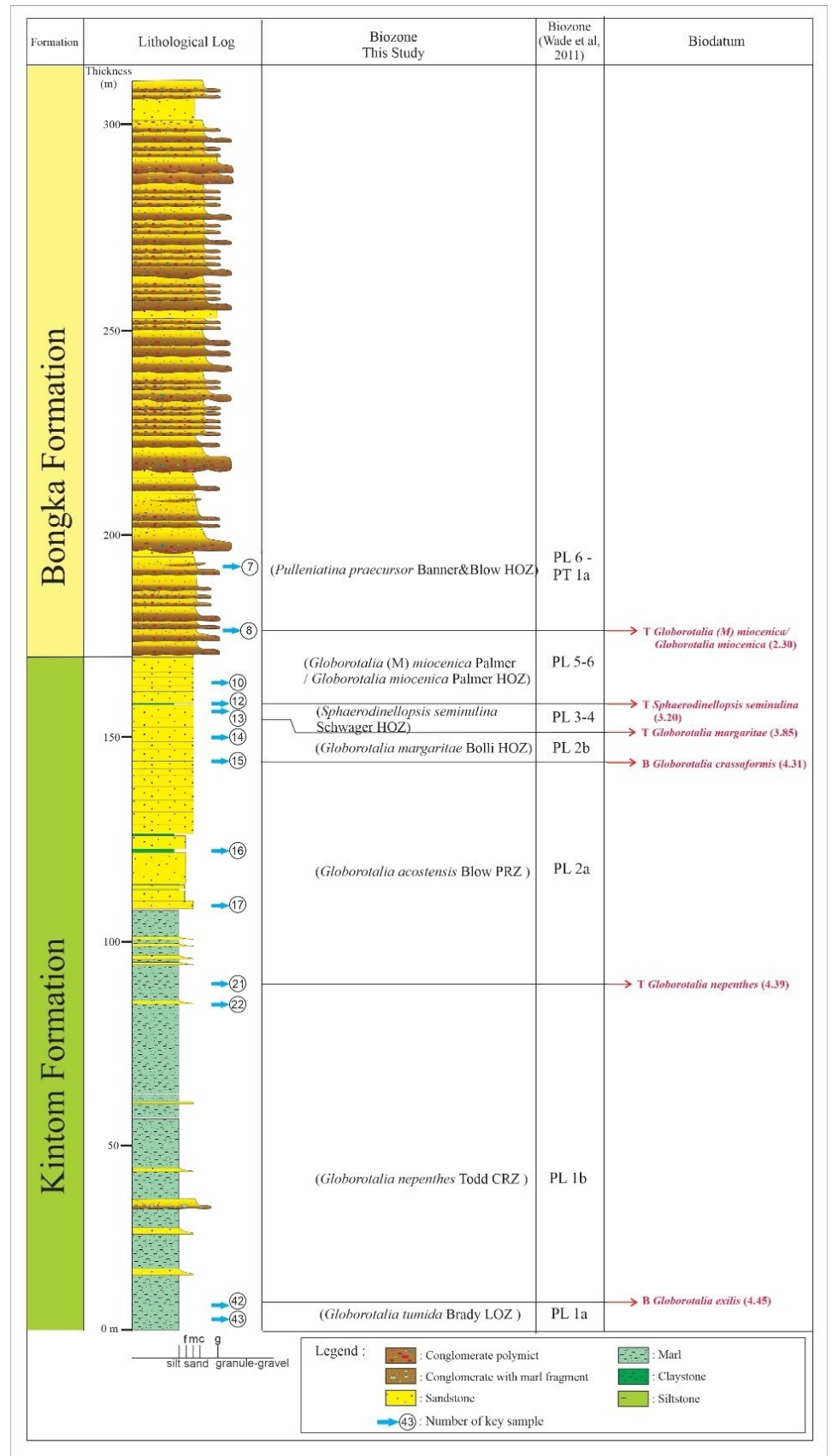
Figure 5. The biozonation position and biodatum of the Kintom and Bongka Formation. The biozonation scheme proposed by Wade et al. (2011) was utilised to compare the nomenclature and age assignment of the biozones and biodata. Please refer to Table 1 on the attached page for the distribution chart of planktonic foraminifera in the Matindok Section.

Globorotalia tumida Brady Lowest Occurrence Zone
Globorotalia tumida Brady Zone Wade et al. (2011), *Globorotalia margaritae margaritae* Bolli & Bermudez Zone Bolli et al. (1985).

Definition: This zone is *Globorotalia tumida* Brady Lowest Occurrence Zone (LOZ), marked by FO of *Globorotalia tumida* Brady to FO of *Globorotalia exilis* Blow and *Globorotalia menardii* B Bolli (Figure 5).

Sample Distribution: No.sample 45 – 43

Remarks: The biozones had a thickness of 10 m in the lithology column of the Matindok Section. The foraminifera identified in this zone are: *Globigerinoides immaturus* Broniman, *Globigerinoides obliquus extremus* Bolli & Bermudez, *Globigerinoides obliquus obliquus* Bolli , *Globigerinoides ruber* D'Orbigny, *Globigerinoides sacculiferus* Brady, *Globoquadrina altispira* Cushman & Jarvis, *Globorotalia acostaensis* Blow, *Globorotalia menardii menardii* (Parker, Jones & Brady), *Globorotalia merotumida* Blow & Banner, *Globorotalia plesiotumida* Blow & Banner, *Globorotalia pseudomiocenica* Bolli & Bermudez, *Globorotalia tumida* Brady, *Hastigerina aequilateralis* Brady, *Orbulina universa* D'Orbigny, *Pulleniatina primalis* Banner & Blow, *Sphaeroidinella dehiscens* Parker & Jones, and *Sphaeroidinellopsis seminulina* Schwager have also been identified. Other species found in these biozones include *Globigerinoides sacculiferus fistulosus* Schubert, *Globorotalia margaritae* Bolli & Bermudez, *Globorotalia menardii A* Bolli, *Globigerinoides altiaperturus* Bolli, *Globigerinoides conglobatus* Brady, *Globigerinoides extremus* Bolli & Bermudez, *Globigerinoides quadrilobatus* D'Orbigny, *Globigerinoides sicanus* de Stefani, *Globigerinoides trilobus* Reuss, *Globoquadrina dehiscens* Jenkins, *Globorotalia cibaoensis* Bermudez, *Globorotalia humerosa* Takayanagi & Saito, *Globorotalia humerosa humerosa* Takayanagi & Saito, and *Globorotalia pseudoopima* Blow.

Stratigraphic Distribution: Marl unit, Matindok section lithology column interval 0 - 10 m.

Horizon: PL 1c (Early Pliocene), B *Globorotalia tumida* Brady (5.59 Ma) – B *Globorotalia exilis* Blow (4.45 Ma) see Table 1.

Globoturborotalita nepenthes Todd Concurrent-range Zone

Globoturborotalita nepenthes Todd CRZ (Wade et al. 2011), *Globorotalia margaritae evoluta* Cita Zone (Bolli et al. 1985).

Definition: This Zone is *Globoturborotalita nepenthes* Todd Concurrent-Range Zone (CRZ), marked by FO of *Globorotalia exilis* Blow to LO of *Globoturborotalita nepenthes* Todd and LO *Globoquadrina venezuelana* Hedberg (Figure 6).

Sample Distribution: No.sample 42 – 22

Remarks: The biozones in the lithology column of the Matindok Section had a thickness of 70 m. The foraminifera identified in this zone include *Dentoglobigerina altispira* Cushman & Jarvis, *Globigerinoides conglobatus* Brady, *Globigerinoides extremus* Bolli & Bermudez, *Globigerinoides immaturus* Broniman, *Globigerinoides obliqus extremus* Bolli & Bermudez, *Globigerinoides obliquus obliquus* Bolli, *Globigerinoides ruber D'Orbigny*, *Globigerinoides sacculiferus* Brady, *Globigerinoides sicanus* de Stefani, *Globigerinoides trilobus* Reuss, *Globoquadrina altispira* Cushman & Jarvis, *Globoquadrina dehiscens* Jenkins, *Globoquadrina praedehiscens* Blow & Banner, *Globoquadrina tripartita* Koch, *Globorotalia acostaensis* Blow, *Globorotalia cibaoensis* Bermudez, *Globorotalia exilis* Blow, *Globorotalia humerosa* Takayanagi & Saito, *Globorotalia humerosa humerosa* Takayanagi & Saito, *Globorotalia margaritae* Bolli & Bermudez, *Globorotalia (Menardella) miocenica* Palmer, *Globorotalia menardii A* Bolli, *Globorotalia menardii B* Bolli, *Globorotalia menardii cultrata* D'Orbigny, *Globorotalia menardii menardii* (Parker, Jones & Brady), *Globorotalia merotumida* Blow & Banner, *Globorotalia multicamerata* Cushman & Jarvis, *Globorotalia plesiotumida* Blow & Banner, *Globorotalia pseudomiocenica* Bolli & Bermudez, *Globorotalia pseudoopima* Blow, *Globorotalia tumida* Brady,

Hastigerina aequilateralis Brady, *Orbulina bilobata* D'Orbigny, *Orbulina universa* D'Orbigny, *Pulleniatina praecursor* Banner & Blow, *Pulleniatina primalis* Banner & Blow, *Sphaeroidinella dehiscens* Parker & Jones, *Sphaeroidinellopsis seminulina* Schwager, and *Sphaeroidinellopsis seminulina seminulina* Schwager.

Stratigraphic Distribution: Marl unit, Matindok section lithology column interval 10 - 80 m.

Horizon: PL 1b (Early Pliocene), B *Globorotalia exilis* Blow (4.45 Ma) – T *Globoturborotalita nepenthes* Todd (4.39 Ma) see Table 1.

Globorotalia acostaensis Blow Partial Range Zone

Globorotalia margaritae Bolli HOZ (Wade et al. 2011), *Globorotalia margaritae evoluta* Cita Zone (Bolli et al. 1985).

Definition: This Zone is *Globorotalia acostaensis* Blow Partial Range Zone (PRZ), marked by LO of *Globoturborotalita nepenthes* Todd and *Globoquadrina venezuelana* Hedberg to FO of *Globorotalia crassaformis crassaformis* Galloway & Wissler (Figure 6).

Sample Distribution: No.sample 21 - 16

Remarks: The biozones in the lithology column of the Matindok Section have a thickness of 65 m. The foraminifera identified in this zone include *Globigerinoides altiaperturus* Bolli, *Globigerinoides conglobatus* Brady, *Globigerinoides immaturus* Broniman, *Globigerinoides obliqus extremus* Bolli & Bermudez, *Globigerinoides obliquus obliquus* Bolli, *Globigerinoides ruber* D'Orbigny, *Globigerinoides sacculiferus* Brady, *Globoquadrina altispira* Cushman & Jarvis, *Globoquadrina dehiscens* Jenkins, *Globorotalia acostaensis* Blow, *Globorotalia exilis* Blow, *Globorotalia humerosa* Takayanagi & Saito *Globorotalia humerosa humerosa* Takayanagi & Saito, *Globorotalia margaritae* Bolli, *Globorotalia (Menardella) miocenica* Palmer, *Globorotalia menardii cultrata* D'Orbigny, *Globorotalia menardii menardii* (Parker, Jones & Brady), *Globorotalia merotumida* Blow & Banner, *Globorotalia plesiotumida* Blow & Banner , *Globorotalia pseudomiocenica* Bolli & Bermudez, *Globorotalia pseudoopima* Blow, *Globorotalia tumida* Brady, *Hastigerina aequilateralis* Brady, *Orbulina universa* D'Orbigny, *Pulleniatina praecursor* Banner & Blow, *Pulleniatina primalis* Banner & Blow, *Sphaeroidinella dehiscens* Schwager, and *Sphaeroidinellopsis seminulina* Schwager.

Stratigraphic Distribution: Upper marl – lower calcareous sandstone unit, Matindok section lithology column interval 80 - 145 m.

Horizon: PL 2a (Early – Late Pliocene), T *Globoturborotalita nepenthes* Todd (4.39 Ma) – B *Globorotalia crassaformis crassaformis*(4.31 Ma) see Table 1.

Globorotalia margaritae Bolli Highest Occurrence Zone

Globorotalia margaritae Bolli HOZ (Wade et al. 2011), *Globorotalia margaritae evoluta* Cita Zone (Bolli et al. 1985)

Definition: Interval from FO *Globorotalia crassaformis crassaformis* Galloway & Wissler to LO *Globorotalia margaritae* Bolli (Figure 6).

Sample Distribution: No.sample 15 – 14

Remarks: The biozones in the lithology column of the Matindok Section had a thickness of 9 m. The foraminifera identified in this zone include *Dentoglobigerina altispira* Cushman & Jarvis , *Globigerinoides conglobatus* Brady, *Globigerinoides immaturus* Broniman, *Globigerinoides obliqus extremus* Bolli & Bermudez, *Globigerinoides obliquus obliquus* Bolli, *Globigerinoides quadrilobatus* D'Orbigny, *Globigerinoides ruber* D'Orbigny, *Globigerinoides sacculiferus fistulosus* Schubert, *Globigerinoides tosaensis* Takayanagi & Saito, *Globigerinoides trilobus* Reuss, *Globoquadrina dehiscens*

Jenkins, *Globorotalia crassaformis crassaformis* Galloway & Wissler, *Globorotalia dutertrei blowi* Rogl & Bolli, *Globorotalia exilis* Blow, *Globorotalia margaritae* Bolli, *Globorotalia menardii A* Boll*i*, *Globorotalia menardii B* Bolli, *Globorotalia menardii menardii* (Parker, Jones & Brady), *Globorotalia merotumida* Blow & Banner, *Globorotalia multicamerata* Cushman & Jarvis, *Globorotalia plesiotumida* Blow & Banner, *Globorotalia pseudomiocenica* Bolli & Bermudez, *Globorotalia pseudoopima* Blow, *Globorotalia tumida* Brady, *Hastigerina aequilateralis* Brady, *Orbulina universa* D'Orbigny, *Pulleniatina praecursor* Banner & Blow, *Pulleniatina* primalis Banner & Blow, *Sphaeroidinella dehiscens* Schwager, and *Sphaeroidinellopsis seminulina* Schwager.

Stratigraphic Distribution: Calcareous sandstone unit, Matindok section lithology column interval 145 – 154 m.

Horizon: PL 2b (Early Pliocene), B *Globorotalia crassaformis crassaformis* (4.31 Ma) – T *Globorotalia margaritae* Bolli (3.85 Ma) see Table 1.

Sphaeroidinellopsis seminulina Schwager Highest Occurrence Zone

Sphaeroidinellopsis seminulina Schwager HOZ (Wade et al. 2011), *Globorotalia margaritae evoluta* Cita Zone (Bolli et al. 1985).

Definition: This Zone is *Sphaeroidinellopsis seminulina* Schwager Highest Occurrence Zone (HOZ), marked by LO of *Globorotalia margaritae* Bolli & Bermudez to LO of *Sphaeroidinellopsis seminulina* Schwager (Figure 6).

Sample Distribution: No.sample 13

Remarks: The biozones in the lithology column of the Matindok Section had a thickness of 2.5 m. The foraminifera identified in this zone include *Globigerinoides extremus* Bolli & Bermudez, *Globigerinoides immaturus* Broniman, *Globigerinoides obliquus obliquus* Bolli, *Globigerinoides ruber* D'Orbigny, *Globigerinoides sacculiferus* Brady, *Globigerinoides trilobus* Reuss, *Globoquadrina altispira* Cushman & Jarvis, *Globorotalia humerosa humerosa* Takayanagi & Saito, *Globorotalia (Menardella) miocenica* Palmer, *Globorotalia miocenica* Palmer, *Globorotalia plesiotumida* Blow & Banner, *Globorotalia pseudoopima* Blow, *Orbulina universa* D'Orbigny, *Pulleniatina praecursor* Banner & Blow, *Sphaeroidinella dehiscens* Schwager, and *Sphaeroidinellopsis seminulina* Schwager.

Stratigraphic Distribution: Calcareous sandstone unit, Matindok section lithology column interval 154 – 156,5 m.

Horizon: PL 3 - 4 (Early – Late Pliocene), T *Globorotalia margaritae* Bolli (3.85 Ma) – T *Sphaeroidinellopsis seminulina* Schwager (3.20 Ma) see Table 1.

Globorotalia (M) miocenica Palmer / *Globorotalia miocenica* Palmer Highest Occurrence Zone

Globorotalia miocenica Palmer HOZ (Wade et al. 2011), *Globorotalia miocenica* Palmer / *Globorotalia trilobus fistulosus* Schubert Zone (Bolli et al. 1985).

Definition: This Zone is *Globorotalia (M) miocenica* Palmer / *Globorotalia miocenica* Palmer Highest Occurrence Zone (HOZ), marked by LO of *Sphaeroidinellopsis seminulina* Schwager to LO of *Globorotalia (M) miocenica* Palmer / *Globorotalia miocenica* Palmer (Figure 6).

Sample Distribution: No.sample 12 - 8

Remarks: The biozones in the lithology column of the Matindok Section had a thickness of 18.5 m. The foraminifera identified in this zone include *Globigerinoides conglobatus* Brady, *Globigerinoides immaturus* Broniman, *Globigerinoides obliquus extremus* Bolli & Bermudez, *Globigerinoides ruber* D'Orbigny, *Globigerinoides trilobus* Reuss, *Globoquadrina altispira* Cushman & Jarvis, *Globorotalia crassaformis*

crassaformis Gallowas & Wissler, *Globorotalia dutertrei blowi* Rogl & Bolli, *Globorotalia dutertrei dutertrei* D'Orbigny, *Globorotalia exilis* Blow, *Globorotalia (Menardella) miocenica* Palmer, *Globorotalia menardii cultrate*, *Globorotalia miocenica* Palmer, *Globorotalia merotumida* Blow & Banner, *Globorotalia plesiotumida* Blow & Banner, *Globorotalia pseudoopima* Blow, *Globorotalia tumida* Brady, *Orbulina universa* D'Orbigny, *Pulleniatina praecursor* Banner & Blow, and *Pulleniatina primalis* Banner & Blow.

Stratigraphic Distribution: Upper calcareous sandstone − lower gravelly sandstone unit Matindok section lithology column interval 156,5 - 175 m.

Horizon: PL 5 - 6 (Late Pliocene), T *Sphaeroidinellopsis seminulina* Schwager (3.20 Ma) − T *Globorotalia miocenica* Palmer (2.30 Ma) see Table 1.

Figure 6. Examples of several species of planktonic foraminifera that can be found in rocks in the Matindok Section are as follows: 1a-b: *Globogerinoides nepenthes* Todd 2a-b: *Globorotalia tumida* Brady 3a-b: *Globorotalia acostaensis* Blow 4a-b: *Globorotalia scitula-margaritae* Bolli & Bermudez 5a-b: *Sphaeroidinellopsis seminulina* Schwager 6a-b: *Globorotalia (M) miocenica* Palmer 7a-b: *Globorotalia miocenica* Palmer 8a-c: *Dentoglobigerina altispira* Cushman & Jarvis 9a-b: *Globorotalia multicamerata* Cushman & Jarvis 10a-b: *Globorotalia menardii* Bolli 11a-c: *Globoquadrina altisipra* Cushman & Jarvis 12a-b: *Pulleniatina praecursor* Banner & Blow.

Pulleniatina praecursor Banner & Blow Highest Occurrence Zone
Pulleniatina praecursor Banner & Blow HOZ from (Wade et al. 2011), *Globorotalia miocenica* Palmer / *Globorotalia tosaensis tosaensis* Takayanagi & Saito Zone (Bolli et al. 1985).

Definition: This Zone is *Pulleniatina praecursor* Banner & Blow Highest Occurrence Zone (HOZ), marked by LO of *Globorotalia (M) miocenica* Palmer / *Globorotalia miocenica* Palmer to LO *Pulleniatina praecursor* Banner & Blow (Figure 6).

Sample Distribution: No.sample 7 – 1

Remarks: Biozones had a thickness of 140 m in the lithology column of the Matindok Section. The foraminifera identified in this zone are: *Globoquadrina* altispira Cushman & Jarvis, *Globorotalia tumida* Brady, *Orbulina universa* D'Orbigny, *Pulleniatina praecursor* Banner & Blow and *Pulleniatina primalis* Banner & Blow.

Stratigraphic Distribution: Gravelly sandstone unit, Matindok section lithology column interval 175 – 315 m.

Horizon: PL 6 – PT1a (Late Pliocene), T *Globorotalia miocenica* Palmer (2.30) – T *Pulleniatina praecursor* Banner & Blow (2.26 Ma) see Table 1.

Discussion

Lithology can be grouped based on different categories with clearly distinguishable characteristics (Darman et al. 2023). This research divided the rocks exposed in the Matindok Section into lithostratigraphic and biostratigraphic units. Lithostratigraphic units divided rock bodies based on lithological characteristics with the official basic unit called formation. Biostratigraphic units were based on the division of rock bodies based on the fossil content in the rock with the basic unit being biozones or zones.

The stratigraphic development in the research area started with marl units with intercalations of sandstone and breccia. Subsequently, it gradually transitioned into sandstone with intercalations of claystone-siltstone and concluded with repetitive conglomerate-sandstone gradations. The stratigraphic development indicated a pattern of coarsening upward in rock changes. This pattern generally signified changes in the depositional environment becoming shallower upwards.

In the marl units, the rock character was poor in sedimentary structure and had an open fabric. This suggests a deposition mechanism involving turbidity currents. The fine grains present in the rock, along with the abundant content of planktic foraminifera and a diverse range of species, particularly within the *Globorotalia* genus, imply a deeper marine depositional environment. It is highly probable that the depositional setting is situated in the distal part of the submarine fan.

The calcareous sandstone units showed an increase in rock grain size. Additionally, sedimentary structures such as graded bedding and parallel bedding were becoming appear frequently, although the subangular grain shape and open fabric suggested a relatively similar depositional mechanism in turbidity currents. The amount of planktic foraminifera slightly decreased with a relatively high variety of species, particularly within the genus *Globorotalia*. The depositional environment was a proximal submarine fan.

The intergrade conglomerate-gravelly sandstone units had a very coarse grain size with a channel, graded bedding, parallel-cross bedding sediment structure, and a rounded grain shape. The deposition mechanism involved the movement of traction current, with a shallowing upward depositional environment in the delta front-prodelta slope of a fan delta. In contrast to the two previous units, which were rich in planktic foraminifera, this unit has a low occurrence of planktic foraminifera. The large depositional energy required for this unit implied that planktic foraminifera would face challenges in being deposited in the same environment. Consequently, there will be only a small amount of planktic foraminifera in this unit.

Table 1. Distribution chart of planktonic foraminifera from the Matindok Section with biodatum, age, biozanation from Wade et al. (2011) and biozonation from this study. R: Rare = 1 – 2 specimens, F: Few = 3 – 5 specimens, C: Common = 6 – 10 specimens, A: Abundant = > 10 specimens.

The characteristics of the first and second rock units can be classified as flysch deposits resulting from a collision, while the characteristics of the third unit can be classified as molasses deposits from a collision (Kurniawan et al 2018; Kotlia et al. 2018; Martín-Martín et al. 2020; Milli et al. 2021; Zhang et al. 2020). Reworked rock fragments, including ultramafic igneous rocks such as serpentinite, gabbro, basalt, and sedimentary rocks such as marl, along with reworked foraminifera fossils such as *Globoquadrina dehiscens* Chapman, Parr & Collins, provide indications of the uplift of the ultramafic rocks of the Sulawesi Plate and the formation of newly generated flysch sediments. This phenomenon is common in collision areas as the two colliding plates approach each other.

Grouping rocks into a formation must refer to the locality type for each formation. Based on the locality type, the grouping of rocks in the Matindok Section will follow the definition of the Kintom and Bongka Formations according to Surono et al. (1993). The rock characteristics, mechanisms, and depositional environment are interconnected, allowing marl units with calcareous sandstone-breccia intercalations and sandstones with claystone-siltstone intercalations to be grouped into a distinct formation. When compared with Surono et al. (1993), these two rock units are classified within the Kintom Formation.

In contrast to the two previous units, the third unit shows distinct characteristics, mechanisms, and depositional environments, allowing its classification within a different formation. The repeating units of conglomerate and sandstone gradation are included in the Bongka Formation.

Wade et al. (2011) determined Zone PL1 to be between FO *Globorotalia tumida* Brady and LO *Globoturborotalita nepenthes* Todd and divided Zone PL1 into 2 based on the extinction of LO *Globorotalia ciboensis* Bermudez. Zone PL1 in the research area is divided into two parts, namely Zone PL1a and 1b. Zone PL 1a is *Globorotalia tumida* Brady LOZ, while PL1b is *Globoturborotalita nepenthes* Todd CRZ. This zone is slightly different from the zone proposed by Wade et al. (2011). The boundaries of Zone PL 1a and 1b are determined based on FO *Globorotalia exilis* Blow. LO *Globorotalia ciboensis* Bermudez was found in the study area but its stratigraphic position is above FO *Globorotalia exilis* Blow so it is considered to be reworked from older rocks.

Zone PL2 according to Wade et al. (2011) is the *Globorotalia margaritae* Bolli HOZ with a biostratigraphic interval between LO *Globoturborotalita nepenthes* Todd and LO *Globorotalia margaritae* Bolli. In this study PL2 can be divided into 2 zones: PL2a and 2b based on FO *Globorotalia crassaformis crassaformis* Galloway & Wissler. PL 2a is *Globorotalia acostaensis* Blow PRZ while PL 2b is *Globorotalia margaritae* Bolli HOZ. *Globorotalia acostaensis* Blow PRZ bordered by LO *Globoturborotalita nepenthes* Todd with FO *Globorotalia crassaformis crassaformis* Galloway & Wissler. *Globorotalia margaritae* Bolli HOZ is bordered by FO *Globorotalia crassaformis crassaformis* Galloway & Wissler with LO *Globorotalia margaritae* Bolli.

The next zone of the research area is PL3-4 with the boundary being LO *Globorotalia margaritae* Bolli and *Sphaeroidinellopsis seminulina* Schwager. PL3 zone according to Wade et al. (2011) is *Sphaeroidinellopsis seminulina* Schwager HOZ while PL4 is *Dentoglobigerina altispira* Cushman & Jarvis HOZ. The PL3-4 zone is only found in one rock sample, namely sample no. 13. This indicates the existence of unconformity after rock formation in PL3 and 4, resulting in stacked biostratigraphic zones. This unconformity can occur due to nondeposition or erosion.

Zone PL5 - 6 in the research area is *Globorotalia (M) miocenica* Palmer/ *Globorotalia miocenica* Palmer HOZ while Zones PL5 and 6 Wade et al. (2011) in the form of *Globorotalia pseudomiocenica* Bolli & Bermudez HOZ and *Globigerinoides fistulosus* Scubert HOZ. PL5 in the study area used LO *Sphaeroidinellopsis seminulina* Schwager with LO *Globorotalia (M) miocenica* Palmer/ *Globorotalia miocenica* Palmer while Wade et al. (2011) used LO *Dentoglobigerina altispira* Cushman & Jarvis with LO *Globorotalia pseudomiocenica* Bolli & Bermudez. The use of the biodatum LO *Sphaeroidinellopsis seminulina* Schwager, as the lower limit of PL5 for the study area, is due to the relatively consistent and continuous presence of this species compared to *Dentoglobigerina altispira* Cushman & Jarvis. Meanwhile, the use of the biodatum LO *Globorotalia (M) miocenica* Palmer/ *Globorotalia miocenica* Palmer in the research area for PL6 is due to the fact that *Globorotalia pseudomiocenica* Bolli & Bermudez has not been found since PL2b and *Globigerinoides fistulosus* Scubert has not been found in the research area since the beginning.

The last zone that developed in the PL6 – PT1a research area was *Pulleniatina praecursor* Banner & Blow HOZ while Zone PL6 and PT1a Wade et al. (2011) are *Globigerinoides fistulosus* Scubert HOZ and *Globorotalia tosaensis* Takayanagi & Saito HOZ. Determination of Zone PL6 – PT1a based on the biodatum LO *Globorotalia (M) miocenica* Palmer/ *Globorotalia miocenica* Palmer and the presence of *Pulleniatina praecursor* Banner & Blow. *Globigerinoides fistulosus* Scubert and *Globorotalia tosaensis* Takayanagi & Saito were used to divide PL6 and PT1a by Wade et al. (2011) not found. The presence of *Pulleniatina praecursor* Banner & Blow in this zone is considered to be the re-presence of the *Pulleniatina* genus in Zone PT1a according to Wade et al. (2011). Based on this, the youngest zone of the research area is included in Zone PL6 – PT1a.

The correlation of lithological units with biostratigraphic units in the research area produces several interesting things. The marl rock unit as the first lithological unit formed in the research area, with a thickness of 115 m contains three biostratigraphic units, namely Zones 1a, 1b and lower part 2a with. The time range for the formation of this unit is approximately 2 My. With a predominantly fine-grained lithology, it takes quite a long time to form this unit.

The calcareous sandstone unit, as the second unit, has a thickness of 55 m containing four biostratigraphic units, namely Upper Zone 2a, 2b, 3 -4 and 5-6. The formation time range is approximately the same as the formation of the first unit, approximately 2 My. The lithology in this second unit has a larger grain size of the constituent material compared to the first unit. Generally, with the same deposition time, coarse-grained lithology will have a greater thickness than fine-grained lithology. The thinner lithology of the second unit compared to the first unit could be due to erosion or non-deposition during the formation of this unit. Erosion can reduce the thickness of the lithology that was originally formed, while non-deposition results in thinner lithology that forms. Nondeposition in submarine fan areas due to lobe/channel displacement is common.

Zones PL3-4 and PL5-6 indicate possible erosion and nondeposition in the second unit. PL3-4 has a measured lithological thickness of 2.2 m. The time required to deposit the lithology is 0.65 My. There are 2 biozonations contained in coarser-grained lithology with a thickness of 2.2 m and over a relatively long time. There were no areas of erosion at the boundaries of the lithological layers, so it is thought that there was a long deposition lag during the displacement of the submarine channel. PL5-6 has a lithological thickness of 25 m. The upper limit of the second unit is at PL5-6 and is eroded by the last unit. Therefore, the lithology

thickness at PL5-6 has decreased.

The intergrade conglomerate-gravelly unit, sandstone as the third and final unit, has a lithological thickness of 145 m and contains 1 biostratigraphic unit, namely Zone PL6-PT1a. The formation time range is short, ranging from $0.2 - 0.4$ My. The coarse-grained lithologies that make up this unit require high depositional energies. Generally, high deposition energy will produce thick deposits in a relatively short time as seen in this last unit.

CONCLUSION

The lithology exposed along the Matindok Section can be categorized into three lithology units: marl units consist of marl with interbedded sandstone-breccia, calcareous sandstone unit consists of calcareous sandstone with interbedded claystone-siltstone, and intergrade conglomerate-gravelly sandstone *gradations*. The first two units belonged to the Kintom Formation and had appropriate characteristics with flysch deposits in the collision area, while the last unit was part of the Bongka Formation and had similarities with molasses deposits. The Kintom Formation was deposited from the Early Pliocene to early Late Pliocene, as indicated by the biozonation of foraminifera, including *Globorotalia tumida* Brady LOZ (PL1a; 5.59 - 4.45 Ma), *Globoturborotalita nepenthes* ToddCRZ (PL1b; 4.45 - 4.39 Ma), *Globotalia acostaensis* Blow PRZ (PL2a; $4.39 - 4.31$ Ma), *Globotalia margaritae* Bolli HOZ (PL2b; 4.31 - 3.85 Ma), *Sphaeroidinellopsis seminulina* Schwager HOZ (PL 3-4; $3.85 - 3.20$ Ma), and *Globorotalia (M) miocenica* Palmer / *Globorotalia miocenica* Palmer HOZ (PL5 – 6; $3.20 - 2.30$ Ma). Above the Kintom Formation, the Bongka Formation was deposited unconformably during the Late Pliocene, based on the biozonation of foraminifera including *Globorotalia (M) miocenica* Palmer / *Globorotalia miocenica* Palmer HOZ (PL5 – 6; $3.20 - 2.30$ Ma) and *Pulleniatina praecursor Banner & Blow* HOZ (PL6 – PT1a; $2.30 - 2.26$ Ma).

AUTHORS CONTRIBUTION

Moch. Indra Novian designed the research, analyzed the paleontology, stratigraphy data and wrote the manuscript; Didit Hadi Barianto collected the data; Salahuddin Husein analysed the sedimentology data; Akmaluddin analysed the paleontology data and Sugeng Sapto Surjono supervised the process.

CONFLICT OF INTEREST

The authors declare no conflicts of interest in preparing this article.

REFERENCES

Badaro, V.C.S. & Petri, S., 2022. A deep-sea foraminiferal assemblage scattered through the late Cenozoic of Antarctic Peninsula and its biostratigraphic and biogeographic implications. *Journal of Paleontology*, 96(3), pp.493-512. doi: 10.1017/jpa.2021.120

Berghuis, H.W.K., Troelstra, S.R. & Zaim, Y., 2019. Plio-Pleistocene foraminiferal biostratigraphy of the eastern Kendeng Zone (Java, Indonesia): The Marmoyo and Sumbering in Sections. *Palaeogeography, Palaeoclimatology, Palaeoecology*, 528, pp.218-231. doi: 10.1016/j.palaeo.2019.05.008.

Bolli, H.M., Saunders, J.B. & Perch-Nielsen, K., 1985. *Plankton Stratigraphy*, Cambridge University Press.

BouDagher-Fadel, M.K., 2015. *Biostratigraphic and Geological Significance of Planktonic Foraminifera*, 2nd Edition. London: UCL Press.

Bown, P. et al., 2024. *Mikrotax*. viewed 20 June 2004, from https://www.mikrotax.org/pforams/

Davies, I.C., 1990. Geological and exploration review of the Tomori PSC, Eastern Indonesia. *Indonesian Petroleum Association, Proceedings 19th Annual Convention*, pp.41–67.

Darman, H. et al., 2023. *Sandi Stratigrafi Indonesia edisi 2023*, Ikatan Ahli Geologi Indonesia.

Ducassou, E. et al., 2015. Origin of the large Pliocene and Pleistocene debris flows on the Algarve margin. *Marine Geology*, 377, pp.58-76. doi: 10.1016/j.margeo.2015.08.018.

Fakhruddin, R. & Kurniadi, D., 2019. Age and Paleobathymetry of Salodik Group in Poh Pagimana section, East Arm of Sulawesi Based on Foraminiferal Assemblages *Journal of Geoscience, Engineering, Environment, and Technology*, 04(01), pp.30-39, doi: 10.25299/jgeet.2019.4.1.2751

Garrard, R.A., Supandjono, J.B. & Surono, 1988. The geology of the Banggai-Sula microcontinent, Eastern Indonesia. *Indonesian Petroleum Association, Proceedings 17th Annual Convention*, pp.23–52.

Kotlia, B.S. et al., 2018. Sedimentary environment and geomorphic development of the uppermost Siwalik molasse in Kumaun Himalayan Foreland Basin, North India. *Geological Journal*, 53(1), pp.159-177. doi: 10.1002/gj.2883.

Kurniawan, A.P. et al., 2018. Pliocene Deep Water Channel System of Celebes Molasse as New Exploration Play in Banggai Sula Foreland Basin, Eastern Sulawesi-Indonesia. *IOP Conference Series: Earth and Environmental Science*, 132, 012005. doi: 10.1088/1755-1315/132/1/012005.

Martín-Martín, M. et al., 2020. Similar Oligo-Miocene tectono-sedimentary evolution of the Paratethyan branches represented by the Moldavidian Basin and Maghrebian Flysch Basin. *Sedimentary Geology*, 396, 105548. doi: 10.1016/j.sedgeo.2019.105548.

Martosuwito, S., 2012. Tectonostratigraphy of The Eastern Part of Sulawesi, Indonesia, in relation to The Terrane Origins. *Jurnal Geologi dan Sumberdaya Mineral*, 22(4), pp.199-207. doi: 10.33332/jgsm.geologi.v22i4.119

Milli, S. et al., 2021. Facies, composition and provenance of the Agnone Flysch in the context of the early Messinian evolution of the southern Apennine foredeep (Molise, Italy). *Italian Journal of Geosciences*, 140(2), pp.275-312. doi: 10.3301/IJG.2021.01.

Nugraha, A.M.S., Hall, R. & Fadel, M.B., 2022. The Celebes Molasse: A revised Neogene stratigraphy for Sulawesi, Indonesia. *Journal of Asian Earth Sciences*, 228, 105140. doi: 10.1016/j.jseaes.2022.105140.

Rusmana, E., Koswara, A. & Simandjuntak, T.O., 1993. *Geological Map of the Luwuk Sheet, Sulawesi quadrangles 2115, 2215, 2315, scale 1:250,000*. Geological Research and Development Centre, Bandung, Indonesia.

Simandjuntak, T.O., 1986. *Sedimentology and Tectonics of the Collision Complex in the East Arm of Sulawesi, Indonesia.* University of London.

Surono et al., 1993. *Geological Map of the Batui Quadrangle, Sulawesi Quadrangle 2214, scale 1:250,000.* Geological Research and Development Centre. Bandung, Indonesia.

van Gorsel, J.T., Lunt, P. & Morley, R., 2014. Introduction to Cenozoic biostratigraphy of Indonesia- SE Asia, Biostratigraphy Of Southeast Asia − Part 1. *Berita Sedimentologi,* 29(1), pp.6 − 40. doi: 10.51835/bsed.2014.29.1.140

Wade, B.S. et al., 2011. Review and Revision Of Cenozoic Tropical Planktonic Foraminiferal Biostratigraphy And Calibration To The Geomagnetic Polarity And Astronomical Time Scale, *Earth-Science Rev.,* 104, pp.111-142.

Zhang, J.-M. et al., 2020. Evolution of the Heihe-Nenjiang Ocean in the eastern Paleo-Asian Ocean: Constraints of sedimentological, geo-chronological and geochemical investigations from Early-Middle Paleozoic Heihe-Dashizhai Orogenic Belt in the northeast China. *Gondwana Research,* 81, pp.339-361. doi: 10.1016/j.gr.2019.11.006.

Research Article

Genetic Variation of Baram River Frog, *Pulchrana baramica* (Boettger, 1900), In Java, Sumatra, and Kalimantan based on *16S* Mitochondrial Gene

Luthfi Fauzi[1], Tuty Arisuryanti[1]*, Katon Waskito Aji[1], Awal Riyanto[2], Eric N. Smith[3], Amir Hamidy[2]

1) Laboratory of Genetics and Breeding, Faculty of Biology, Universitas Gadjah Mada, Jl. Teknika Selatan, Sekip Utara, Yogyakarta 55281, Indonesia
2) Laboratory of Herpetology, Museum Zoologicum Bogoriense, Research Centre for Biosystematics and Evolution, National Research and Innovation Agency (BRIN), Gd. Widyasatwaloka, Jl. Raya Jakarta-Bogor Km 46, Cibinong, West Java, Indonesia
3) The Amphibian and Reptile Diversity Research Centre and Department of Biology; University of Texas at Arlington; 501 S. Nedderman Drive; Arlington, TX 76010; 775-351-5277, USA
* Corresponding author, email: tuty-arisuryanti@ugm.ac.id

ABSTRACT

Baram River Frog (*Pulchrana baramica*) is a ranid species distributed in the Malay Peninsula, Borneo, Sumatra and represents the sole species from the genus *Pulchrana* on Java Island. Cryptic species are commonly encountered within the amphibian group which can cause confusion in the identification process. Due to the broad distribution range of *P. baramica* and the frequent occurrence of cryptic species within the amphibian group, it is important to evaluate the taxonomic status of *P. baramica*. Therefore, we investigated the taxonomic position of *P. baramica* from three populations (Kalimantan, Sumatra, and Java) and identified the interpopulation genetic variation based on molecular data of the *16S* mitochondrial gene. We reconstructed phylogenetic relationships using Neighbour Joining, Maximum Likelihood, and Bayesian Inference. The research results revealed that *Pulchrana baramica* is a monophyletic group and nested within a group together with *P. glandulosa* and *P. laterimaculata*. The monophyletic group of *P. baramica* consisted of four distinct lineages that molecularly showed interspecific genetic variation. Clade 1 represents the population of Sumatra and Borneo (Kalimantan), clade 2 comprises the population from Borneo (Sarawak), clade 3 consists of population from Java, and clade 4 represents the population from Sumatra. Further research is required with the addition of morphological and acoustic data as supportive evidence to obtain more extensive comprehension of species identification.

INTRODUCTION

Baram River Frog or *Pulchrana baramica* is a ranid species and was first described from the Baram River in Sarawak, Malaysia, and described in 1900 by Boettger. Boettger identified the diagnostic characteristics of the Baram River Frog as having reduced webbing on the hind limbs, a granular dorsum, lacking folds on the glands, and expanded toe tips, which are comparable to *Rana signata* Gunther, 1872. This species can be found in areas with elevations up to 600 m asl (Iskandar 1998; Leong & Lim

2003; Das et al. 2007; Chan et al. 2014).

The distribution of the *Pulchrana baramica* species includes Johor, Selangor, Peninsular Malaysia, Singapore, Kalimantan, Sumatera (Riau and Bangka Island), and based on Iskandar's records in 1998, the species was found in Cilebut, Bogor Regency, and 2018 in Haurbentes Village, Bogor Regency on Java Island. Additionally, recent records by Herlambang et al. (2022) reported the presence of *P. baramica* in Bunguran and Tiga Island of the Kepulauan Natuna, Indonesia. To date, the Genus *Pulchrana* comprises 18 species and *Pulchrana baramica* (Boettger, 1900) is known as the only species of the *Pulchrana* genus found on Java Island (Frost 2021).

The determination of taxonomic status for amphibian species generally employs morphometric, molecular, or vocal characteristics. However, taxonomic determination using morphometric approaches can encounter obstacles when it is known that the species in question is a cryptic species that is morphologically similar. The molecular data was proven to be an effective tool for solving taxonomic problems within some cryptic species of amphibians in Sunda land regions (Hamidy et al. 2011; Hamidy et al. 2012; Munir et al. 2018; Munir et al. 2021). In amphibians, the species delimitation process frequently used is the non-tree-based method: genetic distance. In this method, species separation is determined from the value of genetic distance. For amphibian groups, Fouquet et al. (2007) proposed an uncorrected p-distance value of >3% as a species delimitation threshold for the mitochondrial genes *12S* and *16S* rRNA.

According to Inger (1966), frogs in the *Pulchrana* genus can be identified by looking at the webbing on their hind legs. The frog species *P. baramica* is closely related to *P. glandulosa*. Those two species can be distinguished by the webbing on their hind legs, with *P. baramica* having lack of developed webbing than *P. glandulosa* (Van Kampen 1923). However, identifying amphibians based on morphological characteristics has limitations because the morphological characteristics used to differentiate between species are very limited, and require detailed observations and special skills. Therefore, molecular data is needed to strengthen previous identifications for inter and intraspecific populations.

MATERIAL AND METHODS
Sample Collection
The samples used in this study comprised tissue samples from voucher specimens of *Pulchrana baramica* that were deposited in *Museum Zoologicum Bogoriense* (MZB), the National Research and Innovation Agency (BRIN). All ingroup samples represent the population of *P. baramica* from Sumatra, Kalimantan, and Java in Indonesia. The sample collection locations can be seen in Figure 1, and the detailed location and voucher specimen number are presented in Table 1.

DNA Extraction
The complete DNA genomic samples were isolated from muscle using the kit (dneasy Blood and tissue kit from QIAGEN, Valencia, CA, USA) following the manufacturer's protocols.

DNA Amplification, Electrophoresis, and Sequencing
The DNA isolation product was subjected to amplification using *16S* rRNA primers consisting of forward primer L2606 5' CTG ACC GTG CAA AGG TAG CGT AAT CACT-3' and reverse primer H3056 5' CTC CGG TCT GAA CTC AGA TCA CGT-3' (Hedges et al. 1993). The PCR amplification utilized 25 μl reaction consisting of 12.5 μl Redmix PCR
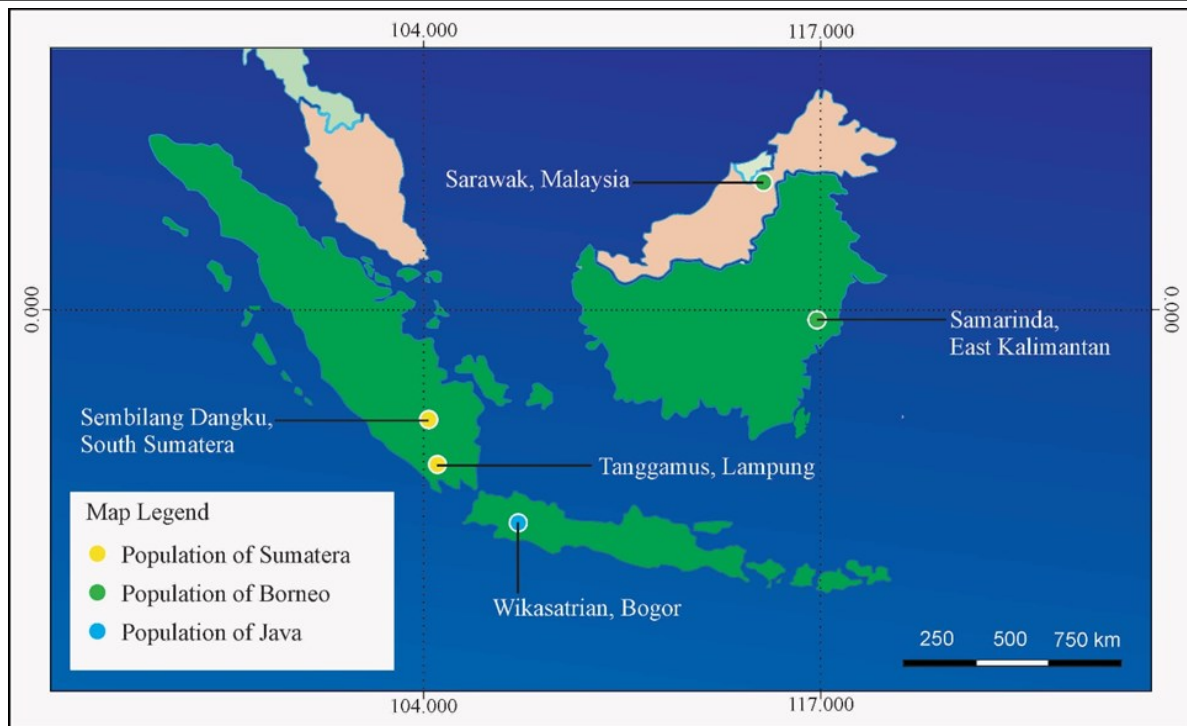
Figure 1. Map of frog sampling locations in this study.

Table 1. List of ingroup samples used in this study.

No	Voucher Number	Genbank Number	Species name	Location	Sources
1	MZB Amph 32583		*Pulchrana baramica*	Java, West Java, Bogor, Pasir Angin, Wikansatrian	This study
2	MZB Amph 32586		*Pulchrana baramica*	Java, West Java, Bogor, Pasir Angin, Wikansatrian	This study
3	MZB Amph 31578		*Pulchrana baramica*	Borneo, East Kalimantan, Samarinda	This study
4	MZB Amph 31579		*Pulchrana baramica*	Borneo, East Kalimantan, Samarinda	This study
5	MZB Amph 32662		*Pulchrana baramica*	Sumatra, South Sumatra, Sembilang Dangku	This study
6	MZB Amph 32665		*Pulchrana baramica*	Sumatra, South Sumatra, Sembilang Dangku	This study
7	MZB Amph 32666		*Pulchrana baramica*	Sumatra, South Sumatra, Sembilang Dangku	This study
8	MZB Amph 32673		*Pulchrana baramica*	Sumatra, South Sumatra, Sembilang Dangku	This study
9	MZB Amph 22327		*Pulchrana baramica*	Sumatra, Lampung, Tanggamus	This study
10	MZB Amph 22329		*Pulchrana baramica*	Sumatra, Lampung, Tanggamus	This study
11	KUHE 53640	AB719234	*Pulchrana baramica*	Borneo, Sarawak, Mulu	Matsui et al. 2012
12	KUHE 53617	AB719232	*Pulchrana baramica*	Borneo, Sarawak, Mulu	Matsui et al. 2012
13	KUHE 53623	AB719233	*Pulchrana baramica*	Borneo, Sarawak, Mulu	Matsui et al. 2012
14	KUHE 53678	AB719231	*Pulchrana baramica*	Borneo, Sarawak, Mulu	Matsui et al. 2012

kit, 1 mm MgCl$_2$, 0.6 mm of forward primer L2606 and reverse primer H3056, 5.5 µl ddH$_2$O, and 3 µl (10-100 ng) of DNA template. All solutions were mixed in a PCR tube for each sample. The solution mixture was vortexed and centrifuged using the spin-down mode before being placed in a Thermocycler with 1 cycle of reaction for 5 minutes of pre-denaturation at 95°C, 35 cycles of reaction for 35 seconds of denaturation at 95°C, 30 seconds of annealing at 50°C, 30 seconds of extension at 72°C and 7 minutes of final extension at 72°C.

The PCR products were subjected to agarose gel electrophoresis on a 1% gel at 100 volts for a duration of 15 minutes. Florosafe (Bioline) was used for staining, while Tris-acetate EDTA (TAE) 1X served as the buffer. The amplification products were visualised under UV light. Purification and sequencing of each amplification sample in the forward and reverse directions were carried out using the Big Dye Terminator (Applied Biosystems) and the Genetic Analyser ABI 3730xl, respectively. These procedures were conducted by P.T. Genetika Science in Jakarta and delivered to First Base (Malaysia).

Sequence Editing
Genestudio software was used to create and to modify the consensus sequence, which was then verified for accuracy through the use of DNASTAR software's seqman and editseq menus (DNASTAR Inc., Madison, USA). While conducting this procedure, careful inspection of the chromatograms was carried out to ensure the absence of any uncertain bases.

Sequence Identification
The sequence of samples was identified using the Nucleotide BLAST analysis available on the NCBI website (https://blast.ncbi.nlm.nih.gov/Blast.cgi). The similarity and the query cover of the sample were used to estimate the species of *P. baramica* compared to the available data in genbank.

Sequence Alignment
The sample sequences were aligned using the Mesquite v.3.70 software on the Opal menu (Maddison & Maddison 2021) and the MEGAX software on the clustalw menu (Kumar et al. 2018).

Intrapopulation and Intraspecies Analysis
The primary objective of the intrapopulation analysis was to determine the nucleotide composition of each sample belonging to the same population. Additionally, the intraspecies analysis aimed to extend the inquiry by examining the nucleotide composition, genetic distance, and phylogenetic relationship across diverse populations.

Nucleotide Composition & Genetic Distance
The nucleotide composition was computed using the MEGAX program. The genetic distance was analysed with the *p*-distance model and visualized in a Neighbour-Joining (NJ) tree, which is a widely employed approach in DNA barcoding research, as described by Hebert et al. (2003).

Phylogenetic Relationship
In this analysis, we used 14 sequences of *P. baramica* as ingroup members, ten of them are from this study and four from the genbank (Table 1). For outgroups, we involved *P. glandulosa* and *P. laterimaculata* from genbank data. The MEGAX software (Kumar et al. 2018) was used to

evaluate the reconstruction of the phylogenetic tree using three methods, Neighbour-Joining, and Maximum Likelihood, both with 1,000 bootstraps, and Bayesian Inference method through the BEAST program ([Suchard et al. 2018](#)). The optimal evolutionary model was identified using the Bayesian Information Criterion (BIC) implemented in jmodeltest 2.1.10 ([Darriba et al. 2012](#)). The HKY with a gamma value of 0.170 (HKY + G) was determined to be the best sequence substitution model based on the Bayesian Inference Criterion. The method of Markov Chain Monte Carlo (MCMC) was employed to estimate the posterior probabilities distribution over 10^7 generations with a sampling frequency of 1,000 generations.

RESULTS AND DISCUSSION
Result
Species verification

We successfully amplified the *16S* mitochondrial gene from 10 samples of Baram River Frogs, yielding fragments of 500 bp (Figure 2). Sequence editing was performed using genestudio software, resulting in consensus sequences ranging from 508 bp to 547 bp in length. Genetic similarity analysis of the samples with reference species in genbank revealed that out of the 10 samples studied, 8 samples exhibited a similarity range of 93.93 to 96.68% with species *Pulchrana baramica*, while 2 samples showed a similarity range from 96.09 to 96.27% with species *Pulchrana laterimaculata* (Table 2).
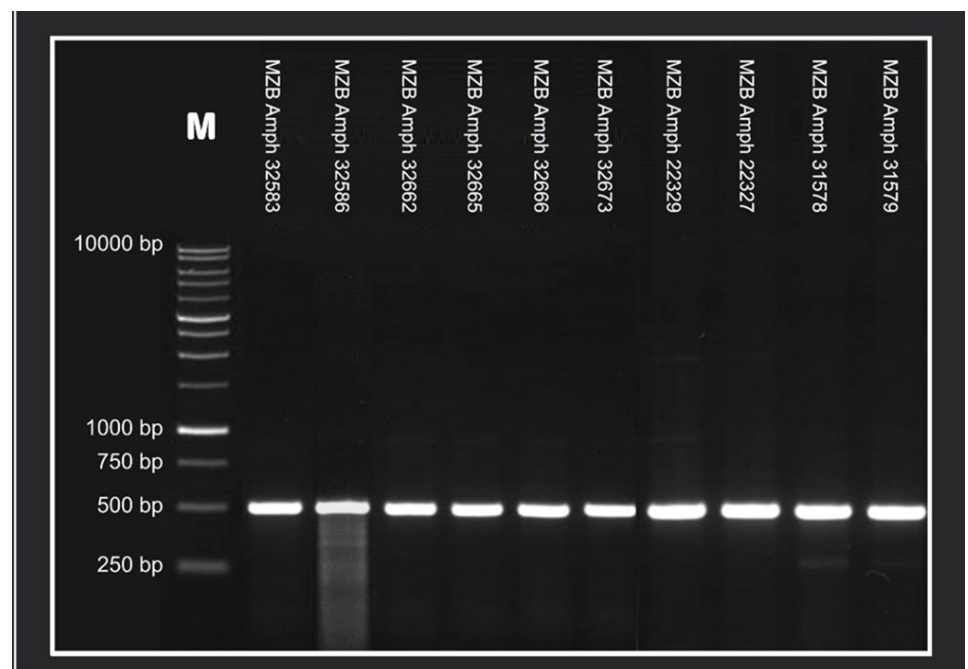
Figure 2. The PCR amplification results of the *16S* mitochondrial gene from frog samples collected from Java, Sumatra, and Kalimantan. The samples were run on 1% agarose gel electrophoresis and identified by the samples *P. baramica* from Indonesia. A 1kb DNA ladder (GENEAID) was included as a reference marker, labelled as "M" in the figure.

We conducted a *16S* mitochondrial gene alignment of in group samples collected from Java, Sumatra, and Kalimantan. The alignment yielded fragment length of 456 base pairs for each species. These sequences were subsequently utilised to conduct intrapopulation analysis for each species. Additionally, we performed intraspecies analysis by comparing the *16S* sequences of Sarawak samples from Mulu, which located in one river system with the Baram River (type locality) as record-

Table 2. Identification of species based on the database of genbank using BLAST.

Specimen number (MZB)	Sample Code	Fragment Length (bp)	BLAST			Genbank Species Identified
			% Identity	% Query Cover	Accession Number Genbank	
MZB Amph 32583	L.J.1	545	95.50	93	DQ835351.1	*Pulchrana baramica*
MZB Amph 32586	L.J.2	508	93.93	99	DQ835351.1	*Pulchrana baramica*
MZB Amph 32662	L.S.1	547	96.29	93	DQ835352.1	*Pulchrana baramica*
MZB Amph 32665	L.S.2	543	96.09	94	EU604193.1	*Pulchrana laterimaculata*
MZB Amph 32666	L.S.3	543	96.27	93	EU604193.1	*Pulchrana laterimaculata*
MZB Amph 32673	L.S.4	546	96.68	93	DQ835352.1	*Pulchrana baramica*
MZB Amph 22329	L.S.5	539	96.48	94	DQ835352.1	*Pulchrana baramica*
MZB Amph 22327	L.S.6	536	96.68	95	DQ835352.1	*Pulchrana baramica*
MZB Amph 31578	L.K.1	538	96.48	94	DQ835352.1	*Pulchrana baramica*
MZB Amph 31579	L.K.2	546	96.48	93	DQ835352.1	*Pulchrana baramica*

ed in genbank and species from Genus *Pulchrana* in Indonesia. To comprehend the evolutionary relationships of the samples, we aligned the sequences from Java (West Java), Sumatera (South Sumatra and Lampung), and Kalimantan (Samarinda) with outgroups member (*P. glandulosa* and *P. laterimaculata*) sequences from genbank. The resulting aligned sequences were then employed to construct a phylogenetic tree.

For intrapopulation analysis, we analysed a total of 10 frog samples from Wikasatrian (West Java), Sembilang Dangku (South Sumatra), Lampung (Sumatra), and Samarinda (East Kalimantan). Our results showed that the average nucleotide composition of samples consisted of 21.96% thymine (T), 27.17% cytosine (C), 30.34% adenine (A), and 20.53% guanine (G), with variations ranging from 0 to 0.9%, 0 to 1.05%, 0 to 0.30%, and 0 to 0.45%. The average composition of nucleotides A+T was found to be 52.30%, while G+C accounted for 47.70%.

The nucleotide composition of A+T is more dominant compared to the composition of nucleotides C+G. In the population of Java Island, the composition of nucleotide T was 22.42%, C ranged from 26.59 to 26.81%, A ranged from 30.33 to 30.55%, and the composition of nucleotide G was 20.44%. In the population of Sumatra Island (clade 1), the composition of nucleotide T ranged from 21.54 to 22.20%, the composition of nucleotide C ranged from 26.75 to 27.91%, A ranged from 30.11 to 30.55%, and G ranged from 20.44 to 20.88%. In the population of Kalimantan Island (clade 1), the composition of nucleotide T ranged from 21.76 to 21.98%, C was 27.25%, A ranged from 30.11 to 30.55%, and G ranged from 20.44 to 20.66%.

The resulting phylogenetic tree revealed the division of the 10 samples into four separate clades, supported by high bootstrap values of 95-100% (NJ), 92-98% (ML), and a posterior probability of 1 (BI). The phylogenetic tree reconstruction is presented in Figure 3, highlighting the distinct separation of clades 1, 2, 3, and 4. Next, our genetic distance analysis results in the estimation of genetic distances between sequences. The sequence fragments used for analysis had a length of 456 bp. The lowest genetic distance among all clades was observed between clade 1 and clade 2, measuring 0.22%. Conversely, the highest genetic distance among all clades was observed between clade 3 and clade 4, measuring 5.45% (Table 3).

Discussion

Genetic identification methods can be employed to rapidly and accurately determine individuals based on their unique genetic information. We ob-
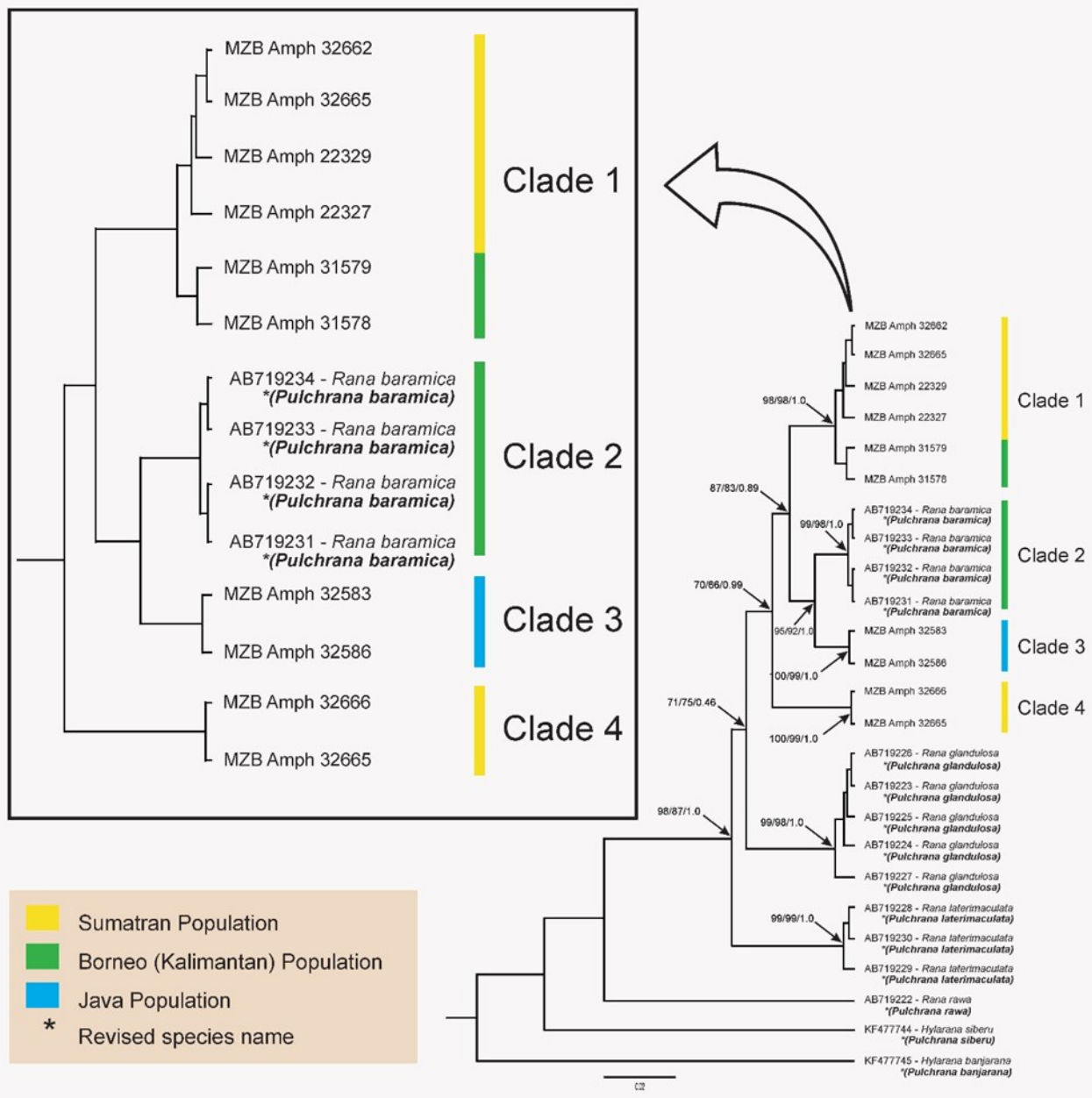
Figure 3. Phylogenetic tree reconstruction based on Neighbour-Joining (NJ), Maximum-Likelihood (ML), Bayesian Inference (BI) topology species sample, species of *Pulchrana baramica* and its outgroup members based on *16S* gene sequences (456 bp). The node represented the number bootstrap (NJ and ML) and Bayesian Posterior Probability (Bayesian Inference).

served that the analysis of nucleotide composition in the *16S* gene of the ten studied frog samples exhibited varying compositions of nucleotides T, C, A, and G. The respective mean nucleotide compositions of T, C, A, and G in the ten studied frog samples were 21.96, 27.17, 30.34, and 20.53%. The average composition of nucleotides A+T was 52.30%, while G+C was 47.70%. In this study, it is evident that the nucleotide base composition follows the order A>C>T>G in descending order. When compared to the research conducted by Chowdhury et al. (2021) on the frog species *Hydrophylax leptoglossa*, which exhibited a nucleotide base composition pattern of A>C>G>T in descending order, it indicates that frogs within the same family may exhibit different patterns of nucleotide base composition.

Our phylogenetic tree revealed the presence of four distinct clades. Clade 1 represents the population from Sumatra and Borneo

Table 3. The percentage (%) of interpopulation genetic distances observed in this research and sample *Pulcrana baramica from* genbank data based on the *16S* rRNA gene.

	Clade 1	Clade 2	Clade 3	Clade 4
Clade 1	0.59% (0.22%-1.10%)			
Clade 2	3.41% (2.08%-3.74%)	0.00% 0.00%		
Clade 3	4.40% (3.96%-4.84%)	2.75% (2.64%-2.86%)	0.22% (0.22%)	
Clade 4	4.07% (3.74%-4.40%)	4.62% (4.62%)	5.16% (5.05%-5.27%)	0.00% 0.00%

(Kalimantan), clade 2 represents a population from Mulu, clade 3 represents a population from Java, and clade 4 comprises a population from Sumatra (South Sumatra). Clade 2 (Borneo, Sarawak, Mulu population) is located in one river system with Baram River (type locality of *P. baramica*), so this clade likely represents "true" *P. baramica.* Therefore, other lineages (clade 1, 3, and 4) are remaining unnamed species. We also found the existence of two distinct lineages from Sumatra Island (clade 1 and clade 4).

We assessed the robustness of our phylogenetic tree by examining the bootstrap values and posterior probabilities, and we found that the formation of clades in the phylogenetic tree had high bootstrap values and posterior probabilities, indicating the robustness of these clades. According to Apriliyanto and Sembiring (2016), if the bootstrap value approaches 100% in the Neighbour-Joining and Maximum Likelihood methods, and the posterior probability value is close to 1 in the Bayesian Inference method, the formation of clades can be deemed robust. In our study, we found that the result aligns with this criterion, providing additional evidence for the dependability and precision of our phylogenetic tree reconstruction.

Our genetic distance analysis revealed significant average genetic divergence ranging from 2.75 to 5.16% among clades. These values closely approach the proposed threshold of 3% for intraspecies genetic divergence, as suggested by Fouquet et al. (2007). Our investigation involved a comprehensive examination of ten carefully selected samples collected from three major island populations in Indonesia. Comparative analysis with the control dataset from the sequence data of *Pulchrana baramica* species obtained from genbank revealed noteworthy outcomes. Specifically, two allopatric populations of Java (clade 3) and Borneo, Mulu (clade 2) exhibited an average genetic divergence of 2.75%, thus supporting interspecific genetic divergence. Conversely, the two clades representing the populations from Sumatra Island and Kalimantan Island (identified as clades 1 and 4, respectively) exhibited genetic divergences of 3.50 and 4.83% respectively, suggesting that they do not belong to the same species as *Pulchrana baramica.* These findings demonstrated that the population from Kalimantan (Samarinda) within clade 1 represents a distinct species, separated from clade 2 Sarawak (Mulu) despite both being on one Island of Borneo.

Our study also revealed that genetic differentiation within Sumatra (clade 1 and clade 4) and Borneo (clade 1 and clade 2) are greater than two allopatric populations of Java and Borneo Mulu (clade 2 and 3). We hypothesised that this result can be attributed to the large population sizes and similar habitat and climate conditions at the sampling locations of clades 2 and 3, which may have limited natural selection. Moreover, larger populations have a higher likelihood of gene flow between individ-

uals within the population and a greater chance of gene exchange with other populations. In small populations, gene flow between individuals or with other populations may be more restricted, leading to genetic isolation and the accumulation of genetic differences between populations. The higher genetic within Borneo (clade 1 and clade 2) can be attributed to factors such as differences in population size and habitat, which could induce adaptation and natural selection, resulting in a higher genetic distance despite being on the same island. Additionally, significant genetic distance is observed for clade 4, whereas it has an average genetic distance ranging from 4.07 to 5.15% compared to other clades (clade 1, 2, 3), this is possibly due to various factors such as population size, habitat variations, and stochastic effects. It is important to note that the lack of supporting data regarding morphological data, habitat types, climate conditions, and population sizes, may have influenced the results of the phylogenetic tree analysis in this study. Future studies with larger sample sizes and comprehensive supporting data including morphological data may be necessary to gain a better understanding of the patterns of genetic diversity within each studied population location.

CONCLUSIONS

Our study provides compelling evidence for the existence of cryptic species within the *Pulchrana baramica* species through analysis of the *16S* mtDNA gene, while also exploring their genetic diversity and relationships. Our phylogenetic tree analysis revealed the existence of four distinct clades within the population of *P. baramica*. Furthermore, additional information on morphological and bioacoustic data is needed to determine the taxonomic status of several unnamed species within the population of the *P. baramica* group.

AUTHOR CONTRIBUTION

T.A. and A.H. were in charge of planning, designing, and supervising the entire research process. L.F. and K.W.A. worked in a laboratory (DNA extraction, DNA amplification, agarose gel electrophoresis, data analysis, and manuscript writing). A.R. and E.N.S. provided support for research materials.

CONFLICT OF INTEREST

The authors declare that they have no conflicts of interest. The authors are responsible for the article's content and writing.

REFERENCES

Apriliyanto, V. & Sembiring, L., 2016. *Filogenetika Molekuler: Teori dan Aplikasi.* Innosain, Yogyakarta

Chan, K.O. et al., 2014. A New Species of Frog (Amphibia: Anura: Ranidae) of the *Hylarana signata* Complex from Peninsular Malaysia. *Herpetologica*, 70(2), pp.228–240. doi: 10.1655/HERPETOLOGICA-D-13-00057

Herlambang, A.E. et al., 2022. After 16 years: an update checklist of herpetofauna on the Natuna Islands, Indonesia. *Treubia*, 49(2), pp.67-84. doi: 10.14203/treubia.v49i2.4379

Chowdhury, M. et al., 2021. Molecular characterization of Copy's Frog *Hydrophylax leptoglossa* based on *16s* rRNA gene. *Bangladesh Journal of Zoology*, 49(1), pp.105–115. doi: 10.3329/bjz.v49i1.53686

Darriba, D. et al., 2012. Jmodeltest 2: more models, new heuristics and parallel computing. *Nature Methods*, 9(8), 772. doi: 10.1038/nmeth.2109.

Das, I. et al., 2007. Species diversity, elevational distribution and reproductive models in an amphibian community at the Matang Range, Sarawak (Borneo). *Mitteilungen aus dem Hamburgischen Zoologischen Museum und Institut*, 158, pp.141–174.

Fouquet, A. et al., 2007. Underestimation of Species Richness in Neotropical Frogs Revealed by mtdna Analyses. *PLoS ONE*, 2(10), e1109. doi: 10.1371/journal.pone.0001109

Frost, D.R. 2021. *Amphibian Species of the World: an Online Reference. Version 6.0 (May, 22nd 2023)*. Electronic Database accessible at http://research.amnh.org/herpetology/amphibia/index.html. New York: American Museum of Natural History.

Hamidy, A. et al., 2011. Morphological and genetic discordance in two species of Bornean *Leptobrachium* (Amphibia, Anura, Megophryidae). *Molecular Phylogenetics and Evolution*, 61, pp.904–913. doi: 10.1016/j.ympev.2011.08.020

Hamidy, A. et al., 2012. Detection of cryptic taxa in *Leptobrachium nigrops* (Amphibia, Anura, Megophryidae) with description of two new species, *Zootaxa*, 3398, pp.22–39.

Hebert, P.D., Ratnasingham, S. & Ward, J.R., 2003. Barcoding Animal Life: Cytochrome C Oxidase Subunit 1 Divergences among Closely Related Species. *Proceedings of The Royal Society*, 270, pp.96-99. doi: 10.1098/rsbl.2003.0025

Hedges, S.B., Nussbaum, R.A. & Maxson, L.R., 1993. Caecilian phylogeny and biogeography inferred from mitochondrial DNA sequences of the *12S* rrna and *16S* rRNA genes (Amphibia: Gymnophiona). *Herpetological Monographs*, 7, pp.64-76. doi: 10.2307/1466952

Inger, R.F., 1966. *The Systematics and Zoogeography of the Amphibia of Kalimantan. Field Museum of Natural History*, 52, pp.160-187.

Iskandar, D.T., 1998. *Amfibi Jawa dan Bali: Seri Panduan Lapangan, Cetakan pertama*, Bogor: Puslitbang Biologi–LIPI.

Kumar, S. et al., 2018. MEGA X: Molecular Evolutionary Genetics Analysis across Computing Platforms. *Molecular Biology and Evolution*, 35(6), pp.1547–1549. doi: 10.1093/molbev/msy096.

Leong, T.M. & Lim, B.L., 2003. A new species of *Rana* (Amphibia: Anura: Ranidae) from the highlands of the Malay Peninsula, with diagnostic larval descriptions. *Raffles Bulletin of Zoology*, 51, pp.115–122. doi: 10.5281/zenodo.13229211

Maddison, W.P. & Maddison, D.R., 2021. Mesquite: a modular system for evolutionary analysis. Ver 3.31. http://mesquiteproject.org.

Matsui, M., Mumpuni M. & Hamidy, A., 2012. Description of a New Species of *Hylarana* from Sumatra (Amphibia, Anura). *Current Herpetology*, 31(1), pp.38-46. doi: 10.5358/hsj.31.38

Munir, M. et al., 2018. A New *Megophrys* Kuhl and Van Hasselt (Amphibia: Megophryidae) from southwestern Sumatra, Indonesia. *Zootaxa*, 4442(3), pp.389-412.

Munir, M. et al., 2021. Two new species of *Megophrys* Kuhl and Van Hasselt (Amphibia: Megophryidae) from Sumatra, Indonesia. *Zootaxa*, 5057(4), pp.503-529

Suchard, M.A. et al., 2018. Bayesian phylogenetic and phylodynamic data integration using BEAST 1.10. *Virus Evolution*, 4(1), vey016. doi: 10.1093/ve/vey016.

Van Kampen, P.N., 1923. *The Amphibia of the Indo–Australian Archipelago.* Leiden: E. Brill Ltd.

Research Article

Morphological Structure of the Tongue of *Gekko gecko* in Yogyakarta, Indonesia

Khairunnisa Aqiilah[1], Teguh Budipitojo[1], Hery Wijayanto[1], Vista Budiariati[1], Tri Wahyu Pangestiningsih[1], Ariana[1], Golda Rani Saragih[1], Ulayatul Kustiati[2], Hevi Wihadmadyatami[1]*

1)Department of Anatomy, Faculty of Veterinary Medicine, Universitas Gadjah Mada, Yogyakarta, Indonesia 55281
2)Laboratory of Veterinary Pharmacology, Faculty of Veterinary Medicine, Universitas Brawijaya, East Java, Indonesia, 65151
* Corresponding author, email: heviwihadmadyatami@ugm.ac.id

ABSTRACT

Gekko gecko is a member of the order Squamata from the family Gekkonidae and mainly feeds on small insects. This study aims to determine the morphology of the tongue of *Gekko gecko* through Scanning Electron Microscopy (SEM), hematoxylin–eosin (HE) staining, and immunohistochemistry (IHC). Six adult *Gekko gecko* were obtained from the Special Region of Yogyakarta, and *Gekko gecko* tongue samples were stored in SEM fixative solution and then observed with SEM. For histochemical and IHC staining, tongue samples were processed into paraffin blocks and cut into 8 µm-thick sections. The SEM revealed three types of papillae: dome-shaped papillae at the apex, fan-shaped papillae at the corpus, and scale–like papillae at the radix. Histological observations showed that the tongue of the *Gekko gecko* was composed of tunica mucosa and tunica muscularis, and goblet cells were present in the lamina of the epithelial mucosa. Meanwhile, no taste buds were found. Immunoreactivity against PGP 9.5 was observed on the tunica muscularis of the apex, corpus, and radix. Taken together, this study provides new insight into the tongue morphology of *Gekko gecko* and is dominated by mechanical papillae on the tongue surface.

INTRODUCTION

The Gekko gecko or house gecko is under the class Reptilia, order Squamata, suborder Sauria (Lacertilian), and family Gekkonidae (Hildyard 2001). *Gekko gecko* in Southeast Asia are naturally found in Indonesia, Malaysia, Singapore, the Philippines, Thailand, Vietnam, and Cambodia and have spread to Northeast India, south China, Hong Kong, and Nepal (Rocha et al. 2015). *Gekko gecko* in Indonesia are found in Java, Sumatra, Kalimantan, Sulawesi, Lesser Sunda (Bali), and Maluku. *Gekko gecko* mainly inhabits areas with many trees, such as forests, but are also often found in the building (Carranza & Arnold 2006; Cahyani et al. 2023). It is nocturnal and mainly feed on small insects (Partasasmita et al. 2016).

The tongue is one of the most important parts of the digestive tract. In most reptiles, amphibians, and mammals, the tongue is used to hold food. The tongues of lepidosaurians are divided into three parts: apex, corpus, and radix (Jamniczky et al. 2009). The tongues of most iguanas and geckos are wide and short with a wide and rounded tip (Schwenk 2000). *Gekko gecko* also uses its tongue to clean it eyes because

it has no eyelids ([Kusrini 2019](#)).

The tongues of geckos in the Gekkonidae family have three types of papillae. For example, *Gekko japonicus* have dome-shaped, fan-shaped, and scale–like papillae ([Iwasaki 1990](#)), and *Tarentola annularis* have dome-shaped, fan-shaped, and broad scale–like papillae ([Bayoumi et al. 2011](#)). In *Gekko japonicus*, the epithelia of dome-shaped papillae comprise stratified columnar epithelial cells, whereas the epithelia of fan-shaped papillae comprises stratified squamous epithelial cells ([Iwasaki 1990](#)). Moreover, the epithelia of the dome-shaped papillae of *Tarentola annularis* are composed of non-keratinised stratified squamous epithelial cells, whereas the epithelia of the fan-shaped and broad scale–like papillae are composed of keratinised layered stratified squamous epithelial cells ([Bayoumi et al. 2011](#)). These studies revealed variations in the morphology and distribution of the papillae on the dorsal tongue surfaces in geckos and lizards, but bibliographical data on the structure of tongue papillae of *Gekko gecko* are limited.

MATERIALS AND METHODS
Ethical approval
The experimental procedures were approved by the ethics committee of the Faculty of Veterinary Medicine, Universitas Gadjah Mada, Yogyakarta, Indonesia (approval number: 0101/EC-FKH/Int./2021).

Animal Sample
Gekko gecko were identified at the Animal Systematics Laboratory, Faculty of Biology, Universitas Gadjah Mada. The tongue samples of *Gekko gecko* were obtained from collectors. A high-dose anesthetic combination of ketamine (Kepro, Maagdenburgstraat, Holand) and xylazine (Interchemie, Metaalweg, Holand) was administered: 20 mg/kg body weight for the ketamine and 3 mg/kg body weight for xylazine. *Gekko gecko* tongue samples were prepared by separating the maxilla and mandible. Then, dirt was removed by brushing the tongues of the *Gekko gecko* with a fine brush. The tongue was removed by cutting the base and separating it from the mandible.

Conservation status
According to the International Union for Conservation of Nature Red List of Threatened Species, *Gekko gecko* is categorised as Least Concern. Furthermore, according to Convention on International Trade in Endangered Species of Wild Fauna and Flora, *Gekko gecko* is included in CITES Appendix 2.

Sample Preparation
Three tongue samples were immersed in 4% paraformaldehyde (KgaA, Darmstadt, Germany) for HE (HE; Bio-Optica, Milan, Spain) staining, and three other samples were immersed in SEM fixative solution (0.5% glutaraldehyde (Chem Cruz, Texas, US), 1.5% paraformaldehyde (Nacalai Tesque, Tokyo, Japan), Hepes (Chemcruz), and PBS (Nacalai Tesque, Tokyo, Japan) for at least 6–8 h.

The length of the tongue was measured using calipers from the tip to the base and each sample was measured in triplicate. The samples were then observed with a camera (Canon EOS 7000D, Tokyo, Japan). After macroscopic observation, the samples were prepared for Scanning Electron Microscopy (SEM) and light microscopy.

Scanning Electron Microscopy

Tongue samples were fixed for at least 24 h, divided into apex, corpus, and radix parts, and washed with PBS (Nacalai Tesque, Tokyo, Japan). Then, the samples were dehydrated in an ethanol solution (KgaA, Darmstadt, Germany) for 5–10 min twice and fixed on a conductive metal plate with carbon tape. The samples were dried using a vacuum system (BUEHLER- Castable Vacuum System, Stuttgart, Germany) for 60 min and then coated with a coater (JEOL-auto fine coater JEC-3000FC, Tokyo, Japan) using platinum for 120 s. Finally, each sample was inserted into an electron microscope (JEOL JSM-6510LA, Tokyo, Japan) and observed at a voltage of 10 kV and magnifications of 30×, 100×, and 300×.

Histological Staining

Tongues fixed in 4% paraformaldehyde (KgaA, Darmstadt, Germany) fixative solution for at least 24 h were cut into three parts: apex, corpus, and radix. The samples were then washed with running water, dehydrated with a graded ethanol solution, cleared with xylol (Leica, Wetzler, Germany), placed in paraffin (Leica Biosystems, Wetzlar, Germany), and embedded in paraffin blocks. The samples were cut transversely and the resulting 8 μm-thick sections were stained with hematoxylin and eosin (HE; Bio-Optica, Milan, Spain).

Immunohistochemistry for PGP 9.5

The samples were fixed in 4% paraformaldehyde (KgaA, Darmstadt, Germany) for 24 h and processed for routine paraffin embedding. The blocks were cut into 8 μm-thick cross-sectional sections, mounted on gelatin-coated microscope slides, and processed for immunohistochemistry. Serial sections were deparaffinized and rehydrated, rinsed several times with PBS, and blocked with 10% normal goat serum for 1 h. Polyclonal rabbit anti-PGP 9.5 (Invitrogen, Waltham, MA, USA) was diluted in a permeabilising solution (PBS, 0.2% Triton X 100, 0.1% sodium azide) according to optimal dilutions and placed on the slides overnight at room temperature. The sections were rinsed with PBS and incubated with secondary antibody poly-HRP goat anti-rabbit IgG (Fine test, Wuhan, China) for 60 min. After DAB was added (Fine test, Wuhan, China), the sections were observed with a light microscope (Nikon, Tokyo, Japan).

RESULTS

Morphology of the Tongue

Gross Morphology

Macroscopic observations of the *Gekko gecko* tongue show four surfaces: a dorsal surface, a ventral surface, and two lateral surfaces. The tongue is triangular, flat, short, and pale pink, with a wide tip and rounded shape, widening and thickening posteriorly. It is attached to the base of the buccal cavity along the ventral median line and has a total length of approximately 2 cm. It is divided into three parts: the apex which is the most anterior part of the tongue, the corpus, and the radix which is the most posterior near the larynx and blackish in color. The difference can be seen through the dorsal view. Papillae lingualis are found on the entire dorsal to lateral surface. The ventral sulcus is found on the ventral surface along the apex region to the radix region of the tongue (Figure 1).

The apex region of the *Gekko gecko* tongue starts from the anterior part to the curve that separates the apex and corpus regions. The *Gekko gecko* tongue in the apex region has a rounded and flattened tip shape anteriorly and its size thickens further posteriorly. Similar to other types of reptiles, *Gekko gecko* has bifurcated or branching tongue. However, the

bifurcation on the *Gekko gecko* tongue is extremely small and does not split the apex of the tongue deeply, and thus the branching or bifurcation can only be seen from an extremely close distance. Papillae lingualis, which has a smooth and flat surface, is found on the dorsal surface of the tongue's apex.

The corpus region is between the apex region on the anterior part of the tongue, and the radix region is on the posterior part. The border of the corpus region with the apex region can be observed from the curve that separates the apex and corpus regions (Figure 1). It can also be located according to changes in the shapes of the scattered papillae (Figures 2 and 3). The tongue papillae scattered on the *Gekko gecko* tongue in the apex region have flat and smooth surfaces. By contrast, the tongue papillae scattered in the corpus region have rougher surfaces than those in the apex region. The border of the corpus and radix regions shows "V"-shaped branching, where the corpus region ends at the beginning of the branching and continues to the radix region.
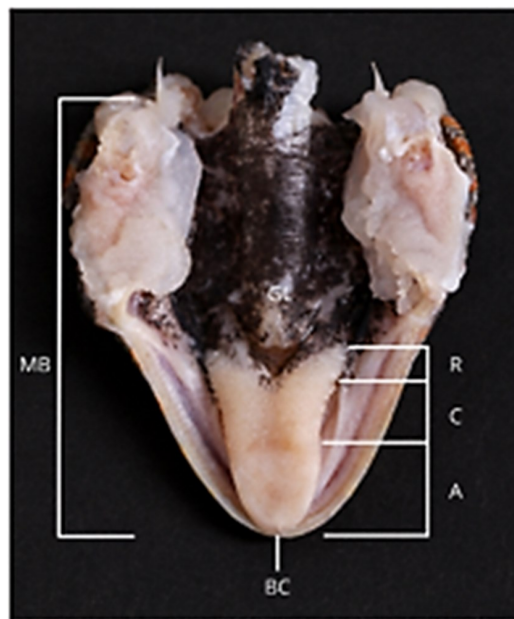
Figure 1. Macroscopic view of *Gekko gecko* tongue in the dorsal section (A = apex region, C = corpus region, R = radix region, BC = bifurcation, = GL = glottis, MB = mandible).

The radix region of the *Gekko gecko*'s tongue is the most posterior, borders the glottis, and is characterised by "V"-shaped branching that splits the region. The glottis is found between the two radix regions. The presence of blackish patches on the posterior part of the tongue radix characterise the radix region.

Scanning Electron Microscopy

Apex

The dorsal surface of the *Gekko gecko*'s tongue at the apex was observed using a scanning electron microscope at 30× magnification. Tongue papillae was found at the apex, and the apex has a smooth texture and flat surfaces and are arranged tightly (100× magnification). Bifurcation or branching on the anterior part of the apex at 100× magnification is fairly small and does not split the apex of the tongue as deeply as that in other types of reptiles. At 300× magnification, the apex contains dome-shaped papillae, which are polygonal and have different shapes. Dome-shaped papillae have short and uniform size, rendering the dorsal surface of the apex smooth and flat (Figure 2).
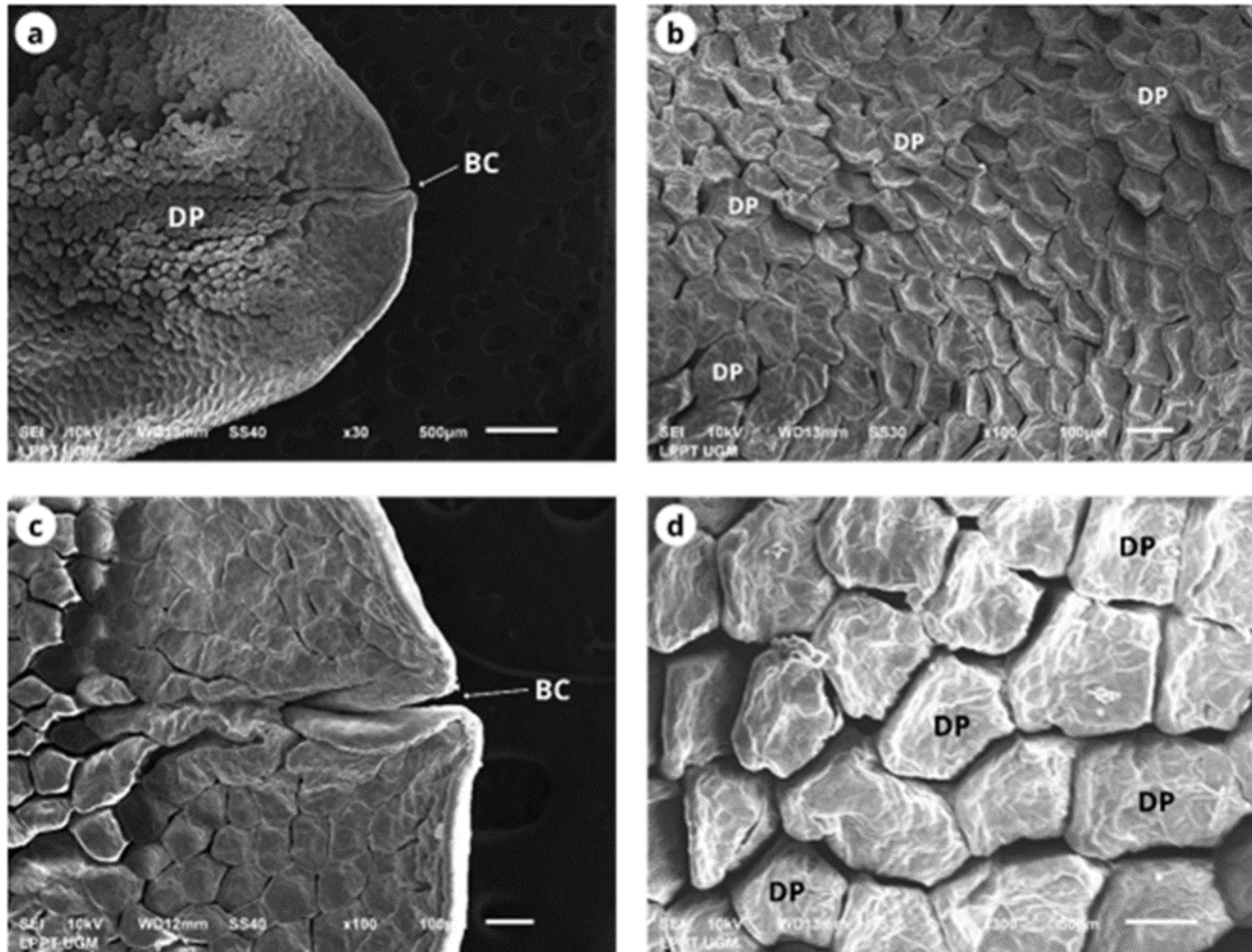
Figure 2. Scanning Electron Microscopy (SEM) image of the tongue of *Gekko gecko* at the apex. (a) *Gekko gecko*'s tongue apex section at 30× magnification; (b) apex at 100× magnification shows visible papillae with smooth and flat surfaces; (c) anterior part of the apex at 100× magnification shows visible bifurcation (BC); (d) apex at 300× magnification shows visible dome-shaped papillae (DP).

Corpus

The dorsal surface of the *Gekko gecko*'s tongue at the corpus was observed with a Scanning Electron Microscopy at 30× magnification. The dorsal surface has uneven and smooth texture, similar to the apex. At 100× magnification, the dorsal surface in the corpus section shows long and slender fan-shaped tongue papillae arranged loosely, thus showing an uneven and smooth surface similar to the dorsal surface of the tongue at the apex. At 300× magnification, the surfaces of the fan-shaped papillae have a small polygonal shapes with tapered ends (Figure 3).

Radix

The dorsal surface of the radix of *Gekko gecko*'s tongue was observed with a Scanning Electron Microscope at 30× magnification. The dorsolateral side has tongue papillae, and the dorsal surface of the radix part has an area without papillae (NP) on the middle dorsal side and can be observed at 30× magnification. At 100× magnification, the dorsolateral side of the radix part of the tongue show tongue papillae with folds and scale–like shapes. At 300× magnification, the papillae have wide triangular shapes and tips that point caudally (Figure 4).

Histological Structure of the Tongue

The histological structure of the *Gekko gecko*'s tongue was observed using the HE-stained cross-sections of the tongue apex, corpus, and radix, and the morphology of each part was further observed. *Gekko gecko*'s tongue is
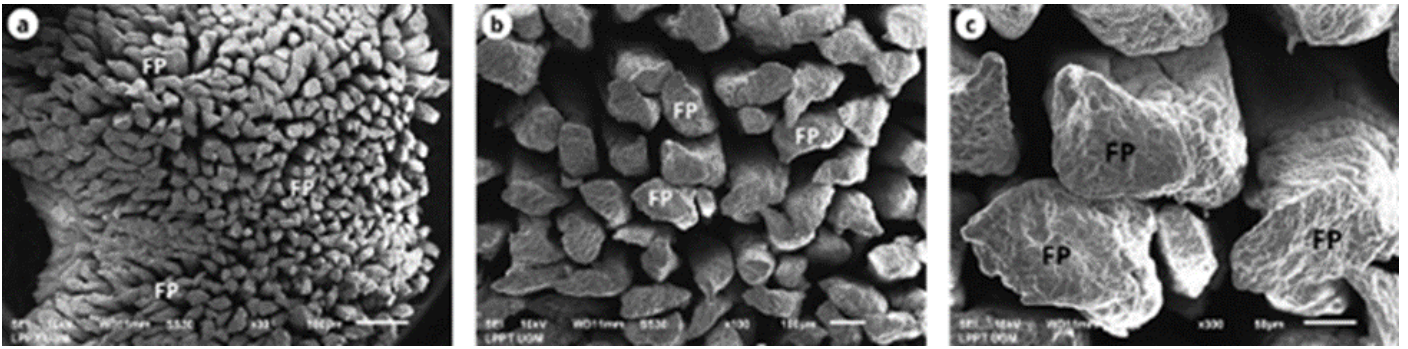
Figure 3. Scanning Electron Microscopy (SEM) image of the corpus of *Gekko gecko*'s tongue: (a) corpus section at 30× magnification; (b) corpus at 100× magnification shows papillae with loose surfaces; (c) corpus with 300× magnification shows the formation of fan-shaped papillae (FP).
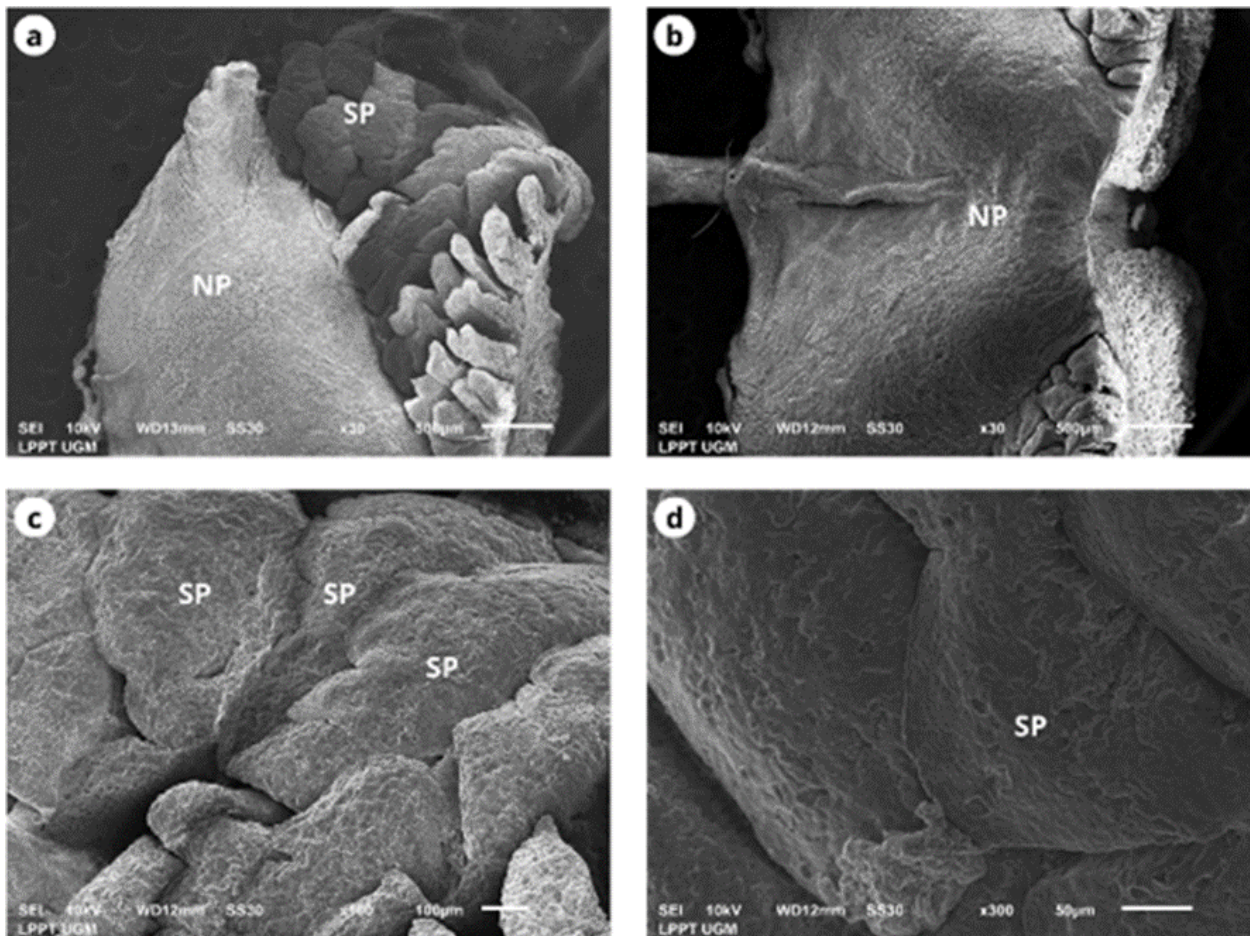
Figure 4. Scanning Electron Microscopy (SEM) image of the radix section. (a) Radix section at 30× magnification; (b) radix at 30× magnification showing the tongue area without papillae; (c) radix at 100× magnification showing scale–like papillae (SP); (d) scale–like papillae at 300× magnification.

microscopically composed of two tunicas: tunica mucosa (lamina epithelial mucosa and lamina propria mucosa) and tunica muscularis composed of several muscles. The histological structures of the *Gekko gecko*'s tongue have similar arrangements in the apex, corpus, and radix, especially in the corpus and radix

Apex
The histological structure of the HE-stained *Gekko gecko*'s tongue at the apex is flat and wide. The apex is histologically composed of two tunica, namely, tunica mucosa and tunica muscularis. The tunica mucosa is composed of lamina epithelial mucosa and lamina propria mucosa. The muco-

sal lining of the tunica mucosa is lined by the stratified squamous epithelium. The tunica muscularis is composed of several types of muscles: dorsal longitudinal muscle, which is in the dorsal part of the tunica muscularis, transverse muscle, and several hyoglossus muscles in the ventral part. The papillae lingualis is found on the dorsal and lateral parts of the tongue. The tongue papillae found on the tongue of *Gekko gecko* at the apex are dome-shaped and appear like short stalks with flat and wide surfaces (Figure 5).

Corpus

The histological structure of the *Gekko gecko*'s tongue was observed using HE-stained corpus section. The structure shows a wide and flat shape but is thicker than that observed in the apex. The corpus is composed of two tunica, namely tunica mucosa and tunica muscularis. Tunica mucosa comprises lamina epithelial mucosa and lamina propria mucosa. The LEM is composed of stratified squamous epithelium. Tunica muscularis is composed of several types of muscles different from those observed in the apex. The muscularis tunica in the corpus is composed of genioglossus muscles on the left and right regions that forms the corpus's lateral border. The entoglossal processus of the hyoid bone is found at the ventral center between the hyoglossus muscles. The tongue of papillae are found on the dorsal to lateral part of the tongue. The tongue papillae found on the corpus are slender and long fan-shaped papillae (Figure 6).
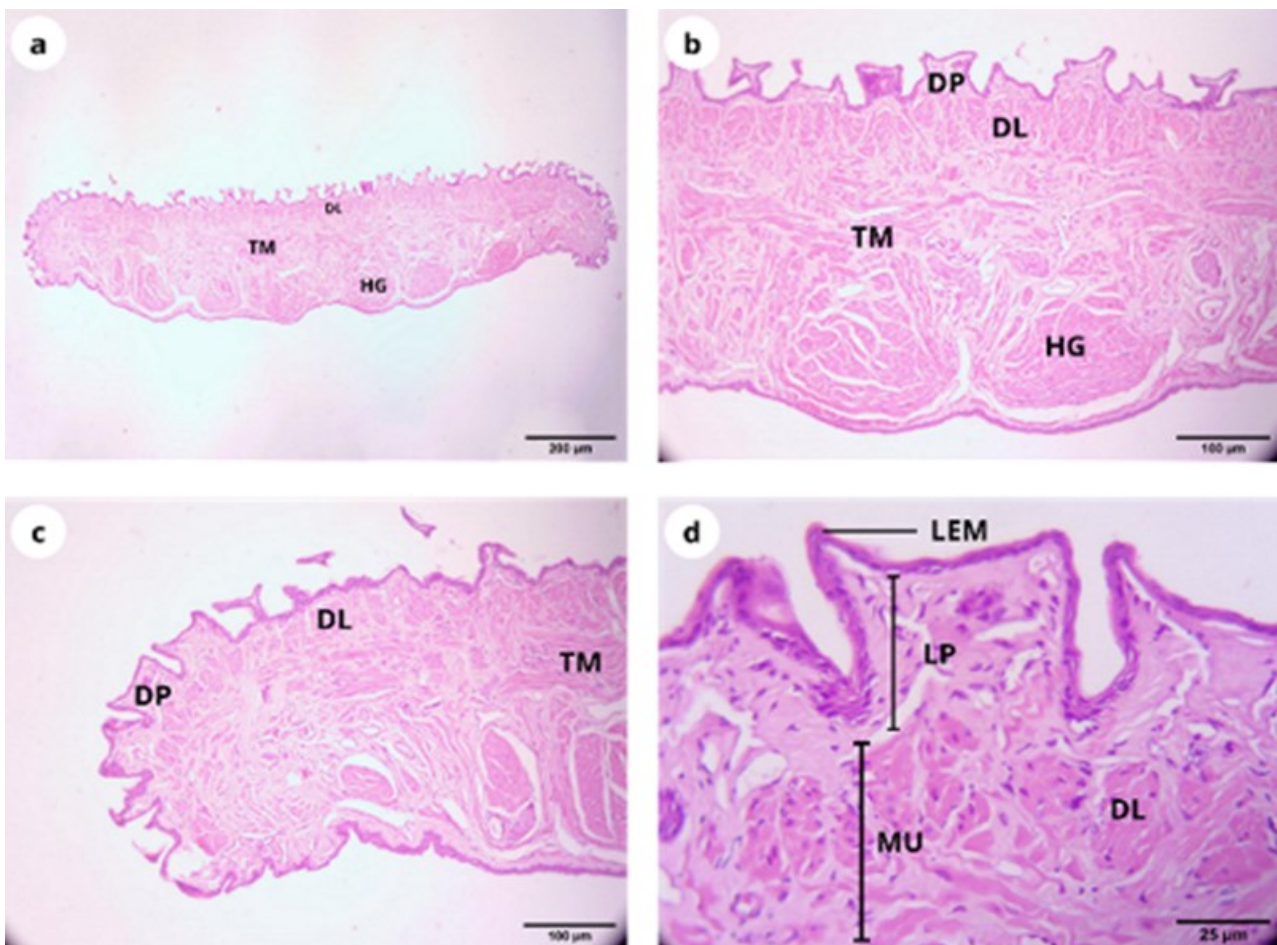
Figure 5. Histological structure of the tongue of a *Gekko gecko* in hematoxylin–eosin-stained apex. (a) The overall shape of the histological structure of the *Gekko gecko*'s tongue at the apex at 4×10 magnification; (b) apex at 10×10 magnification shows the dorsal longitudinal muscle (DL), transverse muscle (TM), and hyoglossus muscle (HG); (c) apex at 10×10 magnification shows the formation of dome-shaped papillae (DP); (d) dome-shaped papillae with a 40×10 magnification shows the lamina epithelial mucosa (LEM), lamina propria mucosa (LP), lamina muscularis (MU).
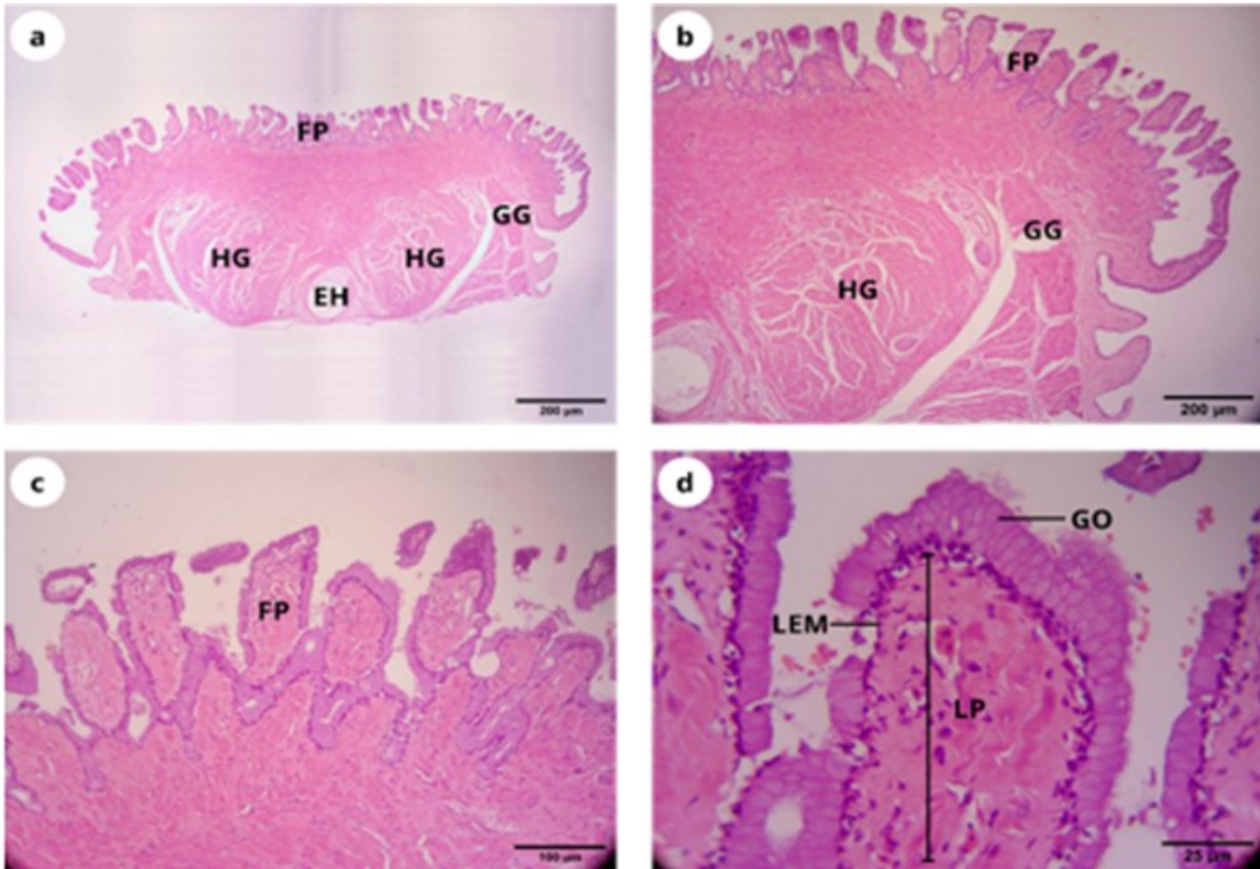
Figure 6. Histological structure of the tongue hematoxylin–eosin–stained corpus. (a) The overall shape of the histological structure of the *Gekko gecko* tongue in the corpus section with a 4 × 10 magnification; (b) corpus with a 10 × 10 magnification showing fan-shaped papillae (FP), genioglossus muscle (GG), and hyoglossus muscle (HG); (c) corpus with 10 × 10 magnification showing fan-shaped papillae (DP); (d) fan-shaped papillae with 40 × 10 magnification showing lamina epithelial mucosa (LEM), lamina propria mucosa (LP), goblet cluster (GO), and hyoid bone (EH).

Radix

The histological structure of the *Gekko gecko*'s tongue in HE-stained radix section was observed. The structure in this section has a wide and flat shape and is thicker than that in the apex but thinner than that in the corpus. The radix and corpus have a similar histological structure arrangement. The radix is composed of two tunics, namely, tunica mucosa and tunica muscularis. Tunica mucosa comprises LEM and lamina propria mucosa. The lamina epithelial mucosa is composed of stratified squamous epithelium. Tunica muscularis in the radix has a similar arrangement to that in the corpus; the genioglossus muscle on the left and right sections of the tongue formed the lateral border of the radix. The entoglossal processus of the hyoid bone on the tongue radix is at the ventral center between the two hyoglossus muscles. The tongue papillae is on the dorsolateral part of the tongue, and the dorsal center has no tongue papillae. The tongue papillae found on the radix part of the *Gekko gecko*'s tongue are scale–like papillae with shaped-like folds resembling scales (Figure 7).

Immunoreactivity of PGP 9.5 on *Gekko gecko*'s tongue

Cells positive for PGP 9.5 protein were observed in the sensory cells of the muscle fiber of the tunica muscularis. Immunoreactive cells are dominant in the genioglossus muscles in the corpus and radix and scattered in the tunica muscularis on the apex (Figures 8A, 8B, 8C).
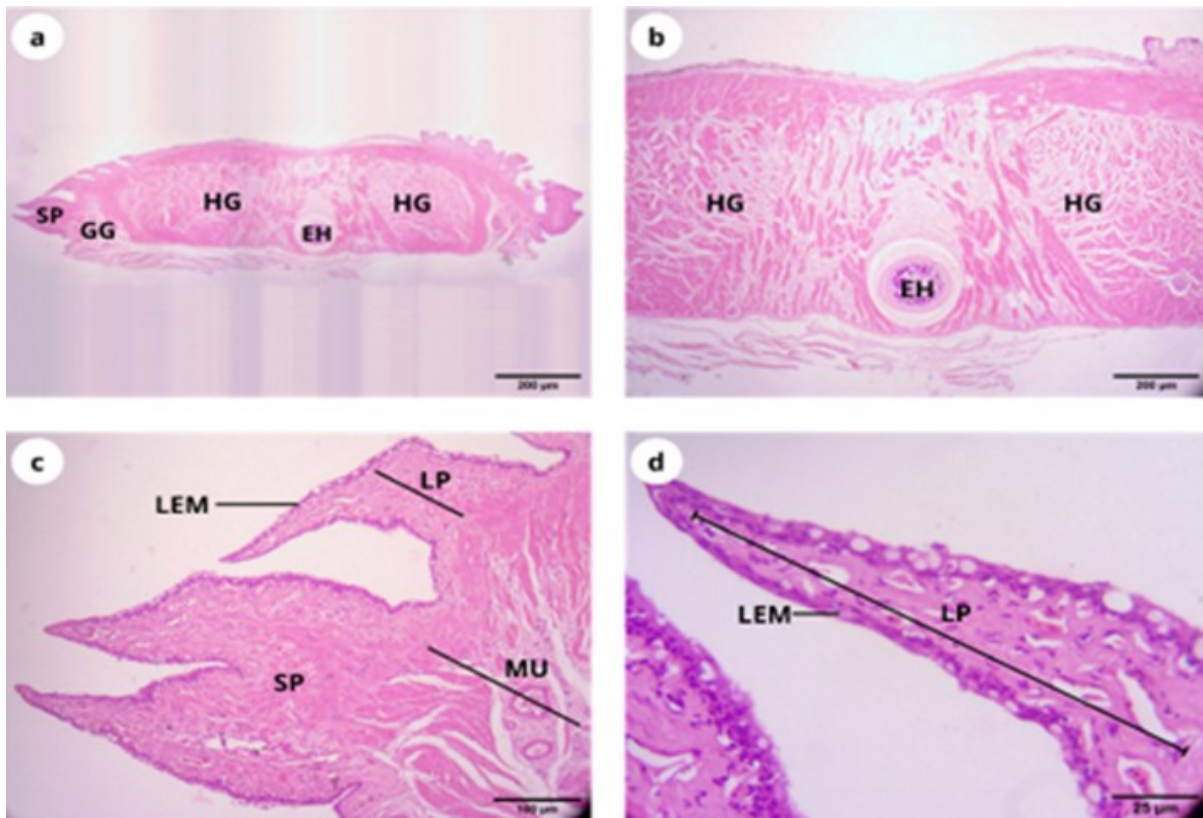
Figure 7. Histological structure of the tongue of a *Gekko gecko* in hematoxylin–eosin-stained radix section. (a) The overall shape of the histological structure of the *Gekko gecko*'s tongue in the radix section at 4 × 10 magnification; (b) radix with a 10 × 10 magnification showing scale–like papillae (SP), genioglossus muscle (GG), and hyoglossus muscle (HG); (c) radix at 10 × 10 magnification showing the formation of scale–like papillae (SP); (d) scale–like papillae with 40 × 10 magnification showing Lamina Epithelial Mucosa (LEM) and Lamina Propria Mucosa (LP); Hyoid Bone (EH), Lamina Muscularis (MU).
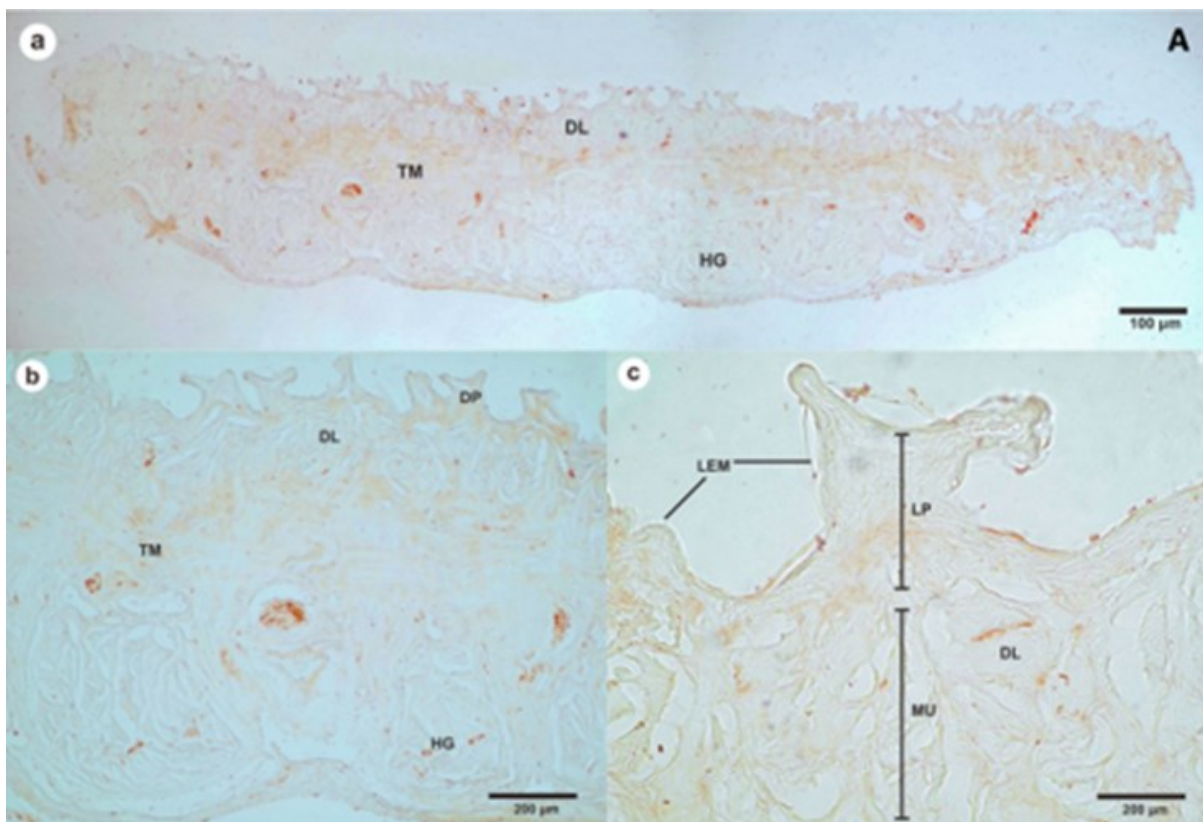
Figure 8A. Micrographs of cells immunoreactive to PGP 9.5 in the apex. The sensory cells immunoreactive for PGP-9.5 protein are scattered in the tunica muscularis, (a) Scale bar: 100 μm; (b and c) Scale bar: 200 μm; dorsal longitudinal muscle (DL); tunica muscularis, transverse muscle (TM); hyoglossus muscle (HG), lamina epithelial mucosa (LEM); Lamina muscularis (LM).
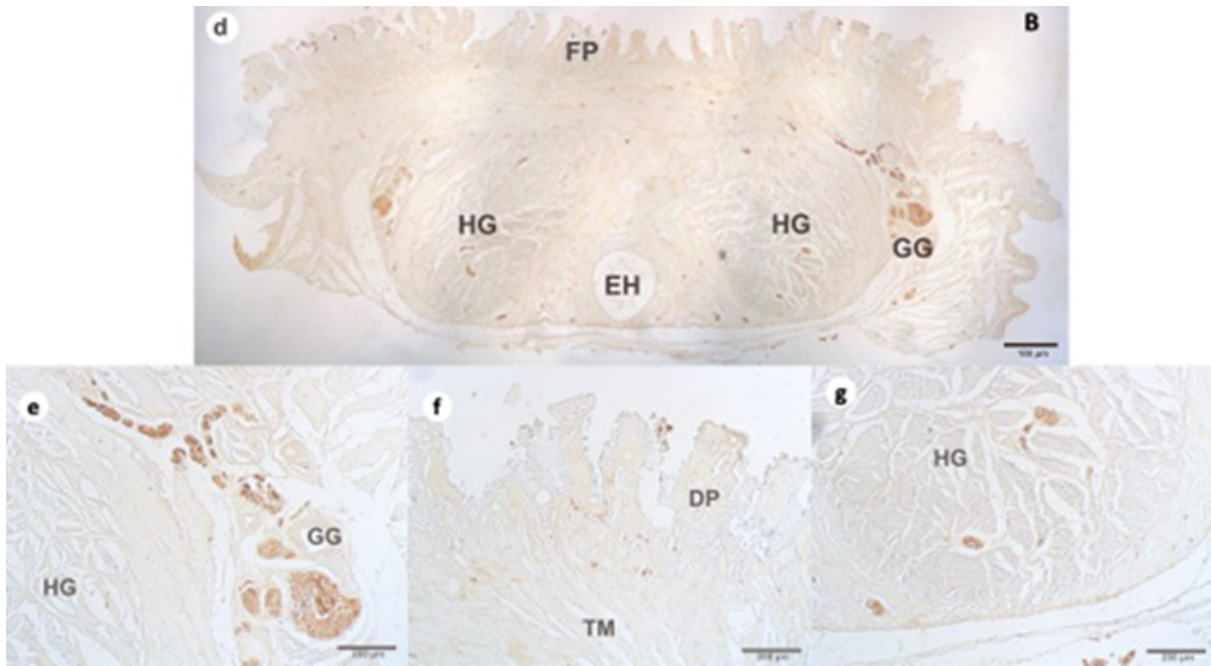
Figure 8B. Micrographs of cells immunoreactive to PGP 9.5 in the corpus. Sensory cells immunoreactive for PGP-9.5 protein are scattered in the tunica muscularis mainly on the genioglossus muscle (GG), (d) Scale bar: 100 µm; (e, f, g) Scale bar: 200 µm; Fan-shaped Papillae (FP); Dome-shaped Papillae (DP); Transverse Muscle (TM); Hyoglossus Muscle (HG), Lamina Epithelial Mucosa (LEM); Lamina muscularis (LM); Hyoglossus Muscle (HG).
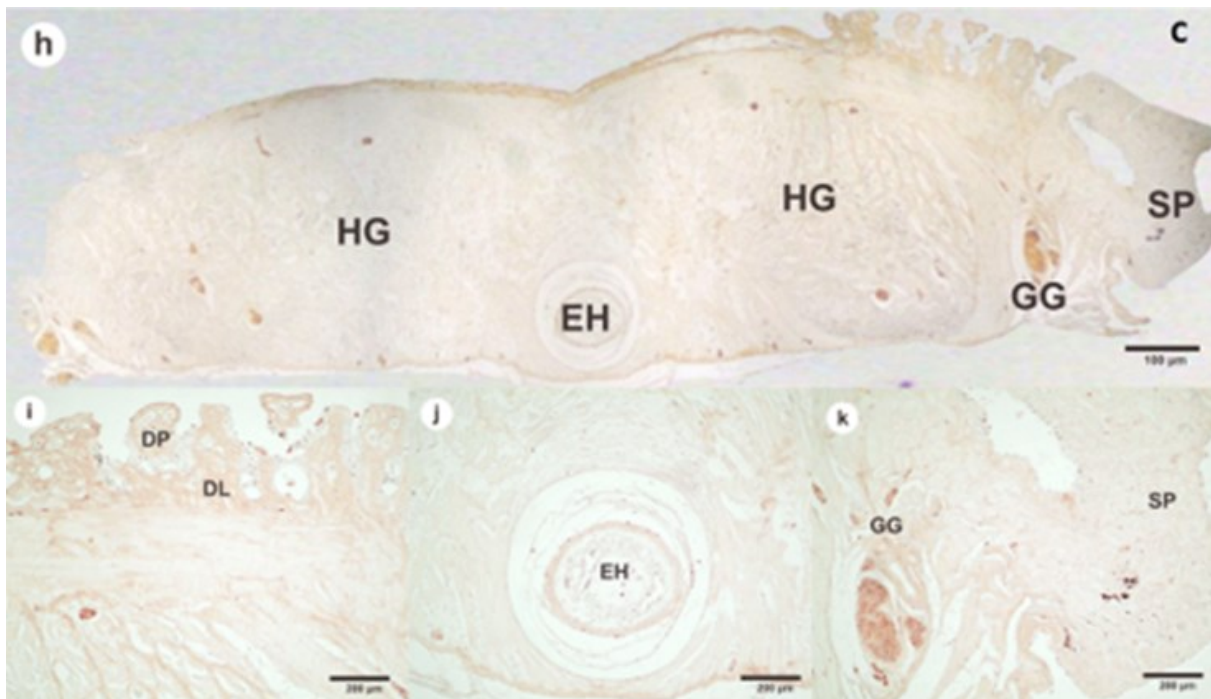
Figure 8C. Micrographs of cell immunoreactive to PGP 9.5 in the radix. The sensory cells immunoreactive to PGP-9.5 protein are present scattered in the tunica muscularis mainly on the genioglossus muscle (GG), (h) Scale bar: 100 µm; (i,j, and k) Scale bar: 200 µm; Scale–like Papillae (SP); Hyoglossus Muscle (HG); Hyoid Bone (EH).

DISCUSSION

Macroscopic observation showed that the *Gekko gecko*'s tongue has a similar shape to the tongues of other lizard species, such as *Gekko japonicus* (Iwasaki 1990), *Eublepharis macularius* (Jamniczky et al. 2009), *Uromastyx aegypticus* (Bayoumi et al. 2011), *Tarentola annularis* (Bayoumi et al. 2011), and *Hemidactylus flaviviridis* (Al-Fartwsy et al. 2016), which have triangular and dorsoventrally flattened tongues. Bifurcation is a special formation found on the apex of a reptile's tongue, dividing the tip of the

apex. *Gekko gecko* shows bifurcation at the apex, but the bifurcation is extremely small and does not split the apex deeply in contrast to the bifurcation found in other reptiles, such *Elaphe climacophora* (Iwasaki et al. 1996), *Psammophis sibilans* (El-Mansi et al. 2020), *Varanus niloticus* (Sheren et al. 2018), and *Varanus bengalensis* (Pathak et al. 2015), which exhibit deep branching. Small and shallow bifurcation is also found in other lizards, such as *Gekko japonicus* (Iwasaki 1990), *Eublepharis macularius* (Jamniczky et al. 2009), *Tarentola annularis* (Bayoumi et al. 2011), and *Hemidactylus flaviviridis* (Al-Fartwsy et al. 2016). The tongue the house gecko is similar to that tongue of a plant-eating lizard. *Gekko gecko* and *Uromastyx aegypticus* have different bifurcation shapes (Bayoumi et al. 2011). According to Bayoumi et al. (2011), bifurcation in reptiles is phylogenetic in nature and thus has no significant effect on diet. However, diet can affect the morphological structure of a bifurcation. Wide and deep bifurcation in *Uromastyx aegypticus*, which is a herbivorous lizard, is suitable for cutting various types of plants, whereas a narrow and shallow bifurcation found in the insectivorous *Tarentola annularis* and *Gekko gecko* is suitable for swallowing insects (Bayoumi et al. 2011). In snakes, the tongue does not function as an organ and help in food ingestion but is used for olfaction in cooperation with the vomeronasal organ (Bayoumi et al. 2011). Difference in bifurcation shape between snakes and monitor lizards has deep ramifications, and the small and shallow bifurcation in the tongues of house geckos may be due to difference in prey search process (Schwenk 1994). Reptiles with deep bifurcations (snakes, amphisbaenians, teiids, varanids, and helodermatids) can follow prey trails through odor or scent, whereas iguanas and gekkonids showing bifurcation with small indentations do not search for prey by following scent trails (Schwenk 1994).

SEM results showed that the tongue papillae on the dorsal surface of *Gekko gecko*'s tongue were similar to those found on the tongues of other lizards, including *Takydromus tachydromoides* (Iwasaki & Miyata 1985), *Gekko japonicus* (Iwasaki 1990), *Eublepharis macularius* (Jamniczky et al. 2009), *Uromastyx aegypticus* (Bayoumi et al. 2011), *Hemidactylus flaviviridus* (Al-Fartwsy et al. 2016; Bayoumi et al. 2011), *Tarentola annularis* (Bayoumi et al. 2011), and *Uromastyx aegypticus* (Bayoumi et al. 2011). The dorsal surface of the apex of *Gekko gecko*'s tongue was smooth and flat and composed of polygonal dome-shaped papillae, which were short, uniform, and tightly arranged. The DP on the tongue of the house gecko are similar to those found on the dorsal surface of the apex in the tongues of *Gekko japonicus* (Iwasaki 1990) and *Tarentola annularis* (Bayoumi et al. 2011). According to Schwenk (2000), papillae on the apex of a gecko's tongue are smooth and flat and can be used to clean the eyes. Long and slender FP are found in the corpus. The papillae are loosely arranged, and thus the dorsal surface has an uneven and smooth surface. The FP on the corpus are similar to those found in *Gekko japonicus* (Iwasaki 1990) and *Tarentola annularis* (Bayoumi et al. 2011). Meanwhile, scale–like papillae on the dorsolateral side in the radix have tight folds resembling wide triangular scale shapes and tips leading to the caudal portion. The scale–like papillae on the radix of the house gecko's tongue are similar to those found on the radices of the tongues of *Gekko japonicus* (Iwasaki 1990) and *Tarentola annularis* (Bayoumi et al. 2011).

The histological structure was then observed using 8 µm-thick samples. The outermost layer of the *Gekko gecko*'s tongue is a LEM composed of stratified squamous epithelial cells. Clusters of goblet cells were found in the LEM in the FP located in the corpus. The mucosal LP is beneath the LEM which is composed of connective tissues. Tunica muscu-

laris is composed of several types of muscles that are in the ventral part of the LP mucosa. The apex of the *Gekko gecko*'s tongue is histologically composed of two tunica, namely, tunica mucosa and tunica muscularis. Tunica mucosa is composed of LEM and LP mucosa. The LEM of the *Gekko gecko*'s tongue at the apex is composed of stratified squamous epithelial cells, similar to that found in the tongues of *Eublepharis macularius* (Jamniczky et al. 2009) and *Tarentola annularis* (Bayoumi et al. 2011). The tunica muscularis is composed of several types of muscles, including the dorsal longitudinal muscle in the most dorsal part of the tunica muscularis, transverse muscle, and several bundles of hyoglossus muscles in the ventral part. The muscle structure found at the apex of the *Gekko gecko*'s tongue is similar to that of *Eublepharis macularius* (Jamniczky et al. 2009). When used in cleaning the eyes, the apex of *Gekko gecko*'s tongue is assisted by several bundles of hyoglossus muscles arranged on the ventral part of the apex (Schwenk 2000). The structure of the muscles that constitutes the apex of the *Gekko gecko*'s tongue is similar to that of the *Gerrhonotus multicarinatus* lizard's tongue (Smith & Mackay 1990), where four bundles of hyoglossus muscles are found, each surrounded by a circular muscle, a transverse muscle on the dorsal part of the hyoglossus muscles, and a DL muscle (Smith & Mackay 1990). The tongue papillae at the apex of the *Gekko gecko*'s tongue—the dome-shaped papillae—appear like short stalks with flat and wide surfaces. Taste buds were not found in the apex of the *Gekko gecko*'s tongue. According to Jamniczky et al. (2009), most geckos may not have taste buds. This feature could have been influenced by the form of adaptation. Interestingly, immunohistochemical staining with PGP 9.5 showed immunoreactivity in the apex, corpus, and radix portions containing tunica muscularis, especially in the genioglossus muscles. These findings demonstrated that the gecko's tongue represented one of the most specialised compound sensory systems among vertebrates. This system may play an important role in chemical and mechanical information processing for preys. Moreover, a correlation may be hypothesised with the vomeronasal system stimulated by tongue flicking. Food odor revealed by the nasal olfaction triggers the mechanism of tongue flicking, and the vomeronasal system provides information on the volatile components of the odor (Filoramo & Schwenk 2009). Furthermore, the tongue papillae found at the apex of the *Gekko gecko*'s tongue are similar to those found at the apex of the tongue of *Eublepharis macularius* (Jamniczky et al. 2009), which are DP called cuboid papillae and at the apex of the tongue of *Tarentola annularis* (Bayoumi et al. 2011), which are DP shaped like short stalks.

The corpus and radix part of the *Gekko gecko*'s tongue are largely the same but differ in the papillae they contain. The corpus and radix of *Gekko gecko*'s tongue are histologically composed of tunica mucosa and tunica muscularis. The lining of lamina epithelialis mucosa is composed of stratified squamous epithelial cells, similar to that in the tongue of Tarentola annularis (Bayoumi et al. 2011). Tunica muscularis in the corpus and radix have similar arrangements, namely, a genioglossus muscles that forms the lateral border of the radix of the tongue and two bundles of hyoglossus muscles on the left and right portions. The entoglossal process of the hyoid bone is found on the tongue radix in the center between two hyoglossus muscles. The muscle structure that composes *Gekko gecko*'s tongue in the corpus and radix is similar to that in the tongue of *Eublepharis macularius* (Jamniczky et al. 2009); that is, two bundles of hyoglossus muscles on the right and left are separated by a connective tissue, and between the two muscles, a processus entoglossal of the hyoid bone is located in the ventral center of the tongue. The muscle structure

in *Gekko gecko*'s in the corpus and radix has a similar arrangement to that in the tongue of the *Gerrhonotus multicarinatus* (Smith & Mackay 1990). Two bundles of hyoglossus and genioglossus muscles form the lateral boundary of the tongue. The histological structures of the corpus and radix of *Gekko gecko*'s tongue differ in the type of papillae. The corpus contains long and slender FP on the dorsal and lateral parts, whereas the radix contains scale–like papillae with folds resembling scales found on the dorsolateral tongue. Papillae found on the corpus and radix are similar to those found on the tongue of *Eublepharis macularius* (Jamniczky et al. 2009). FP are called leaf-like papillae on the corpus, and scale–like papillae are called fungiform papillae on the radix. The papillae on the corpus of the *Gekko gecko*'s tongue are also similar to those found on the corpus of the tongue of *Tarentola annularis* (Bayoumi et al. 2011), which also show FP. Clusters composed of goblet cells are found in the FP in the corpus and produce mucus in the oral cavity (Jamniczky et al. 2009).

The differences in the type of tongue papillae between the *Gekko gecko* and other lizards can be attributed to species-specific variations in tongue morphology. Different reptilian species exhibit distinct types of tongue papillae (Gewily et al. 2021). These variations are observed across different reptilian species and among mammals (Emura & El-Bakary 2014).

Furthermore, the presence of specific tongue papillae types, such as filiform, fungiform, foliate, and vallate papillae, are common in mammals, including rodents (Čížek et al. 2016; Wannaprasert et al. 2019). The diversity, distribution, and morphology of tongue papillae have been studied extensively in various mammals (Erdoğan et al. 2014; Toprak 2023). Additionally, the tongue papillae of different mammalian species exhibit unique characteristics, such as the presence of gustatory and nongustatory papillae, which are distributed in a species-specific manner on the tongue surface (Pastor et al. 2017). In the *Gekko gecko*, the gustatory papillae are not present.

The differences in the type of tongue papillae between *Gekko gecko* and other lizard species can be attributed to species-specific adaptations in tongue morphology. These variations reflect the diverse evolutionary adaptations that have shaped the tongue structures of reptiles and mammals, highlighting the importance of tongue papillae in various functions, such as taste perception, and mechanical manipulation of food (Jackowiak & Godynicki 2007; Manley & Kraus 2010). Additionally, the morphology of tongue papillae can vary regionally within the tongue and is influenced by factors, such as feeding habits, climate conditions, and type of food particles. Moreover, the complexity of tongue structures, including the papillae, can be linked to specific modes of adaptations of reptiles, such as geckos, which are known for their exceptional high-high frequency vision and hearing (Abbate et al. 2019).

CONCLUSION

This work offers the first description of the anatomy of the *Gekko* gecko's tongue in Yogyakarta, Indonesia, also examining the distribution of tongue papillae. This information may offer insight into *Gekko gecko*'s feeding strategies and ecological roles.

AUTHORS CONTRIBUTION

Conceptualisation, H.W.; Methodology, H.W.; Software, K.A., T.W.P., and V.B.; Validation, K.A., A., and T.B.; formal analysis, K.A., G.R.S., HyW., V.B.; Investigation, K.A. and U.K.; Resources, K.A., T.W.P., and HW.; Data Curation, K.A., A.; Writing—Original Draft Preparation,

CONFLICT OF INTEREST
None of the authors have any competing interests to disclose.

REFERENCES

Abbate, F. et al., 2020. The tongue of Leopard Gecko (*Eublepharis macularius*): LM, SEM and confocal laser study. *Anatomia Histologia Embryologia*, 49(1), pp.51-59. doi: 10.1111/ahe.12483.

Al-Fartwsy, A.R., Al-Shuaily, E.H. & Al-Kubaisi, Z.A., 2016. Morphological, Histological and Ultrustructural Study of the Tongue in House Geecko (*Hemidactylus flaviviridis*) Lizard. *Iraqi Journal of Biotechnology*, 15(1), pp.1–11.

Bayoumi, S.S., Abd-Elhameed, A.E. & Mohamed, E.S.M., 2011. Comparative studies on the dorsal lingual surface of two Egyptian squamate reptile with two different feeding habits. *The Egyptian Journal of Experimental Biology (Zoology)*, 7(2), pp.203–211. doi: 10.5455/egyjebb.20230607015627.

Carranza, S. & Arnold, E.N., 2006. Systematics, biogeography, and evolution of Hemi-dactylus Gekko (Reptilia: Gekkonidae) elucidated using mitochondrial DNA sequences. *Molecular Phylogenetics and Evolution*, 38(2), pp.531–545. doi: 10.1016/j.ympev.2005.07.012.

Cahyani, N.K.D. et al., 2023. Population study of tokay gecko (*Gekko gecko*) in Bali Province, Indonesia (Studi populasi Tokek Rumah (*Gekko gecko*) di Provinsi Bali, Indonesia). *Jurnal Biologi Indonesia*, 19(2), pp.125-133. doi: 10.47349/jbi/19022023/125.

Čížek, P. et al., 2017. Light and scanning electron microscopy of the tongue of a degu (*Octodon degus*). *Anatomical Science International*, 92 (4), pp.493-499. doi: 10.1007/s12565-016-0346-x.

El-Mansi, A.A. et al., 2020. Structural and functional characterization of the tongue and digestive tractof *Psammophis sibilans* (Squamata, Lamprophiidae): Adaptive strategies for foraging and feeding behaviors. *Microscopy and Microanalysis*, 26(3), pp.524-541. doi: 10.1017/S1431927620001312

Emura, S. & Bakary, N.E.R.E., 2014. Morphology of the lingual papillae of egyptian buffalo (*Bubalus bubalis*). *Okajimas Folia Anatomica Japonica*, 91(1), pp.13-17. doi: 10.2535/ofaj.91.13.

Erdoğan, S., Arias, S.V. & Pérez, W., 2015. Morphology of the lingual surface of south American fur seal (*Arctocephalus australis*) and sea lion (*Otaria flavescens*). *Microscopy Research and Technique*, 78(2), pp.140-147. doi: 10.1002/jemt.22456.

Filoramo, N.I. & Schwenk, K., 2009. The mechanism of chemical delivery to the vomeronasal organs in squamate reptiles: A comparative morphological approach. *Journal of Experimental Zoology Part A: Ecological Genetics and Physiology*, 311(1), pp.20–34. doi: 10.1002/jez.492.

Gewily, D.I. et al., 2021. Ultrastructural comparison between the tongue of two reptilian species endemic in Egyptian fauna; Bosc's fringe-toed lizard *Acanthodactylus boskianus* and Sinai fan-fingered gecko *Ptyodactylus guttatus*. *Microscopy Research and Technique*, 84(9), pp.1977-1991. doi: 10.1002/jemt.23753.

Hildyard, A., 2001. *Endangered wildlife and plants of the world* (Vol. 5), Marshall Cavendish Corporation.

Iwasaki, S.I. & Miyata, K., 1985. Scanning electron microscopy of the lingual dorsal surface of the Japanese lizard, Takydromus tachydromoides. *Okajimas Folia Anatomica Japonica*, 62(1), pp.15–26. doi: 10.2535/ofaj1936.62.1_15.

Iwasaki S., 1990. Fine structure of the dorsal lingual epithelium of the lizard, *Gekko japonicus* (Lacertilia, Gekkonidae). *American Journal of Anatomy*, 187(1), pp.12-20. doi: 10.1002/aja.1001870103.

Iwasaki, S.I., Yoshizawa, H. & Kawahara, I., 1996. Three dimensional ultrasctructure of the surface of the tongue of the rat snake, *Elaphe climacophora*. *The Anatomical Record*, 245(1), pp.9–12. doi: 10.1002/(sici)1097-0185(199605)245:1%3C9::aid-ar2%3E3.0.co;2-v.

Jackowiak, H. & Godynicki, S., 2007. Light and scanning electron microscopic study on the structure of the lingual papillae of the feather-tail glider (*Acrobates pygmeus*, Burramyidae, Marsupialia). *The Anatomical Record*, 290(11), pp.1355-1365. doi:10.1002/ar.20606.

Jamniczky, H.A. et al., 2009. Morphology and histology of the tongue and oral chamber of *Eublepharis macularius* (Squamata: Gekkonidae), with special reference to the foretongue and its role in fluid uptake and transport. *Evolutionary Biology*, 36(4), pp.11-15. doi: 10.1007/s11692-009-9072-9.

Kusrini, M.D., 2019. *Metode Survei dan Penelitian Herpetofauna*, IPB Press.

Manley, G. & Kraus, J., 2010. Exceptional high frequency hearing and matched vocalizations in Australian pygopod geckos. *Journal of Experimental Biology*, 213(11), pp.1876-1885. doi: 10.1242/jeb.040196.

Partasasmita, R., Iskandar, J. & Malone, N., 2016. Karangwangi people's (South Cianjur, West Java, Indonesia) local knowledge of species, forest utilization and wildlife conservation. *Biodiversitas*, 17(1), pp.8-12. doi: 10.13057/biodiv/d170123.

Pastor et al., 2017. Ultrastructure of lingual papillae in common chimpanzee (*Pan troglodytes*) foetus, newborn and adult specimens. *Anatomia Histologia Embryologia*, 46(5), pp.431-438. doi: 10.1111/ahe.12287.

Pathak, S.K. et al., 2015. Morphological characterization of Bengal Monitor Lizard (*Varanus bengalensis*). *Animal Science Reporter*, 9(2), pp.70-74.

Rocha et al., 2015. Occurrence of the tokay gecko *Gekko gecko* (Linnaeus 1758) (Squamata, Gekkonidae), an exotic species in southern Brazil. *Herpetology Notes*, 8, pp.8-10. doi: 10.1163/15685381-440405SEH.

Schwenk, K., 1994. Why Snakes Have Forked Tongues. *Science*, 263(5153), pp.1573-1577. doi: 10.1126/science.263.5153.1573.

Schwenk, K., 2000. *Feeding: Form, Function, and Evolution in Tetrapod Vertebrates*, Academic Press.

Sheren, A.Z.A., Nasr, E.S. & Hassan, S.S., 2018. Light and scanning electron microscopic observations on the tongue of *Nile monitor, Varanus niloticus niloticus*. *International Journal of Advanced Research in Biological Sciences*, 5(4), pp.1–11. doi: 10.22192/ijarbs.2018.05.04.001

Smith, K.K. & Mackay, K.A., 1990. The morphology of the intrinsic tongue Musculature in snakes (Reptilia, Ophidia): functional and phylogenetic implications. *Journal of Morphology*, 205(3), pp.307–324. doi: 10.1002/jmor.1052050306.

Toprak, B., 2023. Investigations on the light and scanning electron microscopic structure of the lingual papillae in the angora goat (*Capra hircus*): ii. mechanical papillae. *Anatomia Histologia Embryologia*, 52 (2), pp.327-335. doi: 10.1111/ahe.12890.

Wannaprasert, T., Phantuma-opas, P. & Jindatip, D., 2019. Morphology and microstructure of the tongue of the lesser bamboo rat (*Cannomys badius*). *Acta Zoologica*, 101(3), pp.282-291. doi: 10.1111/ azo.12293.

Review Article

Diversity Status of Bamboo in Sumatra: A Review

Muhammad Azli Ritonga[1], Syamsuardi[2]*, Nurainas[2], I Putu Gede P. Damayanto[3]

1) Doctoral Program, Department of Biology, Faculty of Mathematics and Natural Sciences, Universitas Andalas. Jl. Unand, Kampus Limau Manis, Padang, 25163, West Sumatra, Indonesia.
2) Department of Biology, Faculty of Mathematics and Natural Sciences, Universitas Andalas. Jl. Unand, Kampus Limau Manis, Padang, 25163, West Sumatra, Indonesia.
3) Herbarium Bogoriense, Research Center for Biosystematics and Evolution, National Research and Innovation Agency (BRIN), Indonesia. Jl. Raya Jakarta-Bogor, km 46, Cibinong, Bogor, 16911, West Java, Indonesia.
* Corresponding author, email: syamsuardi@sci.unand.ac.id

ABSTRACT

Prior to initiating the conservation effort, conducting a bamboo species inventory in a specific area is crucial for obtaining information about the diversity status of the species in that region. Species inventorying is a fundamental step in ensuring that conservation efforts are targeted, effective, and based on sound scientific data. Regrettably, status of bamboo diversity in Sumatra is unavailable. Therefore, a study was conducted to determine the status of bamboo diversity in Sumatra. The study gathered data from literature review. It covered bamboo species, their statuses (endemic, introduced, ex-situ conservation, and threatened), and encompassed the main Sumatra Island and surrounding smaller islands. Species were re-identified and validated. Conservation status was assessed based on IUCN categories. There are 73 species of bamboo in the Sumatra region, representing 10 genera: *Bambusa* (11 species), *Chimonobambusa* (1 species), *Dendrocalamus* (10 species), *Dinochloa* (2 species), *Gigantochloa* (26 species), *Melocanna* (1 species), *Neololeba* (1 species), *Phyllostachys* (1 species), *Schizostachyum* (19 species), and *Thyrsostachys* (1 species). Eighteen species of Sumatran bamboo are known as introduced species, and 30 species are endemic to Sumatra, with the majority belonging to *Gigantochloa* (15 species). The least represented are *Bambusa* and *Dinochloa*, each having one endemic species. *Bambusa heterostachya*, *Dendrocalamus giganteus*, and *Dendrocalamus membranaceus* fall into the "least concern" (LC) category on the IUCN Red List, while the remaining 70 species have not been evaluated. A total of 44 species have been planted (conserved) in botanical gardens in Indonesia, while the remaining 29 species have not yet been conserved.

INTRODUCTION

Sumatra is an island in the western region of Indonesia, bordered by the Bay of Bengal to the north, the Malacca Strait to the east, the Sunda Strait to the south, and the Indian Ocean to the west (KBBID 2023). Astronomically, the island of Sumatra extends from 95°E to 105°E and from 6°N to 6°S. The island of Sumatra has an area of approximately 480,793.68 km² (Retnowati & Rugayah 2019) dan is surrounded by several small islands, such as the islands of Weh, Simeulue, Nias, Siberut, and Bengkalis. The mainland of Sumatra comprises 8 provinces, from north to south, namely Aceh, North Sumatra, West Sumatra, Riau, Jambi,

Bengkulu, South Sumatra, and Lampung (BPS 2023). Two additional provinces consist of archipelagos territories situated to the east of the primary Sumatran landmass, specifically the provinces of Kepulauan Bangka Belitung and Kepulauan Riau (BPS 2023). This means there are a total of 10 provinces in the Sumatra area.

Sumatra is well-known for its rich biodiversity, making it a significant repository of germplasm and a hub of endemism (Nursanti & Adriadi 2018). In 2017, it was reported that Sumatra harbors 10,259 plant and fungi species (Retnowati & Rugayah 2019). Widjaja et al. (2014) approximated that 23% or 1,891 species out of a total of 8,391 plant species in Sumatra in 2014 were endemic. For example, there are 39 (75%) endemic species of *Impatiens* (Balsaminaceae) in Sumatra from a total of 52 species of Indonesian *Impatiens* (Utami & Damayanto 2023). The mountainous forests of Sumatra harbor a diverse array of plant species (Ismaini et al. 2015; Sujarwanta & Zen 2020). Forest cover in Sumatra was reported to be 11.4 million hectares in 2013 (Purba et al. 2014). One plant species that displays high diversity in Sumatra is bamboo (*see* Widjaja 2019).

Bamboo belongs to the family Poaceae and sub-family Bambusoideae, which is related to grasses. Bamboo typically has a cylindrical, hollow, woody stem known as a culm that is fibrous and has nodes, with branches of leaves growing from each of the nodes. Some species, however, can be found to have rectangular culms, as seen in *Chimonobambusa quadrangularis* (Franceschi) Makino (Damayanto & Muhaimin 2017). Bamboo culms, for example in *Dendrocalamus,* have the potential to grow to significant diameters and heights (Widjaja 2001), reaching up to 25 cm in diameter near the base and 30 meters in height. Culm internodes of bamboo can be more than 1 m long, as seen in some of *Schizostachyum.* Generally, bamboo have erect culm, such as in *Schizostachyum* species (Damayanto & Widjaja 2016). However, bamboo can also be found scrambling in *Chloothamnus* species (Damayanto et al. 2020a) or as a climber in *Dinochloa* species (Damayanto 2018a).

There is an approximate total of 1,439 bamboo species globally (Widjaja et al. 2014), and within Indonesia, it is estimated that there are approximately 176 bamboo species (Widjaja 2019). Most of the bamboos in Indonesia are endemic, and more than half of these species have been used by local communities (Widjaja & Karsono 2005). For example, there are 10 endemic species of bamboo in the Lesser Sunda Islands, and seven among them are used for a variety of purposes, including as building materials, weaving, construction materials, walking sticks, charcoal, handicrafts, baskets, Balinese offerings, and musical instruments (Damayanto et al. 2023). The main issue with the utilization of endemic species of bamboo is the potential for them to become rare or even face the risk of extinction. To prevent extinction, botanical gardens play an important role by having a special responsibility for preserving plants and educating the public about their importance (Sanders et al. 2018).

Prior to initiating the conservation phase, conducting a species inventory in a specific area is crucial for obtaining information about the diversity status of the species in that region. Species inventorying is a fundamental step in ensuring that conservation efforts are targeted, effective, and based on sound scientific data. Regrettably, status of bamboo diversity in Sumatra is unavailable. According to Purba et al. (2014), approximately 1,530,156 hectares, equivalent to an annual rate of 382,539 hectares, were estimated to have been deforested in Sumatra from 2009 to 2013. However, some endemic bamboo species are found growing in the forests of Sumatra (*see* Widjaja 1997). Therefore, a study was conducted to determine the status of bamboo diversity in Sumatra. This re-

search is expected to be used as baseline data by stakeholders in bamboo resource management efforts in Indonesia. Furthermore, this research is also expected to clarify the presence of several bamboo species that are suspected to be questionable in Sumatra, such as *Bambusa lako* Widjaja (Sari 2011), *Bambusa ventricosa* McClure (Ervany et al. 2020), *Dinochloa scandens* (Blume ex Nees) Kuntze (Sujarwanta & Zen 2020), *Gigantochloa baliana* Widjaja & Astuti (Widjaja 2019), and *Schizostachyum blumei* Nees (Riastuti et al. 2019; Sujarwanta & Zen 2020).

MATERIALS AND METHODS

The research was conducted at Andalas University in September–October 2023. Data was gathered through an extensive review of reputable sources including scientific articles, research reports, and related publications focused on bamboo species in Sumatra. The acquired data encompassed bamboo species and their respective statuses, including endemism, introduction, ex-situ conservation, and IUCN Red List, within the region of Sumatra. The region of Sumatra in this study comprises not only the main plains of Sumatra Island but also the surrounding small islands, in accordance with the phytogeographic region outlined by Steenis-Kruseman (1950) (Figure 1). Bamboo species were validated by being re-identified based on the photos and descriptions shown in the references. The established validation criteria involved ensuring that morphological descriptions or photos matched the provided species names. In cases where this information was lacking, the author leaned on their experience from explorations in Sumatra to verify the existing species. All names of the bamboo species were validated using Vorontsova et al. (2016) and several online data sources (Damayanto et al. 2020b). Conservation status was determined based on categories and criteria listed in the International Union for Conservation of Nature's (IUCN) red list, such as not evaluated (NE), data deficient (DD), least concern (LC), near threatened (NT), vulnerable (VU), endangered (EN), critically endangered (CR), extinct in the wild (EW), and extinct (EX), which can be accessed through https://www.iucnredlist.org (IUCN 2023). We referred to the website https://makoyana.brin.go.id (Makoyana 2023) for information on the ex-situ conservation of bamboo species in each of Indonesia's botanical gardens. In order to determine endemic and introduced bamboo species, the information was gathered from the works of Widjaja (2019) and relevant publications. All data were analyzed and presented descriptively.

RESULTS AND DISCUSSION

There are 73 species of bamboo in Sumatra region (Table S1, several photos of the species are in Figure 2), representing 10 genera, namely *Bambusa* Schreb, *Chimonobambusa* Makino, *Dendrocalamus* Nees, *Dinochloa* Buse, *Gigantochloa* Kurz ex Munro, *Melocanna* Trin, *Neololeba* Widjaja, *Phyllostachys* Siebold & Zucc, *Schizostachyum* Nees, and *Thyrsostachys* Gamble. Among these bamboo genera, the most abundant species were *Gigantochloa* (26 species), followed by *Schizostachyum* (19 species), *Bambusa* (11 species), and *Dendrocalamus* (10 species) (Figure 3). The remaining genera each had one to two species. Nine taxa were reported only as identified up to the genus level in Sumatra (Table 1) and several species of bamboo that reportedly found in Sumatra were not included in this study because they did not meet our validation criteria, namely *Bambusa lako* Widjaja, *Bambusa ventricosa* McClure, *Chloothamnus elegantissimus* (Hassk.) Henrard, *Dinochloa scandens* (Blume ex Nees) Kuntze, *Gigantochloa baliana* Widjaja & Astuti, and *Schizostachyum blumei* Nees.

Figure 1. Phytogeographic region of Sumatra (orange colour) based on Steenis-Kruseman (1950). km = kilometers. (Source: QGis Hannover v. 3.16).

Figure 2. Several bamboo species in Sumatra. A. *Bambusa spinosa*, B. *Bambusa tuldoides*, C. *Bambusa vulgaris*, D. *Dendrocalamus luteus*, E. *Dinochloa malayana*, F. *Gigantochloa scortechinii*, G. *Schizostachyum brachycladum*, H. *Schizostachyum silicatum*, I. *Thyrsostachys siamensis* (Photos: Muhammad Azli Ritonga [A, B, C, G, H, I], I Putu Gede P. Damayanto [D, E, F]).

Table 1. Taxa were identified up to the genus level in Sumatra.

Species	References						
	Saputri 2013	Widjaja 2019	Rahayu & Ervianti 2020	Fitmawati et al. 2020	Fitmawati et al. 2021a	Fitmawati et al. 2021b	Syauqi et al. 2023
Bambusa sp.				+			
Dinochloa sp.			+				
Dinochloa sp.3		+					
Schizostachyum sp.	+						
Schizostachyum sp.2		+					
Gigantochloa sp.				+	+	+	
Gigantochloa sp.1							+
Gigantochloa sp.2							+
Gigantochloa sp.3							+

Notes: + = presence/yes

Eighteen species of Sumatran bamboo were known as introduced species, namely *Bambusa* (*B. balcooa, B. bambos, B. farinacea, B. heterostachya, B. multiplex,* and *B. tuldoides*), *Chimonobambusa* (*C. quadrangularis*), *Dendrocalamus* (*D. asper, D. brandisii, D. giganteus, D. latiflorus, D. membranaceus,* and *D. strictus*), *Gigantochloa* (*G. apus*), *Melocanna* (*M. baccifera*), *Phyllostachys* (*P. aurea*), *Schizostachyum* (*S. pergracile*), and *Thyrsostachys* (*T. siamensis*) (Table S1, Figure 4). There are 30 endemic bamboo species in Sumatra, with the majority belonging to *Gigantochloa* (15 species), while the least represented are *Bambusa* and *Dinochloa*, each having one endemic species (Table S1, Figure 4). Among the 73 bamboo species in Sumatra, *B. heterostachya, D. giganteus,* and *D. membranaceus* fall into the least concern (LC) category on the IUCN Red List. The status of the remaining 70 species has not been evaluated (Figure 5). A total of 44 species have been planted (conserved) in botanical gardens in Indonesia, while the remaining 29 species have not yet been conserved (Table S1, Figure 6).
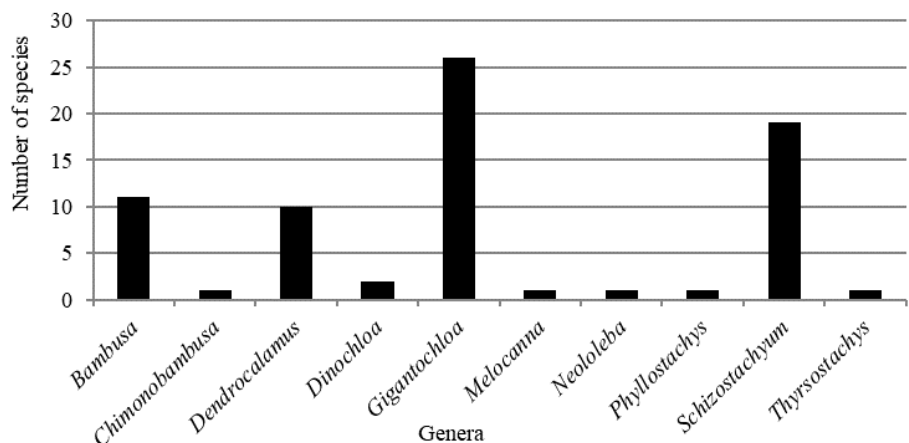
Figure 3. Number of bamboo species in Sumatra.
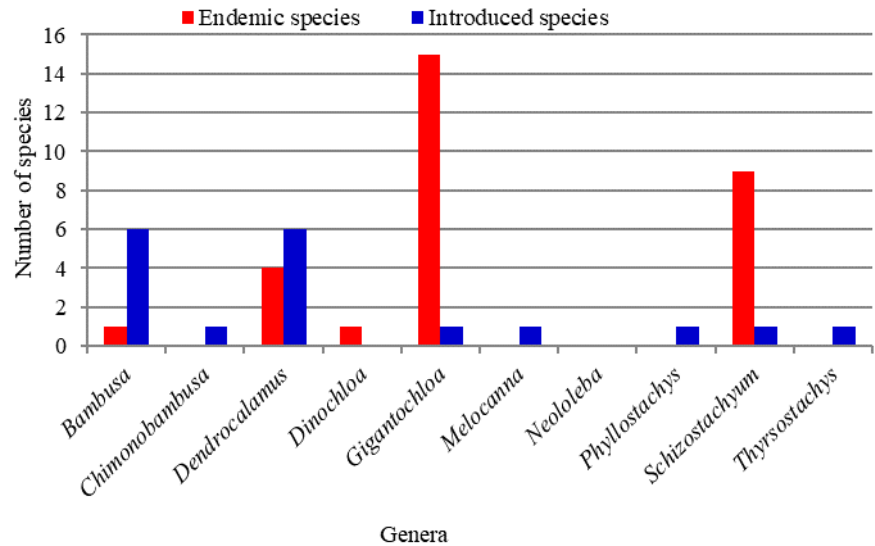
Figure 4. Number of introduced and endemic species of bamboo in Sumatra.
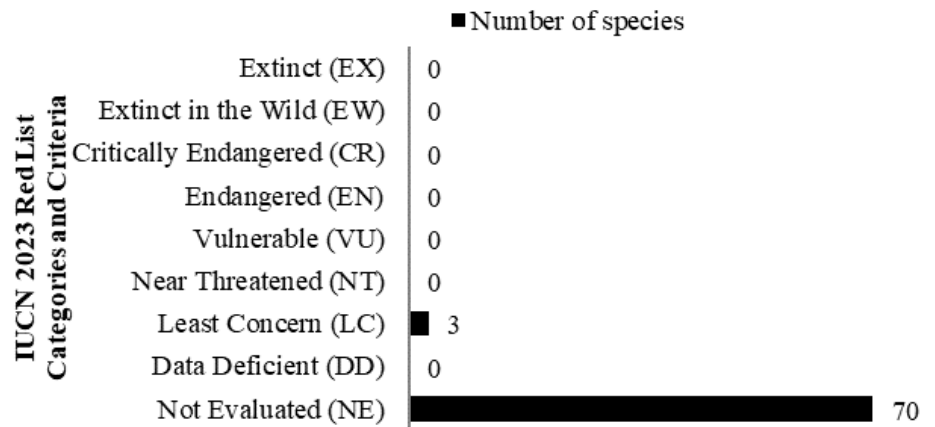
Figure 5. Conservation status of bamboo species in Sumatra based on IUCN 2023 red list.
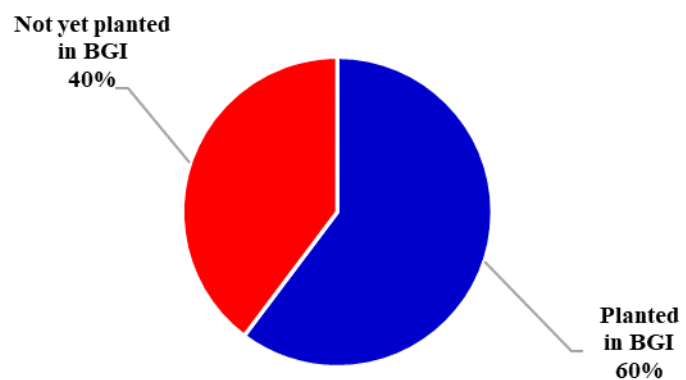
Figure 6. Percentage of ex-situ conservation of bamboo species in Botanical Gardens of Indonesia (BGI).

DISCUSSION

A total of 73 bamboo species and 10 genera were discovered in the Sumatra region. Compared to bamboo genera in Indonesia, the bamboo genera in Sumatra constitute approximately 42% of the total bamboo genera in Indonesia (24 genera) (Damayanto & Fefirenta 2021). Meanwhile, in

comparison to several major islands in Indonesia (Figure 7), the bamboo genera in Sumatra represent about 53% of all bamboo genera in Java (19 genera) (Widjaja 2019) and approximately 83% of all bamboo genera in Sulawesi and Papua respectively (each with 12 genera) (Damayanto et al. 2016b; Ervianti et al. 2019). The bamboo genera in Java are comparatively higher than in Sumatra due to the introduction of several bamboo species, including those from outside Indonesia, into the Botanical Gardens in Java, for instance, in Botanical Gardens of Bogor, Cibodas, Purwodadi, and several other regional botanical gardens (*see* Lestarini et al. 2012; Cahyanto et al. 2016; Ariati et al. 2019; Sujarwo et al. 2019; Wahidah et al. 2021; Kurniawan et al. 2022; Makoyana 2023). The comprehensive flora exploration conducted by botanical garden researchers across Indonesia also contributes to the continual increase in the number of bamboo genera.
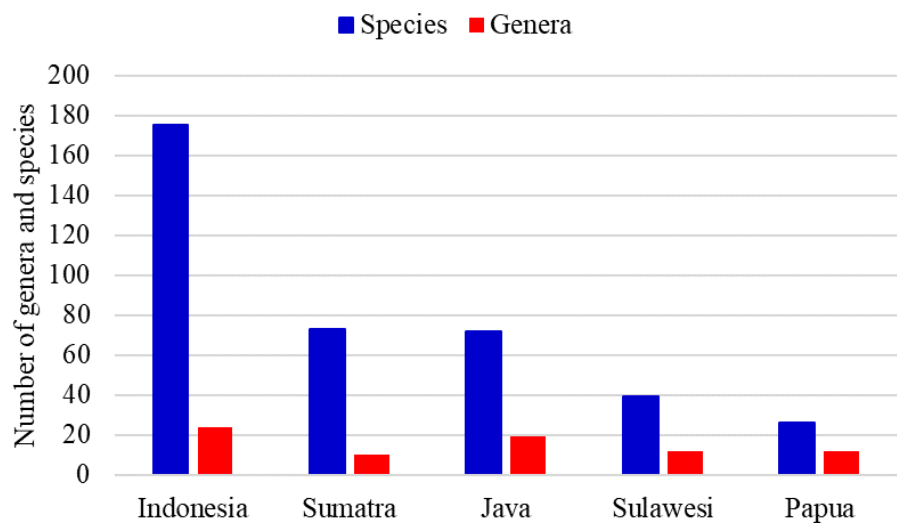
Figure 7. Comparison of bamboo genera and species on several major islands in Indonesia. The data for Indonesia were from Damayanto and Fefirenta (2021), the data for Java were processed from Widjaja (2019), the data for Sulawesi were from Ervianti et al. (2019), and the data for Papua were from Damayanto et al. (2016b).

The bamboo genera in Sumatra mostly (67%) consist of native Indonesian genera (*Bambusa, Dendrocalamus, Dinochloa, Gigantochloa, Neololeba*, and *Schizostachyum*), with only a portion (33%) being introduced genera from outside Indonesia (*Chimonobambusa, Melocanna, Phyllostachys*, and *Thyrsostachys*) (*see* Widjaja et al. 2014; Damayanto & Fefirenta 2021). Widjaja (2019) reported the presence of *Cephalostachyum* (*Cephalostachyum pergracile* Munro) in Sumatra. Additionally, both Widjaja (2001) and Liana (2020) mentioned this genus existence in Java. However, it is important to note that *Cephalostachyum pergracile* is a synonym of *Schizostachyum pergracile* (Munro) R.B.Majumdar (*see* Vorontsova et al. 2016). Consequently, the genus *Cephalostachyum* was not included in this study. *Neololeba* is known to be native to the eastern part of Indonesia, for instance, in Sulawesi, Maluku, and Papua (Widjaja 1997). It is possible that species within the *Neololeba* genus (*Neololeba atra*) and other genera such as *Melocanna* (*Melocanna baccifera*) have been introduced to Sumatra. For example, *Bambusa glaucophylla* has been introduced to Java from Singapore in the 1970s (Widjaja 1997). Later, this bamboo has also been introduced to Great Giant Pineapple Collection Garden in Lampung (Widjaja 1998). On the other hand, Damayanto and Muhaimin (2017) reported that *Chimonobambusa* (*Chimonobambusa quadrangularis*) was introduced

and has become an invasive species in Sumatra, particularly in Gunung Sibayak and Sibolangit Tourist Park, North Sumatra. In Java, this species has become invasive due to its use as a boundary plant between Cibodas Botanical Gardens and Gunung Gede-Pangrango National Parks (Mutaqien et al. 2011). *Chimonobambusa quadrangularis,* which originally comes from South China, was brought to the Cibodas Botanical Gardens in West Java from Japan (Damayanto & Muahimin 2017). Meanwhile, *Phyllostachys* (*Phyllostachys aurea*) and *Thyrsostachys* (*Thyrsostachys siamensis*) are genera that have been introduced in Indonesia for a long time and remain popular as ornamental plants to this day.

The genus which has the most abundant species in Sumatra is *Gigantochloa* (26 species), followed by *Schizostachyum* (19 species), *Bambusa* (11 species), *Dendrocalamus* (10 species), *Dinochloa* (2 species), *Chimonobambusa, Neololeba, Melocanna, Phyllostachys,* and *Thyrsostachys* (1 species respectively). Sumatra emerges as the focal point of *Gigantochloa* species diversity within Indonesia. Upon scrutinizing the bamboo genera's distribution across the archipelago of Indonesia, it becomes evident that *Gigantochloa* predominantly inhabits the western and central regions, gradually tapering in occurrence towards the eastern reaches (*see* Widjaja 2001; Damayanto et al. 2016a; Ervianti et al. 2019; Widjaja 2019; Damayanto & Rahmawati 2020; Robiah et al. 2022). *Gigantochloa* species are characterized by their predominantly erect culms, often featuring relatively substantial diameters. In contrast, Papua displays a scarcity of bamboos exhibiting such erect culms and large diameters (Widjaja et al. 2014). Instead, Papua is predominantly inhabited by scrambling bamboos, particularly of the *Racemobambos* (Damayanto et al. 2016b).

In Sumatra, there are around 42% of the total bamboo species found in Indonesia, which amounts to 175 species (Damayanto & Fefirenta 2021). Additionally, the number of bamboo species in Sumatra is slightly higher, totaling 73 species, compared to Java where there are 72 species (Widjaja 2019). Sumatra hosts almost twice the number of bamboo species as Sulawesi, which has a total of 39 species (Ervianti et al. 2019). Moreover, the bamboo species in Sumatra are nearly three times more numerous than those in Papua, which accounts for 26 species (Damayanto et al. 2016b) (Figure 7). The variation in the number of bamboo species across different regions can be attributed to a combination of factors.

At first, we hypothesized that variations in climate, soil types, and ecological niches in Sumatra and other regions in Indonesia could be factors contributing to the variation in the number of species in each region. However, bamboo is known to thrive in a diverse range of soil conditions, spanning from arid to waterlogged terrain and encompassing both fertile and less productive soils (Aristiatmoko et al. 2012). Its growth is particularly robust in regions characterized by a damp climate, coupled with low temperatures and high humidity, as bamboo has a pronounced need for ample water to support its vigorous development (Hamzah et al. 2016). Report indicate that bamboo demonstrates adaptability to temperatures ranging from 8.8 to 36°C, provided there is a minimum annual precipitation of 1,020 mm and humidity levels of at least 80% (Ediningtyas & Winarto 2012). Notably, bamboo can also flourish in natural settings, without human intervention (Wicaksono et al. 2023). Damayanto et al. (2023) stated that altitude seems to have a lesser impact on bamboo growth.

The diversity in species count across regions is thought to be contingent on the extent of bamboo exploration and the geographical expanse of the area. Varying levels of scientific exploration and documenta-

tion in different regions may contribute to the observed differences in species counts. Regions that have undergone limited flora inventorying, particularly when of considerable size, may lack comprehensive data concerning botanical diversity. This phenomenon is exemplified by the flora of Bali, as elucidated by van Balgooy and Widjaja (2014). Despite Bali's larger landmass compared to Singapore, it registers a lower tally of floral species. This discrepancy is attributed to the limited exploration and field -based inventory, including specimen collection, of its flora (van Balgooy & Widjaja 2014). Additionally, human activities, such as introductions, cultivation, and habitat modification, can also influence the distribution and abundance of bamboo species.

Nine taxa were reported only as identified up to the genus level in Sumatra (Table 1). We were unable to re-identify them mainly because most of them do not provide clear descriptions and photos of the species. It is possible that the taxa reported may be candidates for new species in Sumatra. Widjaja (1991) once reported the existence of 19 bamboo species in Sumatra, which were only identified at the genus level, and one species whose genus was unknown. Widjaja (1991) stated that all 20 taxa were endemic to Sumatra. Many of these species are believed to have been formally described as new species in Widjaja's publication in 1997. Hence, we have omitted the information from Widjaja's (1991) study in this paper. We expected that Sumatra still harbors potential new species waiting to be discovered in the future. This belief is substantiated by Damayanto (2018a) who found *Dinochloa malayana* S.Dransf. in the Riau Islands, which had previously not been reported in Indonesia and was only found in Malay Peninsula (*see* Dransfield 1996a, 1996b; Turner 1995-1996; Chua et al. 2005; Neamsuvan & Tanthien 2015; Vorontsova et al. 2016). Additionally, Damayanto and Widjaja (2016) also published a new species, *Dendrocalamus luteus* Damayanto & Widjaja, discovered in the forest between Jambi and South Sumatra.

A total of six bamboo species (accepted names) that reportedly found in Sumatra were not included in this study because they did not meet our validation criteria, namely *Bambusa lako*, *Bambusa ventricosa*, *Chloothamnus elegantissimus*, *Dinochloa scandens*, *Gigantochloa baliana*, and *Schizostachyum blumei*. Detailed reasons for their exclusion from our list of Sumatran bamboo species in this study can be found in Table 2. Conversely, some bamboo species names that also reported to be found in Sumatra, such as *Bambusa arundinacea* (Retz.) Willd., *Bambusa blumeana* Schult.f., *Bambusa glaucescens* (Willd.) Merr., *Cephalostachyum pergracile* Munro, and *Gigantochloa pseudoarundinacea* (Steud.) Widjaja (*see* Yani 2014; Ami et al. 2017; Widjaja 2019; Ervany et al. 2020; Sujarwanta & Zen 2020; Fitmawati et al. 2021a), were found to be synonym names (Table 3).

Several species of bamboo reported in Sumatra are believed to have identification errors, with some lacking descriptions and/or images. After re-identifying based on the provided descriptions and/or images, we decided not to include that data in the species list for this study. For example, *Bambusa glaucophylla* reported by Sujarwanta and Zen (2020) is suspected to be *Thyrsostachys siamensis*. *Bambusa multiplex* reported by Ami et al. (2017) is suspected to be *Schizostachyum*. *Bambusa multiplex* reported by Sari (2011) does not provide an image. *Bambusa multiplex* reported by Sujarwanta and Zen (2020) is suspected to be *Gigantochloa*. *Bambusa vulgaris* reported by Ami et al. (2017) shows an image of *Gigantochloa apus*. Even Ervany et al. (2020) reported *Dracaena surculosa* Lindl. as a bamboo, which actually belongs to the family of Asparagaceae. The image provided by Ervany et al. (2020) for the species *Dracaena surculosa* resembles

Table 2. List of bamboo species not included in the study.

Species	References	Notes
Bambusa lako Widjaja	Sari 2011	Picture provided by Sari (2011) was similar to *Thyrsostachys siamensis*. *Bambusa lako* occurred in the Lesser Sunda Islands (*see* Widjaja 1997; Widjaja 2019).
Bambusa ventricosa McClure	Ervany et al. 2020	This species is distributed in Southeast China to Vietnam (*see* Vorontsova et al. 2016). Detailed descriptions of Ervany et al. (2020) were not clear. Based on the presented picture, it is suspected that the bamboo is either *Bambusa vulgaris* 'Wamin' or *Bambusa tuldoides*, due to the presence of a "belly" culm.
Chloothamnus elegantissimus (Hassk.) Henrard	Henrard 1936; Holttum 1955; Widjaja 2019	Wong and Dransfield (2016) and Damayanto et al. (2020a) still doubt the presence of this species in Sumatra. This species is reported to be endemic to West Java (Widjaja 2001; Damayanto et al. 2020a).
Dinochloa scandens (Blume ex Nees) Kuntze	Sujarwanta & Zen 2020	Picture provided by Sujarwanta and Zen (2020) was less clear and morphological description was also not very detailed. Damayanto et al. (2021) suspected that this species is *Dinochloa glabrescens.*
Gigantochloa baliana Widjaja & Astuti	Widjaja 2019	This species was endemic to Bali (Widjaja et al. 2004, 2005; Arinasa & Peneng 2013; Arinasa & Sujarwo 2015; Vorontsova et al. 2016; Damayanto et al. 2023).
Schizostachyum blumei Nees	Riastuti et al. 2019; Sujarwanta & Zen 2020	Picture provided by Riastuti et al. (2019) was less clear and morphological description was not provided. Picture provided by Sujarwanta and Zen (2020) was *Schizostachyum brachyladum.*

Table 3. List of synonym names of bamboo species in Sumatra.

Species	References	Notes
Bambusa arundinacea (Retz.) Willd.	Ervany et al. 2020	Synonym of *Bambusa bambos* (*see* Widjaja 2019).
Bambusa blumeana Schult.f.	Ami et al. 2017; Sujarwanta & Zen 2020; Fitmawati et al. 2021a	Synonym of *Bambusa spinosa* (*see* Widjaja 2019; Damayanto et al. 2020c; Ritonga et al. 2020a; Robiah et al. 2022; Ritonga et al. 2023a).
Bambusa glaucescens (Willd.) Merr.	Saputri 2013; Ami et al. 2017; Riastuti et al. 2019	Synonym of *Bambusa multiplex* (*see* Vorontsova et al. 2016).
Cephalostachyum pergracile Munro	Widjaja 2019	Synonym of *Schizostachyum pergracile* (Munro) R.B.Majumdar (*see* Vorontsova et al. 2016).
Gigantochloa pseudoarundinacea (Steud.) Widjaja	Yani 2014; Ami et al. 2017; Riastuti et al. 2019; Sujarwanta & Zen 2020; Sari et al. 2021	Synonym of *Gigantochloa verticillata* (*see* Widjaja 2019).

Thyrsostachys siamensis. Schizostachyum brachycladum reported by Ervany et al. (2020) is suspected to be *Bambusa. Schizostachyum brachyladum* mentioned by Ami et al. (2017) has an image of *Bambusa vulgaris*. On the other hand, Rahayu et al. (2023) reported the presence of *S. bamban*, *S. brachycladum*, and *S. caudatum* in Lampung, Sumatra. Unfortunately, the publication by Rahayu et al. (2023) only provides an abstract. Rahayu (2024, personal communication) stated that their full paper is currently under review. Therefore, we have not included the data from Rahayu et al. (2023) in Table S1 for the time being, pending the publication of the full paper. Nevertheless, the species mentioned by Rahayu et al. (2023) are indeed species that are distributed in Sumatra.

All bamboo species reported by Hastuti et al. (2018) have rather questionable morphological descriptions. Consequently, none of these species were included in this study. For instance, Hastuti et al. (2018) mentioned the presence of "Schyzotyum lima" (the correct spelling is

Schizostachyum lima) in Sumatra, describing it as having one branch larger than the others. However, in reality, *Schizostachyum* exhibits branches that are nearly uniform in size. On the other hand, certain species reported to occur in Sumatra by Riastuti et al. (2019), such as *Bambusa glaucescens* (now accepted as *Bambusa multiplex*), *Dendrocalamus asper*, *Gigantochloa apus*, *Gigantochloa pseudoarundinacea* (initially written as "Gigantochloa pseudoarundin" and currently accepted as *Gigantochloa verticillata*), and *Schizostachyum blumei*, were not included in the list of Sumatran bamboo species in Table S1. This exclusion was due to unclear provided pictures and the absence of a morphological description. Much like the previous situation, the majority of bamboo species documented by Sari et al. (2021) were omitted from the bamboo species list in Table S1 due to a potential identification mistake. For instance, the image intended for *Dendrocalamus asper* was identified as *Bambusa multiplex* by Sari et al. (2021).

Eighteen species of Sumatran bamboo were known as introduced species, namely *Bambusa* (*B. balcooa*, *B. bambos*, *B. farinacea*, *B. heterostachya*, *B. multiplex*, and *B. tuldoides*), *Chimonobambusa* (*C. quadrangularis*), *Dendrocalamus* (*D. asper*, *D. brandisii*, *D. giganteus*, *D. latiflorus*, *D. membranaceus*, and *D. strictus*), *Gigantochloa* (*G. apus*), *Melocanna* (*M. baccifera*), *Phyllostachys* (*P. aurea*), *Schizostachyum* (*S. pergracile*), and *Thyrsostachys* (*T. siamensis*). Species with introduced status are usually brought in as a result of material exchange by botanical gardens in Indonesia, for example, the addition of non-native bamboo collections, *Thyrsostachys oliveri* Gamble, in the "Eka Karya" Bali Botanical Gardens, which were imported from Thailand (*see* Kurniawan et al. 2022). This species has never been reported before occurring in Indonesia. From this garden, this species might eventually spread in various ways, one of which is with the assistance of humans. Humans play a role in bringing some species to Sumatra, where they then grow and even become naturalized or invaded. As an example case, *Chimonobambusa quadrangularis*, which was initially introduced to Cibodas Botanical Gardens, in Java then transported to Sibolangit, and is now invading that area (Damayanto & Muhaimin 2017). This invasive ability of this bamboo is supported by the bamboo's monopodial (running bamboo) root system. The young shoot can grow far from its clump in all directions and dominate the area.

In addition to introduced species, there are 30 endemic bamboo species in Sumatra, with the majority belonging to *Gigantochloa* (15 species), followed by *Dendrocalamus* (4 species), *Schizostachyum* (9 species), while the least represented are *Bambusa* and *Dinochloa*, each having one endemic species. In 1991, Widjaja (1991) reported that there were 25 endemic bamboo species in Sumatra, although for the most part, their taxonomic status was still unclear (only identified up to the genus level). It is suspected that most of these species were later published as new species in Widjaja's publication in 1997.

In Sumatra, there are 5 genera and 30 species of bamboo that are endemic to the area. This number is relatively high when compared to other areas in Indonesia, for instance, in Lesser Sunda Islands, where there are 6 genera and 10 species of bamboo endemic to the area (Damayanto et al. 2023). Endemic species are importance for various reasons. Firstly, they significantly contribute to the overall biodiversity of a specific region, offering unique adaptations to local conditions. Secondly, these species play vital roles within their respective ecosystems, often possessing specialized ecological functions that ensure balance and stability. Culturally, they can be of great significance to indigenous communities, carrying traditional uses and cultural connections, and may also hold

economic value for local industries and economies. Moreover, endemic species can serve as indicators of ecosystem health (Montefalcone 2009), offering early warnings of environmental changes.

Bambusa heterostachya, *Dendrocalamus giganteus*, and *Dendrocalamus membranaceus* fall into the "least concern" (LC) category on the IUCN Red List, indicating they have the lowest risk of being threatened. The status of the remaining 70 species has not been evaluated. It is necessary to conduct an evaluation of the IUCN Red List conservation status of bamboo species, especially for endemic species in Sumatra. Accessing conservation status is crucial for several reasons. It provides a standardized evaluation of extinction risk, guides resource allocation, influences policies, aids research and management, establishes baselines for monitoring, fosters global collaboration, and raises public awareness. The conservation status assessment for endemic bamboo species in Indonesia is rarely conducted. Nevertheless, Damayanto et al. (2023) and Damayanto (2024) have assessed several endemic bamboo species in Lesser Sunda Islands, and the results can serve as a database for stakeholders to initiate conservation efforts. On the other hand, ex-situ conservation efforts are also necessary as the next step after assessing the conservation status. Fortunately, the majority (44 species) of bamboo in Sumatra have been planted and conserved in botanical gardens in Indonesia, while the remaining 29 species have not yet been conserved. Ex-situ conservation helps preserve genetic diversity, preventing potential loss of genetic variations that may be crucial in the future. Additionally, ex-situ conservation provides an opportunity to safeguard bamboo species that are endangered or experiencing significant population declines in the wild, within a controlled and protected environment. Conservation facilities also enable research on the biology, ecology, and management of bamboo species, as well as the development of sustainable cultivation techniques and management practices. Ex-situ preserved bamboo can also serve as a resource for researchers, entrepreneurs, and artisans for scientific research, product development, and bamboo-related commercial activities.

CONCLUSIONS

There are 73 species of bamboo in the Sumatra region, representing 10 genera: *Bambusa* (11 species), *Chimonobambusa* (1 species), *Dendrocalamus* (10 species), *Dinochloa* (2 species), *Gigantochloa* (26 species), *Melocanna* (1 species), *Neololeba* (1 species), *Phyllostachys* (1 species), *Schizostachyum* (19 species), and *Thyrsostachys* (1 species). Eighteen species of Sumatran bamboo are known as introduced species, and 30 species are endemic to Sumatra, with the majority belonging to *Gigantochloa* (15 species). The least represented are *Bambusa* and *Dinochloa*, each having one endemic species. *Bambusa heterostachya*, *Dendrocalamus giganteus*, and *Dendrocalamus membranaceus* fall into the "least concern" (LC) category on the IUCN Red List, while the remaining 70 species have not been evaluated. A total of 44 species have been planted (conserved) in botanical gardens in Indonesia, while the remaining 29 species have not yet been conserved. Research on bamboo in Sumatra is still needed, especially for species not included in the study and several taxa were identified up to the genus level, to clarify their status. Additionally, an assessment of endemic species in Sumatra is necessary to understand their conservation status.

AUTHOR CONTRIBUTION

M.A.R. conducted the literature search and wrote the manuscript. I.P.G.P.D. wrote and contributed to improving the manuscript. S. and N. supervised the process.

CONFLICT OF INTEREST

The authors declare no conflicts of interest but are accountable for the article's content and composition.

REFERENCES

Ami, E. et al., 2017. Bamboo distribution in Musi Rawas District South Sumatera Province. *Science and Technology Indonesia*, 2(4), pp.105-109. doi: 10.26554/sti.2017.2.4.105-109.

Ariati, S.R. et al., 2019. *An Alphabetical List of Plant Species Cultivated in the Bogor Botanic Gardens.* Bogor: Indonesian Institute of Sciences, Center for Plant Conservation, Bogor Botanic Gardens.

Arinasa, I.B.K., & Peneng, I.N., 2013. *Jenis-jenis Bambu di Bali dan Potensinya*, Jakarta: LIPI Press.

Arinasa, I.B.K., & Sujarwo, W., 2015. The diversity of endemic bamboo in Bali and conservation efforts. *Bamboo Journal*, 29, pp.85-92.

Aristiatmoko, P. et al., 2011. Sebaran dan potensi pemanfaatan bambu di Desa Purwobinangun, Kecamatan Pakem, Kabupaten Sleman, Yogyakarta. *Prosiding Seminar Nasional Agroforestry*, 3(29), pp.289-294.

Backer, C., 1928. *Handboek voor de Flora van Java 2.* Batavia: Ruygrock & Co.

BPS (Badan Pusat Statistik)., 2023. *Statistik Indonesia 2023. Statistical Yearbook of Indonesia 2023.* Jakarta: Badan Pusat Statistik/BPS-Statistics Indonesia.

Cahyanto, T. et al., 2016. Keanekaragaman jenis bambu di Taman Bambu Siageung Kebun Raya Kuningan Jawa Barat. *Prosiding Seminar Nasional MIPA dan Pendidikan MIPA. Fakultas Ilmu Tarbiyah dan Keguruan IAIN Sulthan Thaha Saifuddin Jambi*, pp.161-168. doi: 10.24252/bio.v4i2.2513.

Chua, L.S.L. et al., 2005. A preliminary checklist of vascular plants at the Machinchang Range, Pulau Langkawi, Peninsular Malaysia. *Malayan Nature Journal*, 57(2), pp.155-172.

Damayanto, I.P.G.P. & Fefirenta, A.D., 2021. Pola persebaran marga bambu di Indonesia. *Prosiding Seminar Nasional Biologi*, 7(1), pp.24-41. doi: 10.24252/psb.v7i1.22233.

Damayanto, I.P.G.P. & Muhaimin, M., 2017. Notes on *Chimonobambusa quadrangularis* (Franceschi) Makino (Poaceae: Bambusoideae) as an invasive alien plant species in Indonesia. *Floribunda*, 5(7), pp.253-257. doi: 10.32556/floribunda.v5i7.2017.201.

Damayanto, I.P.G.P. & Widjaja, E.A., 2017. A noteworthy *Dendrocalamus* (Poaceae: Bambusoideae) from Sumatra, Indonesia. *The Gradens' Bulletin Singapore*, 69(1), pp.75-80. doi: 10.26492/GBS69%281%29.2017-04.

Damayanto, I.P.G.P. et al., 2016a. A new species of *Schizostachyum* (Poaceae: Bambusoideae) from Sumba Island, Indonesia. *Reinwardtia*, 15(2), pp.119-122. doi: 10.14203/reinwardtia.v15i2.2946.

Damayanto, I.P.G.P. et al., 2016b. Bamboos (Poaceae: Bambusoideae) of Papua, Indonesia. *Jurnal Biologi Papua*, 8(2), pp.57-61. doi: 10.31957/jbp.52.

Damayanto, I.P.G.P. et al., 2020a. A new record of *Chloothamnus* Buse (Poaceae: Bambusoideae) from Sumbawa Island and notes on the genus in Malesia. *Floribunda*, 6(4), pp.127-132. doi: 10.32556/floribunda.v6i4.2020.282.

Damayanto, I.P.G.P. et al., 2020b. Pemanfaatan portal basis data daring dalam validasi nama ilmiah jenis dan suku tumbuhan. *Berkala Ilmu Perpustakaan dan Informasi*, 16(2), pp.170-183. doi: 10.22146/bip.v16i2.770.

Damayanto, I.P.G.P. et al., 2020c. A synopsis of Bambusoideae (Poaceae) in Lombok, Indonesia. *Biodiversitas Journal of Biological Diversity*, 21(10), pp.4489-4500. doi: 10.13057/biodiv/d211004.

Damayanto, I.P.G.P. et al., 2021. *Dinochloa scandens* (Poaceae-Bambusoideae): distribution, habitat preference, and notes on synonymy. *Jurnal Biodjati*, 6(2), pp.174-189. doi: 10.15575/biodjati.v6i2.12485.

Damayanto, I.P.G.P. et al., 2023. Endemic bamboo (Poaceae, Bambusoideae) of the Lesser Sunda Islands. *Jurnal Biodjati*, 8(1), pp.13-28. doi: 10.15575/biodjati.v8i1.25015.

Damayanto, I.P.G.P. & Rahmawati, K., 2020. Bamboos diversity in Banggai Kepulauan, Central Sulawesi, Indonesia. *Jurnal Biodjati*, 5(1), pp.1-14. doi: 10.15575/biodjati.v5i1.6230.

Damayanto, I.P.G.P., 2018a. *Dinochloa malayana* S.Dransf. (Poaceae: Bambusoideae), a new record for Indonesia. *Reinwardtia*, 17(1), pp.35-37. doi: 10.14203/reinwardtia.v17i1.3351.

Damayanto, I.P.G.P., 2018b. Koleksi bambu Taman Eden 100, Kabupaten Toba Samosir, Sumatera Utara dan perannya dalam taman. *Jurnal Arsitektur Lansekap*, 4(2), pp.210-218. doi: 10.24843/JAL.2018.v04.i02.p11.

Damayanto, I.P.G.P., 2024. *Keanekaragaman Jenis Bambu (Poaceae-Bambusoideae) Kepulauan Sunda Kecil.* IPB University.

Dransfield, S., 1983. Notes on *Schizostachyum* (Gramineae-Bambusoideae) from Borneo and Sumatra. *Kew Bulletin*, 38(2), pp.321-332. doi: 10.2307/4108116.

Dransfield, S., 1996a. New species of *Dinochloa* (Gramineae-Bambusoideae) in Malesia and notes on the genus. *Kew Bulletin*, 51(1), pp.103-117. doi: 10.2307/4118748.

Dransfield, S., 1996b. Report on the fieldtrip to Southern Thailand 2 to 29 April 1996. *Thai Forest Bulletin (Botany)*, 24, pp.66-71.

Ediningtyas, D. & Winarto, V., 2012. *Want to Know on Bamboo?*. Jakarta: Forestry Extension Center, the Ministry of Forestry.

Ervany, H. et al., 2020. Etnobotani bambu di Kecamatan Darul Imarah Kabupaten Aceh Besar. *BIOTIK: Jurnal Ilmiah Biologi Teknologi dan Kependidikan*, 8(1), pp.24-36. doi: 10.22373/biotik.v8i1.5836.

Ervianti, D. et al., 2019. Bamboo diversity of Sulawesi, Indonesia. *Biodiversitas Journal of Biological Diversity*, 20(1), pp.91-109. doi: 10.13057/biodiv/d200112.

Fitmawati. et al., 2020. Diversity utilization of bamboo (Bambusoideae) in five islands around Riau Province, Indonesia. *Sabrao Journal of Breeding and Genetics*, 52(2), pp.177-190.

Fitmawati. et al., 2021a. Species diversity and environmental effects on bamboo (Bambusoideae) in estuaries along the east coast of Sumatra. *Sabrao Journal of Breeding and Genetics*, 53(3), pp.403-416.

Fitmawati. et al., 2021b. Inventarisasi keanekaragaman bambu (Poaceae: Bambusoideae) di Pulau Rupat, Kabupaten Bengkalis. *Majalah Ilmiah Biologi Biosfera: A Scientific Journal*, 38(2), pp.69-78. doi: 10.20884/1.mib.2021.38.2.1282.

Hamzah, T.N.T. et al., 2016. Proteomics of Bamboo, the Fast-growing Grass. In *Plant Omics: Trends and Applications*. Basel, Switzerland: Springer, pp.365. doi: 10.1007/978-3-319-31703-8_13.

Hasibuan, M., 2020. *Identifikasi dan Karakteristik Beberapa Jenis Bambu di Kabupaten Batu Bara dan Kabupaten Simalungun*. Universitas Sumatera Utara.

Hastuti, R.W. et al., 2018. Studi keanekaragaman jenis bambu di Desa Tanjung Terdana Bengkulu Tengah. *Diklabio: Jurnal Pendidikan dan Pembelajaran Biologi*, 2(1), pp.96-102. doi: 10.33369/diklabio.2.1.96-102.

Henrard, J.T., 1936. *Chloothamnus*, a neglected genus of Bambusaceae. *Blumea*, 11(2), pp.60-73.

Holttum, R.E., 1955. The bamboo-genera *Nastus* and *Chloothamnus*. *Kew Bulletin*, 10(4), pp.591-594. doi: 10.2307/4113771.

Ismaini, L. et al., 2015. Analisis komposisi dan keanekaragaman tumbuhan di Gunung Dempo, Sumatera Selatan. *Prosiding Seminar Nasional Biodiversitas Indonesia* (1)6, pp.13-18. doi: 10.13057/psnmbi/m010623.

IUCN (International Union for Conservation of Nature)., 2023, 'Guidelines for using the IUCN Red List categories and criteria. Version 15.1. Prepared by the standards and petitions committee' in *IUCN Red List*, viewed 19 November 2023, from https://www.iucnredlist.org/resources/redlistguidelines.

KBBID (Kamus Besar Bahasa Indonesia Daring)., 2023, 'Sumatra', in *Kamus Besar Bahasa Indonesia Daring*, viewed 19 November 2023, from https://kbbi.kemdikbud.go.id/entri/sumatra.

Kurnia, H.B., 2022. *Pemanfaatan Jenis-jenis Bambu (Bambusoideae) di Kecamatan Pangkalan Koto Baru Kabupaten Lima Puluh Kota Provinsi Sumatra Barat*. Universitas Riau.

Kurniawan, A. et al., 2022. *An Alphabetical List of Plant Species Cultivated in "Eka Karya" Bali Botanic Garden*. Jakarta: BRIN Pub.

Lestarini, W. et al., 2012. *An Alphabetical List of Plant Species Cultivated in Purwodadi Botanic Garden*. Purwodadi: Purwodadi Botanic Garden, Indonesian Institute of Sciences.

Liana, A., 2020. Keanekaragaman genus bambu (Poaceace: Bambusoideae) di Indonesia. *Prosiding Seminar Nasional Biologi*, 6(1), pp.54-57. doi: 10.24252/PSB.V6I1.15539.

Makoyana., 2023, *Makoyana*, viewed 19 November 2023, from https://makoyana.brin.go.id.

Montefalcone, M., 2009. Ecosystem health assessment using the Mediterranean seagrass *Posidonia oceanica*: A review. *Ecological Indicators*, 9(4), pp. 595-604. doi: 10.1016/j.ecolind.2008.09.013.

Mutaqien, Z. et al., 2011. Penyebaran tumbuhan asing di Hutan Wornojiwo Kebun Raya Cibodas, Cianjur, Jawa Barat. *Prosiding Seminar Nasional HUT Kebun Raya Cibodas ke-159*, pp.550-558.

Nasution, E.Z., 2018. *Keanekaragaman Jenis dan Pemanfaatan Bambu (Bambusa sp) oleh Masyarakat Sekitar Hutan Kawasan Taman Nasional Batang Gadis*. Universitas Sumatera Utara.

Neamsuvan, O. & Tanthien, S., 2015. Medicinal plants used for women's healthcare from Khao Phanom Bencha National Park, Krabi Province. *Burapha Science Journal*, 20(1), pp.118-132.

Nuraetin, E., 2014. *Invenarisasi dan Identifikasi Jenis Bambu di Kawasan Hutan Bambu Pagar Alam Provinsi Sumatera Selatan.* Universitas Sriwijaya.

Nursanti, & Adriadi, A., 2018. Keanekaragaman tumbuhan invasif di kawasan Taman Hutan Raya Sultan Thaha Saifuddin, Jambi. *Media Konservasi*, 23(1), pp.85-91.

Owen, Y.R., 2021. *Eksplorasi dan Inventarisasi Jenis-jenis Bambu (Poaceae-Bambusoidae) di Kabupaten Kampar.* Universitas Riau.

Purba, C.P.P. et al., 2014. *Potret Keadaan Hutan Indonesia Periode 2009-2013*, Bogor: Forest Watch Indonesia, pp. 129.

Rahayu, Y. et al., 2020. Bamboo in the area of Sumatra Institute of Technology and its potency in landscape gardens. *Biologica Samudra*, 2 (2), pp.79-86. doi: 10.33059/jbs.v2i2.2310.

Rahayu, Y. et al., 2023. *Schizostachyum caudatum* Backer ex Heyne: a sacred bamboo from the foothills of Mt. Pesagi, West Lampung, Indonesia. *Current Trends in Biotechnology & Pharmacy*, 17(Suppl Issue 2023), pp.57.

Rahayu, Y. & Ervianti D., 2020. Bamboos of the Batu Putu Biodiversity Park Lampung. *Bioma*, 16(1), pp.14-20. doi: 10.21009/Bioma16 (1).2.

Retnowati, A. & Rugayah., 2019. Keanekaragaman Tumbuhan dan Jamur Indonesia. In *Status Keanekaragaman Hayati Indonesia: Kekayaan Jenis Tumbuhan dan Jamur Indonesia.* Jakarta: LIPI Press, pp.1-14.

Riastuti, R.D. et al., 2019. Eksplorasi jenis bambu di Kecamatan Rawas Ulu Kabupaten Muratara. *BIOEDUSAINS: Jurnal Pendidikan Biologi dan Sains*, 2(1), pp.13-25. doi: 10.31539/bioedusains.v2i1.641.

Rijaya, I. & Fitmawati., 2019. Jenis-jenis bambu (Bambusoideae) di Pulau Bengkalis, Provinsi Riau, Indonesia. *Floribunda*, 6(2), pp.41-52. doi: 10.32556/floribunda.v6i2.2019.229.

Ritonga, M.A. et al., 2020a. Keragaman jenis bambu di Kawasan Ekosistem Leuser, Kecamatan Tenggulun, Kabupaten Aceh Tamiang, Aceh. *Buletin Plasma Nutfah*, 26(2), pp.109-122. doi: 10.21082/ blpn.v26n2.2020.p109-122.

Ritonga, M.A. et al., 2020b. Penelusuran ragam jenis bambu di Kota Langsa, Aceh. *Al-Hayat: Journal of Biology and Applied Biology*, 3(1), pp.8-14. doi: 10.21580/ah.v3i1.6065.

Ritonga, M.A. et al., 2020c. Pemanfaatan bambu oleh masyarakat di Kecamatan Tenggulun, Kabupaten Aceh Tamiang. *Jurnal Biologica Samudra*, 2(1), pp.10-19. doi: 10.33059/jbs.v2i1.2232.

Ritonga, M.A. et al., 2023a. Bamboo diversity in Weh Island, Aceh, Indonesia. *Biodiversitas Journal of Biological Diversity*, 24(5), pp.2563-2576. doi: 10.13057/biodiv/d240508.

Ritonga, M.A. et al., 2023b. Ethnobotany of bamboo on Weh Island, Aceh, Indonesia. *Ethnobotany Research and Applications*, 26(75), pp.1-19. doi: 10.32859/era.26.75.1-19.

Robiah, Y. et al., 2022. Bamboo diversity in the Maluku Islands, Indonesia. *Jurnal Biodjati*, 7(2), pp. 292-308. doi: 10.15575/ biodjati.v7i2.18713.

Sanders, D.L. et al., 2018. Navigating nature, culture and education in contemporary botanic gardens. *Environmental Education Research*, 24(8), pp.1077-1084. doi: 10.1080/13504622.2018.1477122.

Saputri, A., 2013. *Biodiversitas Bambu di Sumatera Utara Bagian Timur.* Universitas Sumatera Utara.

Sari, N., 2011. *Inventarisasi dan Pemanfaatan Bambu di Desa Sekitar Tahura kabupaten Karo*. Universitas Sumatera Utara.

Sari, R.P. et al., 2021. Keanekaragaman bambu di Bukit Cogong Kabupaten Musi Rawas. *Borneo Journal of Biology Education (BJBE)*, 3(1), pp.8-17. doi: 10.35334/bjbe.v3i1.1886.

Sitepu, M.R., 2022. *Identifikasi dan Karakteristik Jenis Bambu (Studi Kasus di Desa Suka Makmur Kecamatan Sibolangit Kabupaten Deli Serdang)*. Universitas Sumatera Utara.

Steenis-Kruseman, M.J.V., 1950. Malaysian plant collectors and collections being a Cyclopaedia of botanical exploration in Malaysia and a guide to the concerned literature up to the year 1950. *Flora Malesiana*, 1(1), pp.1-639.

Sujarwanta, A. & Zen, S., 2020. Identifikasi jenis dan potensi bambu (*Bambusa* sp.) sebagai senyawa antimalaria. *BIOEDUKASI (Jurnal Pendidikan Biologi)*, 11(2), pp.131-151. doi: 10.24127/bioedukasi.v11i2.3423.

Sujarwo, W. et al., 2019. *List of Living Plants Collection Cultivated in Cibodas Botanic Gardens*, Cibodas: Cibodas Botanic Garden, Indonesian Institute of Sciences.

Syauqi, M.F. et al., 2023. Diversity, ecology and habitat suitability of *Gigantochloa* in Central Sumatra. *Agriculture and Natural Resources*, 57 (2), pp.343-352.

Tarigan, T.T., 2008. *Kajian Pemanfaatan Bambu di Kecamatan Sibolangit Kabupaten Deli Serdang*. Universitas Sumatera Utara.

Turner, I.M., 1995-1996. A catalogue of the vascular plants of Malaya. *The Gardens' Bulletin Singapore*, 47(1&2), pp.17-57.

Utami, N. & Damayanto, I.P.G.P., 2023. Annotated checklist of Indonesian *Impatiens* (Balsaminaceae). *Nordic Journal of Botany*, 2023 (e04088), pp.1-19. doi: 10.1111/njb.04088.

van Balgooy, M.M.J., & Widjaja, E.A., 2014. Flora of Bali: a provisional checklist. *Reinwardtia*, 14(1), pp.219-221. doi: 10.55981/reinwardtia.2014.418.

Vorontsova, M.S. et al., 2016. World checklist of bamboos and rattans. *INBAR Technical Report*, 37, pp.1-454.

Wahidah, B.F. et al., 2021. Bamboo diversity in Indrokilo Botanical Garden, Central Java. *Buletin Plasma Nutfah*, 27(1), pp.57-70. doi: 10.21082/blpn.v27n1.2021.57-70.

Wicaksono, D. et al., 2023. Identifikasi persebaran bambu pada daerah aliran sungai Pepe Desa Sawahan. *Nusantara Hasana Journal*, 2(8), pp.349-373.

Widjaja, E.A. & Karsono, K., 2005. Bamboo diversity in Sumba Island. *Biodiversitas Journal of Biological Diversity*, 6(2), pp.95-99. doi: 10.13057/biodiv/d060205.

Widjaja, E.A. et al., 2004. New species of bamboos (Poaceae-Bambusoideae) from Bali. *Reinwardtia*, 12(2), pp.199-204. doi: 10.14203/reinwardtia.v12i2.73.

Widjaja, E.A. et al., 2005. *Identikit Bambu di Bali*, Bogor: Puslit Biologi, LIPI.

Widjaja, E.A. et al., 2014. *Kekinian Keanekaragaman Hayati Indonesia, 2014*, Jakarta: LIPI Press.

Widjaja, E.A., 1987. A revision of Malesian *Gigantochloa* (Poaceae Bambusoideae). *Reinwardtia*, 10(3), pp.291-380. doi: 10.14203/reinwardtia.v10i3.274.

Widjaja, E.A., 1991. Endemic bamboos from Sumatra. *The IV International Bamboo Workshop, Chiangmai, Thailand*, pp.1-6.

Widjaja, E.A., 1997. New taxa in Indonesian bamboos. *Reinwardtia*, 11(2), pp.57-152. doi: 10.14203/reinwardtia.v11i2.588.

Widjaja, E.A., 1998. State of the art of Indonesian Bamboo. *Proceedings of Training Course Cum Workshop 10-17 May 1998, Kunming and Xishuanbanna, Yunnan, China*, pp.1-275.

Widjaja, E.A., 2001. *Identikit Jenis-jenis Bambu di Jawa*, Jakarta: LIPI Press.

Widjaja, E.A., 2019. *The Spectacular Indonesian Bamboos*, Jakarta: Polagrade.

Wong, K.M., & Dransfield, S., 2016. *Ruhooglandia* and *Widjajachloa*, two new genera of Malesian bamboos (Poaceae: Bambusoideae) and their distinction from *Nastus* and *Chloothamnus. Sandakania*, 22, pp.1 -9.

Yani, A.P., 2014. Keanekaragaman bambu dan manfaatnya di Desa Tabalagan Bengkulu Tengah. *Jurnal Gradien*, 10(2), pp.987-991.

APPENDICES

Table S1. List of bamboo species in Sumatra including the source of refereRitongances, IUCN conservation status, introduced species, endemic species, and ex-situ conservation status.

Species	Cultivated in BGI (Makoyana 2023)	Endemic species	Introduced species	IUCN conservation status (IUCN 2023)	Syauqi et al. 2023	Ritonga et al. 2023a, 2023b	Sitepu 2022	Kurnia 2022	Tampubolo 2021	Sari et al. 2021	Owen 2021	Fitmawati et al. 2021b	Fitmawati et al. 2021a	Togatorop et al. 2020	Sujarwanta & Zen 2020	Ritonga et al. 2020b	Ritonga et al. 2020a, 2020c	Rahayu et al. 2020	Rahayu & Ervianti 2020	Hasibuan 2020	Fitmawati et al. 2020	Ervany et al. 2020	Widjaja 2019	Rijaya & Fitmawati 2019	Riastuti et al. 2019	Nasution 2018	Damayanto 2018b	Damayanto 2018a	Damayanto & Widjaja 2017	Ami et al. 2017	Yani 2014	Nuraetin 2014	Saputri 2013	Sari 2011	Tarigan 2008	Widjaja 1997	Backer 1928	Widjaja 1987	Dransfield 1983
Bambusa balcooa Roxb.	+		+	NE																			+												+				
Bambusa bambos (L.) Voss	+		+	NE																			+																
Bambusa farinacea K.M.Wong	+		+	NE																			+																
Bambusa glaucophylla Widjaja	+	+		NE							+	+						+			+		+	+									+						
Bambusa heterostachya (Munro) Holttum	+		+	LC							+	+	+								+		+	+															
Bambusa maculata Widjaja		+		NE											+								+																
Bambusa multiplex (Lour.) Raeusch. ex Schult.f.	+		+	NE		+		+			+	+	+			+		+			+		+	+			+			+	+	+			+				
Bambusa riauensis Widjaja	+	+		NE												+		+			+		+	+						+	+	+				+			
Bambusa spinosa Roxb.	+			NE		+		+				+			+		+				+		+	+									+		+				
Bambusa tuldoides Munro	+		+	NE		+																	+																
Bambusa vulgaris Schrad. ex J.C.Wendl.	+		+	NE		+	+	+			+	+	+		+	+	+	+			+	+	+	+	+	+	+			+	+	+	+	+	+				
Chimonobambusa quadrangularis (Franceschi) Makino			+	NE																			+																
Dendrocalamus asper (Schult. & Schult.f.) Backer	+		+	NE		+		+			+	+	+	+	+		+	+			+		+	+	+	+	+			+	+	+	+	+	+				
Dendrocalamus bengkalisensis Widjaja	+	+		NE																			+						+										
Dendrocalamus brandisii (Munro) Kurz			+	NE																			+						+										
Dendrocalamus buar Widjaja	+	+		NE																			+						+										
Dendrocalamus giganteus Munro	+		+	LC																			+						+										
Dendrocalamus hait Widjaja	+	+		NE																			+						+										
Dendrocalamus latiflorus Munro	+		+	NE																			+						+										
Dendrocalamus luteus Damayanto & Widjaja		+		NE																			+						+										
Dendrocalamus menbranaceus Munro			+	LC																			+						+										
Dendrocalamus strictus (Roxb.) Nees	+		+	NE		+														+			+																
Dinochloa glabrescens Widjaja		+		NE																			+					+											
Dinochloa malayana S.Dransf.				NE																			+					+											

Table S1. Contd.

Species	Cultivated in BGI (Makoyana 2023)	Endemic species	Introduced species	IUCN conservation status (IUCN 2023)	Syauqi et al. 2023	Ritonga et al. 2023a, 2023b	Sitepu 2022	Kurnia 2022	Tampubolo 2021	Sari et al. 2021	Owen 2021	Fitmawati et al. 2021b	Fitmawati et al. 2021a	Togatorop et al. 2020	Sujarwanta & Zen 2020	Ritonga et al. 2020b	Ritonga et al. 2020a, 2020c	Rahayu et al. 2020	Rahayu & Ervianti 2020	Hasibuan 2020	Fitmawati et al. 2020	Ervany et al. 2020	Widjaja 2019	Rijaya & Fitmawati 2019	Riastuti et al. 2019	Nasution 2018	Damayanto 2018b	Damayanto 2018a	Damayanto & Widjaja 2017	Ami et al. 2017	Yani 2014	Nuraetin 2014	Saputri 2013	Sari 2011	Tarigan 2008	Widjaja 1997	Backer 1928	Widjaja 1987	Dransfield 1983
Gigantochloa achmadii Widjaja		+		NE																			+										+			+		+	
Gigantochloa apus (Schult.f.) Kurz ex Munro	+		+	NE	+		+		+					+	+	+	+			+	+		+											+	+				
Gigantochloa atter (Hassk.) Kurz ex Munro	+			NE	+									+		+	+			+	+		+										+			+			
Gigantochloa atroviolacea Widjaja	+			NE	+										+				+				+							+			+						
Gigantochloa calcicola Widjaja		+		NE																			+													+			
Gigantochloa hasskarliana (Kurz) Backer	+	+		NE	+			+				+	+						+		+		+	+															
Gigantochloa hirtinoda Widjaja		+		NE																			+													+			
Gigantochloa kuring Widjaja	+	+		NE	+																+		+													+			
Gigantochloa levis (Blanco) Merr.	+		+	NE	+																+		+																
Gigantochloa longiprophylla Widjaja		+		NE																			+													+			
Gigantochloa luteostriata Widjaja		+		NE																			+																
Gigantochloa magentea Widjaja		+		NE																			+													+			
Gigantochloa membranoidea Widjaja		+		NE																			+													+			
Gigantochloa nigrociliata (Buse) Kurz	+	+		NE	+																		+													+			
Gigantochloa papyracea Widjaja		+		NE																			+													+			
Gigantochloa prurieus Widjaja	+	+		NE	+		+	+													+		+										+					+	
Gigantochloa pubinervis Widjaja	+	+		NE																			+													+			
Gigantochloa pubipetiolata Widjaja	+	+		NE																			+													+			
Gigantochloa robusta Kurz	+	+		NE	+																		+							+	+	+	+						
Gigantochloa scortechinii Gamble	+	+		NE	+																		+								+	+							
Gigantochloa serik Widjaja	+	+		NE	+							+								+			+			+										+			
Gigantochloa thoi K.M.Wong	+	+		NE																			+																
Gigantochloa tomentosa Widjaja	+	+		NE																			+													+			
Gigantochloa velutina Widjaja	+	+		NE										+	+								+							+						+			
Gigantochloa verticillata (Willd.) Munro	+	+		NE																			+																
Gigantochloa wrayi Gamble				NE																			+									+							
Melocanna baccifera (Roxb.) Kurz	+		+	NE																			+																

Table S1. Contd.

Species	Cultivated in BGI (Makoyana 2023)	Endemic species	Introduced species	IUCN conservation status (IUCN 2023)	Ritonga et al. 2023a, 2023b	Sitepu 2022	Kurnia 2022	Fitmawati et al. 2021a	Sujarwanta & Zen 2020	Ritonga et al. 2020b	Ritonga et al. 2020a, 2020c	Rahayu & Ervianti 2020	Fitmawati et al. 2020	Widjaja 2019	Rijaya & Fitmawati 2019	Nasution 2018	Damayanto 2018b	Ami et al. 2017	Nuraetin 2014	Saputri 2013	Tarigan 2008	Widjaja 1997	Backer 1928	Dransfield 1983
Neololeba atra (Lindl.) Widjaja	+			NE										+							+			
Phyllostachys aurea (André) Rivière & C.Rivière	+		+	NE										+										
Schizostachyum aciculare Gamble		+		NE															+					
Schizostachyum atrocingulare Widjaja	+	+		NE										+								+		
Schizostachyum banban Widjaja	+	+		NE										+								+		
Schizostachyum brachycladum (Kurz ex Munro) Kurz	+	+		NE	+		+	+	+	+			+	+	+	+		+		+	+			
Schizostachyum caudatum Backer ex K.Heyne	+	+		NE										+									+	
Schizostachyum cornutum Widjaja		+		NE										+								+		
Schizostachyum cuspidatum Widjaja	+	+		NE										+								+		
Schizostachyum grande Ridl.	+	+		NE										+										
Schizostachyum iraten Steud.	+	+		NE										+										
Schizostachyum latifolium Gamble	+	+		NE			+							+	+									
Schizostachyum lengguanii K.M.Wong	+	+		NE										+										
Schizostachyum lutescens Widjaja		+		NE										+								+		
Schizostachyum mampouw Widjaja	+	+		NE										+								+		
Schizostachyum pergracile (Munro) R.B.Majumdar	+			NE										+										
Schizostachyum pleianthemum S.Dransf.	+	+		NE										+										+
Schizostachyum silicatum Widjaja	+			NE	+								+	+			+					+		
Schizostachyum terminale Holttum		+		NE										+										
Schizostachyum undulatum S.Dransf.	+	+		NE										+										+
Schizostachyum zollingeri Steud.	+			NE		+	+	+			+	+		+						+	+			
Thyrsostachys siamensis Gamble	+		+	NE			+	+		+			+	+	+							+		
Neololeba atra (Lindl.) Widjaja	+			NE										+										
Phyllostachys aurea (André) Rivière & C.Rivière	+			NE										+										

Notes: + = presence/yes, BGI = Botanical Gardens of Indonesia, LC = least concern, NE = not evaluated